Contents of Lecture Script for the IAEA/RCA Regional Training Course on Digital Industrial Radiology and Computed Tomography Applications in Industry Kajang, Malaysia, 2 – 6 November 2009

Contents of Lecture Script for the IAEA/RCA Regional Training Course on Digital Industrial Radiology and Computed Tomography Applications in Industry Kajang, Malaysia, 2 – 6 November 2009

L 01 Physical Basics of the X-ray Technology

Content

1.1 Introduction

The X-rays feature a class of **electromagnetic radiation.** An overview of the whole spectrum of electromagnetic radiation is given in Figure 1.1 together with the corresponding energies. Based on its **energy** level higher than that of visible light, X-rays are capable to penetrate objects not transparent to visible light. This kind of **permeability** and the linear propagation of X-rays form the base for all radiographic (using X-ray film or CR) and radioscopic (real time and film free) testing methods. The information gained by these techniques consists of a descriptive image showing the thickness of layers and material density distributions within a test specimen.

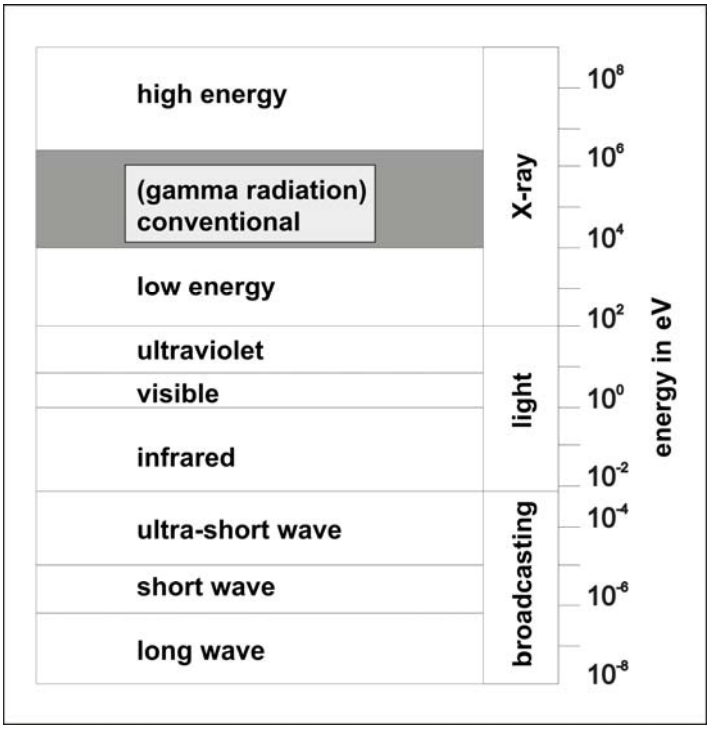

Figure 1.1: Whole spectrum of electromagnetic radiation together with corresponding energies and fields of applications (according to Becker)

1.2 Generation of X-rays

The principle of the generation of X-rays is shown schematically in Figure 1.2.

Within an evacuated tube made of glass (glass-tubes) or of a combination of metal and ceramics (metal-ceramic-tubes) electrons are **emitted** from a heated spiral-wound filament**.** The free electrons then are accelerated by the high potential **(tube voltage)** between the **cathode (electrically negative polarity)** and the **anode (electrically positive polarity)** towards the anode. Hitting the anode material **(target)** the electrons are decelerated. During this physically rather complicated event the electrons loose their

kinetic energy. This loss is transformed mainly into heat and a minor part (some 1%) into X-radiation ("bremsstrahlung"). As a consequence the X-ray tube needs an efficient cooling.

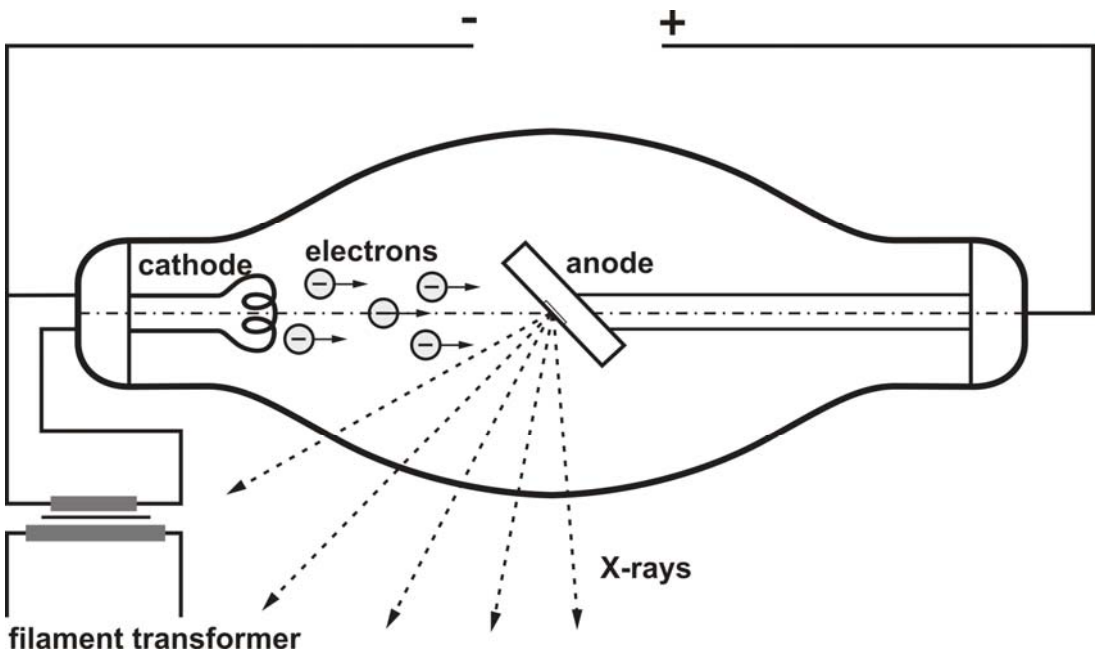

Figure 1.2: Principle of the generation of X-rays

The X-rays emitted from the anode by the deceleration process is characterised by a certain continuous spectrum typical for the **Bremsstrahlung**. The term spectrum is understood as a graphic presentation of the **radiation intensity I_0 against the radiation energy E**. Continuous means that any energy is present within a certain range, even if the intensity varies. The highest occurring energy is denoted as the **accelerating energy E_I**.

The accelerating energy E_I is only of limited use to describe the radiation property since the theoretical case is assumed that whole energy of the electron beam will be transformed. Therefore, it is common practice to choose the average energy or the position of the maximal intensity to describe the radiation property. The **total intensity** of the spectrum depends on the **tube current I** and the **tube voltage U**. The material of the anode can be neglected referring to its influence on the total intensity when applied for the radiography and the radioscopy.

1.3 Parameter adjustment on the X-ray generator operating console

The following adjustments which can be set on the control console of the X-ray generating device will be discussed in view of their effect on the spectrum:

1.3.1 Choice of the tube current

Modifying the current I results in a change of the radiation intensity I_0 of each energy lower than the limiting one (Figure.1.3). The average energy, the position of the maximum and the accelerating energy itself remain unchanged.

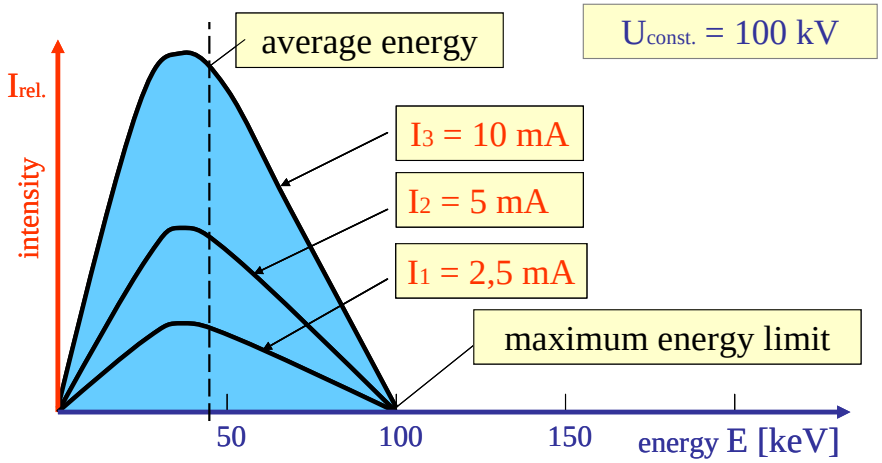

Figure.1.3: Intensity changes I_0 upon modification of the current I

1.3.2 Choice of the accelerating potential (tube voltage)

Increasing the voltage U results in a shift of the maximal intensity to a higher energy, towards increased limiting and average energies and thus to a more than proportional risen total intensity (Figure 1.4).

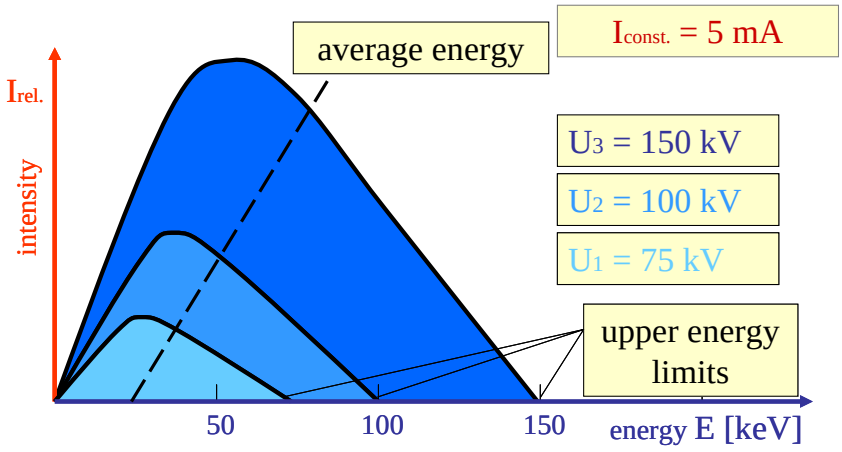

Figure 1.4: Altered spectrum responding to a modified voltage U

1.4 Attenuating the radiation

The most eminent property of X-rays is their penetrability. This means that the radiation penetrates the test specimen while undergoing an attenuation. The resulting **attenuation profile** is being recorded with a suitable detector and thus forms the **radiographic image.**

To understand the interactions between the penetrating radiation and the specimen it should be helpful to understand the radiation as a stream of particles of certain energies. In case of an electromagnetic radiation these particles are referred to as **photons** or **quanta**. The attenuation then can be understood as impulsive interaction with the electrons of the atoms or molecules of the specimen. Within the range of energies used in the applications that will be presented in this course (10 – 450 keV) the attenuation can be described as a sum of two processes: **photo absorption and scattering.**

The very complex secondary processes ongoing to revert the temporary ionisation of atoms will not be discussed any further. In addition, it should be mentioned that the interacting processes between X-rays and matter is much more complicated in reality. The simplified presentation given here should be completely sufficient for the purpose of this course.

1.4.1 Attenuation of radiation by photo absorption

The actual desired and image generating effect is the photo absorption. Here the energy of the hitting X-ray photon is totally transferred to the related counterpart **(absorbed).** One part of the energy will be dissipated in turn by the release of a photo electron and the generation of X-ray fluorescence radiation (Figure 1.5).

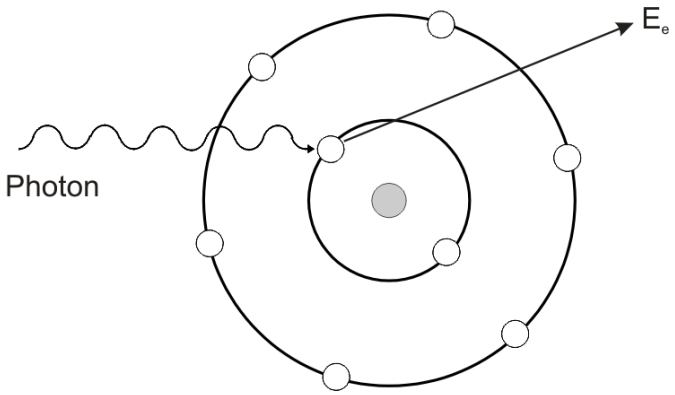

Abb.1.5: Photo absorption of a photon at an orbital electron

1.4.2 Attenuation by scattering

In case of scattering the electron is subjected to a change of its direction **(scatter)** with or without loss of energy (Compton- or Rayleigh scatter). Since the Compton scatter predominates over the Rayleigh scatter at energies from 40-60 keV on only the Compton effect will be considered further. Here the energy of the photon is reduced by the impact, and a so-called Compton electron is being released (Figure 1.6). The scatter radiation generated here is distributed equally into all directions and thus does **not contribute to image contours** in the radioscopy. This may be compared with a subject illuminated from all sides without producing visibly a shadow.

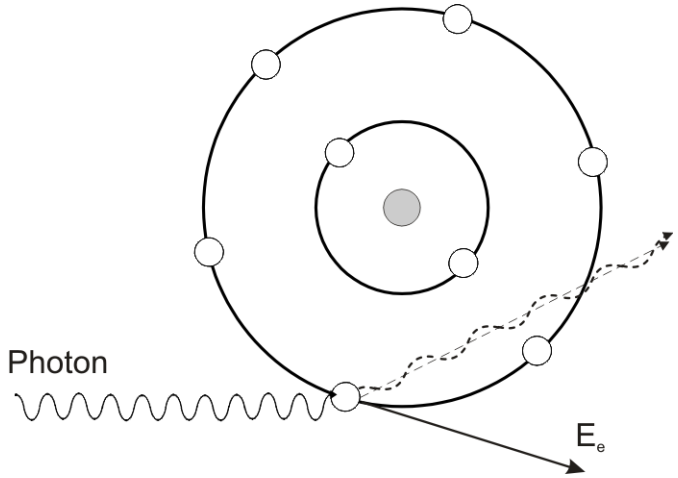

Figure 1.6: Scattering of a photon at an orbital electon

The attenuation of the radiation, understood as the sum of both effects, depends deeply on the energy E of the radiation. A rising energy is followed by a decrease in attenuation. The domination of either effect depends also on the atomic order number of the material of the specimen (Figure 1.7).

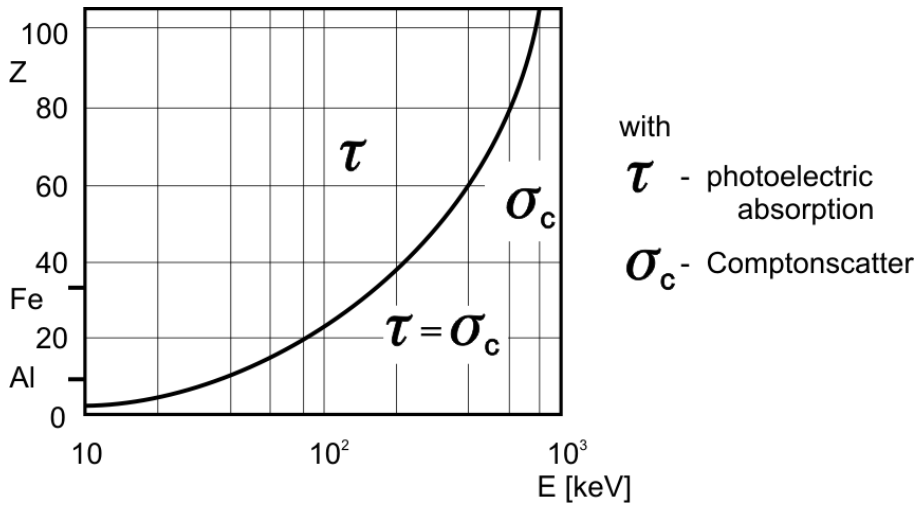

Figure 1.7: Dependence of absorption and scatter on energy and the atomic order number

1.4.3 Law of the attenuation of X-rays

The mathematical reconstruction is very complex in how the intensity and/or attenuation profile is altered behind a specimen by the attenuation processes for any individual case. A quantitative description of the attenuation of the radiation is only possible with simplified assumptions, but far from reality:

- narrow collimated beam
- mono-energetic radiation (just a single spectral line)

However, it is still useful for many application to describe the attenuation behaviour of radiation mathematically with these assumptions (see Figure 1.8):

$$I = I_0 \cdot e^{-\mu \cdot w}$$

with **I** Intensity behind the specimen

I_0 Radiation intensity without attenuation

μ Attenuation coefficient

w Penetrated wall thickness of the specimen

Wherein the attenuation coefficient μ is determined by:

- the energy
- the material

The attenuation coefficient decreases with increasing radiation energy (Figure 1.8), in other terms, the specimen becomes more and more transparent, that means, less radiation is absorbed. As a consequence, two walls of different thickness within a specimen will be displayed with lower **intensity differences (radiation contrast K_S)** with rising energies.

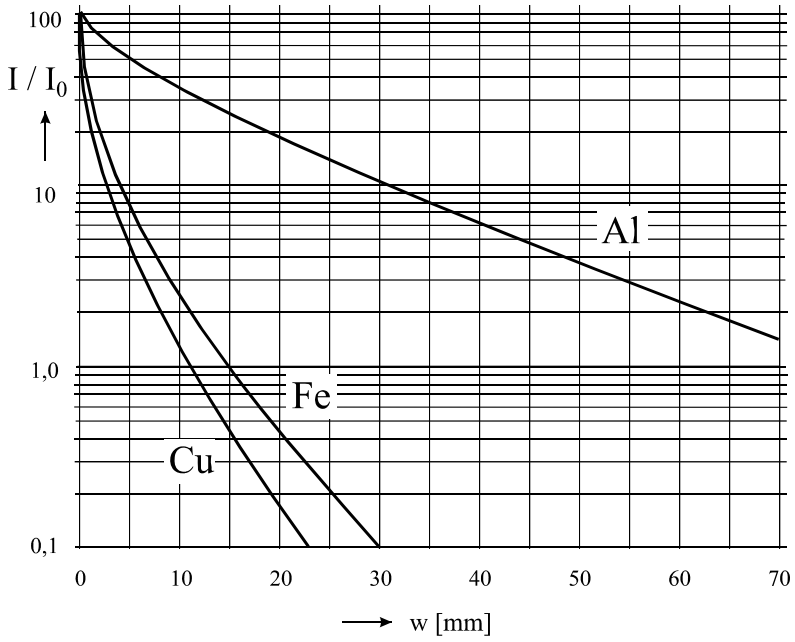

Figure 1.8: Attenuation curves of various materials

1.5 Hardening by pre-filtering

The total intensity decreases while the average energy and the position of the maximal intensity is shifted to higher energies (Figure 1.9).

Common materials used for pre-filtering are aluminium (Al) with a layer thickness of 1-5 mm and copper (Cu) from 0.2 – 1 mm thickness on.

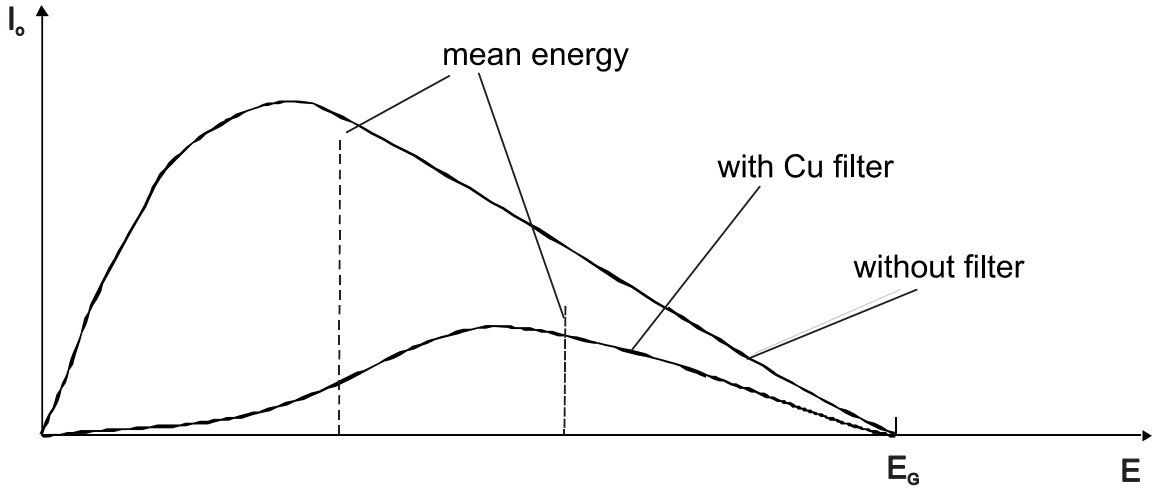

Figure 1.9: Modification of the spectrum by pre-filtering

Conclusions:

Increasing the voltage	→ raises the energy of the radiation
	→ increases the penetrability of the radiation
	→ causes higher radiation intensity

„The radiation passes through materials more readily → it is possible to penetrate also thicker and denser materials easily“

Increasing the current	→ raises radiation intensity without improved penetrability
Pre-filtering	→ reduces the portions of the radiation with lower energies
	→ reduces the intensity
	→ enables penetration of layers in a larger thickness range

L 02 Radiation Contrast, Noise and Imaging Requirements

Content

2.1 Introduction

The **radiation contrast** is of particular interest when inspecting radiographically since there is a fundamental link between the ability to detect a flaw in the material and the noise which determines the contrast sensitivity in the radiographic image.

The attenuation coefficient decreases with increasing radiation energy, in other words, the specimen becomes more transparent since it absorbs less radiation. That means that two different wall thicknesses within a specimen appear only with a smaller **intensity difference ΔI** in the resulting image when increasing the energy (see Fig. 2.1).

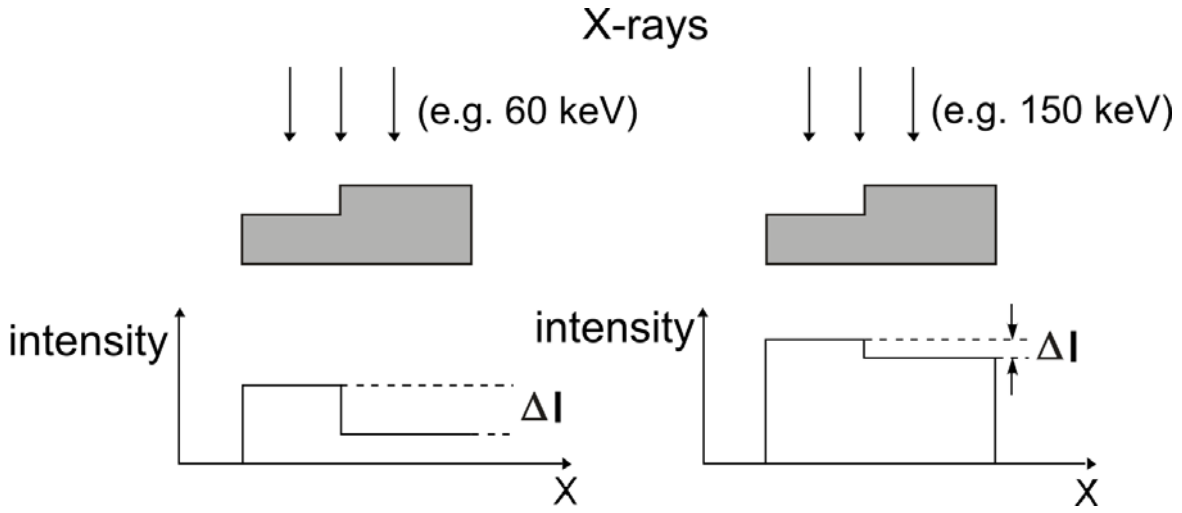

Fig. 2.1: Dependency of the intensity difference on the energy

To conclude:

With increasing energy, the intensity differences within a feature of a specimen (e.g. a cavity), i.e. the contrast, decreases regardless of the chosen detector.

This has to be taken into account in any inspection task!

„More is better" is the wrong approach when adjusting the accelerating potential for optimal flaw recognition!

2.2 Quantitative considerations

The radiation is described mathematically based on the intensity changes during a radiographic inspection (Fig.2.2. This approach illustrates the essential factors determining the radiation contrast for the practical work.

The intensity changes of the radiation during a radiographic inspection are explained in Fig.2.2. Following the physical processes of attenuating radiation (s. a. Lecture 1), the **total intensity behind the specimen** always results from both, the attenuated primary beam and the scattered radiation.

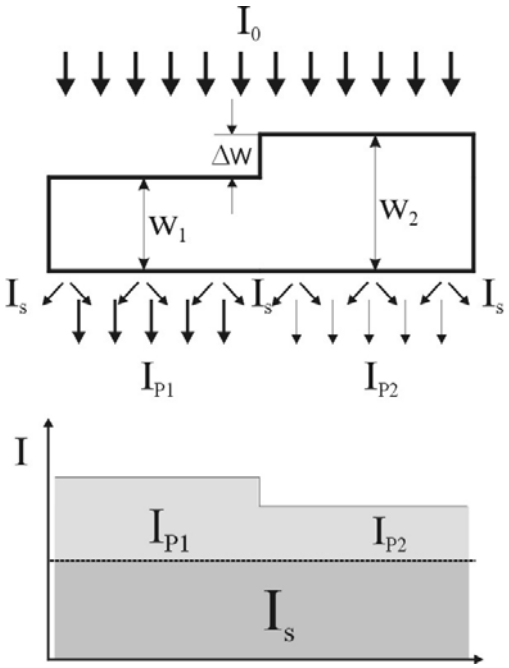

Fig. 2.2: Formation of the radiation contrast

The total intensity I_g behind the specimen equals the sum of the intensity of the attenuated primary beam I_p and that one of the scatter radiation I_s:

$$I_g = I_P + I_S$$

Since the scatter radiation I_s spreads out into all spatial directions it contributes homogeneously to the total everywhere directly behind the specimen as long as the difference in material thickness Δw remains small. As a consequence, the „diffuse" nature of the scatter radiation results in an **offset intensity or basic brightness** in the radiographic image as shown in Fig.2.2.

The intensity difference ΔI that is of fundamental importance to enable flaw detection, since it is caused by the alterations of the (*penetrated*) wall thickness Δw, now appears simply as the difference between the intensities of the two primary beams I_{p1} und I_{p2}

$$\Delta I = I_{P1} - I_{P2}$$

When applying the law of attenuation here (s. a. Lecture V1),

$$I = I_0 \cdot e^{-\mu \cdot w}$$

then a relationship can be concluded between ΔI und Δw as well as with the X-ray attenuation coefficient which is energy dependent. This results in:

$$\Delta I \approx I_P \cdot \mu \cdot \Delta w$$

The relative radiation contrast K_S denotes the ratio of the intensity difference ΔI to the total intensity I_g.

$$K_S = \frac{\Delta I}{I_g} = \frac{\mu \cdot \Delta w}{1 + \frac{I_S}{I_P}}$$

More commonly said with regard to the difference between two attenuation coefficients (e.g. μ of the specimen and μ_f of the material flaw), the radiation contrast which is fundamental for the radiographic inspection is defined as:

$$K_S = \frac{(\mu - \mu_f) \cdot \Delta w}{1 + \frac{I_S}{I_P}}$$

In this context, the **scatter ratio k** is defined as: $k = \frac{I_S}{I_P}$

With I_s – scattered radiation

I_p – primary radiation.

The ratio $c_S = \frac{(\mu - \mu_f)}{1 + k}$ is known as specific contrast.

As a consequence, the radiation contrast is directly influenced by three factors:

- the difference between the attenuation coefficients $(\mu - \mu_f)$
- the extension of the flaw Δw along the radiation beam
- the scatter ratio k

The Formula $c_S = (\mu-\mu_f)/(1+k)$ is a useful approach for weld inspection if the flaws are small in depth and in lateral dimension in comparison to the constant material thickness in the base material. The scatter ration depends for steel dominantly on the material thickness. The scatter ratio for steel inspection is as about proportional to the penetrated wall thickness w if the X-ray voltage is selected close to the maximum energy of EN 444 and ISO 5579. For a step wedge exposure (see fig. 2.3) with the wedge directly in contact with the detector the scatter ratio is about $k \approx 0.06 \cdot w$ (the factor can vary between 0,06 to 0.1 if w is given in mm). The radiation intensity after the object is calculated by

$$I = I_o \cdot (1+k) \cdot e^{-\mu \cdot w}$$

That means, the image of the primary radiation is intensified by the scattered radiation. Therefore, (1-k) is also called build up factor (B_u). Finally the image of the primary radiation is overlaid with a second image, which is the blurred scatter image. This needs to be considered for casting inspection if objects have different large areas with different wall thickness. Fig 2.3 shows the schemes for the two different models for the specific contrast; called weld model (classic specific contrast) and casting model ("revised" specific contrast 2).

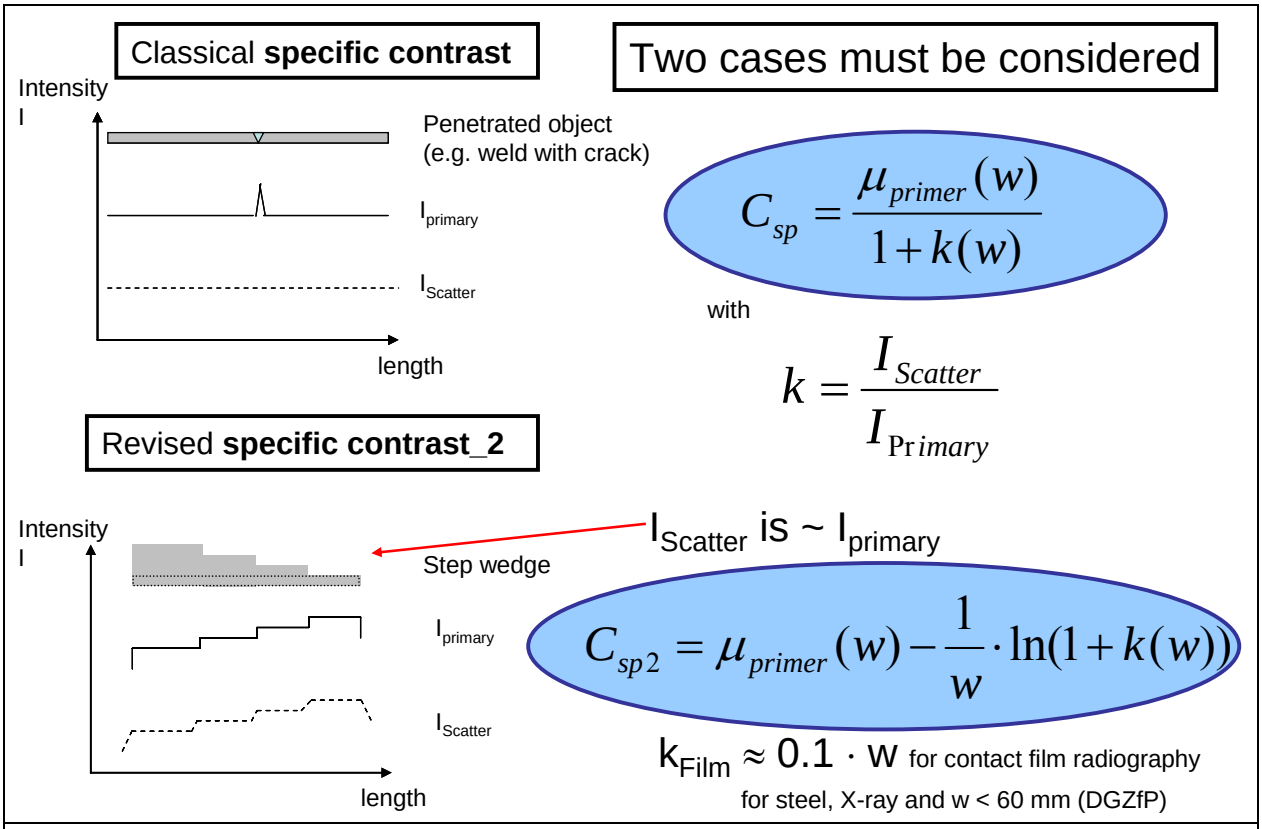

Fig. 2.3: Specific contrast for contact radiography at a given radiation energy. The classic specific contrast is a useful approach for inspection of plates with fine flaws (weld model). The revised specific contrast 2 is the more accurate formula for calculation of the specific contrast at object areas with different thickness as shown for a step wedge.

Considering the models of the specific contrast has the following consequences for the practical inspection:

- In case of an air bubbles or gaseous voids ($\mu_f \approx 0$) such as cavities etc. a high radiation contrast will be achieved which is only determined by the spatial depth of the flaw Δw, the material of the specimen and the scatter ratio. This also applies to laminar defects and cracks. **In this case, it appears of an advantage to the radioscopic inspection that the flaw can be brought into an optimal position along the radiation beam with respect to its orientation.**
- In case of metallic inclusions high radiation contrasts are yielded whenever there is a large difference in the attenuation coefficients between the material of the specimen and that of the inclusion. This is encountered rather frequently particularly in light metal alloy castings. It is evident also in this case that optimal radiation contrast can be achieved by varying the alignment with the radiation beam.
- Diminishing the scatter ratio will be achieved commonly by collimating the primary beam at the X-ray tube in the direction towards the radiographic area of interest. Such measures have always to be taken to achieve an optimal image quality or the best available radiation contrast, respectively.

2.3 Noise

In the Lecture 1, the so-called "particle model" has been used to illustrate the "quantum nature" of radiation. Said in a more imaginative way, the radiation could be treated as a stream of particles. This means that penetration of a material layer of constant thickness makes intensities surrounding a mean value with a certain deviation. As a consequence, radiographic inspection of a material layer with a homogeneous thickness always results in a mean value surrounded by deviating intensities (Fig. 2.4). The deviation around the mean value is called "noise".

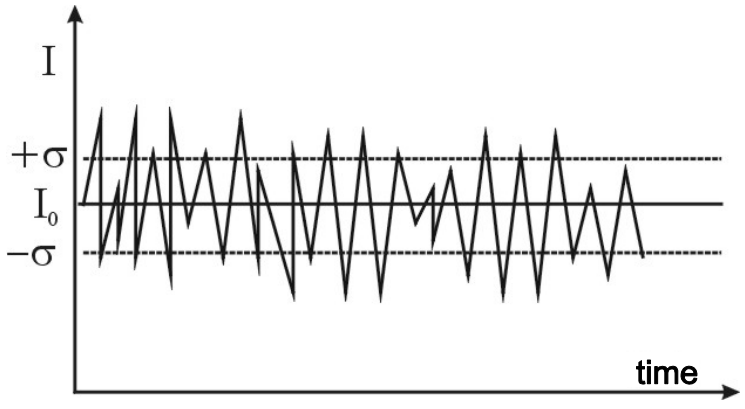

Fig. 2.4: Overlay of a mean intensity by noise

To quantify the effect of the noise on the actually wanted signal, the so-called **signal-to-noise-ratio (SNR)** is defined as the ratio of the mean intensity value I_0 (signal) to the

noise amplitudeσ. The **contrast-to-noise ratio (CNR)** is defined as the ratio of the mean intensity difference between the intensities in the flaw and the surrounding material in the radiograph to the noise amplitude σ. The principle is described in fig. 2.5 for the exposure of a steel plate with a notch.

It is common practice in defining **SNR** to relate the noise amplitude to the intensity mean:

- large SNR → the wanted signal, i.e. the mean intensity I_0 is large as compared to the noise → high image quality
- small SNR → the wanted signal, i.e. the mean intensity I_0 is small as compared to the noise → low image quality

The SNR depends on the intensity. The higher the intensity of the X-ray may become the larger (better) the SNR will be (see controlling the radiation intensity in L01).

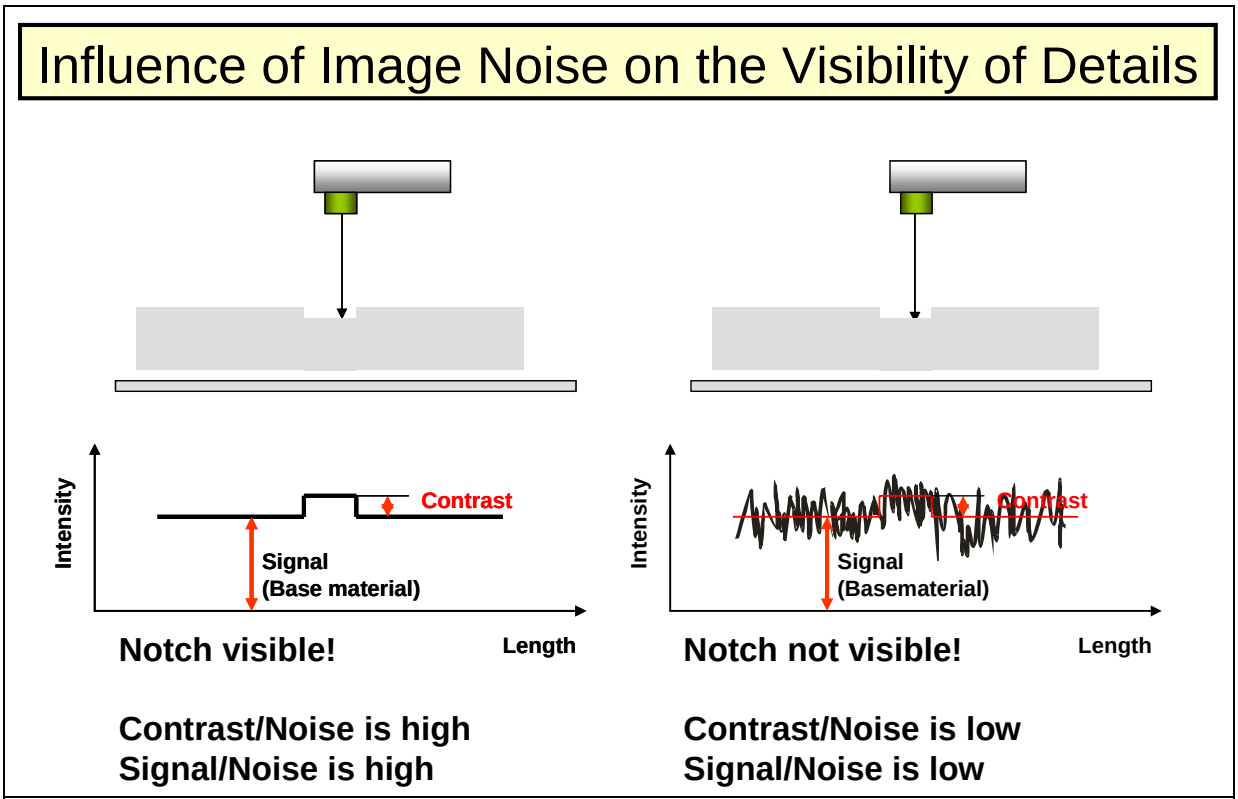

Fig. 2.5: Influence of the SNR and CNR at the visibility of a notch in a radiography of a steel plate.

In difference to film radiography the signal-to-noise ratio is of considerable importance in digital radiology since the generated radiological images can be viewed directly ("live") with suitable detectors. In case of the film radiography, the accumulation of a mean intensity value may be already achieved by the substantially longer exposure time of the films leading to large SNR values. Fine grained films have a higher SNR than coarse grained films. Therefore, the fine grained films provide higher contrast sensitivity at

longer exposure time. For purposes in digital radiology either sufficient high radiation intensities need to be applied or long enough image integration has to be achieved by means of the digital image processing facilities to guarantee a sufficient high SNR ratio and a minimum image quality in the digital image.

The visibility of fine flaws depends on the **CNR** per material thickness difference (small flaws). Fig. 2.6 illustrates the contributing parameters. The visibility of flaws of the same size depends on the product of SNR and μ_{eff}. This is an essential context for digital radiography.

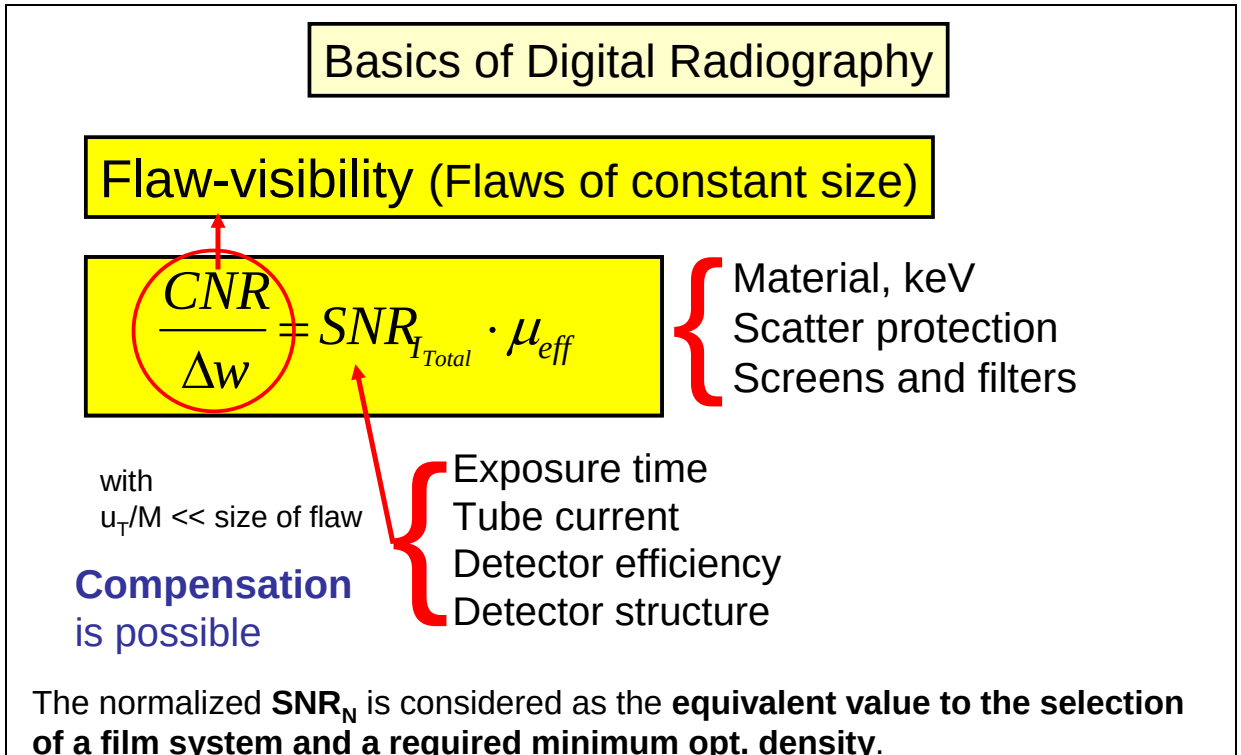

Fig. 2.6: The flaw visibility in a digital radiograph depends on the product of SNR and μ_{eff}. The SNR increases with the exposure dose. The operator controls the contrast sensitivity by the exposure time.

The visibility of flaws and IQIs depends also on its lateral dimension. The human operator can percept larger flaws at a lower CNR and therefore also at a lower SNR. Almost all contrast IQIs change its diameter with the thickness, this applies to wire IQIs (EN 462-1, ISO 19232-1 ASTM E 747) as well as to the hole diameters in plate and step hole IQIs (ASTM E 1025, EN 462-2, ISO 19232-2). The human IQI perception depends on the square root of the SNR. In ASTM E 747 and E 1742 and others the effective penetrameter sensitivity (EPS) is used to describe the contrast sensitivity of an operator in % of the wall thickness. A sensitivity of e.g. 2% means that a hole in a thin plate of 2% thickness of the material to inspect and a hole diameter of 2 times plate thickness is just visible in the radiograph.

$$EPS(\%) = \frac{\text{const.}}{\sqrt{SNR_{I_{Total}} \cdot \mu_{eff}}}$$

This formula applies if the image unsharpness is much smaller than the wire or hole diameter of the IQI to be visualized.

Since digital detectors have typically a significantly higher unsharpness than X-ray films (with leas screens), the visibility of flaws and IQIs is significantly influenced by the inherent detector unsharpness. If the detector unsharpness increases, the ratio of SNR to detector element size (or effective detector element size) increases at same exposure dose. If different detectors with different efficiency values shall be compared, it is required to normalize the achieved SNR to the detector size (diameter). As reference size a diaphragm of 100 µm diameter (aperture) is selected as required for film classification in EN 584-1, ASTM E 1815, ISO 11699-1. The normalised SNR_N is calculated as follows:

$$SNR_N = SNR \cdot 88{,}6\ \mu m / SR_b$$

SR_b is the basic spatial resolution, which is defined as exactly one half of the detector unsharpness.

The following major noise sources contribute to the noise in the image:

- Photon noise depending on exposure dose (e.g. mA · s or GBq · min)
- Structure noise of imaging plates (roughness of sensitive IP-layer and protection layer)
- Crystalline structure of material (e.g. nickel based steel, mottling)
- Surface roughness of test object.

2.4 Focal spot of X-ray tubes

The area of the anode material which is bombarded with electrons emitted from the cathode is defined as the so-called thermal focal spot. The size of this thermal focal spot depends on the focussing of the electron beam on the target and arrangement of the heating coil. Since the slow down of the electrons within the anode material results in only about 1% X-rays and some 99% heat, the anode material and the focussing of the electron beam have to meet certain requirements:

- **high melting point of the anode materials**

Tungsten (W, melting point ca. 3000°C) is the common choice. The mean temperature at the focal spot is around 800°C, but can be higher in peak loads.

- **Limited focussing of the electron beam**

Shaping the focal spot depends on the intensity requirements. High intensities need a large focal spot.

The optically effective focal spot is defined as the projection of the thermal focal spot onto the plane perpendicular to the centric core beam (fig.2.7). Its size is of principal importance for the image quality particularly in the field of radioscopy. The geometric size of the effective focal spot depends, in addition to that one of the thermal spot, on the **tilt angle** β of the anode. As in common X-ray tubes designed for resolving coarse structures the size of this angle is around 20°. The X-rays disperse into all spatial directions. The anodal angle and the radiation window of the tube limit the utilisable aperture

angle to typically 40°. The largest geometrical size of the focal spot ranges between 0.3 mm and maximally 1.5 mm, depending on the radioscopic applications, and may reach several millimetres for film and film replacement radiographic purposes. For top imaging quality requirements micro-focus tubes are employed with focal spot geometries of less than 0.1 mm. Micro and nano focus tubes are available for high magnifying radiography and radioscopy.

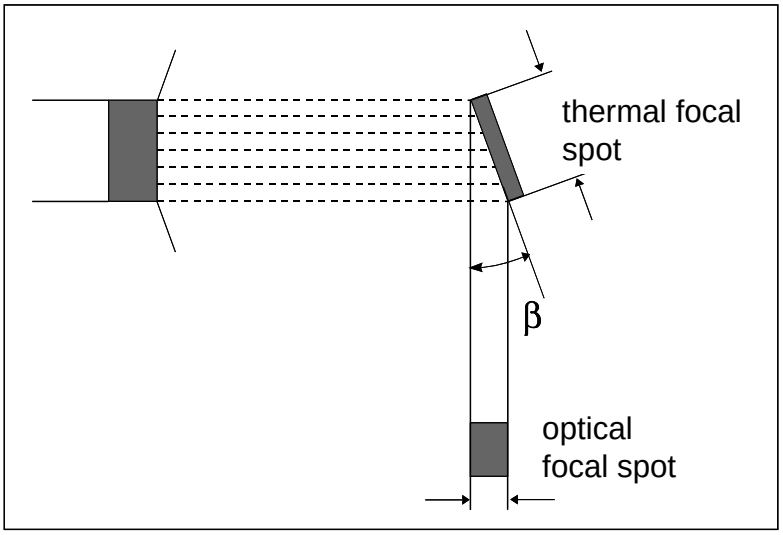

Fig. 2.7: Thermal and optically effective focal spot

2.4.1 Ideal imaging geometry

Due to the geometrical magnification of the shape of the specimens, the focal spot properties have a decisive impact on the image quality. For a better understanding of the focal spot effects, only the ideal imaging geometry will be considered to begin with (which may be not relevant for practical purposes).

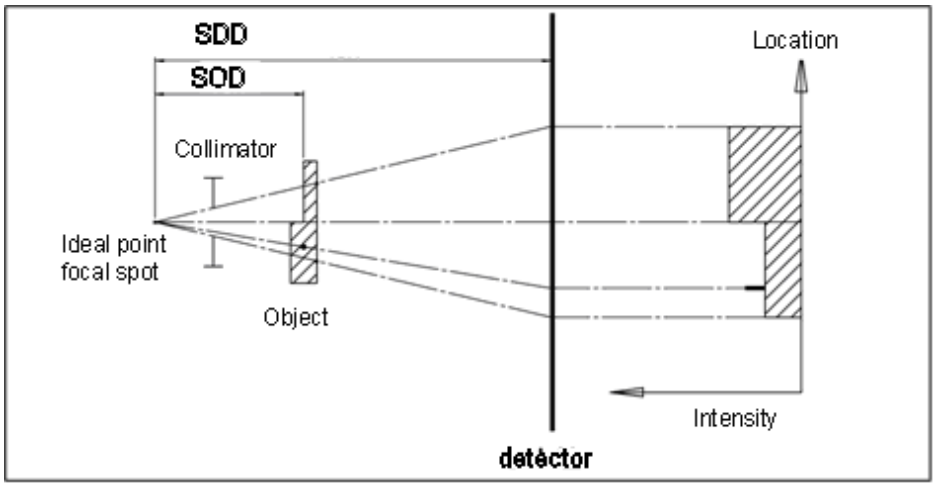

Fig. 2.8: Ideal imaging conditions

Fig.2.8 shows the **ideal imaging geometry** assuming a **point shaped X-ray focal spot.** The image of the specimen only depends on its position between the focal spot and the detector; a sharp edge within the specimen, exactly aligned with the beam direction, always appears as a distinct jump in the intensity distribution of the detector. By this way, any arbitrarily small detail of the specimen can be displayed, or visualised in the radioscopic image, theoretically just taking advantage of a larger **geometrical** or **direct magnification**. The **magnification factor M** is determined by the ratio of the **source-detector-distance (SDD)** over the **source-object-distance (SOD):**

Geometric magnification factor $$M = \frac{SDD}{SOD}$$

Some cases of magnifications will be considered more in detail:

- The magnification factor M will be the larger the closer the object will be moved towards the X-ray generator!
- The magnification factor assumes the value „2", if the object is located half way between the focal spot and the detector!
- The magnification factor M approaches the value „one", if the object is positioned directly on the detector (as it is the case in many radiographic imaging situations)!

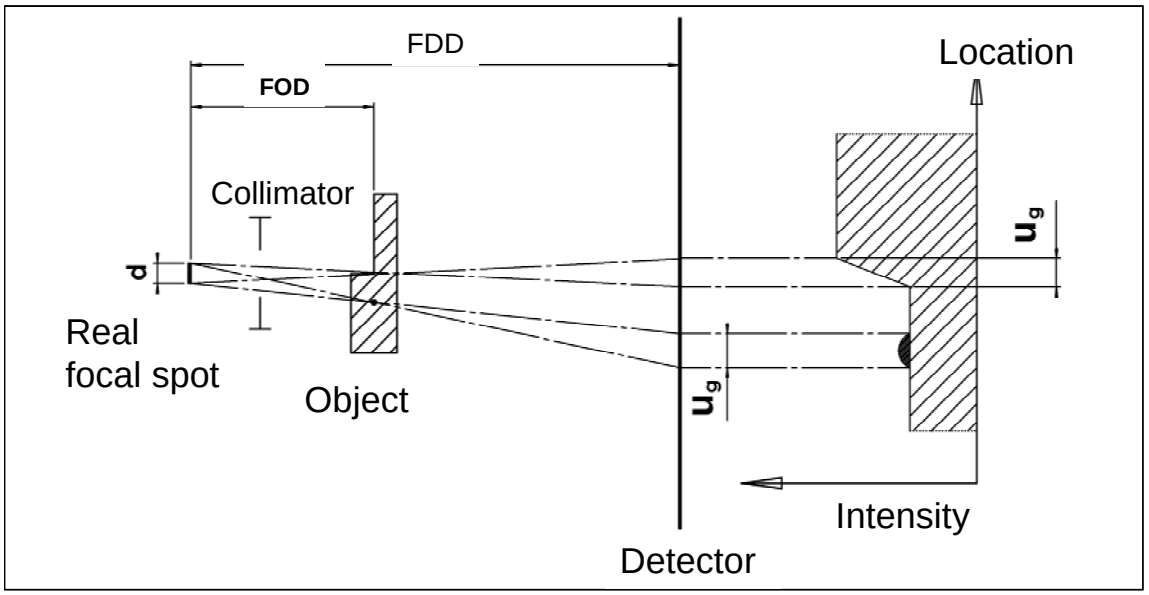

Fig.2.9: Realistic imaging situation

2.4.2 Real imaging geometry

Based on the spatial dimensions of the X-ray focal spot the realistic imaging conditions appear differently to ideal (Fig. 2.9). The focal spot causes a so-called **geometric un-**

sharpness u_g which depends on the **size of the focal spot d** and the **adjusted magnification M**.

The geometric unsharpness u_g results from the presentation in Fig. 2.9 together with the mathematical theorem on intersecting lines:

$$\frac{u_g}{d} = \frac{SDD - SOD}{SOD} \qquad \text{or} \qquad u_g = d \cdot (\frac{SDD}{SOD} - 1)$$

Inserting the geometrical magnification M turns it into the:

Geometric unsharpness $$u_g = d \cdot (M - 1)$$

Within the intensity profile, the appearance of the geometric unsharpness results in displaying an edge or a sharp contour as an unsharp pattern and not as a distinct intensity jump any more.

Whenever flaws within a specimen are of the same size of the geometric unsharpness the contrast will be diminished noticeably. In case of a small object detail, this means that the loss of contrast due to the **"smearing"** could make details **vanishing in the noise** so they finally become invisible in the radioscopic image.

The geometric unsharpness caused by the focal spot gives rise to **limited capability to detect flaws** of the whole **radioscopic inspection system** independently from the detector in use. This effect becomes even more pronounced

- with a larger focal spot d and
- with an enhanced geometric magnification M.

With a known detector unsharpness u_i and a given focal spot size d, the magnification M_{opt} best for an optimal perceptibility of a fine flaw (flaw size - fls) can be taken from the graphic *(Fig. 2.10)* or calculated by using the following formula:

$$M_{opt} = \frac{u_i}{d} + 1 \qquad \text{optimal magnification}$$

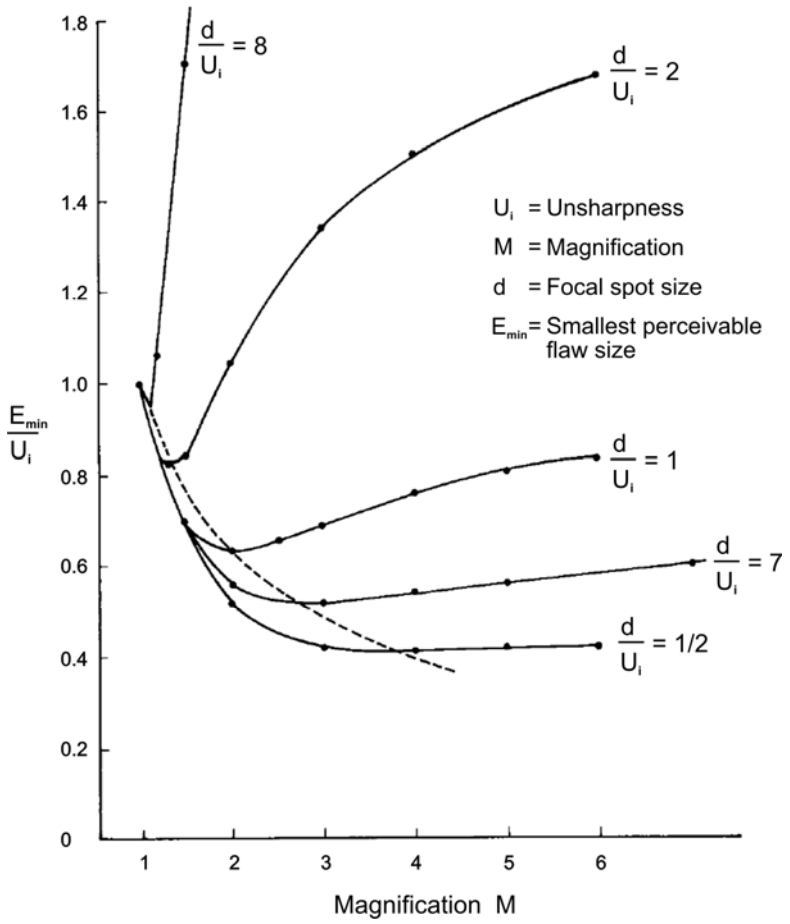

Fig. 2.10: Smallest perceivable flaw size fls related to the detector unsharpness u_i as a function of the magnification M

The geometric unsharpness is calculated as: $u_g = d \cdot (M - 1)$

The total unsharpness is approximately given by: $u_T \approx \sqrt[3]{u_g^{\,3} + u_i^{\,3}}$

The projected unsharpness (image unsharpness) denotes the ratio of the total unsharpness over the magnification:

$$u_P = \frac{u_{tot}}{M}$$

This determines the perceptibility of fine details.

Fig. 2.10 shows that the optimal magnification can be determined as a function of the detector unsharpness and the focal spot size!

Conclusion:

With an optimally adjusted magnification the smallest perceivable flaw E_{min} is smaller than the focal spot size or the detector unsharpness, respectively!

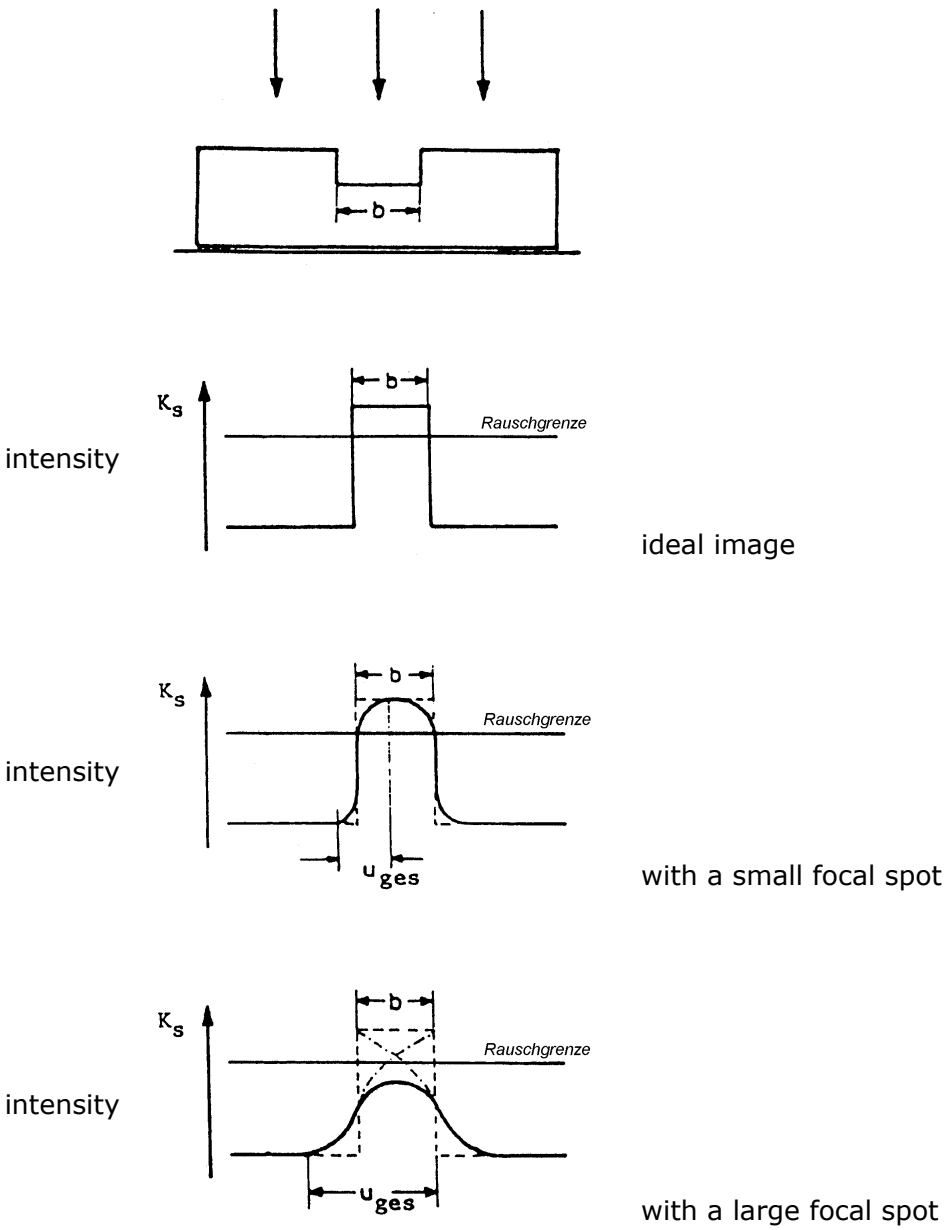

Fig. 2.11: Ideal and realistic images of a small object detail just above the noise limit.

In the field of **radioscopy** it is nearly always essential to operate with a geometric magnification of M > 1

- to keep a safety distance to the detector,
- to display a flaw inside a large specimen or
- to compensate a low spatial resolution of the detector as compared to the film.

As a consequence, raised demands have to be made on the size of the focal spot. They typically range from 0.2 to maximally 2 mm for radioscopic purposes (according to EN 12543) in the field of inspecting cast parts and weld seams.

The film radiography and film replacement techniques can, in part, make use of considerably larger focal spots since the magnification factor is close to M=1. It has to be taken into account that flaws located more towards the X-ray tube will be displayed with a magnification of M>1! This gave rise to predefine minimum distances in relation to the focal spot size as in the relevant NDT standards (EN 1435 / EN 444 or ISO 17636 / ISO 5579). Fig. 2.11 shows the effect of contrast reduction if the flaw size is smaller than the image unsharpness.

2.5 Law of the squared distances

At a given focal spot size and a given distance between the specimen and the detector the geometric unsharpness could be improved just mathematically by enlarging the distance between the generator and the detector. However, this does not make sense in most cases by several reasons. First of all, an enlargement of the SDD would entail a decreased geometric magnification and thus an impaired perceptibility of details. Another essential objection can be derived from the consideration of the intensity relations.

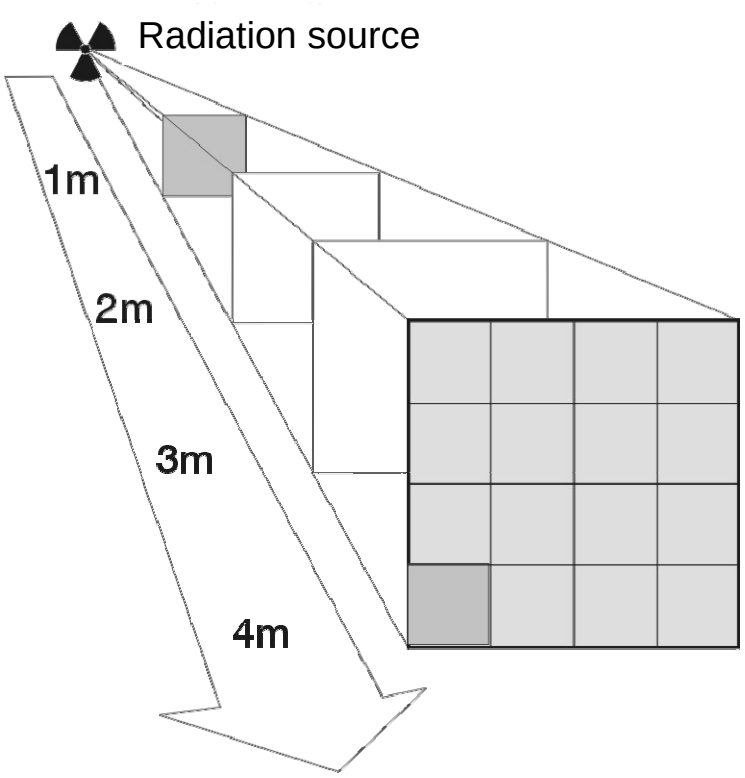

Abb.2.12: Law of the squared distances

The **law of squared distances** means that a doubling of the distance between the focal spot and the detector results in receiving only a quarter ($2^2=4$) of the intensity per surface element of the detector. Fig. 2.12 shows a quadruplicating of the distance with a decrease of the intensity by one sixteenth ($2^4=16$). To achieve a reasonable signal-to-noise ratio nevertheless, this drawback in radiological applications can be compensated by **a extraordinarily increased tube current** (which normally is limited).

The corresponding equivalent in the radioscopy is the **integration of radioscopic images** by employing the digital image processing. A N-fold integration usually means the addition of N images followed by a division by the number of images N; the *resulting* image does not become brighter but comes with less noise!

The dependency of the radiation intensity on the square of the distance in addition has an influence on the **maximally penetrable wall thickness**. Any data on wall thicknesses (e.g. ca. 25 mm steel at 160 kV and 640 W generator power in combination with an image intensifier) must be taken in conjunction with a certain SDD (e.g. 500 mm).

Conclusion:

Since always a compromise has to be found between the requested radiation intensity and the focal spot size when using X-ray generators, always a system has to be assembled specifically for the individual purpose (X-ray tube, detector, geometry) with a defined minimum perceptibility of flaws suitable for the intended application!

L 03 Standardisation I

Content

3.1 Introduction

Rules *(norms)* and standards have been introduced to harmonise modes of operations and procedures so that testing results become comparable independently from the operator. There are different standards specifically for operations, devices and for evaluations.

In the following, the international standards will be compared with each other first and then the essential European standards will be presented in detail for the tackled application.

3.2 Basic standard for radiography EN 444, ISO 5579

All film based standards in the world require:

- Minimum optical Density (e.g. > 2.0)
- Maximum film system class (e.g. ≤ ASTM class II)
- Maximum unsharpness (< 0.1 mm, SDD/SOD)
- Minimum IQI perception

It is now the task to introduce some of these standards as precondition for the requirement to digital radiography (DR). All DR techniques shall provide the same testing sensitivity as film radiography or even better to enable the present status of industrial quality assurance and provide the basis for manufacturer customer agreements for product acceptance.

3.2.1 Contrast

3.2.1.1 Radiation energy

Decreasing the energy of X-rays or the application of X-ray generators instead of the gamma radiation which is relatively easy to operate makes a remarkable gain in contrast in case of lower wall thicknesses so it could happen that a first image already rated as "satisfying" has to be regarded as "insufficient" when flaws have become visible in a repeated exposure. ISO 5579 is very similar to EN 444. Invalid film system class names are currently referenced in ISO 5579, since the ISO 11699-1 (film classification) was revised recently. Therefore, it will be made reference to EN 444 only in the following.

A hint in the DIN EN 444:

p.4, Figure 1: maximal accelerating potential ... up to 500 kV

p.4, Table 1: thickness range for gamma-radiography.

3.2.1.2 Minimum optical film density

Since the contrast increases with raising density in the film radiography, a minimum density is required in the standard in accordance with the related test category.

A hint in the DIN EN 444:

p.8, Table 4: optical density D ≥ 2.0 in the testing class A

optical density D ≥ 2.3 in the testing class B

3.2.1.3 Scattered radiation

The scattered radiation is a combination of ambient radiation together with that one generated inside the specimen.

The scattered radiation is being reduced by the use of collimators, diaphragms and shielding plates at the sides and at the rear.

In order to protect the film from ambient scattered radiation the back of the film is provided with a lead sheet. In addition, a tin foil can be inserted between the film cassette and the lead sheet for suppressing the scattered radiation that is generated in the lead shielding. Covering the back side only makes sense if walls or other scattering objects are located closer than about 2 to 3 metres behind the film.

A way to check if scattered radiation may have reached the film is to attach a lead character on the back-side of the film-sheet combination. If the character appears bright and clearly readable on the developed film then it has to be assumed that the contribution of the scatter ratio to the total density was too high.

The use of collimators as well as the application of back shielding can only incompletely be controlled based of the developed film. The masking of the primary beam at the tube window avoids unnecessary additional exposition of non-interesting areas of the specimen to X-rays or gamma radiation. Attaching a protection from scattered radiation behind the film is hardly enforceable in practical inspections. Nevertheless, the operator should always reduce the scattered radiation by applying a rear shielding.

The hint in DIN EN 444:

p.6, Figure 6.5: reduction of the scattered radiation.

3.2.2 Granularity / inherent unsharpness u_i

3.2.2.1 Choosing a fine-grained film system

Taking a fine-grained film system (low film system class number) entails a prolongation of the exposure time. However, the gain in image quality (better contrast sensitivity due to reduced granularity) allows a more detailed visualisation of flaws. It should be brought to mind that optimal results can only be achieved by a correct developing process.

A hint in the DIN EN 444:

p.5, Table 2: Film system class and choice of screens.

3.2.3 Unsharpness

3.2.3.1 Geometric unsharpness u_g

To keep the geometric unsharpness small, the following formula will be applied:

$$u_g = \frac{d \cdot b}{f}$$

this requires a small focal spot d and exceeding a minimum distance f_{min} (as higher the distance f as smaller u_g).

The proposition to choose a geometric unsharpness equal to the inherent unsharpness is hardly realisable in practical testing when inspecting thicker specimens or from a large distance b since a large distance f would require long exposure times. Complying with the minimum distances f_{min} that are stated in the DIN EN 444 can be regarded as sufficient. See also ASTM E 94.

This is based in EN 444 on the following relations:

Conforming to testing class A $f_{min} = 7{,}5 \cdot d \cdot b^{\frac{2}{3}}$

Conforming to testing class B $f_{min} = 15 \cdot d \cdot b^{\frac{2}{3}}$

Conforming to test class B requires a minimum distance twice as large as to that one of test class A.

In addition, there is a hint in DIN EN 444 that a better sharpness is required for materials being sensitive for cracks implying that the distance f needs to be enlarged.

The hint in DIN EN 444:

p.6, paragraph 6.6: distance between radiation source and test object

p.6, paragraph 6.6: (last paragraph) enlarging of f_{min} in case of crack sensitive materials

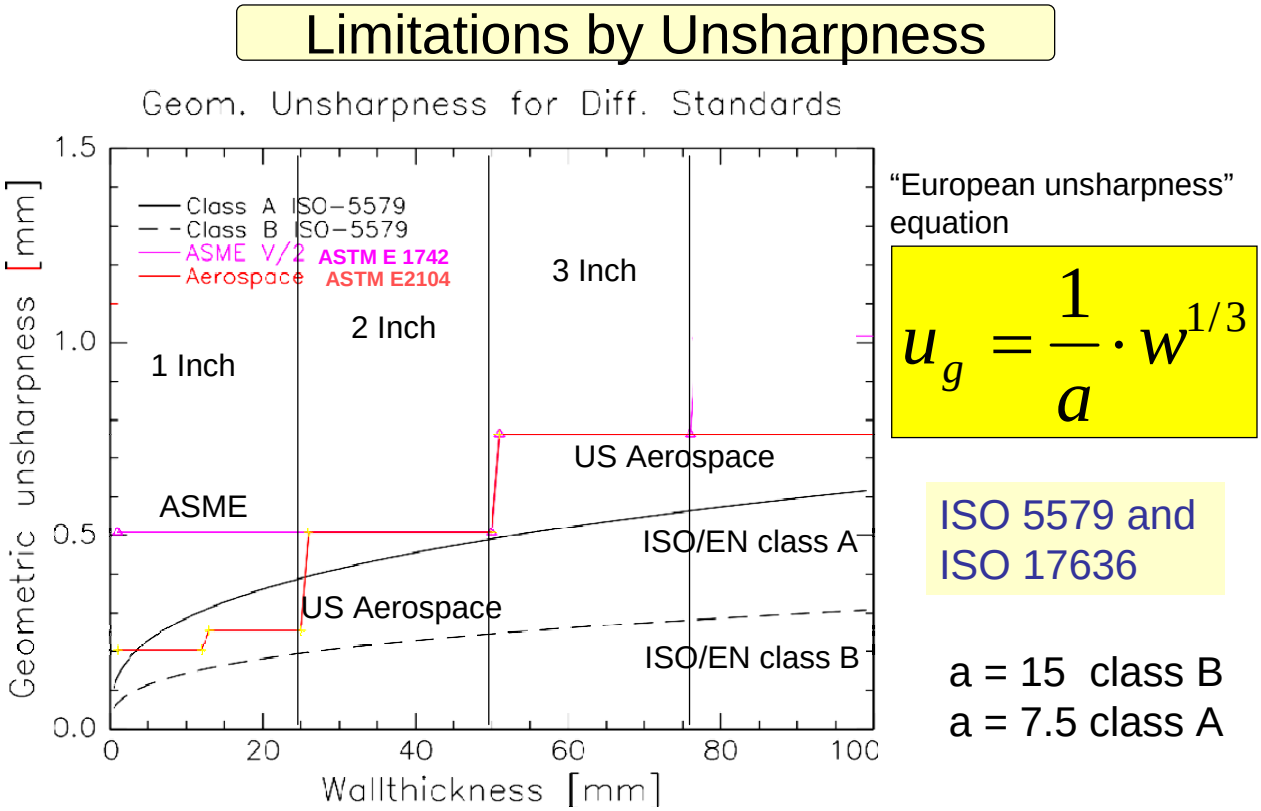

Fig. 3.01: Comparison of unsharpness requirements of international standards.

The requirements for the geometric unsharpness are in the different standards world wide very different, especially for the range of thickness below 50 mm (2 inches). Fig. 3.01 informs graphically about the differences of some selected international standards.

3.2.3.2 Film-screen-contact (inherent unsharpness u_i)

The influence of a good or bad contact between film and screen on the exposure and thus on the image quality has been investigated systematically not before the eighties. They have shown two possibilities of taking action. First, the inherent unsharpness increases remarkably whenever the screen is not in close contact with the film, and second, the loss in image quality becomes measurable even at a distance of a few tenth of a millimetre between the screen and the film as it can be demonstrated by the IQI value. The presumable free pathway of the electrons generated in the screen may well explain the increased unsharpness as well as the emerging light (intensifying fluorescent screen) and the influence by the energy. In this context, the necessity should be mentioned of using cassettes that can be evacuated or commercially available film-screen combinations that are already evacuated.

A hint in the DIN EN 444:

p.4, paragraph 6.3: film systems and intensifying screens

see also ASTM E 1742 tab. 1

3.3 Radiographic inspection of weld seams EN 1435, ISO 17636

The minimum requirements for testing weld seams with conventional films are regulated in the EN 1435 and the ISO 17636 as well as in ASTM E 1032. EN 1435 and ISO 636 are almost identical. For simplicity the following discussion will make reference to EN 1435 only. Herein, the specifications are largely taken from the EN 444 and specific testing situations are considered by amendments. Various arrangements for the inspection of flat and circular weld seams are presented in the EN 1435 illustrated as samples for easy orientation and writing records. This includes the description of minimum requirements associated with exposure setups that cannot be found in the EN 444 (e.g. elliptic exposures for external diameters < 100 mm). In order to provide the operator on site with rules and standards as concisely as possible, the number of projections required for a 100 % inspection and the rules for controlling the image quality employing the image quality indicators according to EN 462-1,-2 or ISO 19232-1,-2, have been transferred into the amendments of the standard.

3.4 Measurement of the focal spot size according to EN 12543

Fig. 3.02 provides an overview about the European standards for qualification of classical radiographic equipment. A definition of a dimensionless nominal size of the focal spot (nominal focal spot value) has been found in the previous DIN/IEC standard. IEC 60336 uses still the concept of measurement of nominal spot size and is used for medical characterisation of X-ray tubes. The result of a focal spot determination with the pin-hole method has been compared with reference values listed in that DIN/IEC and the corresponding nominal value has been taken for characterisation. The problem with this ap-

proach was that the value found by this way poorly described the real physical dimensions of the focal spot.

In the course of the European standardisation related to the properties of X-ray generators (CEN TC 138 WG1) the necessity has been taken into consideration to provide an exact determination of the focal spot size particularly for radioscopic purposes. By this reason, a reference measuring procedure has been defined in the part 1 of the draft standard that has to be referred to by all other methods. Moreover, a precise determination of the focal spot size based on the measured results is also defined within this draft which has to be used for further calculations of limits set in the standards.

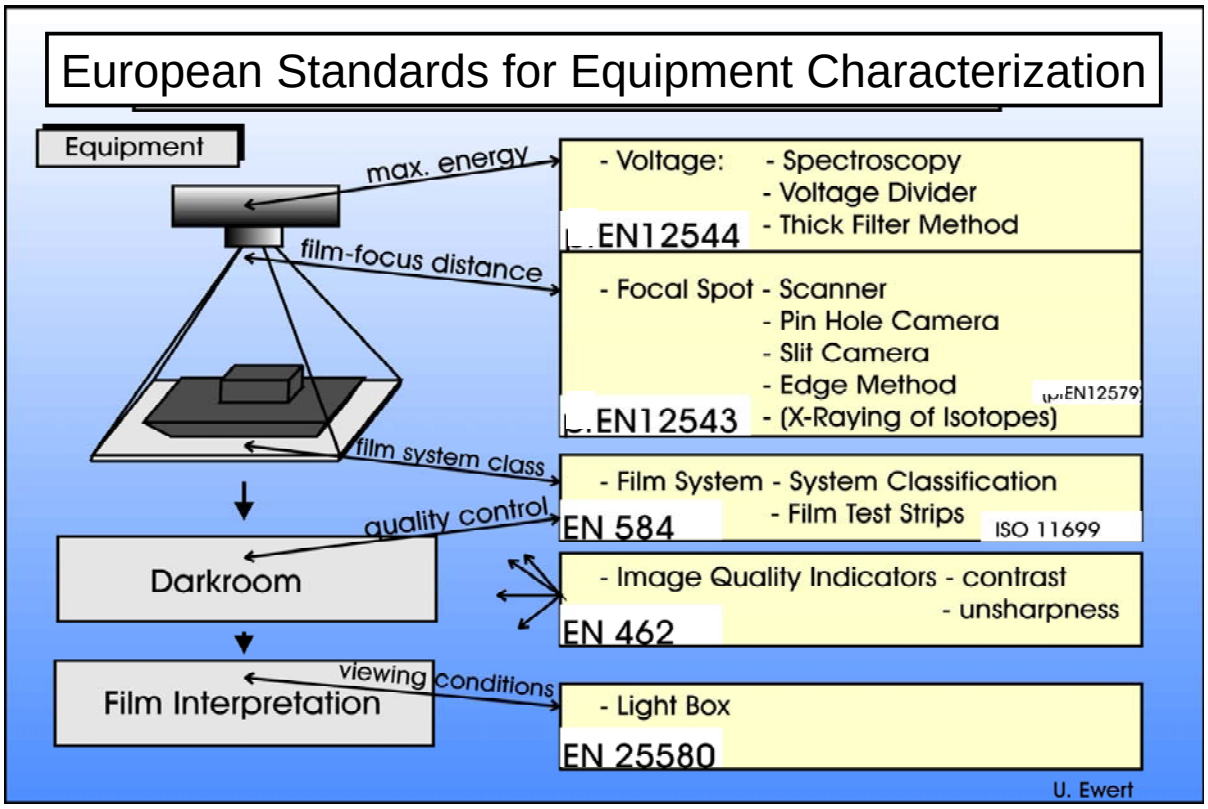

Fig. 3.02: European standards for qualification of radiographic equipment.

3.4.1 EN 12543 - part 1 „scanning method“

The so-called „scanning method“ is understood as a radiometric method to measure the focal spot based on scanning it point by point followed by computationally determining its size together with a three-dimensional graphic presentation.

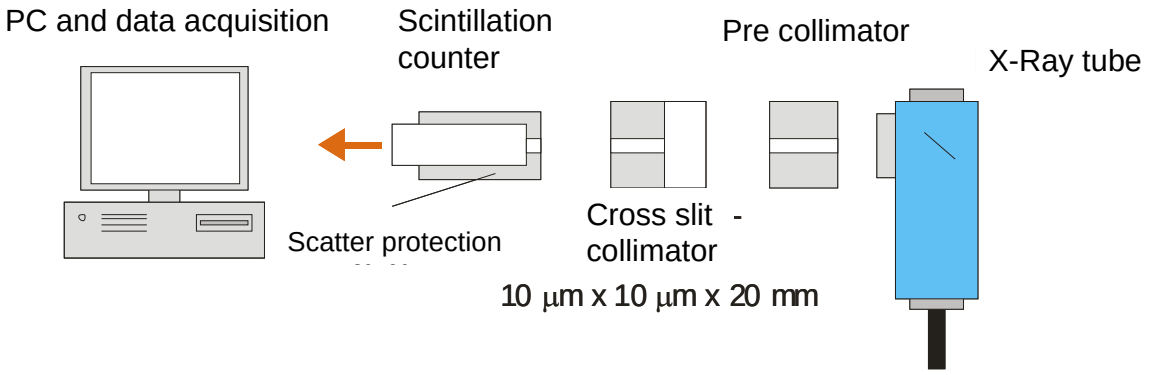

Fig. 3.1: Arrangement to measure radiometrically the focal spot

The coarsely collimated core beam of the X-ray tube is scanned with a cross-slit collimator which has an effective window of 10 µm x 10 µm in size and a scintillation counter (Fig. 3.1). The divergence of the measuring collimator amounts to 1:2000. Pre-collimator, collimator and scintillation counter are mounted on a high precision cross slide and are operated by two stepper motors. The output signal is collected by a computer equipped with a data acquisition module that must carefully be synchronised with the control of the cross slide stepper motors. Line scans are recorded with a given step width. This has to be defined in accordance to the desired spatial resolution. The software is capable to present the result graphically in a very understandable way and to determine precisely the size of the focal spot.

Figure 3.2 shows the result of a typical focal spot measurement with a pronounced saddle shaped structure. The maximum values of the spatially presented intensity distribution correspond with the highest intensities represented by the densities determined by the pin-hole camera method.

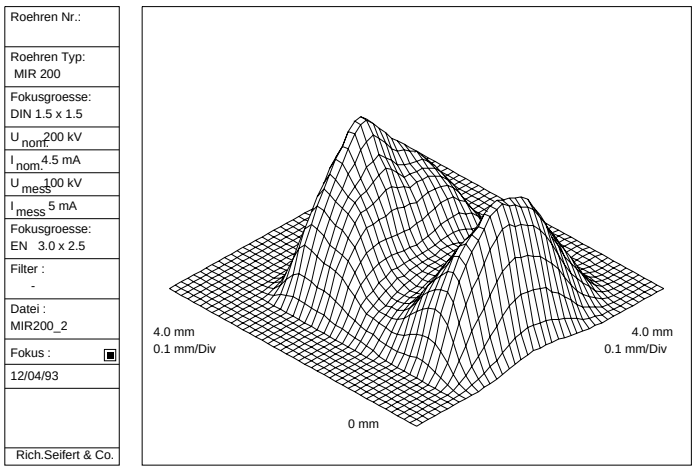

Fig. 3.2: Result of the scanning procedure

The density distribution of the focal spot can also be presented as a contour line diagram as shown in Figure 3.3. The contour lines ("isodose" presentation) present levels of equivalent doses between 10% and 90% of the maximal intensity.

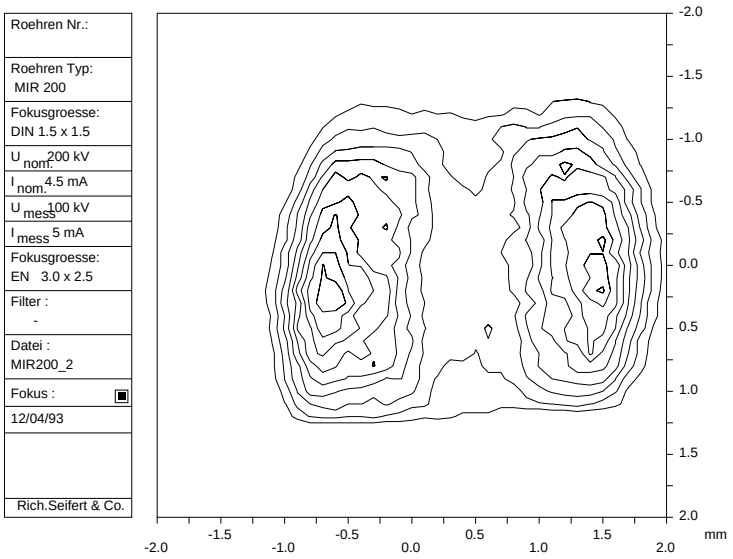

Fig. 3.3: Result of the scanning in a contour-line presentation

According to the new standards, the maximal extensions in length **and** width between the the 10% contour lines ("iso-doses") are defined as focal spot size. The **larger of these two distances** will be taken as the focal spot size value in the terms of radiography.

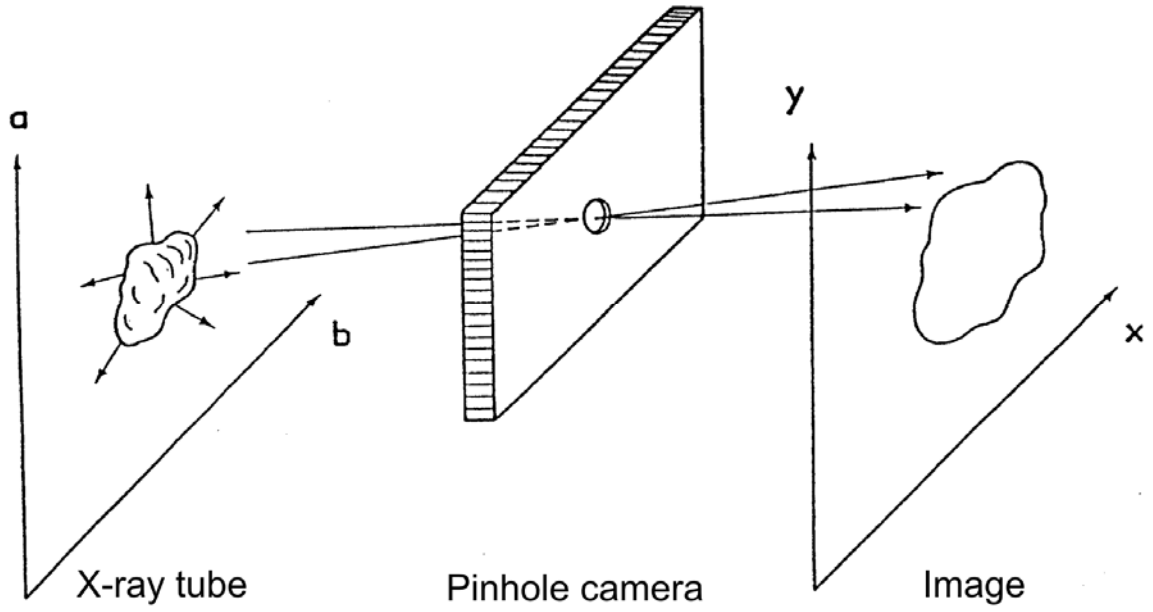

Fig. 3.4: Focal spot measurement with a diaphragm

3.4.2 EN 12543 – part 2 „pinhole method“

This part of the standard defines the imaging conditions and the setup of the diaphragm or pin-hole camera.

A diaphragm wrapped in lead (pinhole camera) is placed in front of the window of an X-ray tube for the focal spot size determination. The size of the diaphragm opening is 100 µm if the nominal focal spot size is larger than 1 mm, and 30 µm for mini-focus tubes with a nominal focal spot size less than 1 mm. An X-ray film or digital detector (CR or DDA) is taken for imaging the focal spot. Figure Fig. 3.5 shows the enlarged images of the big and the small focal spot of an X-ray tube. They are measured on the film directly, and the result is corrected in accordance to the magnification given by the pinhole camera setup.

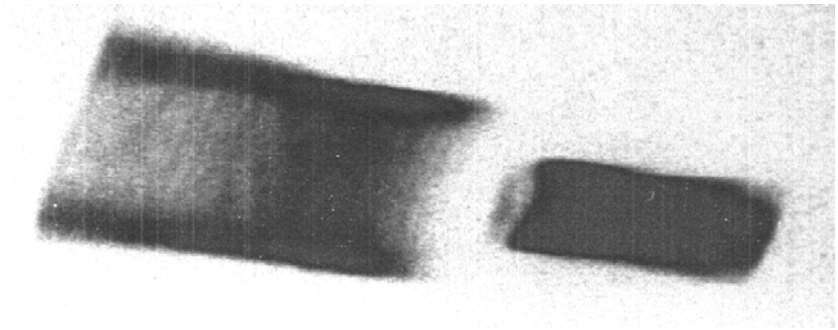

Fig. 3.5: Image taken of focal spots with a pinhole camera (film image)

Several problems have been encountered applying this measurement which may have a strong influence on the result:

- The diaphragm opening causes an unsharp image of the focal spot
- Sufficient precise mounting of the pinhole camera in the core beam

The biggest disadvantage of the method is given by the limited energy range within which this method can be applied. This amounts to maximally 200 kV (to be measured at 75% of maximum kV) when using film since the lead case will be penetrated at higher energies. Focal spots at higher kVs can be measured with digital detectors in combination with digital image processing. Therefore, this method can replace the time consuming scanning method when using a digital image detector.

The focal spot image displayed on an X-ray film shall be evaluated with a magnifying glass.

3.4.3 EN 12543 – part 3 „slit camera method“, part 4 „edge method“

These two procedures to determine the size of a focal spot are similar to the "pinhole camera method" to be found in part 2 of the EN 12543. When applying the slit camera and the edge method, the geometric unsharpness along a line caused by the focal spot is determined followed by the estimation of the focal spot size.

The slit camera method is employed in the production surveillance of X-ray generators. The edge method represents a simplified procedure for continuously monitoring the focal spot size on site. Both procedures are applied rather rarely so they cannot be accounted for as a standard procedure anymore.

3.4.4 EN 12543 – part 5 „focal spot size measurement of micro focus tubes“

This procedure has been introduced for the focal spot size determination of micro-focus X-ray tubes. Analogously to part 3 and part 4 of the standard, the geometric unsharpness caused by the focal spot is determined with the aid of a cross made of platinum wires or a lead sphere of 1 mm diameter followed by calculating the geometrical unsharpness according to

geometrical unsharpness $\mathbf{u_g = d \cdot (M - 1)}$

together with the **geometrical magnification factor** $M = \frac{SDD}{SOD}$ (see also L02).

To ensure the determination of the focal spot size as precisely as possible, the platinum cross or lead sphere is placed as close to the focal spot of the micro-focus tube as possible – i.e. with the highest possible magnification. The realisation of this part of the standard to determine the focal spot size turns out to be difficult in practice since the core beam of the tube has to be directed exactly in the centre of the platinum cross. Otherwise, different unsharpness values will be achieved at the shoulders of the wire-cross because of the divergence of the rays.

3.5 Energy limits of X-ray generators according to EN 12544

In order to comply with the energy limits given in EN 444 / EN 1435 and EN 13068 (s. a. L04) and consequently to achieve radiographs or radiographic images rich in contrast, it is essential to determine the energy limit of the X-ray generators precisely and comparably. This subject is accommodated in EN 12544 from part 1 to part 3. In these 3 parts of the standard, procedures are described to allow determining energy limits with various efforts. A reference procedure is defined also here – similarly to the EN 12543 – which other methods have to refer to.

3.5.1 EN 12544 – part 3 „spectrometry“

This elaborated procedure allows the precise determination of the limit energy by measuring the total spectrum of the X-ray bremsstrahlung (Fig. 3.6). This measurement is conducted with an energy-sensitive semi-conductor detector. This procedure represents the reference method of the EN 12544.

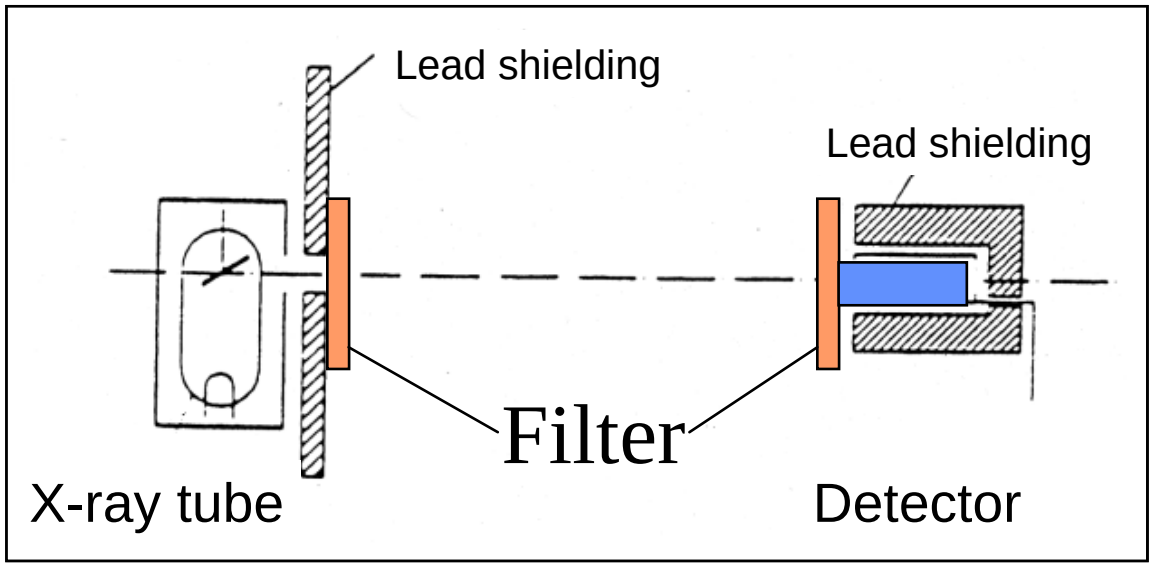

Fig. 3.6: Arrangement to determine the energy limit

The intensity is measured in dependence of the radiation energy and this is the base to determine the energy limit (Fig. 3.7).

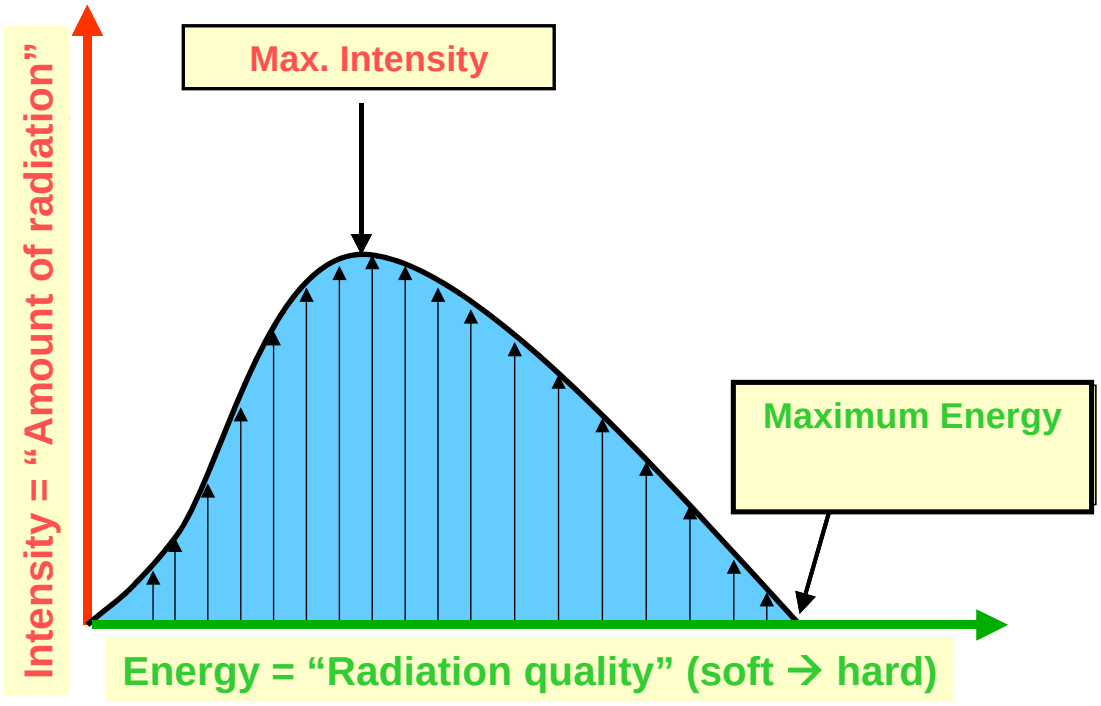

Fig. 3.7: Measured spectrum of the X-ray bremsstrahlung

In practice the energy limit is determined by fitting a regression line to the falling slope of the spectrum of the bremsstrahlung (Fig. 3.8). The intercept of this line with the energy axis (i.e. zero energy) is defined as the energy limit of the X-ray generator.

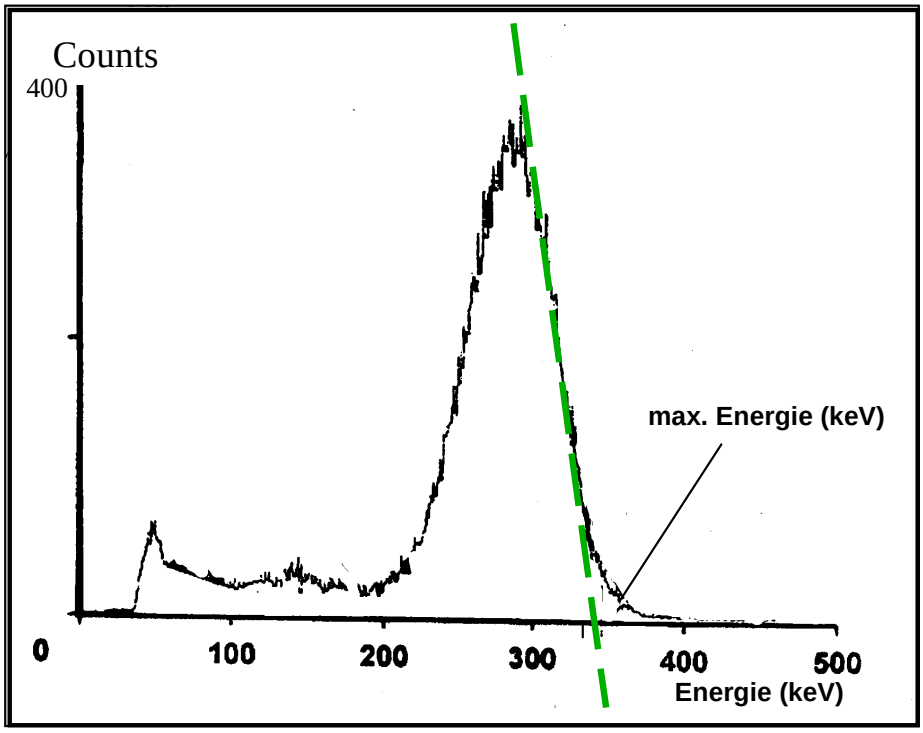

Fig. 3.8: Measured spectrum of the bremsstrahlung with the determined energy limit

3.5.2 EN 12544 – part 1 „voltage divider method“

Practically, the so-called voltage divider method according to part 1 of the standard is applied for the in process measurement and calibration of the energy limit during the production of X-ray tubes. For this purpose, the high voltage is reduced to a potential measurable with ordinary voltmeters with the aid of a voltage divider. The high voltage then will be recalculated from the low voltage reading and the splitting factor of the voltage divider.

3.5.3 EN 12544 – part 2 „filter method“

This method uses pre-filters to record a spectrum of the hardened bremsstrahlung to determine the energy limit. This approach is suitable for in-service inspections of X-ray generators*(see Fig. 3.8!).*

3.6 ASTM rules and standards (USA) as compared to the EN standards and ISO standards

Comparison of available standards in Europe and the USA (status 2006)

	radiography		radioscopy		imaging plates (CR)		computed tomography
	ASTM	**CEN**	**ASTM**	**CEN**	**ASTM**	**CEN**	**ASTM**
terms		EN 1330-3/ ISO 5576	E1316	EN 1330-3/ISO 5576			E1441 - Gloss.
equipment, radiation source	E1165	EN 12543, EN 12544, EN 12579					
equipment, detector	E1815	EN 584 / ISO 11699, EN 25580		EN 13068-1,2	E 2445 E 2446	EN 14784-1	
equipment, system			E1411				E1672, E1695
image quality indicators and their application	E2002, E142, E592, E747, E1025, E1936 - Digitization	EN 462 ISO 19232	E1647, E1817				
common rules	E94, E1742	EN 444/ ISO 5579, EN 14096	E1000	EN 13068-3	E2033, E2007	EN 14784-2	E1441, E1570, E1931

		radiography		radioscopy		imaging plates (CR)		computed tomography
		ASTM	**CEN**	**ASTM**	**CEN**	**ASTM**	**CEN**	**ASTM**
inspection								
	weld seam	E1032	EN 1435 / ISO 17636	E1416				
	reference catalogue weld seam	E390	ISO 5817 cat					
	cast part	E1030	EN 12681	E1734				E1814
	reference catalogue cast parts	E155, E1320, E280; E186, E446						
	steel pipe		EN 10246-10					
evaluation			EN 12517 Quality levels, ISO 17635 / EN 12062: General rules					
	weld seam		ISO EN 2517					
	cast part							
	electronics	E431						

Method	Standard organisation	qualification	stability tests	guide	general practice	Welding general	welding practice	welding evaluation	casting practice	casting catalogue	IQI	IQI-spatial resolution	IQI step wedge
film RT	ISO	11699-1	11699-2		5579	prISO17635	17636	10675			2504, 19232-1,2	2504,19232-5	
	CEN	584-1	584-2		444	12062	1435	12517	12681		462-1, 462-2	462-5	
	ASTM	1815		94	1742		1032		1030	155, …	747, 1025	2002	
Fluoroscope, Intensifier	ISO					prISO17635		10675					
	CEN	13068-1	13068-2	13068-1	13068-3	pr EN 12062		12517					
	ASTM	1411		1000	1255		1416		1734	2422	1647		
Film digitisation	ISO	14096-1	14096-1		14096-2								
	CEN	14096-1	14096-1		14096-2								
	ASTM	1936											
CR	ISO					prISO17635		10675			2504, 19232-1,2	2504,19232-5	
	CEN	14784-1	14784-1		14784-2	pr EN 12062		12517			462-1, 462-2	462-5	
	ASTM	2446	2445	2007	2033					2422	747, 1025	2002	
DDA	ISO										2504, 19232-1,2	2504,19232-5	
	CEN										462-1, 462-2	462-5	
	ASTM	2597								2422	747, 1025	2002	WK12340
Radiation source size	ISO				3999-1								
	CEN				12679								
	ASTM				1114								

L 04 Standards II

Content

4.1 Introduction

Image quality is a rather common term that expresses if a radiographic or radioscopic image complies or does not comply with the requirements to evaluate a defective component. It is common practice to describe how good or poor is an image quality by relating it to an **image quality value (IQI value)**. The IQI value is determined by employing so-called **image quality indicators (IQI)**.

Within the radiography, there exist specifications regulating the examination of weld seams precisely and in full length since a long time. Imaging conditions, upper limits for radiation energies and the essential perceivable image quality values are described in comprehensive rules and standards (EN 444, EN 1435). In the meantime, even film systems (properties of films **and** conditions of development) are described conclusively in the frame of the European standardisation (EN 584, 1-2).

The film-free X-ray inspection called radioscopy has given rise to develop the EN 13068 „Radioscopic Testing".

4.2 Image Quality Indicator (IQI) EN 462 part 1-5, ISO 19232 part 1-5

Important remark:
The only purpose of image quality indicators is to determine a measure for the image quality as contrast sensitivity and unsharpness, respectively, in the system.

BUT:
There is no direct relationship between the perceptibility of image quality indicators and that of genuine flaws!

4.2.1 Wire type IQI

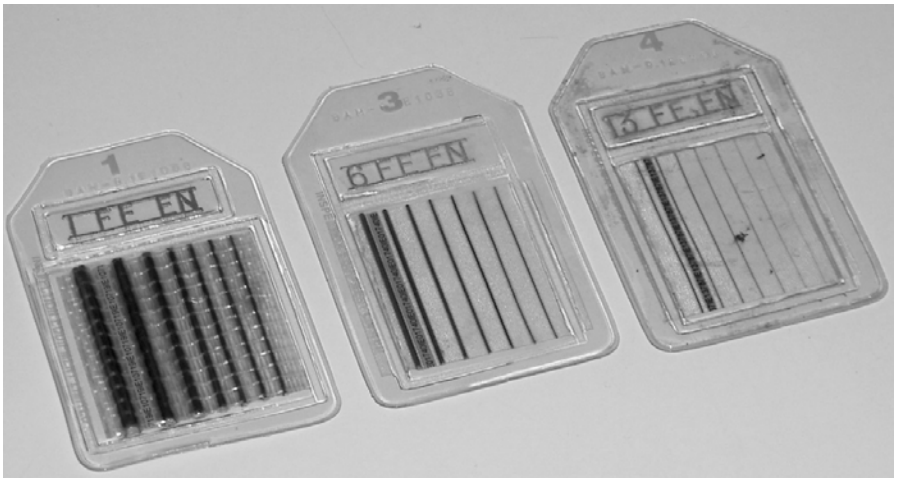

Fig. 4.1: Wire IQI according to EN 462-1 (and ISO 19232-1)

The question how good or poor is an X-ray image can be answered by referring to an **image quality value (IQI Value)**. To determine the IQI value, one way is to attach e.g. **wire IQIs according to EN 462-1 and ISO 19232-1** at the specimen so both will appear on the image. The diameter of the wires decreases in a geometric sequence from 3.2 mm (wire W1) down to 0.05 mm (wire W19). The number of the thinnest just perceivable wire represents the image quality value (e.g. if the wire W11 is just visible then the image has an image quality value of IQI value 11). The wire is supposed to be made out of the same material as the inspected specimen.

Rather frequently and particularly in radioscopic applications the image quality of an X-ray image is rated by a so-called **relative wire perceptibility** or **testing sensitivity**. This means that the ratio of the wire diameter over the penetrated wall thickness is calculated and expressed in percent. A wire diameter of 1mm on a 100mm thick wall thus results in a wire perceptibility of 1%.

Figure 4.2 shows the wire perceptibility plotted as a function of the penetrated wall thickness of aluminium (low percentage means high wire perceptibility) for image intensifiers with and without digital image processing as well as for digital detector arrays with various read-out times.

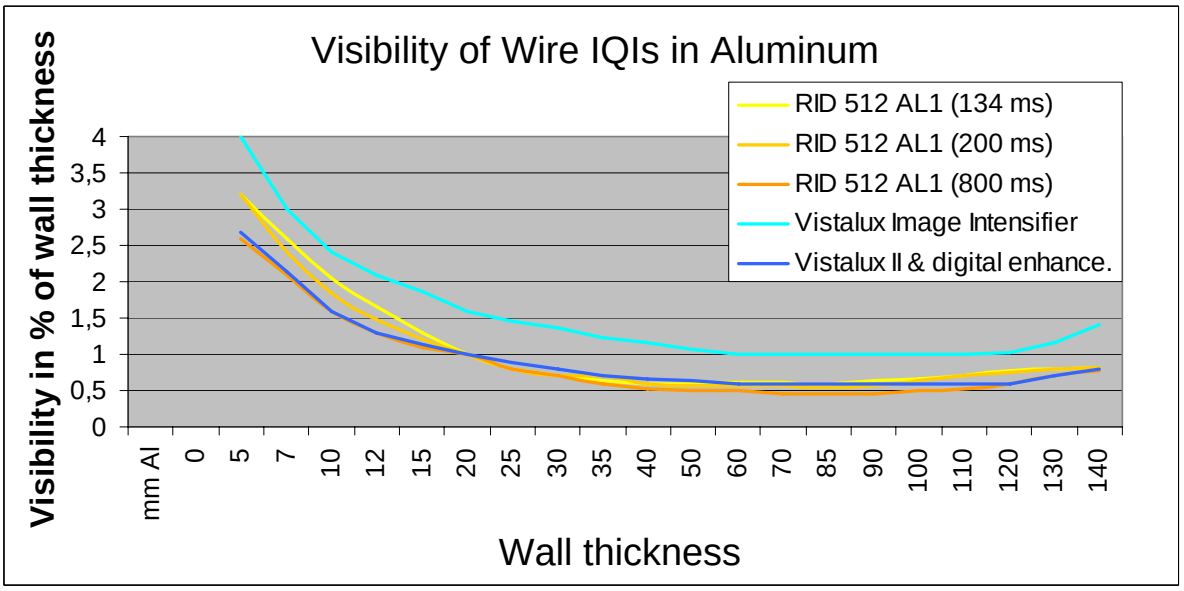

Fig. 4.2: Wire perceptibility on aluminium

Figure 4.3 shows the wire perceptibility in percent plotted as a function of penetrated steel wall thicknesses for image intensifiers with and without digital image processing as well as a further detector in real time and in the high resolution mode.

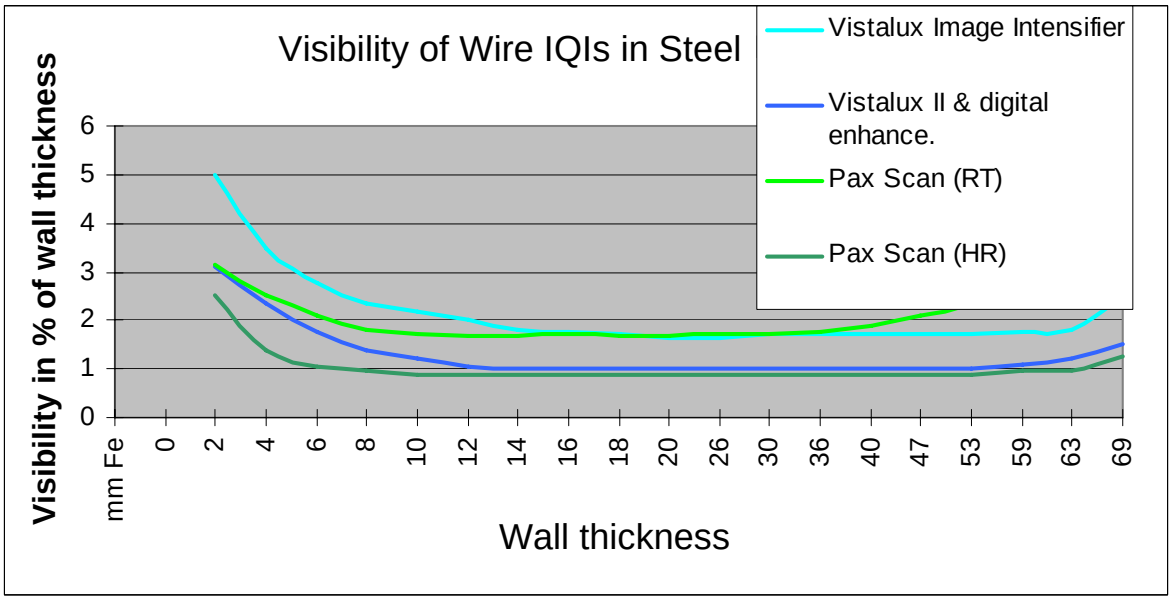

Fig. 4.3: Wire perceptibility for steel

Remark: It should be pointed out that the wire perceptibility depends both on the contrast resolution and the spatial resolution of the imaging system. As a consequence, the wire type IQI is inappropriate if the spatial resolution is less than the wire diameter. In this case a plaque type with step/hole combination has to be preferred.

4.2.2 Plate hole and step hole type IQI

The system of this image quality indicator according to EN 462-2 is based on a row of 18 steps with holes of different thicknesses and corresponding diameters. The image quality value results from the number of the least just visible hole. The handling is analogous to that one of the wire IQIs.

Fig. 4.4: Step hole penetrameter according to EN 462-2 (and ISO 19232-2)

4.2.3 Contrast sensitivity IQI

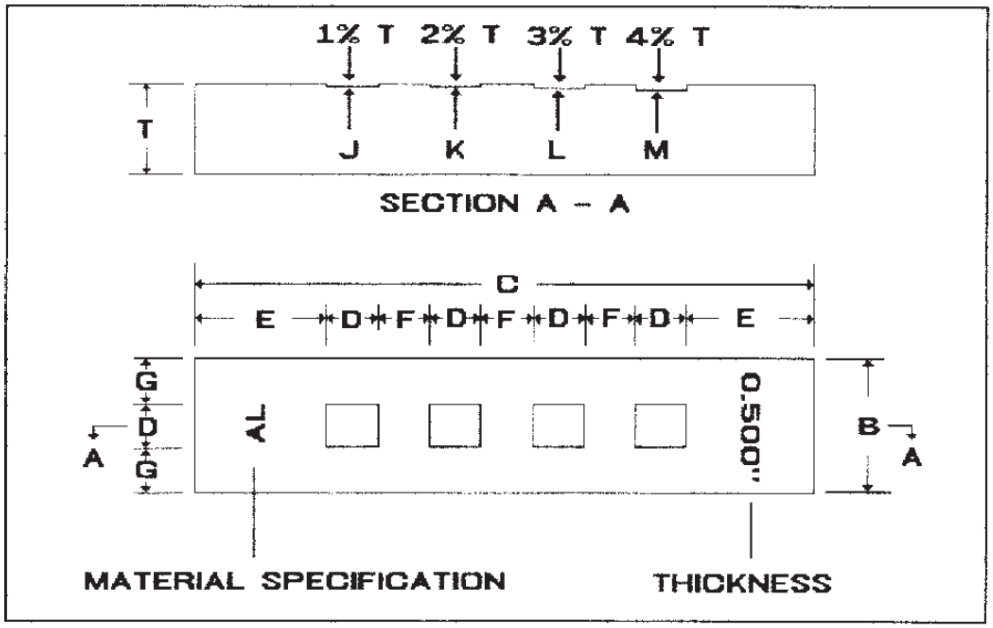

Fig. 4.5: Contrast sensitivity gage in accordance with ASTM E 1647

Fig. 4.5 represents the scheme of the ASTM E 1647 IQI which is designed for measurement of the contrast sensitivity of unsharp radioscopic systems. It is also included in the phantom IQI of EN 14784-1 and ASTM E 2445 for long term stability check in computed radiography. It consists of a metal plate of given thickness and material. Four milled squares are in the material with 1, 2, 3, 4 % depth of the IQI block. The operator can evaluate the contrast sensitivity by visual evaluation of the number of visible squares.

4.2.4 Platinum duplex wire IQI (EN 462-5, ASTM E 2002, ISO 19232-5)

The duplex wire IQI system consists of a series of 13 elements. Each element consists of a pair of wires with a circular diameter. The distance between the wires of each pair is equivalent to their diameters. The elements are cast into a rigid block of plastics as shown in the figure.

The pair of wires which just cannot be resolved as such in the image is regarded as the indication of the **limit of what can be distinguished**. Then the **image unsharpness** is given by the double of the wire diameter. This image quality indicator suits for determination of the unsharpness only and therefore should be applied only in conjunction with wire IQIs or the plaque systems for sensitivity measurement.

In order to determine the total unsharpness of a system the duplex IQI is fixed onto the specimen on the side toward the radiation source. When determining the internal unsharpness of the detector the duplex IQI is positioned directly on the detector surface.

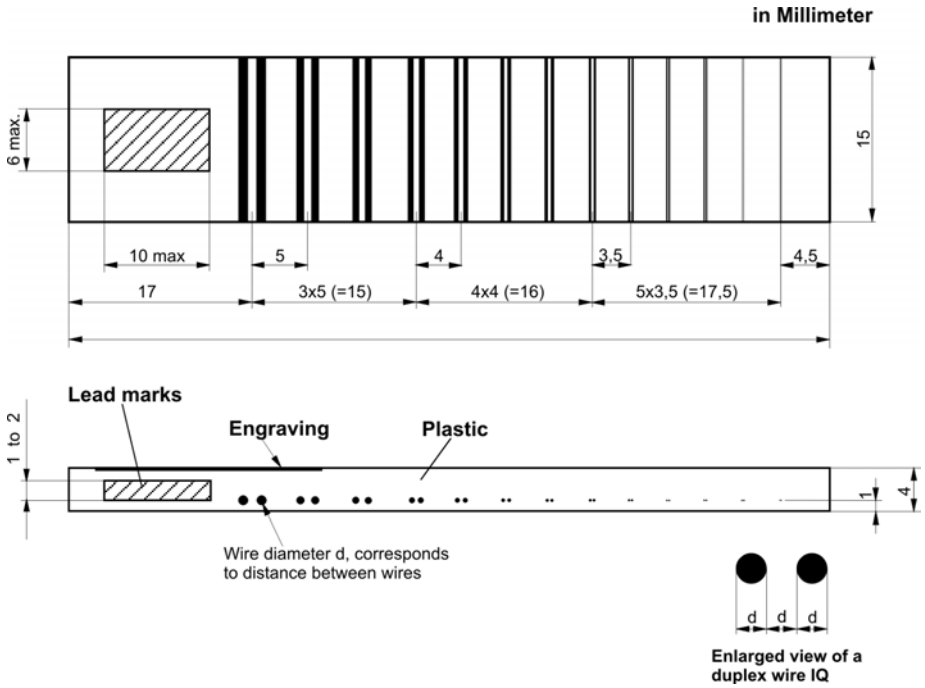

Fig. 4.6 Duplex wire IQI for determination of unsharpness and basic spatial resolution in accordance with EN 462-5, ASTM E 2002, ISO 19232-5.

4.3 Standardisation of digital industrial radiology

CEN EN 13068	**Radioscopy**
CEN EN 14096, ISO 14096	**Film Digitisation**
CEN EN 14784 **CR**	Part 1: Classification of Systems, Part 2: General principles
ASTM **CR**	Classification (E 2446), Long term stability (E2445), Guide (E 2007), Practice (E 2033)
ASME (BPVC, S.XI) **CR** Code Case 2476 integrated	Radiography (CR) with Phosphor Imaging Plates
ASTM E 2597-07 **DDA**	DDA: Standard practice for manufacturer characterisation
ASTM E 07 **DDA**	DDA: Guide, user qualification and practice under development
ASTM E 2422	First **digital catalogue**, light alloy casting

Table 4.0: Overview of selected standards on radioscopy and digital radiology

Table 4.0 gives an overview about the standards using digital radiology. All CR standards were published in 2005. There exist more standards on Radioscopy in ASTM, but they are currently (2009) under revision for considering digital technologies. More DDA standards

are under development as e.g. a standard practice a standard guide and a user qualification standard. The practice will be published probably in 2010.

4.3.1 Standardisation of radioscopic systems

In the past years, tremendous efforts have been undertaken to develop a standard for radioscopy. Ample work has been accomplished particularly in the International Institute of Welding (IIW). The sub-commission in charge V A working party „Radioscopic Systems for Weld Inspection" has agreed upon the elaboration of a standard in three parts. This group also formed the nucleus of the CEN (European Committee of standardisation) standardisation group „Radioscopy" (TC 138 WG1) since 1993. The European Standard for "Radioscopic Testing" was published in the years 1999 and 2002:

Part I: Quantitative measurement of imaging properties

Part II: Check of long term stability of imaging devices

Part III: General principles of radioscopic testing of metallic materials by X- and gamma rays

4.3.1.1 EN 13068-1: Quantitative measurement of imaging properties

In the first part of this standard basic requirements are defined for the measuring instruments used and the procedures to determine the relevant parameters of the imaging system.

From the radioscopic image, the following parameters are determined (among others):

Inherent unsharpness of the imaging system (U_i): By placing an edge made of a strong absorbing material in the centre of the detector the contour and the width of its "smoothed" illustration will be determined. The unsharpness will be determined between the 10% und 90% of the amplitude of the output signal.

Contrast ratio: The contrast ratio is determined by the ratio of the amplitude of the unimpeded free radiation over the attenuated one having passed the specimen. This test object consists of a lead disk placed centrally on the detector covering 10% of the total detector area.

Contrast sensitivity: For this purpose, a test object is employed whose thinnest in the image resolvable material layer indicates the contrast sensitivity. A plaque type IQI with steps and holes according to EN 462-2 may serve this purpose.

Material thickness range: The penetrable range of wall thicknesses is determined by means of a step-wedge with a step to step difference of 1 mm each. This step-wedge is placed directly on the entrance window of the detector. The tube parameters current and voltage have to be kept constant during the whole measurement.

Linearity: In order to determine the linearity of the imaging system the differential and integral distortion ($V_{d,i}$) and the homogeneity ($H_{d,i}$) are determined at various locations on the detector surface.

The purpose of the determined parameters is to enable a comparison of radioscopic systems with regard to their instrumental properties. In part three of the standards, the determined parameters then are associated with different classes of requisition so that in each case minimum application requirements can be specified for the applicable radioscopic system.

4.3.1.2 EN 13068-2: Check of long term stability of imaging devices

In general, the performance of a radioscopic system should always be checked by means of a test object with genuine flaws. Standardised image quality indicators have to be employed for the monitoring of essential image quality parameter such as spatial resolution and unsharpness, respectively, as well as the contrast sensitivity to ensure compatibility in addition.

Spatial resolution respectively unsharpness: The total resolution of the system should be determined by means of a duplex wire type IQI according to EN 462-5. The spatial resolution determined with the aid of this IQI is directly converted into the system unsharpness.

Contrast sensitivity: For the sake of monitoring, a step-wedge should be chosen of the same material as of the specimen. In addition, IQIs according to EN 462-1 or EN 462-2 (wire type ore plaque type IQIs) can also be taken to ensure comparability to the film radiography.

Homogeneity ($H_{d,i}$): Image quality indicators according to EN 462-1 oder EN 462-2 can also be taken to monitor the homogeneity. Typical inhomogeneities may arise e.g. from burning-in plaques at the entrance window of the image converter.

4.3.1.3 EN 13068-3: General principles of radioscopic testing of metallic materials by X- and gamma rays

The part 3 of the radioscopy standard defines the minimum requirements concerning a radioscopic system requested for various applications (weld seams, cast components etc.).

In the first step, minimum requirements are given for the parameters defined in part 1 such as internal unsharpness, distortion and homogeneity and subsequently categorised into three different system classes SC1, SC2, SC3 (Table 1).

Parameter	System class		
	SC 1	SC 2	SC 3
U_i (100 kV)	0,35 mm	0,5 mm	0,5 mm
$V_{d,i}$	5%	10%	20%
$H_{d,i}$	20%	30%	30%

Table 4.1: Definition of device system classes

The performance of the whole system consisting of the imaging system and the geometric imaging conditions as well as its suitability for certain inspection tasks is verified by the requested perceptibility of certain image quality indicators. The specimens of choice are the wire type IQI (EN 462-1) and the duplex wire type IQI (EN 462-5). The application of both image quality indicators facilitates independently from each other a determination of the geometric and the contrast resolution. Analogously to the film radiography a **basic testing class SA** and an **enhanced testing class SB** are defined for each application (Table 4.2).

The **testing class SA** is supposed to satisfy the requirement of real time serial testing that can be achieved with a standard mini-focus X-ray tube (< 1 mm focal spot size).

The **testing class SB** covers the requirements beyond serial testing that require an X-ray tube with a focal spot size of < 0.5 mm.

SA			**SB**		
System class SC2			System class SC1		
thickness [mm]	IQI wire No.	IQI duplex wire	thickness [mm]	IQI wire No.	IQI duplex wire
1,2-2,0	W17	11D	-1,5	W19	13D
2,0-3,5	W16	10D	1,5-2,5	W18	12D
3,5-5,0	W15	9D	2,5-4,0	W17	11D
5,0-7,0	W14	8D	4,0-6,0	W16	10D
7,0-10	W13	7D	6,0-8,0	W15	9D
10-15	W12	7D	8,0-12	W14	9D
15-25	W11	7D	12-20	W13	9D
25-32	W10	7D	20-30	W12	9D
32-40	W9	7D	30-35	W11	9D
40-55	W8	7D	35-45	W10	9D
55-85	W7	6D	45-65	W9	9D

Table 4.2: Performance of the system for metallic materials testing classes SA and SB except aluminium and light alloys

The testing classes SA und SB of the table 4.2 are based on the EN 462-3.

Because of the totally different requirements in serial inspections of aluminium cast components, different claims are defined for the perceptibility of the image quality indicators (Table 4.3). Herein, the testing class SA complies with the specific requirements for serial inspections.

Testing class	SA		SB	
System class	SC3		SC2	
IQI	Wire No.	Duplex wire	Wire No.	Duplex wire
Wall thickness mm				
5	W12	8D	W16	10D
10	W11	7D	W14	9D
15	W10	7D	W13	9D
25	W9	7D	W12	9D
35	W8	7D	W10	9D
45	W7	7D	W9	9D
55	W6	7D	W9	9D
70	W5	7D	W8	9D
85	W5	7D	W8	9D
100	W5	7D	W8	9D
120	W4	7D	W7	9D

Table 4.3: Performance of the systems for aluminium and light alloys

Remark: In case of testing of light alloys, the **testing class SA** complies with the requirements for the real time serial inspection that are covered by the standard mini-focus X-ray tubes (0.1 ... 1 mm according to EN 12543).

The **testing class SB** complies with the requirements beyond the serial inspections for higher geometric resolution and contrast sensitivity (according to EN 462-3).

To achieve a good capability to detect flaws, the tube voltage (according to EN 12544-1 and -3) should be chosen as low as possible. Depending on the thickness, the maximal values of the tube voltage are listed in the Table 4.4 for aluminium, light alloys and for steel.

Steel		Aluminium and light alloys	
thickness in mm	maximal tube voltage kV	thickness in mm	maximal tube voltage kV
1,2 to 2,0	90	≥ 5	45

2,0 to 3,5	100	≥ 10	50
3,5 to 5,0	110	≥ 15	55
5,0 to 7,0	120	≥ 25	65
7,0 to 10	135	≥ 35	75
10 to 15	160	≥ 45	85
15 to 25	210	≥ 55	95
25 to 32	265	≥ 70	110
32 to 40	315	≥ 85	125
40 to 55	390	≥ 100	140
55 to 85	450	≥ 120	160

Table 4.4: Maximal tube voltage

Remark considering the application: If it becomes necessary to deviate from the maximal tube voltage by instrumental reasons, the image quality requests according to the Tables 4.2 and 4.3 have to be ensured by other measures.

4.3.2 Standards for film digitisation

The two ISO/European and one ASTM standards are entitled:

- ISO/EN 14096-1: Non-destructive testing - Qualification of radiographic film digitisation systems - Part 1: Definitions, quantitative measurements of image quality parameters, standard reference film and qualitative control
- ISO/EN 14096-2: Non-destructive testing - Qualification of radiographic film digitisation systems - Part 2: Minimum requirements
- ASTM E 1936: Standard reference radiograph for evaluating the performance of radiographic digitization systems.

On the basis of the image quality of film radiography and the state of the art of digitising systems, three quality classes were defined; DA, DB and DS. The user may select the testing class based on the needs of the problem. The three testing classes are defined as follows:

DS - The enhanced technique, which performs the digitisation with an insignificant reduction of signal-to-noise-ratio and spatial resolution, Application field : digital archiving of films (digital storage);

DB - The enhanced technique, which permits some reduction of image quality, Application field : digital analysis of films, films have to be archived;

DA - The basic technique, which permits some reduction of image quality and further reduced spatial resolution, Application field : digital analysis of films, films have to be archived;

Due to the required international harmonisation, the standard reference film is taken over from ASTM E 1936 for test and evaluation as well as for long term stability tests of digitisation systems.

Beside the requirements for maximum density and SNR, X-ray films require a very high spatial resolution. The limiting structure for very low X-ray energies is the grain size of the photo active silver based crystals, which is below 1 µm. This is particularly important for micro radiography. General NDT applications require X-ray energies between 50 and 12000 keV. In medicine, the application range is normally below 150 keV only. Due to this large energy range for NDT radiography, it was decided to reduce the requirements for spatial resolution to the unsharpness, which is caused by interaction of high energy X-rays with the lead screen film system. Measured functions provide unsharpness values between 30 and 800 µm, depending on the energy and the screen film system. Based on these measurements and the experience from the evaluation of different film digitisation systems the following tables define the minimum requirements (see ISO EN 14096, part 2: minimum requirements).

Table 1: Minimum density range of the radiographic digitisation system with a minimum density contrast sensitivity

parameter	**Class DS**	**Class DB**	**Class DA**
density range* D_R [OD]	0.5 – 4.5	0.5 – 4.0	0.5 – 3.5
digital resolution [bit]	≥ 12	≥ 10	≥ 10
density contrast sensitivity ΔD_{CS} [OD] within D_R	≤0.02	≤0.02	≤0.02

Table 4.5: Minimum requirements for the different testing classes of digitisation systems.

Table 4.5 defines the minimum working range of the radiographic film digitisation system. In this working range, the digitizer shall provide an optical density contrast sensitivity ΔDcs which is ΔDcs ≤ 0.02. The minimum digital resolution is given for all devices converting the digital value proportional to the optical density. If the digital value is converted proportional to the light intensity, the digital resolution must be increased by at least 2 additional bits.

In fig. 4.6 an image of the reference radiograph, developed by EPRI Charlotte (U.S.A.), is shown for the evaluation of the digitisation systems. This radiograph is used by the ASME, ASTM and CEN standards. With the help of this test film all the basic parameters of a film digitisation system can be evaluated. The reference radiograph contains five types of targets for the parameter evaluation of the digitisation system. The targets are located within a background density of D=3:

- Spatial resolution targets, consisting of converging line pairs in a range of 1 ... 20 lp/mm,

- Density contrast sensitivity targets, block targets of 1 cm² with ΔD =0.05 at D=2 and ΔD=0.1 at a darker background of D=3.5,
- Stepped density targets, a series of 13 1cm² blocks with density between D=0.5 and 4.5 : 4.5, 4.02, 4.0, 3.5, 3.02, 3.0, 2.5, 2.02, 2.0, 1.5, 1.02, 1.0 and 0.5,
- Linearity targets, these targets provide a geometrical measurement scale in horizontal and vertical direction of 25.4 mm units,
- Parallel line pair target, a parallel line pair gage with a resolution between 0.5 and 20 lp/mm.

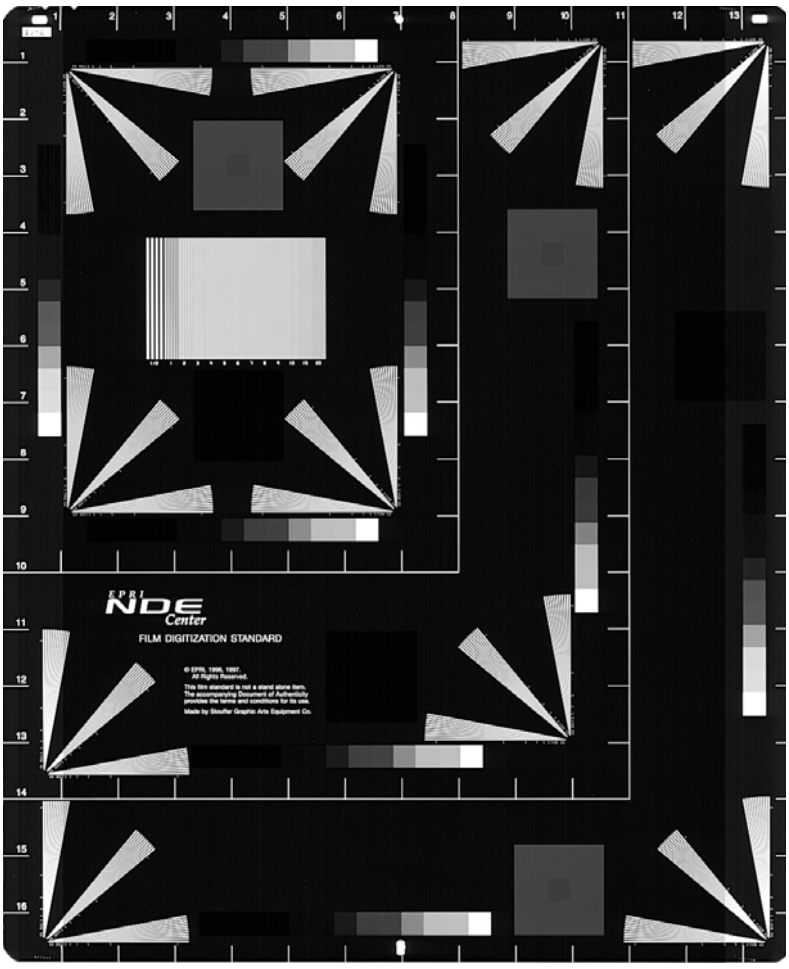

Fig. 4.6: EPRI test film of ASTM 1936

The size of the reference radiograph (14”x17”) may be cut to custom fit a particular digitisation system (down to 8”x10”) and still contain all of the necessary targets.

4.3.3 Standards for Computed Radiography

The complete set of CR standards has been published at CEN and ASTM in 2005; see tab. 4.0. Since then, there is an ongoing discussion on new revisions. The classification and qualification standards ASTM E 2445, E 2446 and EN 14784-1 are similar. The practice at ASTM and CEN shows differences as it does in film radiography.

4.3.3.1 Comparison of image quality for film and digital detection systems

X-ray film has been used since more than 100 years. The most important innovations are the development of double coated films, intensifying screens and vacuum packed flexible cassettes. The film quality has been improved over the years, but with different goals in medicine and NDT. Medical film systems are optimised for low patient dose and medium, but sufficient image quality. Special film systems yield also high image quality (e.g. mammography films). NDT films yield an excellent image quality but need 10 to 100 times higher dose for sufficient exposure. Any radiation damage of "NDT objects" is usually negligible (risks may exist for electronic products).

Therefore, NDT films are exposed to an optical density (o.D.) between 2 and 4 (EN 444, ISO 5579), which is the double of the typical value for medical applications. Critical NDT objects, as e.g. castings and weldments, require the visualisation of fine cracks and fine wall thickness changes. This leads to higher demands for the image contrast and sharpness. The basic requirements are described in the several film based standards standards.

4.3.3.2 Normalized signal-to-noise ratio and basic spatial resolution

SNR of film systems

The signal-to-noise ratios SNR of industrial film systems are indirectly given in EN 584-1, E 1815, K 7627 and ISO 11699-1 (see table 4.6). Film systems are characterised by the gradient G_D (at D = 2 and D = 4 above fog and base) and the granularity σ_D at D = 2 above fog and base. The most important parameter for the perception of fine flaws is the gradient over granularity ratio $G2/\sigma_D$, which can be used to calculate the equivalent SNR. The reader of the standards should know that the gradient over granularity ratio is the up rounded quotient of gradient and granularity limits in the standard tables. Tab. 4.6 shows the different $G2/\sigma_D$ and SNR values and system classes. Even though the different nations and committees decided to use different names and ranges for the film system classes, they, nevertheless, did agree on the same limit values.

The conversion of $G2/\sigma_D$ into SNR values is based on the assumption that both systems, NDT film system and digital detector systems, provide signals (opt. Density, photo stimulated luminescence, or digital grey values), which are approximately proportional to the exposure dose. Non-linear signals have to be linearised before SNR and spatial resolution can be determined. The "W"-film systems of Tab. 4.6 and film fluorescence screen systems are excluded, because they have a relatively non-linear characteristic. **The equivalent SNR to a given film system class (table 4.6) can be calculated for linear systems from $G2/\sigma_D$ measured at optical density of 2 above fog and base**, by:

$$SNR = (G2/\sigma_D) / \ln(10) \qquad (1)$$

Tab. 4.6: Overview about the film system classes in different standards and the corresponding SNR values and G2/σ_D values.

System class				Minimum gradient-noise ratio at	Signal to Noise Ratio
World ISO 11699-1	Europe CEN 584-1	USA ASTM E1815-01	Japan K7627-97	D=2 above D_0	D=2 above D_0
				G_2/σ_D	SNR
C1	C1	Special		300	130
C2	C2	I	T1	270	117
C3	C3			180	78
C4	C4		T2	150	65
C5	C5	II	T3	120	52
C6	C6	III	T4	100	43
		W-A	W-A	135	
		W-B	W-B	110	
		W-C	W-C	80	

The SNR values in table 4.6 are the equivalent values to the optical density of 2 of digitized radiographs of a given film system. For film replacement the operator shall expose a digital detector until he will achieve in the digital image the equivalent SNR value of the selected film system.

The SNR is the equivalent value for the optical density and the film system class in radiography!

Measurement of SNR

The measurement of the SNR can be performed with an exposure setup as seen in fig 4.7. The most accurate method (image 1 in fig. 4.7) is based on a step exposure. An imaging plate is shifted step by step behind a collimating diaphragm. The exposure time will be changed from step to step. The radiation quality is the same for all exposed steps, only the exposure time is different. The same equipment is used by film manufacturers to produce step tablets for film classification and/or for production of step tablets for densitometer calibration. The simpler method (image 2 in fig. 4.7) for users requires the exposure of a step wedge. The operator shall determine the grey value and the SNR in each step of the digital radiograph. All grey values (for CR only) and/or SNR values higher than selected from table 4.6 for a given system class are acceptable for exposures with sufficient image quality.

The normalised SNR_N

The SNR values of films are measured (see EN 584-1, ISO 11699-1, ASTM E 1815) with a circular diaphragm of 100 µm diameter after exposure to a diffuse optical density of 2 above fog and base. The effective diaphragm area (aperture) has to be converted into a square shaped area for comparison of scanned films to digital images of digital detectors. The equivalent square of a picture element (pixel) amounts to 88.6 x 88.6 µm², which corresponds to a resolution of 287 dpi. The pixel size/area is important, because the measured SNR per exposure dose depends on the detector area. The SNR increases proportionally to the square root of the pixel area under same exposure conditions (same radiation quality and exposure time).

Therefore, the standards for CR and DDA radiology require minimum normalised SNR_N limits for classification (CEN EN 14784-1, ASTM E 2446). The measured SNR_{meas} has to be corrected to calculate the SNR_N as follows:

$$SNR_N = SNR_{meas} \cdot \frac{88.6\mu m}{SR_b} \qquad (2)$$

The basic spatial resolution (SR_b)

SR_b is the basic spatial resolution (in µm), which corresponds to the effective pixel size (square root of pixel area). SRb can be measured at different kind and manner. In the standard committees it was recommended to use the duplex wire method due to its simplicity (EN 462-5, ISO 19232-5, E 2002). The duplex wire IQI standards describe a procedure to measure a total unsharpness value (u_T) in µm which is equivalent to the spatial resolution. The basic spatial resolution SR_b is calculated by:

$$SR_b = u_T / 2 \qquad (3)$$

SR_b corresponds usually to the pixel size (pixel limited unsharpness) of direct converting systems (e.g. α-Se flat panel or CdTe- flat panel). It is greater than the pixel size for CR and DDA's with fluorescent converter screens.

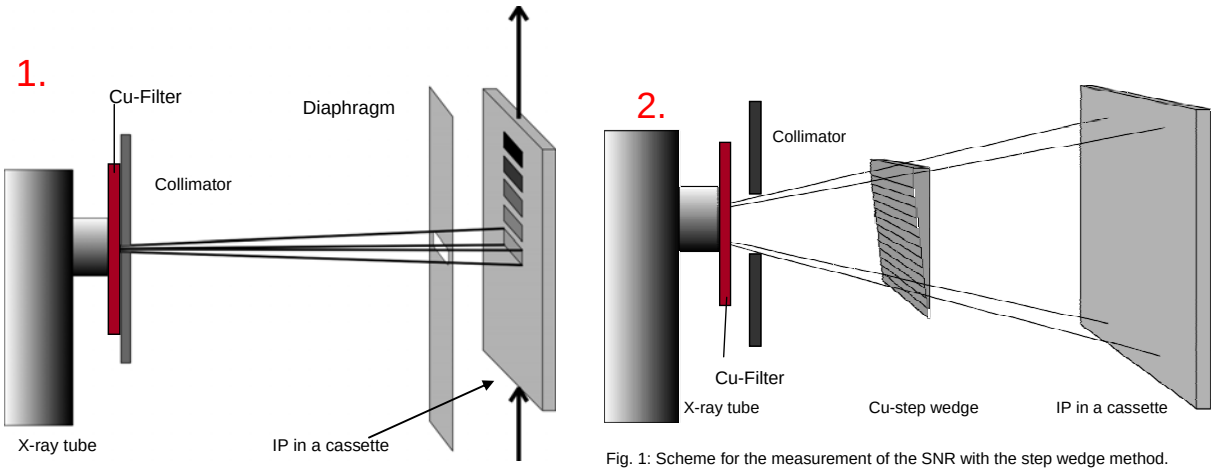

Fig. 1: Scheme for the measurement of the SNR with the step wedge method.

Fig. 4.7: Test exposure configuration for CR measurements of SNR dependence on dose and grey values.

The measurement of SR_b can be done in different ways. The standards EN 14784, ASTM E 2445, E 2446, E 2597 refer to the duplex wire IQI for the measurement. Fig. 4.8 shows a typical exposure of the duplex wire. EN 462-5, ISO 19232-5 and ASTM 2002 describe the IQI and the procedure for unsharpness measurement. The first "unsharp" wire pair shall be determined and the corresponding unsharpness can be read from the table 1 of the standard. SR_b is just ½ of the unsharpness. For better accuracy it is recommended to use image processing software with a profile function. The profile of the IQI image is shown in fig. 4.8. The first wire pair with a dip less than 20% shall be read and the value shall be taken for unsharpness and SR_b determination.

Other IQIs for unsharpness measurement are e.g. line pair pattern based as e.g. MTF gages and converging line pair gages (see fig. 4.8). These IQIs are useful for low energy applications. Nevertheless, they provide mostly different values than the duplex wire IQI.

Its reading can be influenced by the SNR and so called aliasing effects. They were accepted for the integration in the CR test phantom as described in EN 14784-1 and ASTM E 2445. The EPRI test film, described in E1936 uses also line pair IQIs.

4.3.3.3 Classification of CR systems

CR system classification was developed in analogy to the film classification of EN 584-1, ISO 11699-1 and ASTM 1815. The classification intends to classify systems which allow the replacement of film systems at optical density of 2 above fog and base. The motivation for film replacement by digital detectors is given as following:

- Shorter test and interpretation time
- New application areas by higher inspection quality and wall thickness range
- No chemicals and dangerous waste
- Less consumables

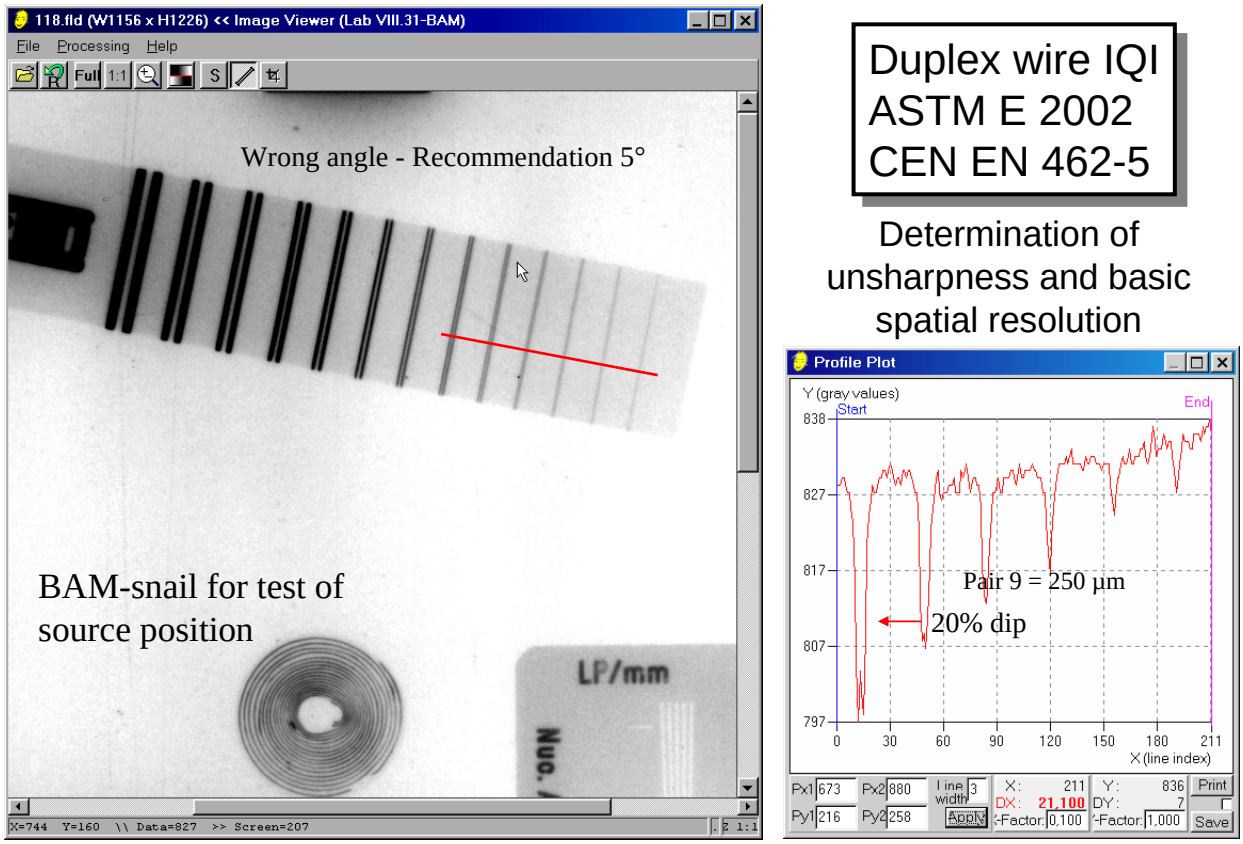

Fig. 4.8: Measurement of unsharpness and basic spatial resolution with the duplex wire IQI according to EN 462-5, ISO 19232-5 and E 2002 for classification and long term stability test as required in EN 14784- 1 and ASTM E 2445.

Digital radiography with sorter test and interpretation time requires achieving the same image quality or better than qualified radiographic testing with film. The classification of a digital detector system for comparison to NDT film systems needs two parameters:

- basic spatial resolution SR_b and

- normalised SNR_N as function of exposure conditions (usually speed at defined radiation quality).

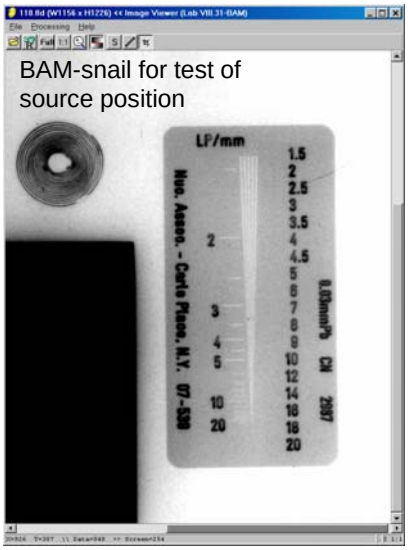

Basic spatial resolution SR_b and Spatial Frequency

Basic spatial resolution means: "effective pixel size"

$$SR_b = 0.5 \cdot u_i \text{ [mm]}$$

ISO 19232-5, EN 462-5, E 2002 measure: $u_i = 2 \cdot SR_b \text{ [mm]}$

Converging line pairs measure:

$$lp \text{ [1/mm]} = 1/u_i = 1/(2 \cdot SR_b)$$

lp – line pairs

Line pairs have problems with
- Aliasing
- the result may depend on the SNR

Fig. 4.9: Converging line pair gage and conversion formulas for line pairs per mm (lp), unsharpness (u_i) and basic spatial resolution (SR_b).

Tab. 4.7 shows the parameters of the IP system classes on the basis of SNR_N as given in EN 14784-1 and E 2446. The classification statement requires additionally posting the value of the SR_b measurement of the detector system. The standards EN 14784-1 and E 2446 recommend calculating the speed of the used detector. The speed is defined as the inverse dose value (in Gray), which is necessary to obtain a certain SNR_N class limit of Tab. 4.7.

For any testing problem the required image quality shall be defined. Standardized NDT applications use defined film systems, which are usually film lead screen systems. The corresponding SNR_N can than be taken from Tab. 4.6.

The required basic spatial resolution (SR_b) can also be determined accordingly to the standards. Film systems (with lead screens) are distinguished by a very low unsharpness, which depends on radiation quality, screen thickness and screen material. The SR_b film values are in general much smaller than the required geometrical unsharpness. Usually, a detector unsharpness can be accepted in the range of (or smaller than) the required geometrical unsharpness. Unfortunately, these unsharpness values are not harmonized world wide. European standards define the geometric unsharpness as a function of the material thickness for the two testing classes (standard A and enhanced B in E444 and ISO 5579).

ASTM and ASME standards require quite moderate unsharpness values, especially in the lower material thickness range (see lecture V03). The typical NDT testing sensitivity in USA requires the 2-2T IQI (penetrameter) perceptibility, which even allows an unsharpness of 4% of the material thickness. Only the standard E2104 (Standard Practice for Radiographic Examination of Advanced Aero and Turbine Materials and Components) contains reduced unsharpness requirements. ASME V/2 is equivalent to ASTM E 1032.

As general conclusion of these standard based requirements, the user shall define the minimum required SNR_N (see tables 4.6 and 4.7) and the basic spatial resolution of the detection system in dependence on the inspected material thickness, energy and company procedures.

The European EN 444, EN 1435 and EN 12681 require for instance:

1st a minimum geometric unsharpness as function of thickness (w) and testing class and

2nd film usage of system classes between C3 and C5 ($SNR_N \geq 52 \ldots 78$ at D=2) as function of wall thickness, radiation energy and testing class.

The total unsharpness u_T is substituted now by the maximum geometrical unsharpness u_g which is calculated in EN 444 by:

$$u_g = \frac{1}{a} \cdot w^{1/3} \qquad (4)$$

with a = 15 for class B testing and a = 7.5 for class A testing and

with w - in mm.

The "European" requirement as given by equation 4, enables the calculation of the required pixel size of the detector for a European testing problem. Due to the difference between u_g and SR_b the recommended pixel size is one half of u_g. If the detector unsharpness is higher than the required one, a magnification technique should be used. Tab. 4.8 summarizes the requirements for system selection of CR systems as function of kV and material thickness (EN 14784-2). It is planned to revise this table, since many users are obtaining also sufficient results with slightly unsharper digital detectors.

Table 1: IP-scanner system classes in dependence on the minimum SNR

IP System classes		
System class CEN	System class ASTM	Minimum Signal-noise ratio
IP 1	ASTM IPSpecial	130
IP 2		117
IP 3		78
IP 4	ASTM IP 1	65
IP 5	ASTM IP 2	52
IP 6	ASTM IP 3	43

IP System classes

EN 14784-1
ASTM E 2446

NOTE:The SNR-values of table 1 are equivalent to EN 584-1, ISO 11699-1, ASTM E 1815-96 They are calculated by: SNR = log (e) · (Gradient/Granularity) of table 1 of the corresponding standards and up-rounded. The calculation of measured SNR values shall be performed from dose proportional data.

Table 4.7: Imaging system classes according to EN 14784-2 and ASTM E 2445.

It is pointed out that the described procedure above focuses to the strict applications of the E 444 based standards. There exist a variety of testing tasks, which do not need the strong unsharpness requirements of testing class B or even class A. Companies can define their own limits. This is the typical case for automated X-ray inspection systems.

The minimum unsharpness is derived from fracture mechanics and time constrains. The European standard EN 13068-3 (Radioscopy) allows higher unsharpness values in the lower material thickness range, but requires the usage of lower radiation energy to compensate with increased contrast.

The ASTM/ASME standards are characterized by moderate requirements for the unsharpness, especially in the low material thickness range. This promotes the application of new digital techniques considerably. The NDT operator should know about the risk of reduced probability of detection for fine details if using unsharp systems. Usually the written procedure of the company defines the required sharpness/unsharpness in dependence on the testing problem.

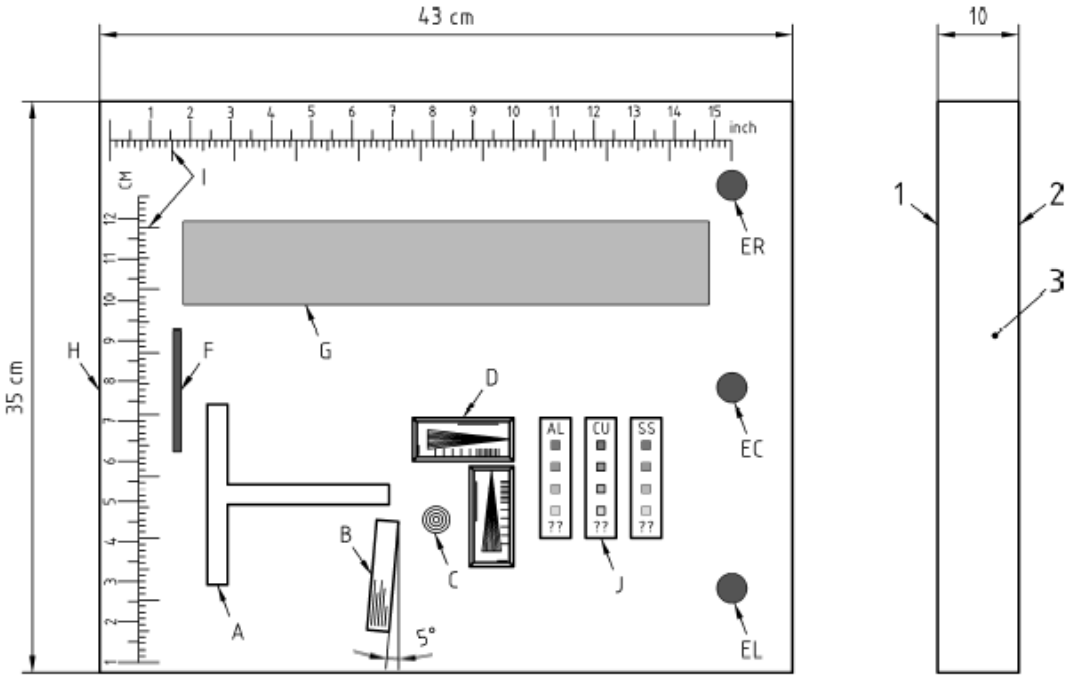

Key

A T-target for laser jitter test and MTF-measurement (length 114 mm, 5 mm, brass)
B duplex wire IQI according to EN 462-5
C central beam alignment (BAM-snail)
D converging line pair quality indicators
E EL, EC, ER: measuring points for shading correction (19 mm diameter, 0,3 mm Lucite removed)
F cassette positioning locator (does not appear on radiographic image)
G homogeneous strip (Al, 0,5 mm)
H lucite plate
I inch/cm ruler for linearity check
J contrast sensitivity quality indicators (aluminium: 12,7 mm, copper: 6,4 mm, stainless steel: 6,4 mm thick)

Figure B.1 — Example of CR phantom containing CR quality indicators for qualification of computed radiography systems (dimension approximately: 43 cm × 35 cm)

Fig. 4.10: CR phantom of EN 14784-1 and ASTM E 2445.

Scattered radiation and lead screens

Some digital detectors are characterized by considerable differences in its spectral sensitivity. Fluorescence screen based DDAs and CR have a higher sensitivity for radiation of low energy than lead screen film systems. This contributes to an increased

sensitivity against scattered radiation. The effective object contrast decreases in comparison to film systems. This effect must be considered and the scattered radiation should be reduced by application of lead or steel screens for filtration. A typical value for CR systems (steel inspection) is the application of 3 times thicker lead screens than typical for film based inspection. Since the lead screens do not intensify the effective exposure of imaging plates as they do it for films, it is also possible to work without lead screens for tube voltages below 250 kV. A reduction of the used kV is recommended if no lead screens are used. The exposure time shall be increased to increase the SNR for compensation.

Table 4 — Required spatial system resolution in dependence on energy and wall thickness

Radiation source	Wall thickness	Class IPA		Class IPB	
	w in mm	Max. pixel[a] size µm	Double wire IQI number[b]	Max. pixel[a] size µm	Double wire IQI number[b]
X-ray $U_p \leq 50$ kV	$w < 4$	40	> 13[c]	30	>> 13[d]
	$4 \leq w$	60	13	40	> 13[c]
X-ray 50 kV < $U_p \leq$ 150 kV	$w < 4$	60	13	30	>> 13[d]
	$4 \leq w < 12$	70	12	40	> 13[c]
	$w \geq 12$	85	11	60	13
X-ray 150 kV < $U_p \leq$ 250 kV	$w < 4$	60	13	30	>> 13[d]
	$4 \leq w < 12$	70	12	40	> 13[c]
	$w \geq 12$	85	11	60	13[c]
X-ray 250 kV < $U_p \leq$ 350 kV	$12 \leq w < 50$	110	10	70	12
	$w \geq 50$	125	9	110	10
X-ray 350 kV < $U_p <$ 450 kV	$w < 50$	125	9	85	11
	$w \geq 50$	160	8	110	10
Yb 169, Tm 170		85	11	60	13
Se 75, Ir 192	$w < 40$	160	8	110	10
	$w \geq 40$	200	7	125	9
Co 60		250	6	200	7
X-ray $U_p >$ 1 MeV		250	6	200	7

[a] If magnification technique is used, double wire IQI readout is required only.

[b] The given IQI numbers indicate the readout value of the first unresolved wire pair corresponding to EN 462-5.

[c] The symbol "> 13" requires the 13th wire pair to be resolved with a dip separation larger than 20 % (see Figure 3 of EN 14784-1:2004).

[d] The symbol ">> 13" requires the 13th wire pair to be resolved with a dip separation larger than 50 %.

U_P = tube voltage.

Table 4.8: System unsharpness requirements for selection of CR systems for NDT of metals in dependence on material thickness and selected tube voltage.

Usage of IQIs

The human eye percepts the contrast-to-noise ratio (CNR) instead of the SNR. Due to the difficulties of the measurement of CNR, the required minimum SNR limits shall be chosen for the standard procedures. Nevertheless, the contrast IQIs (e.g. wires or step hole penetrameters) shall also be used for all applications to guarantee that the sufficient CNR is achieved.

CR phantom

Fig. 4.10 shows the test phantom of EN 14784-1 and ASTM 2445 for user qualification and long term stability tests. All test targets are listed in fig. 4.10. The test phantom includes all IQIs which are useful for qualification. The user can evaluate the CR system in a short time and document the key quality parameters.

4.3.4 Standards for radiography with digital detector arrays

ASTM has published in 2007 the first standard (ASTM E 2597) for manufacturing classification of digital detector arrays (DDA). This standard describes different tests to characterise a DDA and provides information on the correct way to report these parameters. The standard requires finally the measurement of the following key parameters, which shall be provided in a table and a spider graph (see fig. 4.11):

- Efficiency
- Contrast sensitivity
- Specific material thickness range
- Image lag
- Basic spatial resolution

Bad pixel Types and Classifications

***Dead Pixel*— Pixels that have no response, or that give a constant response independent of radiation dose on the detector.**

***Over responding pixel* — Pixels whose gray values are greater than 1.3 times the median gray value of an area of a minimum of 21×21 pixels. This test is done on an offset corrected image.**

***Under responding pixel* — Pixels whose gray values are less than 0.6 times the median gray value of an area of in a minimum of 21×21 pixels. This test is done on an offset corrected image.**

***Noisy pixel* — Pixels whose standard deviation in a sequence of 30 to 100 images without radiation is more than 6 times the median pixel standard deviation for the complete DDA.**

***Non-uniform pixel* — Pixel whose value exceeds a deviation of more than +/-1 % of the median value of its 9×9 neighbor pixel. The test should be performed on an image where the average gray value is at or above 75% of the DDA's linear range. This test is done on an offset and gain corrected image.**

***Persistence / Lag pixel* — Pixel whose value exceeds a deviation of more than a factor of 2 of the median value of its 9×9 neighbors in the first image after X-ray shut down**

***Bad neighborhood pixel*— Pixel, where all 8 neighboring pixels are bad pixels, is also considered a bad pixel.**

Single bad pixel	Cluster bad pixels	CKP

Cluster kernel pixel (CKP) are pixels, which only have four or less good neighborhood pixels

Line of bad pixels

Table 4.9: List of bad pixels (underperforming detector elements in a DDA) and clusters and lines.

Furthermore information is required about the amount and location of bad pixels as well as clusters and lines of bad pixels. Table 4.9 contains a list of all types of

underperforming pixels called "bad pixels". This includes also dead pixels which are not responding to radiation and are white or black spots in the digital images if no correction software will be used.

Fig. 4.11 shows a matrix with bad pixels, bad lines and bad pixel clusters. For detector qualification it is required to inform the customer if the detector contains cluster kernel pixels (CKP). It is presupposed that a bad pixel value in an image can be replaced by numeric interpolation best, if the pixel has at least 5 "good" pixels as next neighbour pixels to be used for interpolation. Fig. 4.11 contains one bad pixel cluster with 2 bad pixels which are not correctable from the values of 5 good neighbour pixels. This is a CKP, also named relevant 3x4 cluster 7-2. The last no. 2 stands for two uncorrectable pixels. It is mentioned here, that almost all manufacturer provide software which is able to correct also CKPs and multiple bad lines. Finally it depends of the user how many bad pixels, clusters and lines he or she may accept. Generally, it can be recommended, that CRPs are acceptable it they are << than the flaws or structures to detect. It shall also be considered that DDAs are products which develop bad pixels during its usage due to the interaction with the ionising radiation. A DDA has a limited live time since its performance decays due to radiation damages.

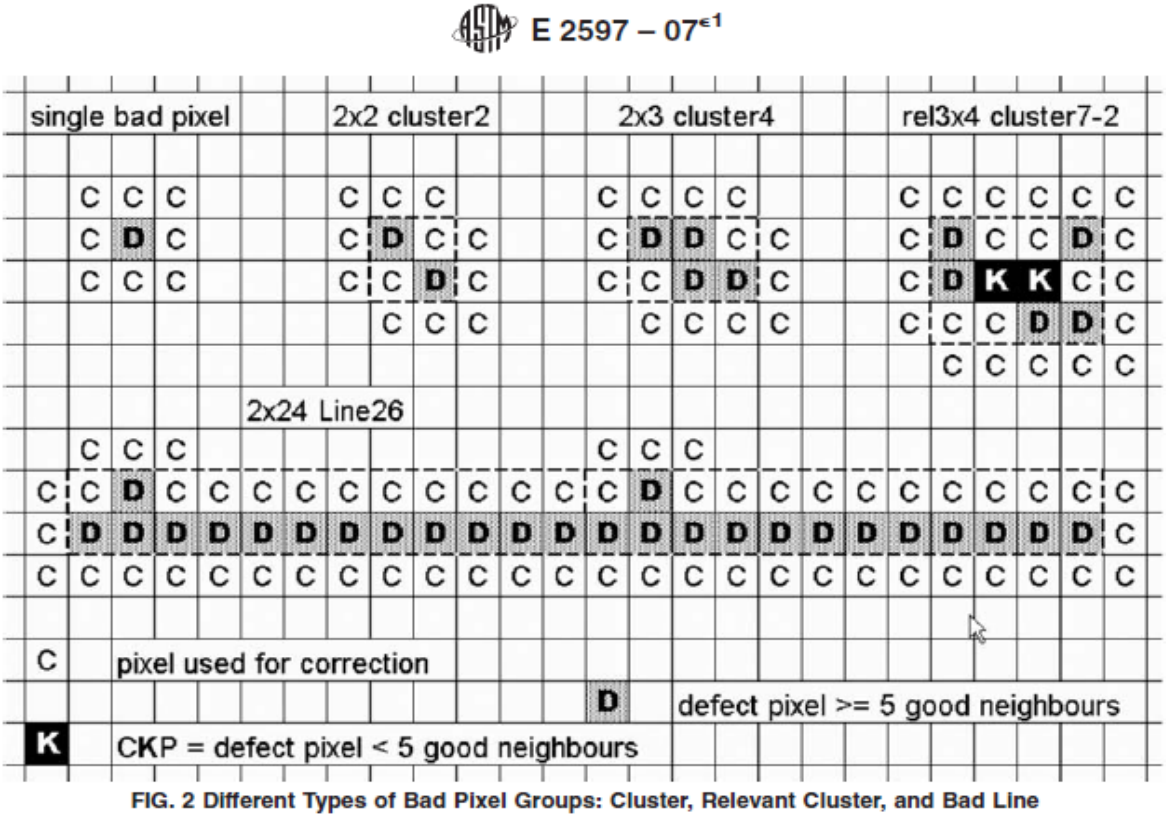

Fig. 4.16: Scheme for the different appearance of bad pixels and its correction according to ASTM E 2597.

4.3.4.1 Efficiency test

The efficiency test is based on two sequential detector exposures under given conditions. The subtraction of these images compensates for the differences in the pixel characteristics. Finally, the statistic noise, which is photonic noise (quantum statistics), remains in the difference image. The mean value of a single exposed image divided by the standard deviation of the difference image (to be corrected by square root of 2) and normalised to the detector element size, provides the efficiency value taken for 1 mGy exposure and a given radiation quality. Fig. 4.12 shows the result of these measurements as illustrated in ASTM E 2597.

4.3.4.2 Contrast Sensitivity (CS)

CS is measured after exposure of a grooved step wedge onto the digital detector for different exposure conditions. The reciprocal contrast-to-noise is plotted as CS versus the wall thickness. The graph informs about the contrast sensitivity which can be achieved in a certain material thickness range.

4.3.4.3 Specific material thickness range (SMTR)

The SMTR informs about the thickness range which can be inspected with one exposure. Two different SNR values are required for the determination of a CS of 1% and 2%. This is SNR = 250 and SNR = 130, respectively. The same step wedge, which is used for the CS measurement, can be taken for the measurement of SMTR.

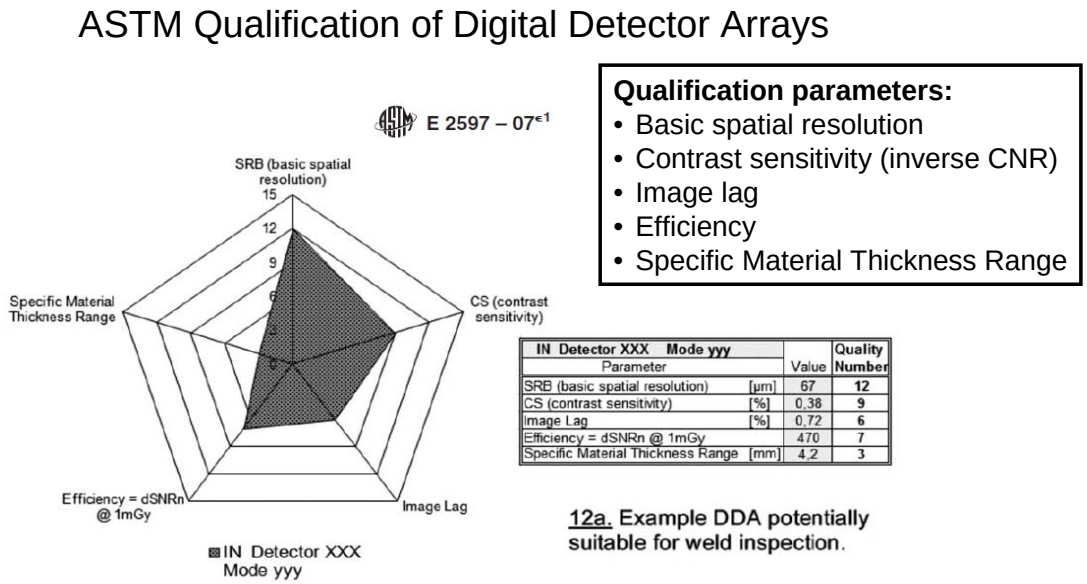

Fig. 4.11: Qualification result on the basis of the tests of ASTM E 2597.

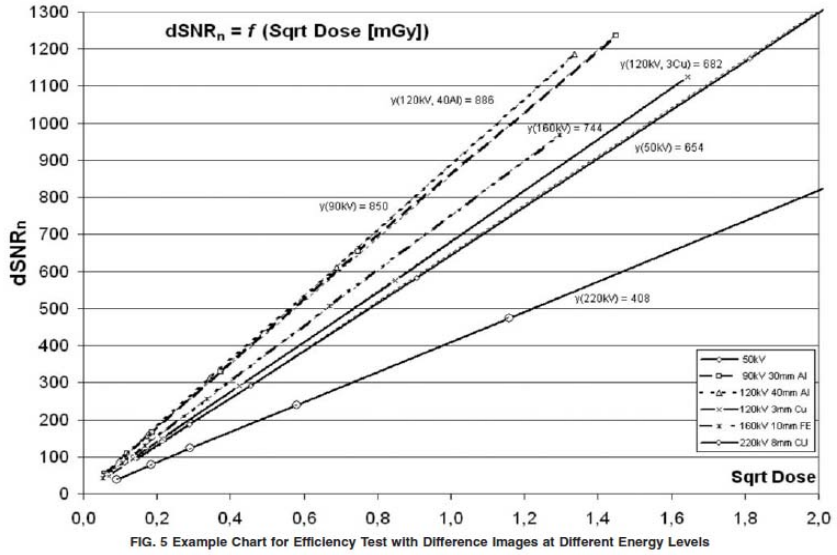

FIG. 5 Example Chart for Efficiency Test with Difference Images at Different Energy Levels

Efficiency is defined as normalized Detector $dSNR_N$ at defined exposure dose (1 mGy) determined from the difference of two measurements.

Fig. 4.12: Example of efficiency tests of DDAs at different radiation qualities based on ASTM E 2597.

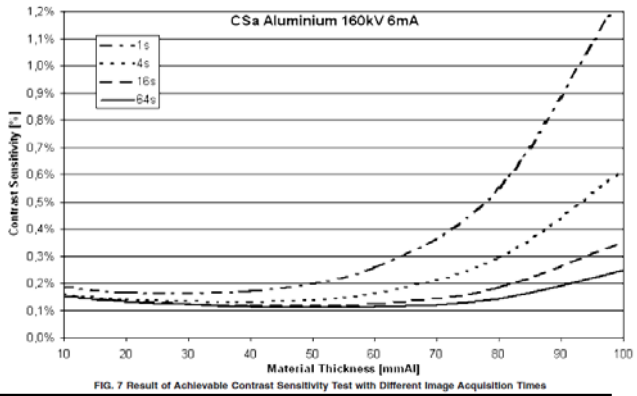

FIG. 7 Result of Achievable Contrast Sensitivity Test with Different Image Acquisition Times

Contrast Sensitivity is defined as reciprocal CNR, measured with a grooved step wedge at given radiation quality.

Fig. 4.13a: Contrast sensitivity measurement for DDAs according to ASTM E 2597

Step wedge exposure for measurement of **contrast sensitivity**

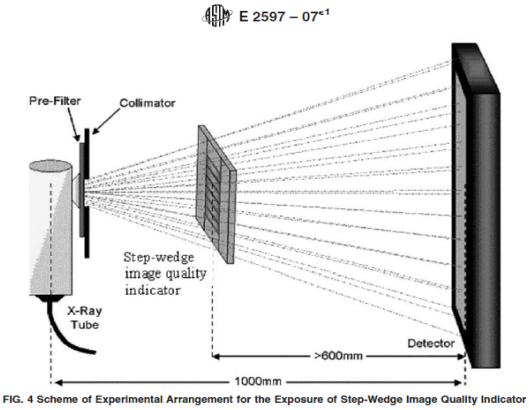

FIG. 4 Scheme of Experimental Arrangement for the Exposure of Step-Wedge Image Quality Indicator

Fig. 4.13b: Exposure geometry for the measurement of the contrast sensitivity as given in fig. 13a.

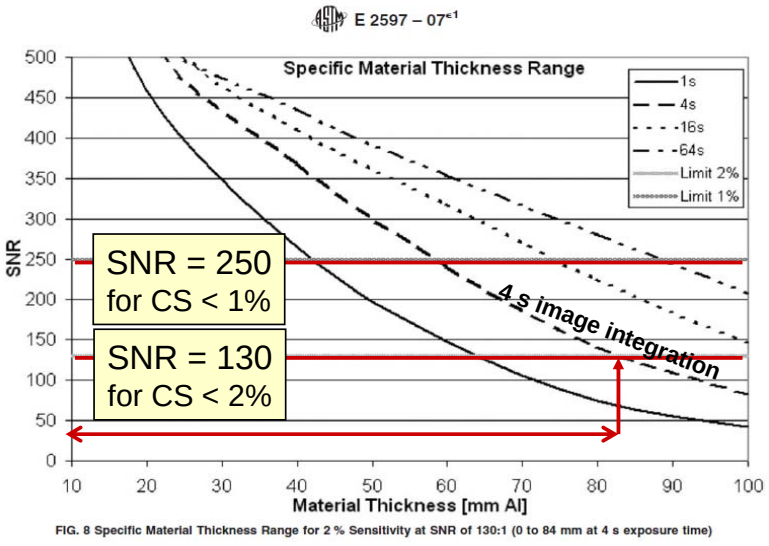

Specific Material Thickness Range is defined as inspectable material thickness range from detector saturation (low thickness limit) to a thickness where the digital radiograph falls below a SNR of 130 for 2% CS and below a SNR of 250 for 1% CS (large thickness limit).

Measurement obtained from step wedge measurement in analogy to the CS measurement.

Fig. 4.14: Specific material thickness range, determined according to ASTM E 2597.

4.3.4.4 Image lag (IL)

All detector elements respond with a time delay and its pixel value (gray value in the image) decays after the exposure with a different time delay. Since the next exposure may add the information to the incomplete decayed image of the previous exposure, it is important to know this time constants. Fig. 4.15 shows a typical example for an image lag. The pixel values need 45 seconds to decay at 1% of the image information, measured immediately after the exposure. Since the contrast sensitivity of DDAs is typically better than 1% this may distort the inspection of serial products. It means in practice that the inspected product of the exposure before may still be visible in the next exposure. This will also distort computed tomography applications.

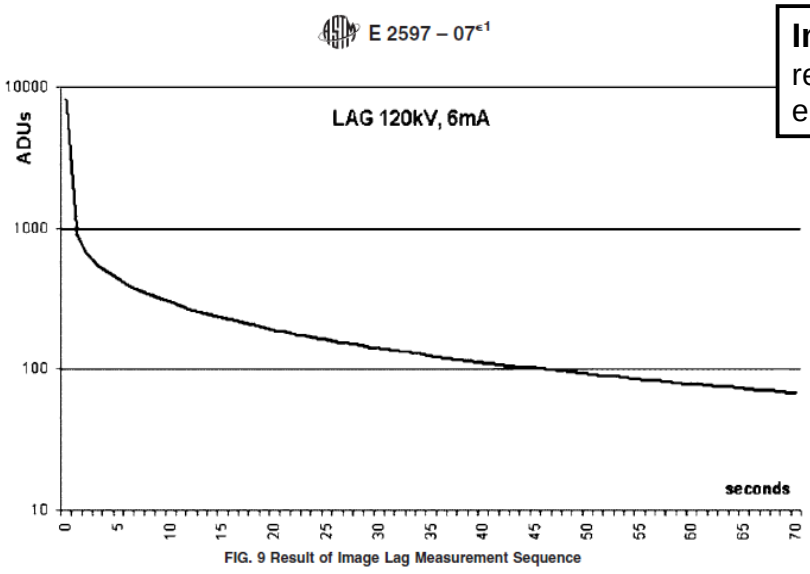

Image Lag is defined as relaxation time of detector elements after exposure.

Fig. 4.15: Image lag measurement according to ASTM E 2597.

The test for the determination of the basic spatial resolution SR_b is equivalent to the procedure for CR qualification. For DDA qualification it is required to interpolate between the duplex wire pair which shows a dip of more than 20% depth and the next duplex wire showing a smaller dip than 20%.

New standards are under development, as e.g. a standard practice for DR with DDAs a user guide for DDA based radiography and a user test standard for long term stability tests and user qualification with simpler means.

L 05 Fundamentals of Digital Image Processing

Content

5.1 Introduction

Images comprise a tremendous pile of information. Nevertheless, much more information is perceived “at a glance” when viewing an image rather than reading a description. Obviously, the information content of an image is wrapped in a way that is rather perceptible for the human brain. Man is capable to process a large amount of data with the visual system much faster than with any other sense organ.

In spite of the similarities between the concept of a “technical viewing system” and the human visual system (Figure 5.1) it has become evident that profound differences exist between the ways of processing image information. While the technical system is capable to process the information only sequentially and thus needs much time and large calculating efforts to relate between individual pixels the human visual system operates associatively and thus has the ability also to analyse rather quickly very complex relationships. Because of these differences, the human visual system is also capable to extract the essential information even from images with very defective information contents. On the other hand, a technical viewing system requires the best possible image quality to gain the desired information from the image.

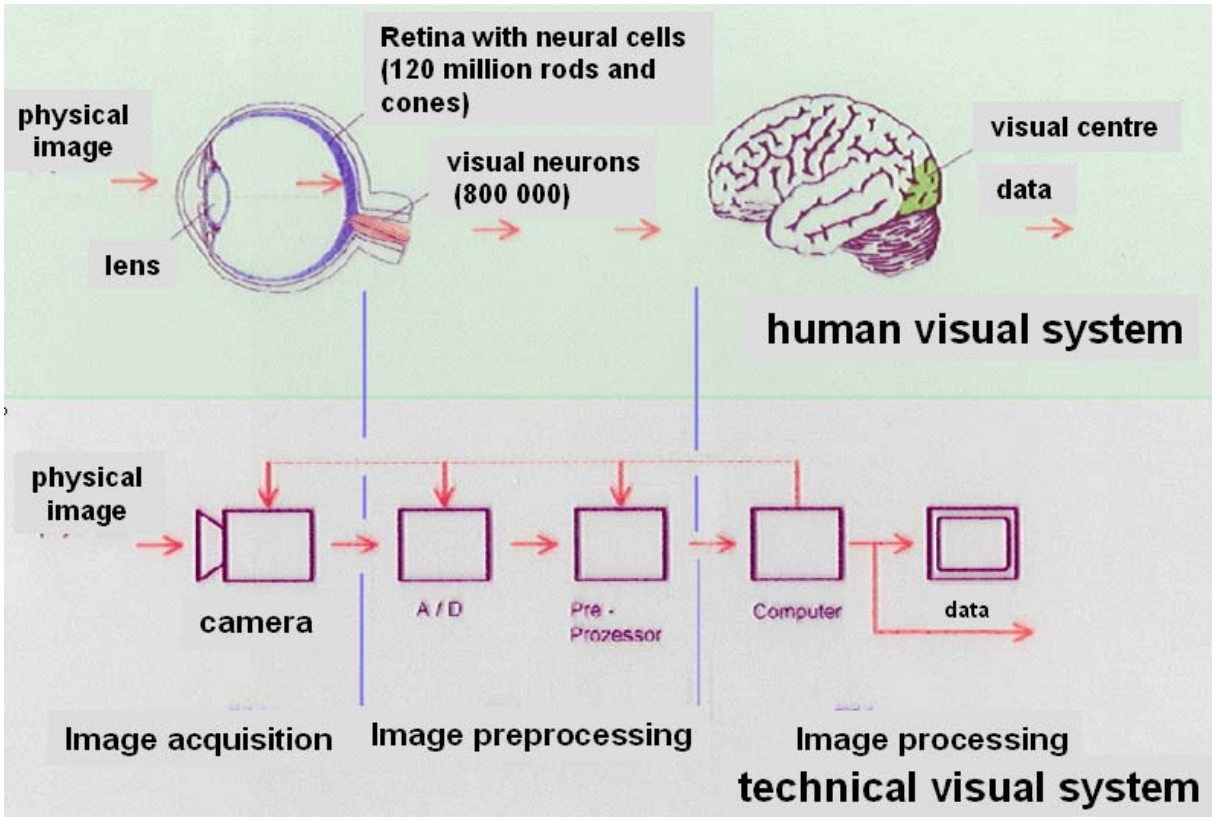

Fig. 5.1: Comparison between the human and the technical viewing system

The term “digital” is of Greek origin and means “countable”. This means that the image information has to be transformed into a format a computer is capable to operate with. Only thereafter it is possible to apply the desired methods of the digital image processing. These are usually separated into procedures for **image improvement** and those for **image analysis and evaluation**. Both tasks are of eminent importance in the industrial X-ray inspection.

5.2 Image acquisition

The first step of image processing is the image acquisition. All factors of the acquisition process need to be completely understood for a quantitative image evaluation or analysis. The pathway from the object to the digital image in the memory of a image processing system can be divided into three separate steps:

visualisation: the attenuation of the X-ray by the object

imaging: the projection of the spatial (three dimensional) object onto an image plane (two dimensions)

digitisation: the continuous image is converted into a matrix of discrete dots (*“picture element”* = “pixel”). The existing analogue intensity values have to be converted (rounded) into a set of grey values (quantification).

5.2.1 Digitisation

Digitisation is understood as the scanning of an image into a two dimensional matrix. A single image dot is called pixel. The number of scanned values or pixels that have been generated in the digitalising procedure has a decisive influence on the quality of the digital image or the image resolution (Figure 5.2 a - c).

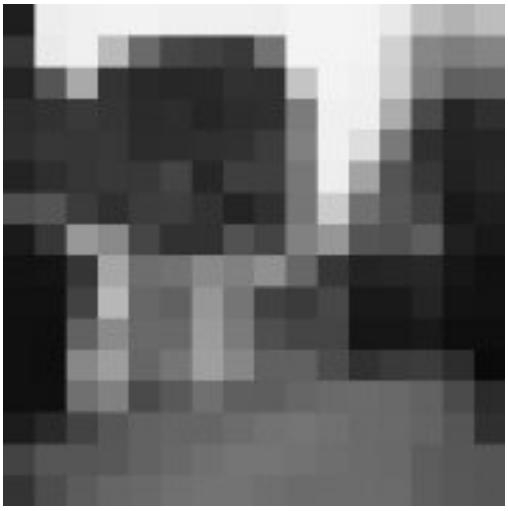

left: **16x16** scanned values (pixels)

right: **32x32** scanned values (pixels)

Fig. 5.2 a: Effect of the number of pixels on the image resolution

left: **64x64** scanned values (pixels)

right: **256x256** scanned values (pixels)

Fig. 5.2 b: Effect of the number of pixels on the image resolution

left: **512x512** scanned values

right: **1024x1024** scanned values

Fig. 5.2 c: Effect of the number of pixels on the image resolution

Nowadays, at least 512 x 512 pixels are taken to digitalise an industrial X-ray for image processing, typically it has several Mega pixels.

5.2.2 Quantification

Not only the number of pixels the original continuous image has been converted to is of decisive importance for the resulting digital image quality but obviously also the assignment to discrete intensity levels, the so-called grey values GV (Figure 5.3 a-c).

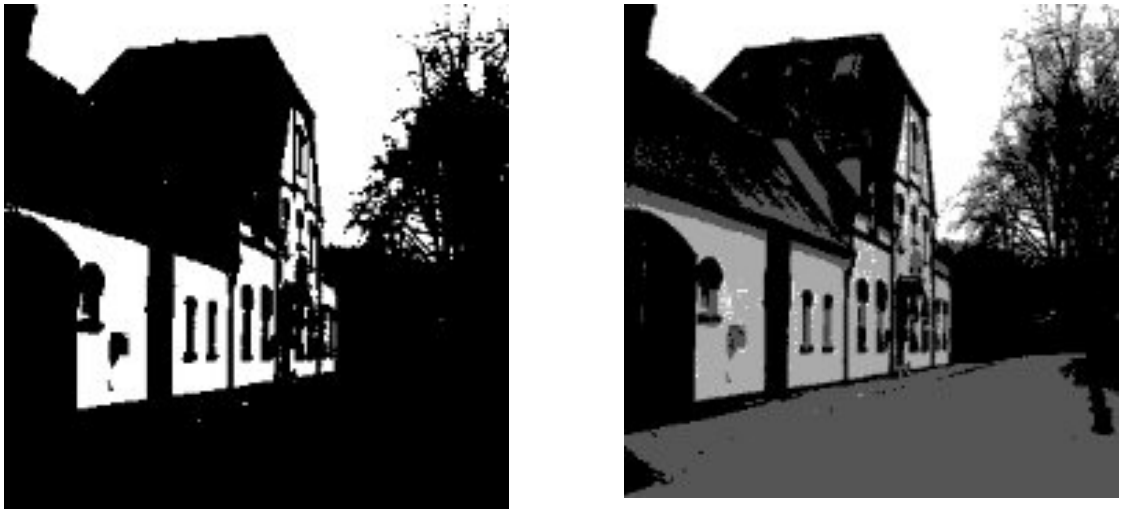

left: **1 Bit** (2 GV) right: **2 Bit** (4 GV)

Fig. 5.3 a: Effect of the grey value resolution (quantification)

left: **3 Bit** (8 GV) right: **5 Bit** (32 GV)

Fig. 5.3 b: Effect of the grey value resolution (quantification)

left: **6 Bit** (64 GV) Right: **8 Bit** (256 GV)

Fig. 5.3 c: Effect of the grey value resolution (quantification)

While the human eye has a limited capacity of some 60 grey values, depending on the viewing and the environmental conditions, the industrial X-ray image processing starts compulsorily with 8 bit, i.e. 256 grey values. Depending on the detector in use, grey value resolutions of 12 bit or 16 bit and more are quite common nowadays.

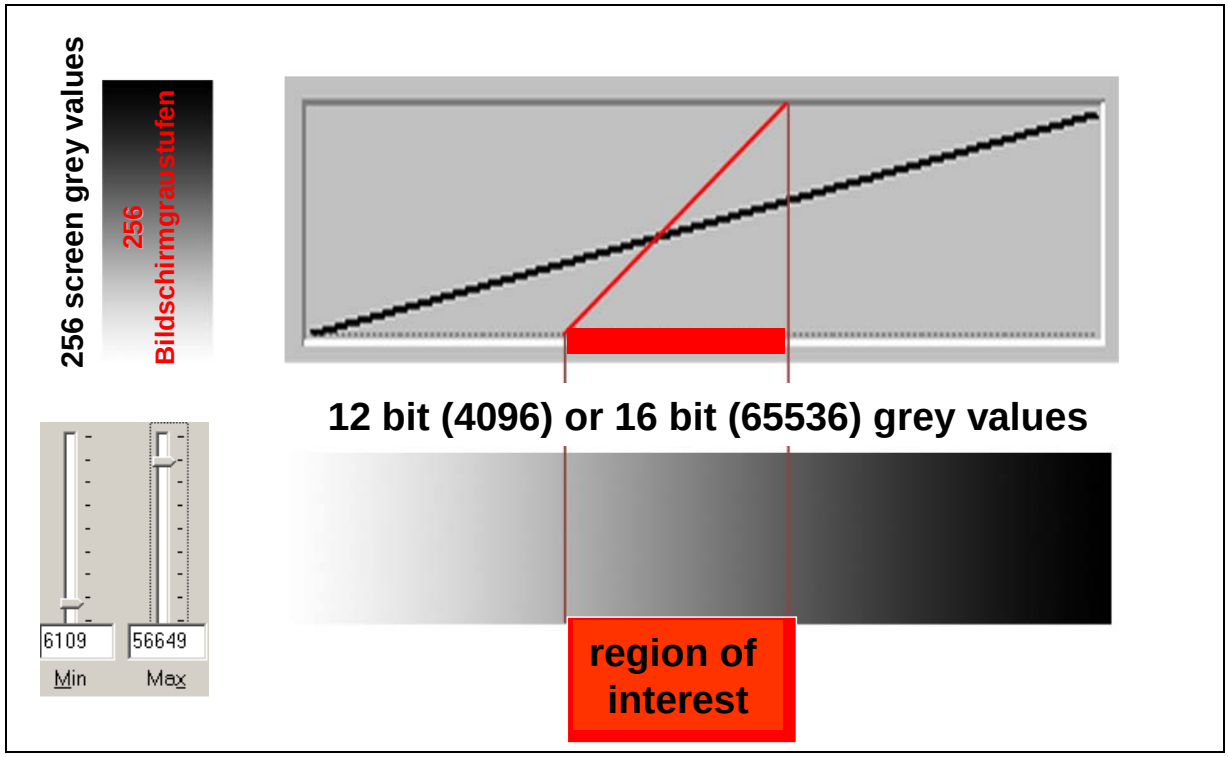

Fig. 5.4: Presentation of 256 grey values from a 12 or 16 bit range

Problems are encountered when more than 256 grey values have to be displayed on a PC-monitor. The monitor screens *usually* are capable to display several millions of different colours but only 256 grey values. This means that 256 grey values have to be selected for displaying on the monitor in an appropriate way from e.g. 4096 grey values (12 bit) or some 65000 grey values (16 bit) (Figure 5.4).

The selection of 256 grey values out of a larger set of grey values is related to the presentation of a certain range of wall thicknesses in the industrial X-ray inspection.

5.3 Image pre-processing

Depending on the radiation intensity and the reading time of the detector, a noticeable noise becomes visible in the radioscopic image due to the quantum nature of the X-rays. As a consequence, improving the signal-to-noise ratio, or a noise reduction, respectively, is a usual step in the image pre-processing.

A marked reduction of the noise can be achieved by averaging several single X-ray images **(digital image integration)** (Fig. 5.5). A prerequisite for this approach is that the object and its position remain unchanged. In case of objects in motion, so-called recursive procedures could be employed (recursive filters) for noise reduction.

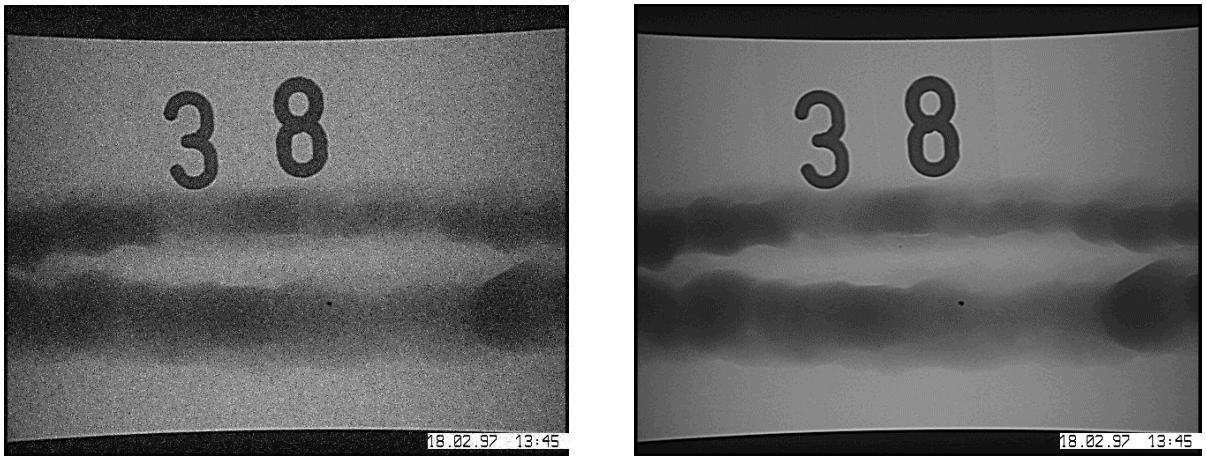

Fig. 5.5: Noise reduction by digital image integration (prior/after)

In addition, images poor in contrast can be improved significantly by subsequent **spreading the contrast**. In such cases advantage is taken from the fact that only a rather limited range of grey values actually exists within the whole scale in *faint* images (poor in contrast), e.g.: only grey values between 100 and 200 are present in an 8 bit image with 256 possible grey values. These 100 grey values then are spread to the total length ranging from 0 to 255 (Fig. 5.6).

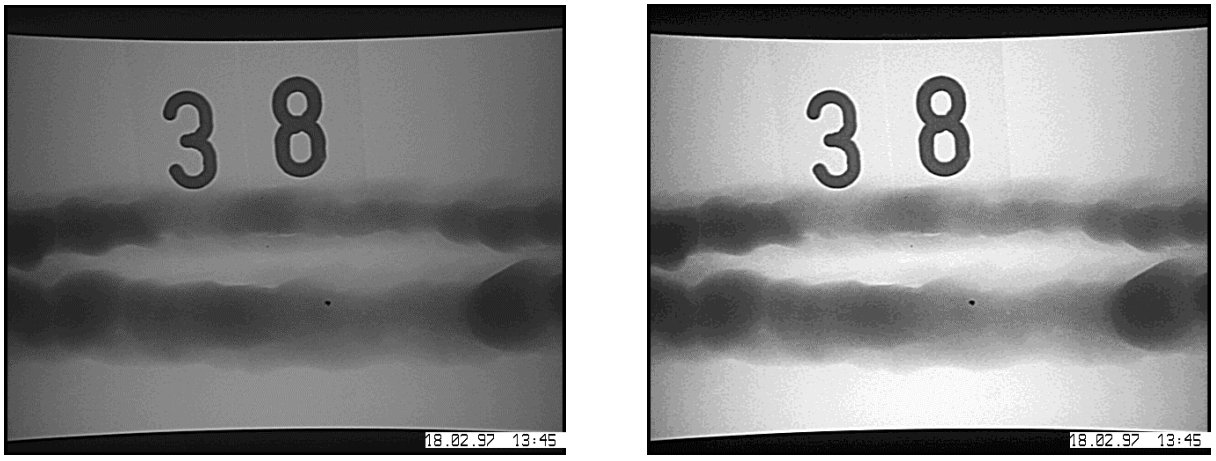

Fig. 5.6: Improving the perceptibility of details by spreading the contrast

Wile the spreading of the contrast only displays one and the same image information one or the other way, and can be undone any time, other methods are introduced to change the informal content of an image purposely to achieve an improvement of the perceptibility of details – the **digital filtering**. Fig. 5.7 exemplifies the result of such a digital filtering. The gain of various filters needs to be assessed accordingly to the *postulated* purpose.

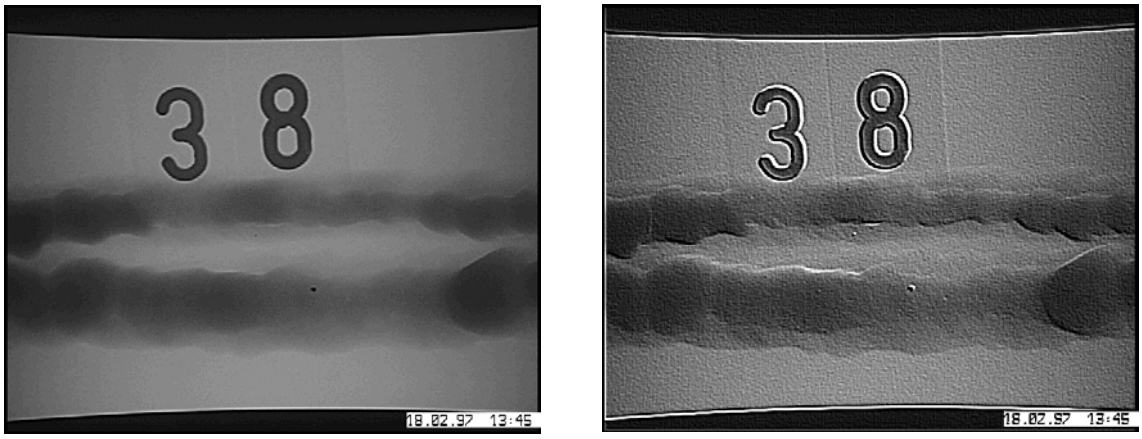

Abb. 5.7: Result of digital filtering (right)

5.4 Intensity profiles and measurements

A simple tool to analyse distribution of grey values in digital images is given by the so-called grey value profile (Fig.5.8). This enables to present intensity distribution of grey values simply, descriptive and easily interpretable in a diagram.

Distance between image details or their dimension also could easily be determined by means of the intensity profile. This plays an important role in the assessment of X-ray images.

Common measurements are:
- distances
- lengths
- areas

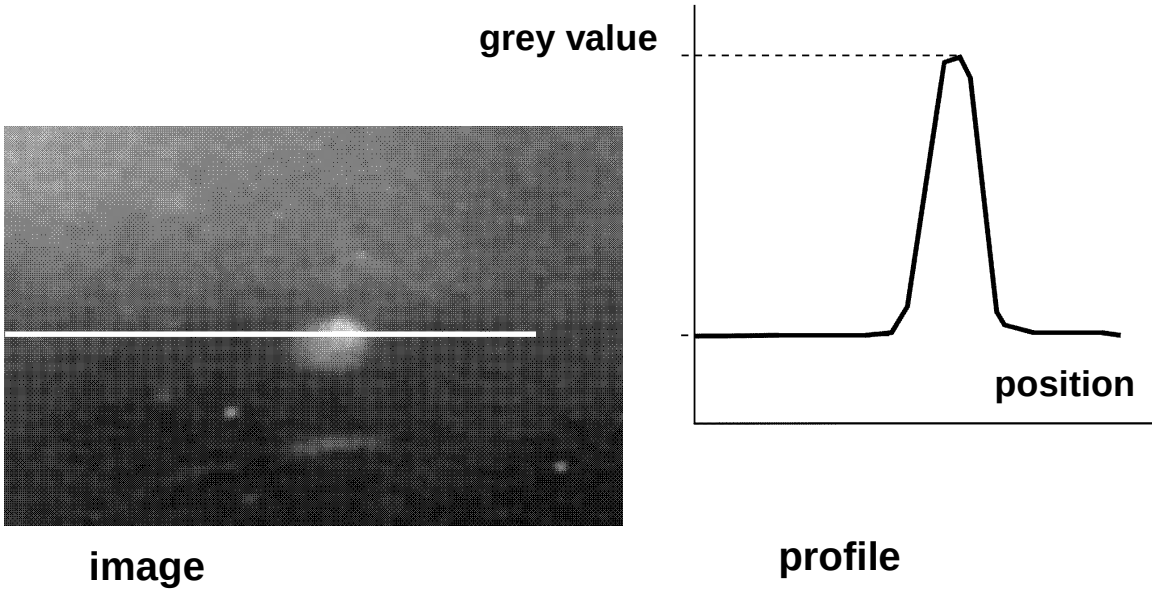

Fig. 5.8: Grey value profile along the line indicated in the image

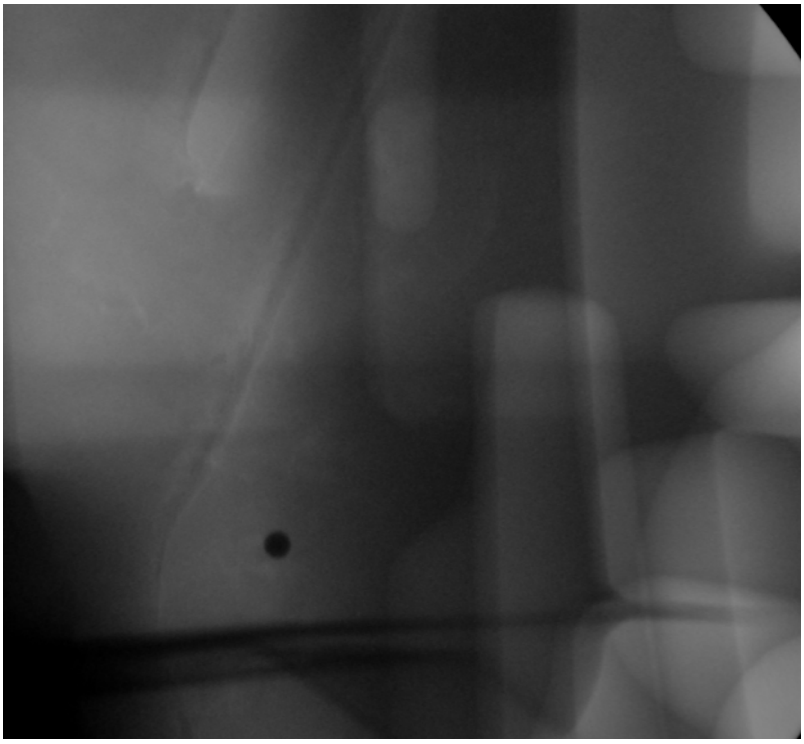

Fig. 5.9: Al cast component with a Fe-sphere (diameter = 2mm)

If a measurement of image details is desired true to scale then the geometric resolution of the X-ray image has to be taken into account. This needs to relate the dimensions of a known calibrated reference to the resolution per pixel. Since this relationship changes dependently on the exposure geometry (the chosen geometric magnification) the calibration has to be redone each time for various geometric magnifications. Figure 5.9 shows a Fe-sphere of 2 mm diameter which is chosen as a reference for calibrating the measurements of a cast component made of aluminium.

L 06 X-ray Sensitive Detectors I

Content

6.1 Principles of film digitisation

The development of high resolution scanning systems facilitates the digitalisation of X-ray films in the field of non-destructive material testing. This technology has been applied in medical fields since years. The digitisation opens a series of new opportunities for the conventional radiographic inspection:

- Archiving on digital media (no more image degradation over the years, copies of the same quality, availability in data bases to reduce the searching time)
- Quantitative evaluation (measurements, differences in wall thickness taken from alterations in density)
- Image processing (to improve visual evaluation, as a preparatory step for the computer aided image interpretation)
- Fast image transfer (utilisation of telecommunication, "remote expertise")
- Computer aided image evaluation (automatic flaw recognition)
- Combination of radiographic inspection with other testing methods
- Reconstruction (Calculation of spatial (3D) volume data from multiple 2D-projections)

The problem of film digitisation consists of transposing the high image quality of the film radiograph (object range, resolution of the wall thickness as well as the spatial resolution) into the digital image. This high image quality makes the difference between the film radiography and other film-free X-ray methods such as radioscopy or the application of imaging plates. Requirements on film digitisation equipment applied for NDT films can be found in ISO EN 14096.

6.2 Phosphor imaging plates

Phosphor imaging plates (IPs) are media for film-free radiography. This technology is commonly called „computed radiography" or CR. This technology has been applied in medicine and biology since 30 years. This technique has also been introduced in the fields of NDT. The fact that these systems have been developed for medical applications by far does not imply that they are capable to replace completely the NDT film. On the other hand, CR could pave the way to new areas of applications since higher sensitivities allow shorter exposure times and the results can be directly evaluated digitally. Standards for NDT applications are EN 14784 and ASTM E2007, E2033 2445 and 2446.

6.2.1 Principles

Imaging plates are exposed analogously to films. The image information is readout from the plates with a laser scanner and the plates are erased at the same time or in a follow up erasure unit (see fig. 6.1). This makes any chemical developing process as for films obsolete, the results are available on the computer for evaluation immediately after the readout. The plates can be reused up to a thousand times without any significant loss in quality if no mechanical damages appear.

The imaging plate consists of a flexible polymer carrier foil covered with a layer sensitive to X-rays consisting of a BaFBr mixture doped with Eu^{2+}. A thin protection layer prevents the surface from mechanical damages (see fig 6.2).

The **advantages** of the imaging plate technology:	The **disadvantages** of the imaging plate technology:
High linearity	Limited spatial resolution (see Fig. 6.7)
High dynamic range > 10^5	High sensitivity at low energies
High sensitivity	Therefore largely influenced by scatter radiation
Thousand times reusable	
No chemical processing	
Can be integrated into digital image processing	

Physical background:

The sensitive layer of the most common systems consists of a mixture of BaFBr doped with Eu^{2+}. X-ray or gamma ray quanta result in an avalanche of charge carriers i.e. electrons and holes in the crystal lattice (see fig. 6.3). These charge carriers may be trapped at impurity sites i.e. electrons at a halogen vacancy (F centre) or holes at an interstitial Br^{2+} molecule (H center). Red laser light (600-700nm) excites electrons trapped in a Br^- vacancy (FBr^- centre) to a higher state from which they may tunnel and recombine with a nearby trapped hole. Transfer of the recombination energy excites a nearby located Eu^{2+} ion. Upon return to its ground state this Eu^{2+} ion emits a blue photon (390 nm). This process is described as PSL or photo stimulated luminescence. Essential is the occurrence of defect aggregates consisting of a hole trap, an electron trap and a luminescent point defect such as a Eu^{2+} ion substituted at a Ba lattice site. Aggregating defects are located within a range of typically 10 lattice cells.

6.2.2 Maximum achievable SNR

It should be noted as a disadvantage as compared to the digital detector arrays that there is a limited maximum signal-to-noise ratio SNR because of structural noise from the IP production process, which cannot be reduced by system calibration.

The saturation effect of the SNR with increasing exposure dose is illustrated in. fig. 6.4. With increasing exposure dosage the maximum achievable SNR_N value is limited. This is caused by structure noise of the used imaging plate. Scanner effects may cause additional noise as e.g. line ripple. The structure noise of the IP is a side effect of production inhomogeneities of the phosphor layer. This effect is also known from fluorescent

screens. At high exposure dosage the contribution of quantum noise of the X-rays is low compared to these image structures, and as result the image quality is finally limited.

An example for achievable image quality at weld inspection is given in fig. 6.5. The exposure times are high enough, that the image noise is determined by the structure noise of these CR systems. Clearly it shows, that a standard CR system has a poorer image quality (both in SR_b and SNR_N values) compared with the best NDT film system, whereas the high definition CR system (HD-CR) system can reach a slightly higher SNR_N value compared with film, but with 8 times longer exposure time than film.

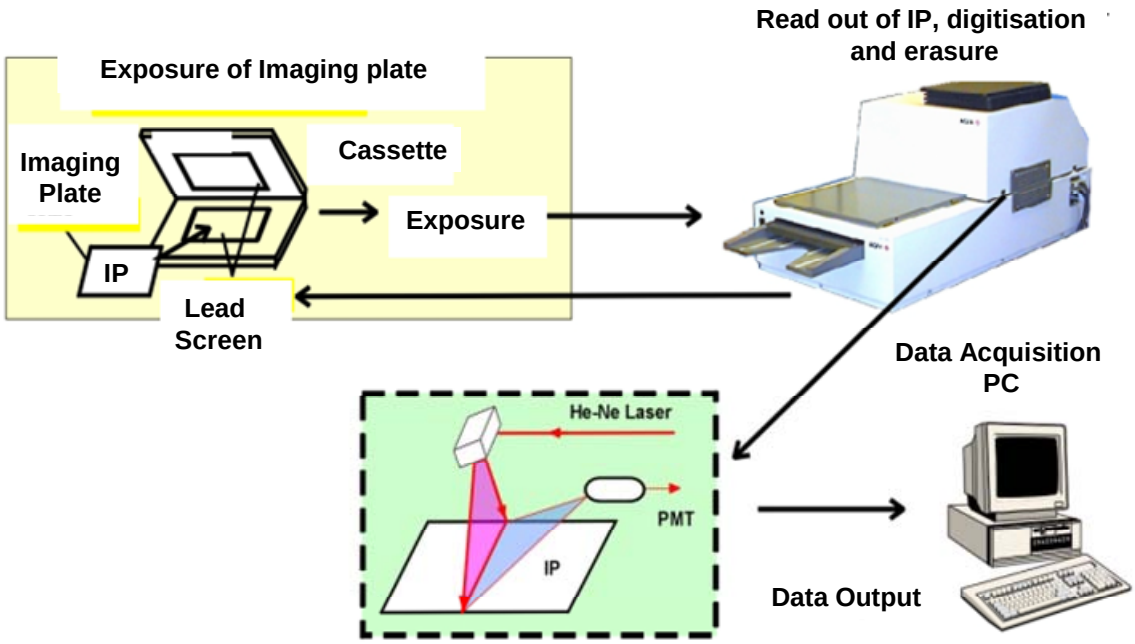

Fig. 6.1: Principle of application of phosphor imaging plates (IP) for Computed Radiography (CR). The plate is exposed in a light proof cassette. The scanner reads the IP with a red laser beam. All exposed areas emit stimulated blue light. The photo multiplier collects the blue light through a blue filter and converts it to an electrical signal. The signal intensity values are converted to digital grey values and stored in a digital image file. Remnants of the image on the IP's can be erased by intensive light. They can be used usually 100 -1000 times, if they are handled carefully.

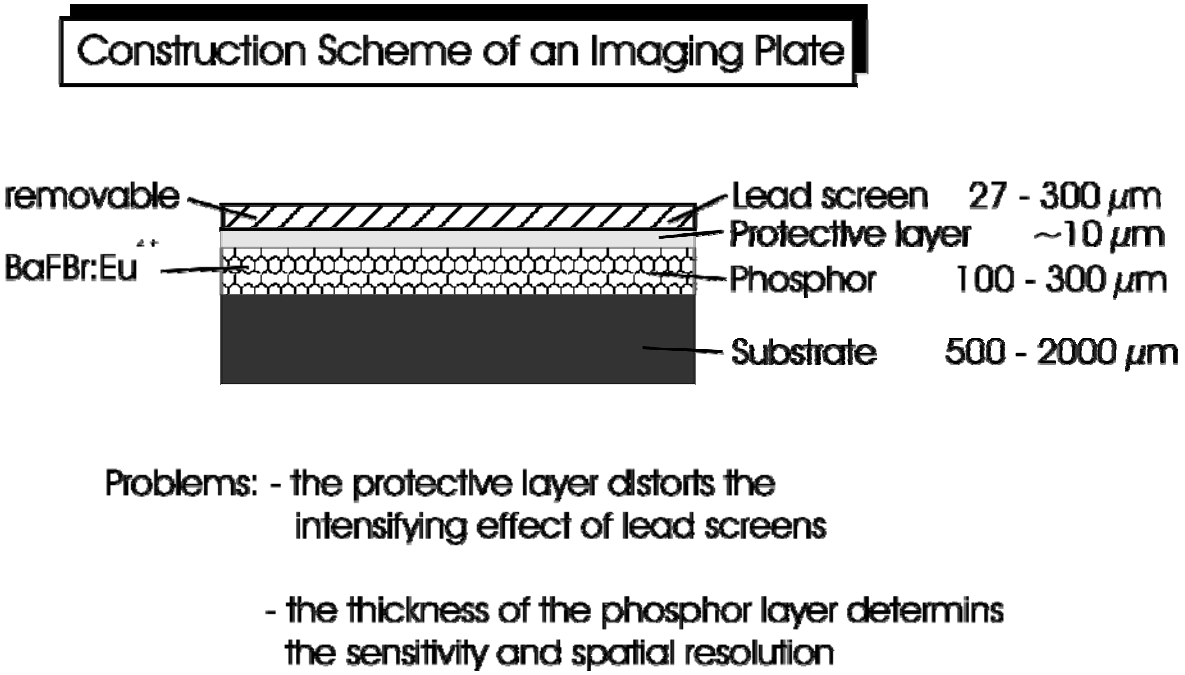

Fig. 6.2: Construction scheme of an imaging plate

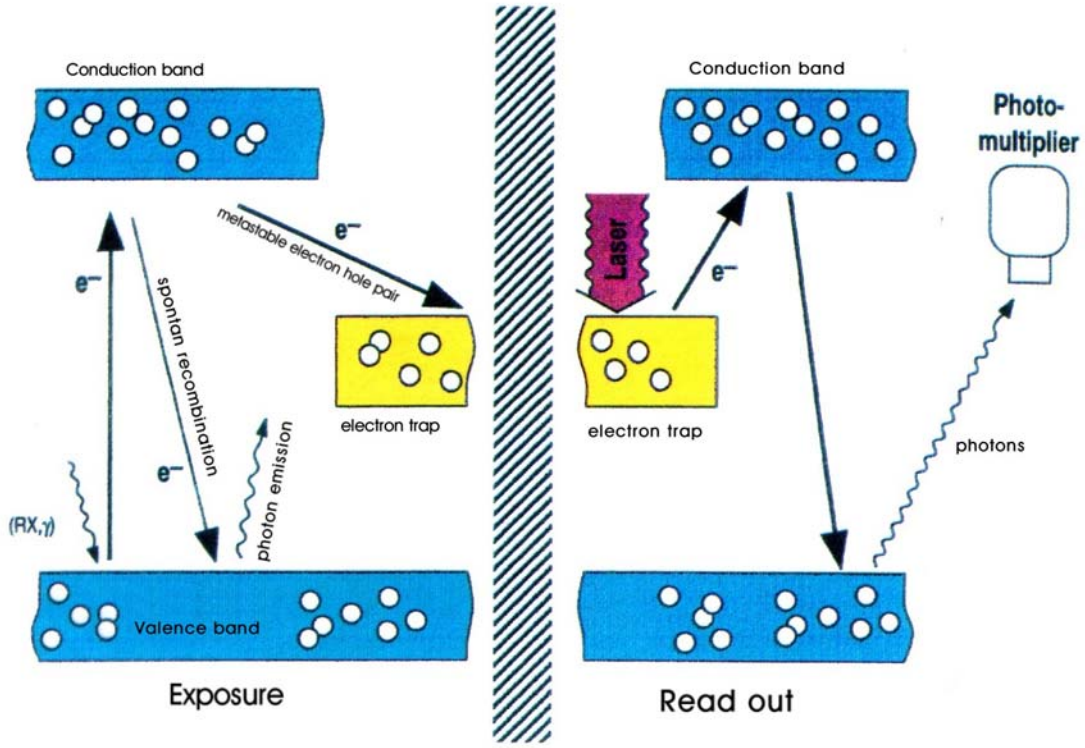

Fig. 6.3: Physics of the exposure and photo stimulated luminescence of the sensitive layer of an imaging plate

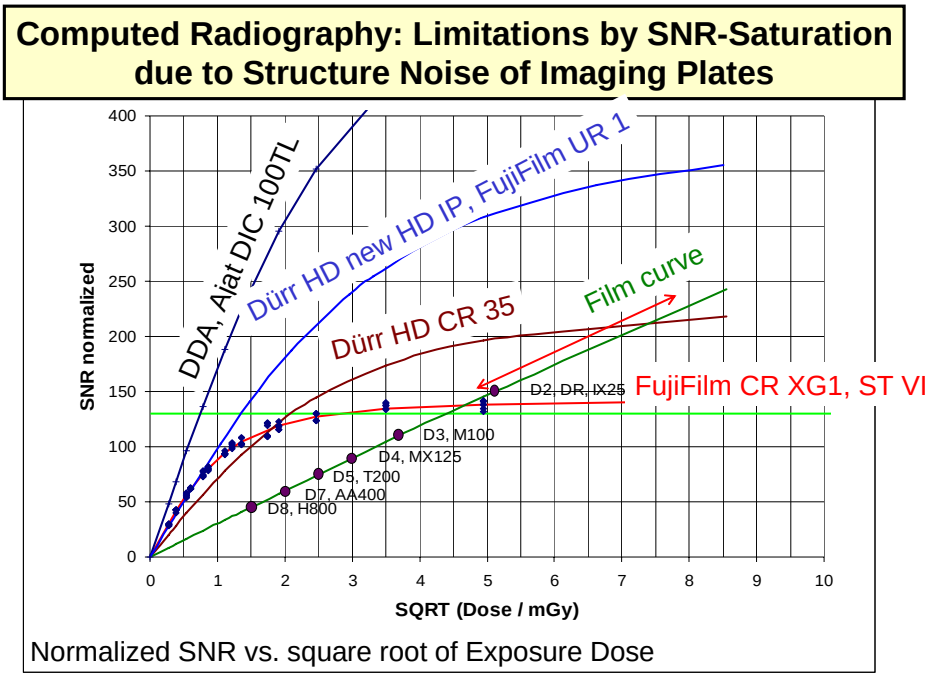

Fig. 6.4: Example of saturation of SNR_N by IP structure noise.

- The maximum achievable SNR_N (saturation) value for XG-1/ST VI is 142 and 232 for HD-CR 35 NDT/HD-IP.
- X-ray films from all major suppliers were measured. Its parameters are at the same line.
- The slope of the curves is a measure for the detector efficiency. The DDA DIC 100 TL of Ajat, based on CdTe semiconductor has the highest efficiency of the compared detectors.

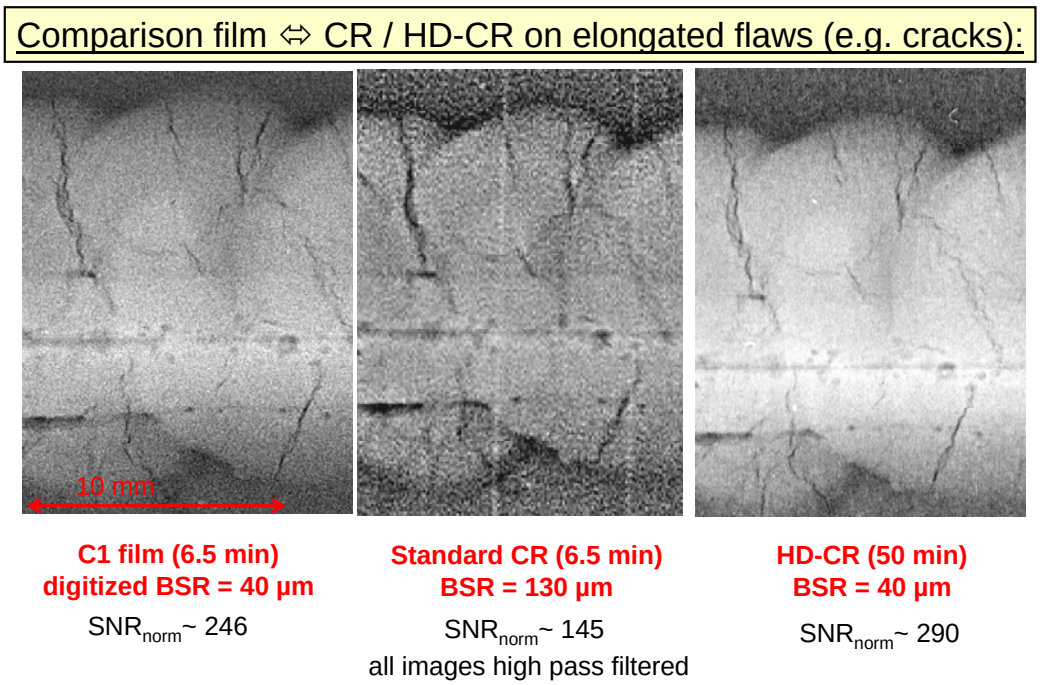

Fig .6.5: Comparison of a section of the BAM 5 test weld obtained with the best NDT film system class C1 (left), a standard CR system (middle) and a HD-CR system (right).

6.2.3 Applications

Requirements for application of film digitisation systems for NDT purposes are regulated in EN 14096.

A typical application for film digitisation and CR is the quantification of corrosion effects in pipe walls (shadow technique or projection radiography). The inspection for corrosion in pipes is one of the most important NDT precaution measures in the chemical industry. The pipes are thermally insulated and the insulation material is held together with a aluminium collar. The radiographic inspection is accomplished without removing the insulation. This is an advantage over the ultrasonic method that needs a direct contact with the pipe.

The currently available phosphor imaging plate systems together with the corresponding laser scanner are capable to cover more than 10 000 dose levels. This is equivalent to far more grey values perceivable by the human eye.

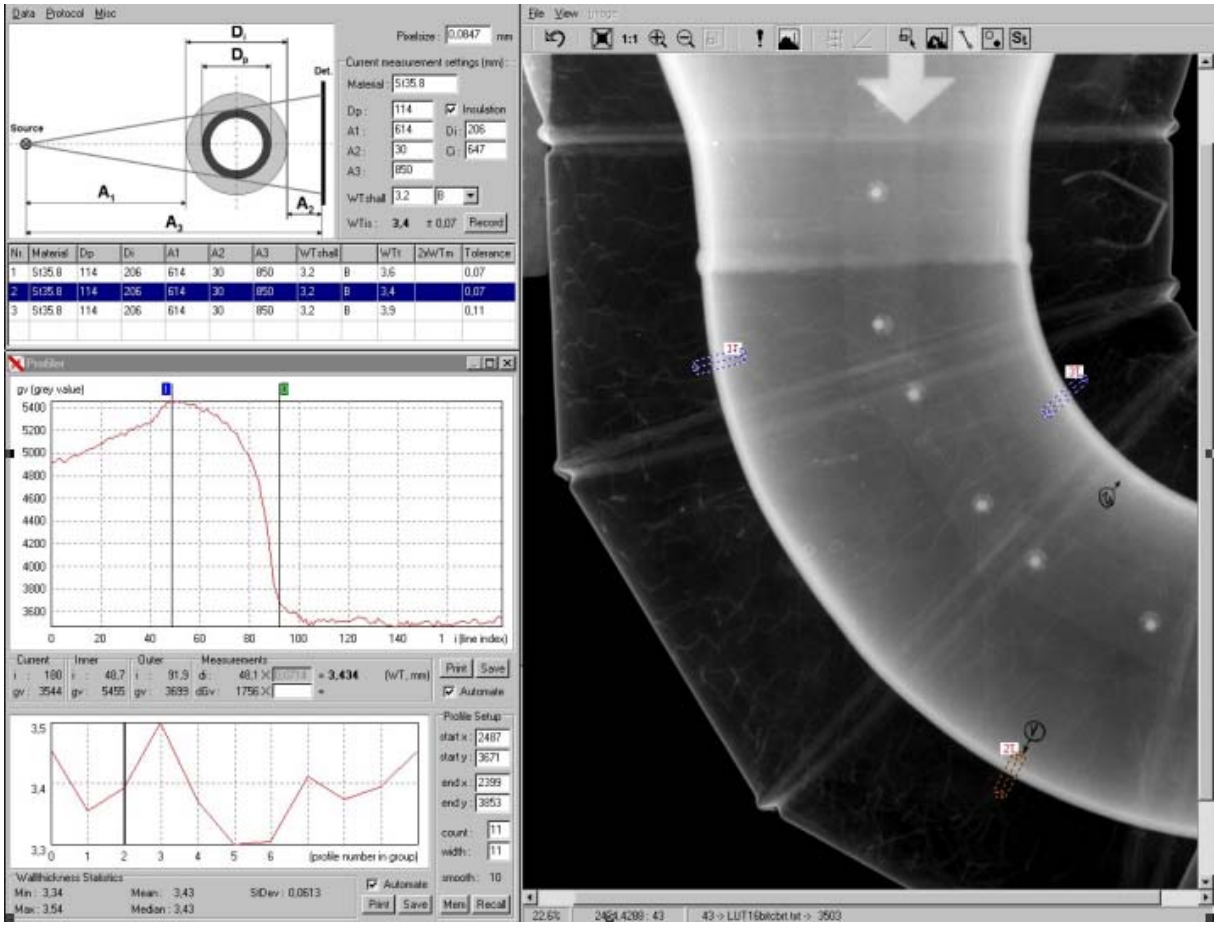

Fig. 6.6: Computer aided inspection of an insulated pipe by means of the projection radiography. The wall thickness can be determined, corrosion is not visible (Interactive evaluation computer program developed in the frame of a joint research project of BAM and BASF)

The advantage of the phosphor imaging plate system is demonstrated in Figure 6.6. The low absorbing wrap (insulation) and the pipe are imaged with the same parameters (a single exposure). Both features are visualised with sufficient brightness and sufficient contrast without the application of any enhancing digital image processing. Different types of imaging plates are available. As with the film radiography, they have to be chosen according to the specific application. A universal imaging plate as it is offered by some providers does not produce acceptable results. Figure 6.7 shows the resolution of different imaging plate systems. The images have been accomplished with duplex wire image quality indicators that illustrate fine structured flaws like cracks.

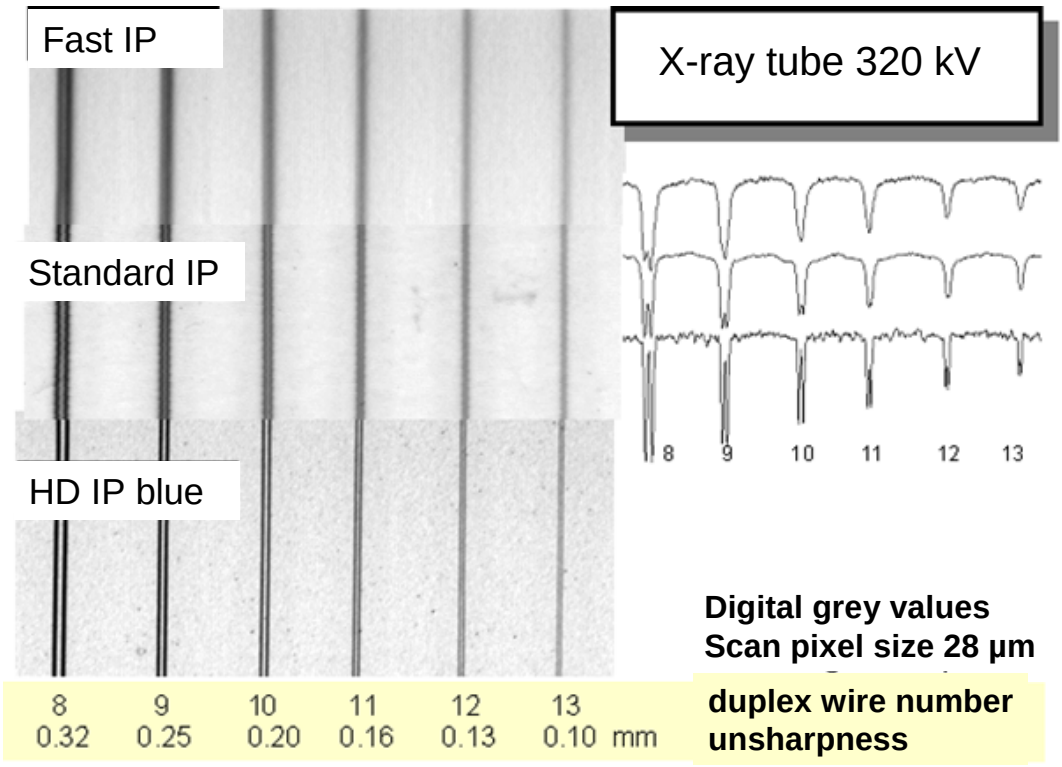

Fig. 6.7: Images of the duplex wire IQI (EN 462-5, ASTM E2002 or ISO19232-5) together with their profiles taken with different imaging plates. They were readout with a highly resolving scanner (DPS by AGFA). The resulting basic spatial resolutions ranged from 160 µm for Fast IPs via 100 µm for Standard IPs down to the better 50 µm for the blue coloured High Definition HD-IPs.

All imaging plates were exposed to 220 kV and readout with a AGFA-scanner with a resolution of 900 dpi (System AGFA DPS, 28 µm pixel size; laser beam of 40 µm). The Fast IP plates (ST-VN) are optimised for scanners with 100 µm pixel size. Standard IPs can be scanned with pixel sizes down to 50 µm and the High Definition IPs are scanned with pixel sizes as small as 20 µm for applications requiring a high resolution. The last one was capable to visualise all line pairs and had a spatial unsharpness better than 100 µm (MTF: 80 µm).

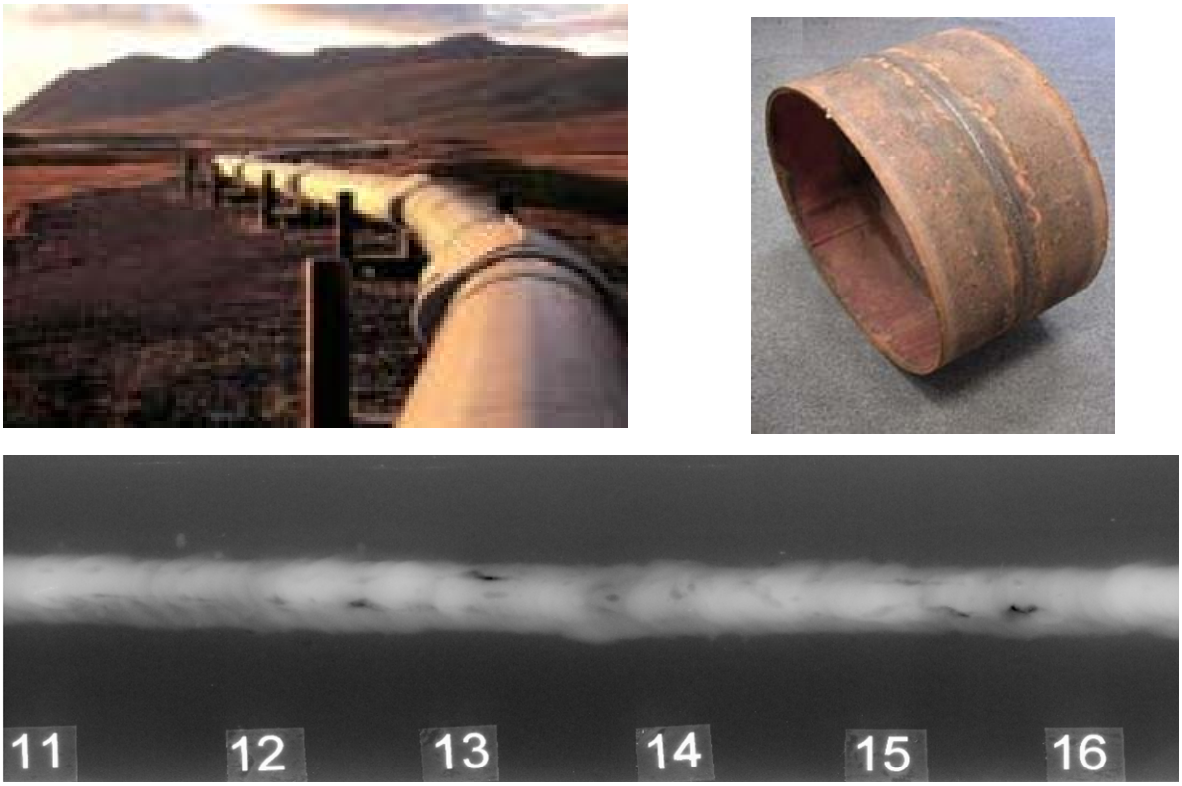

Fig. 6.8: Pipeline inspection with CR.

The blue high definition IP (HD-IP) is the slowest detector. As compared with the Fast IPs, it is by a factor of 100 times slower related to the same SNR, and with respect to the standardised SNR_N it was some 10 times slower. The standardised area (to which the SNR is normalised) has a size of $\mathbf{88{,}6 \cdot 88{,}6\ \mu m^2}$. The standardised SNR_N of all other (white) imaging plates is similar (applied range: 3 - 300 mAs). Exposure parameters: 220 kV, 936 mm FDA, 8mm Cu filter.

Experimental results show that the discussed advantage of a shorter exposure time really exists as compared to the film radiography with lead screens (see also fig. 6.4) when inspecting thick walled construction parts, in cases of working with energies greater than 300 keV or when applying Ir-192 or Co-60. Imaging plates with a high spatial resolution need exposure times comparable to those of conventional X-ray films but have the advantage that the result is already available in a digital format. The high resolving imaging plates can be applied for low energy applications as well as for weld seams inspections.

6.2.4 High definition CR for X-ray inspection of thin material components

Weld inspection with X-rays of thin components (< 12 mm) requires the application of high definition systems. These are CR systems with a pixel resolution ≤ 50 µm and a basic spatial resolution ≤ 60 µm. Fig. 6.8 shows a CR application for pipeline inspection. Systems are available which are equipped with long IPs for panoramic inspection ena-

bling fast and efficient testing. HD-CR inspection systems provide with similar exposure time as X-ray film adequate image quality. Due to the construction of the HD-IPs the exposure time cannot be shortened significantly to the film applications. For improvement of contrast sensitivity a reduction of the tube voltage by about 20 % is recommended. The new IPs with high normalised saturation SNR_N can be used even with higher kV than films. This is based on the compensation principle I as described in lecture 07. This allows the testing with shorter exposure time at sufficient image quality. Basically this can be reproduced for 2-2T testing (E1742) and class A testing (EN 444, ISO 5579).

6.3 Image intensifier and digital imaging

The X-ray image intensifier still is the most applied image converter for the industrial radiographic inspection until nowadays.

6.3.1 Principle of the X-ray image intensifier

The X-ray image intensifier (fig. 6.9) consists of a luminescent screen sensitive to X-rays at the front side which is made of CsI (caesium-iodide). This luminescent layer converts the radiographic image into visible light. The light generated by this causes electrons leaving the photo cathode. These are accelerated by an electrical field between the cathode and the electrodes of the so-called electron optics and directed onto the output screen. By means of a second fluorescent screen the electrons are converted back again into visible light to generate the final radioscopic image.

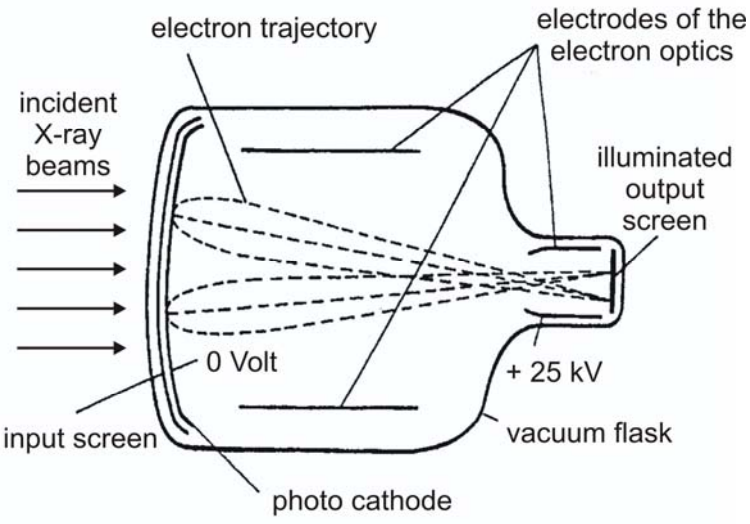

Fig. 6.9: Basic construction of an X-ray image intensifier

The amplification of the light intensity amount to some 10000 – 15000 times. The achievable image contrast is comparable to that of the radiographic film, in spite of the "online" image generation. However, this makes a rather noisy image. On the other hand, with the aid of digital image processing, the noise can be reduced considerably by

suitable methods in analogy to the prolongation of the exposure time in the film radiography (see also. L09, L11).

Admittedly, with an internal unsharpness (detector resolution) of some 0.3 mm, the image intensifier produces a noticeable lower spatial resolution as compared to the X-ray film. On the other hand, this can be compensated partially by a geometrical magnification. However, an improved perceptibility of details only can be achieved by the increase of the geometrical magnification if the effective focal spot of the X-ray tube used is sufficiently small.

Another possibility to enhance the perceptibility of details is the "zooming" function of the image intensifier. This means that the input field of the image intensifier is switched / reduced in size and thus a magnification effect is yielded at the output window.

The size of the input screen of the usual image intensifiers ranges between 6 and 12 inch (150-300mm) diagonally, whereas a margin of a considerable size has to be taken into account.

6.3.2 Image intensifier with CCD-cameras according to TV standards

The output image of the X-ray image intensifier is scanned by a TV camera and transferred to a monitor, or made available to an image processing system.

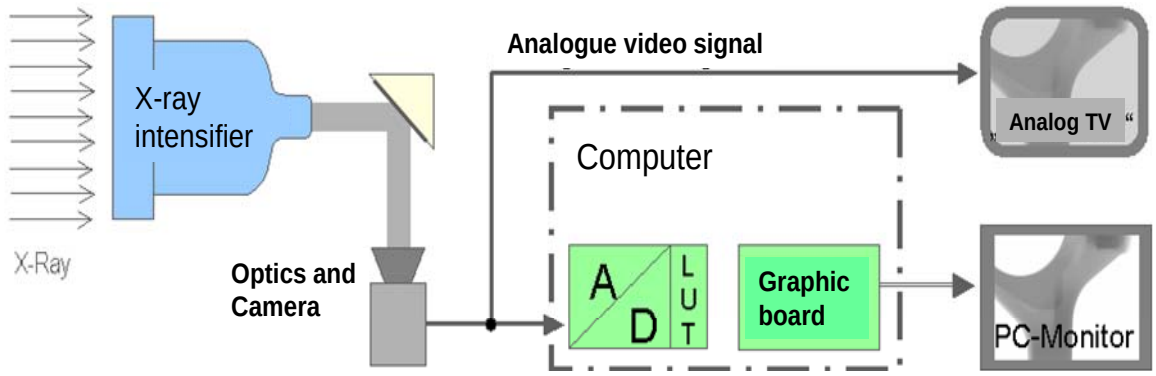

Fig. 6.10: Analogue camera attached at the image intensifier; presentation on a TV- or PC- monitor

The image signal is transferred usually in accordance to the TV standards:

- CCIR (Europe) with 50 half frames per second and 625 lines or
- RS170 (USA) with 60 half frames per second and 480 lines

The light intensity at the output screen of the image intensifier is imaged onto a CCD chip and is scanned line by line therein and converted into an electric signal (see fig. 6.10).

A high light intensity (white) is equivalent a high voltage level in the video signal (Figure 6.11). The individual video lines are separated from each other by line synchronising impulses. Within the period of 64µs per line the information is displayed for 52.48µs on the screen, the remaining time is needed for the return to the beginning of the line. The signal band width is limited to 5 MHz, so that 25 images/s can be transferred.

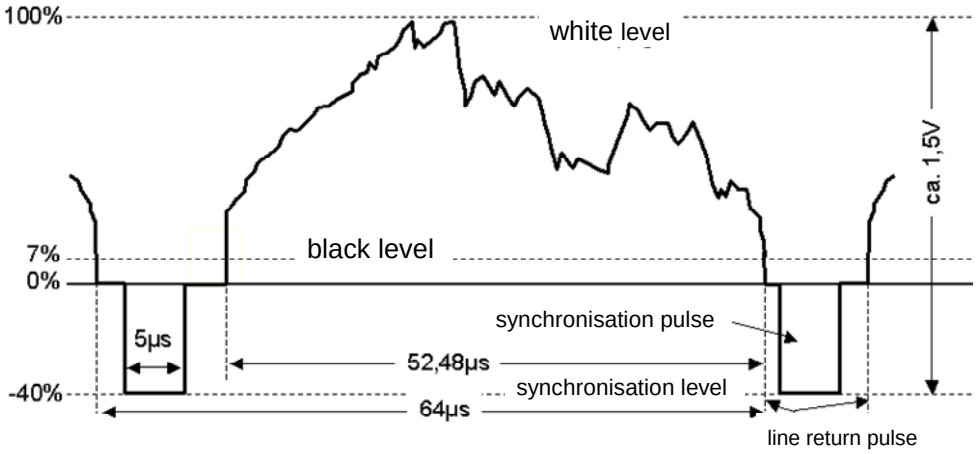

Fig. 6.11: Analogue Video-Signal according to CCIR
(somewhat more than just a line is shown)

Since 25 images per second only cause a strong flickering in the human vision, alternating only every other line is transferred within an image frame (line spacing technology) and displayed on the monitor. A complete ("full") image is composed of two half fames. Such a 50 Hz half frame frequency leaves an impression of a relatively flicker free image.

The electron tube cameras of earlier times have disturbing smearing effects (smearing when specimens are moved) so that they are used only for special applications (high radiation tolerance). Nowadays, **CCD-cameras** are mainly employed (Figure 6.12), which, among other advantageous properties, in particular feature a very low inertness.

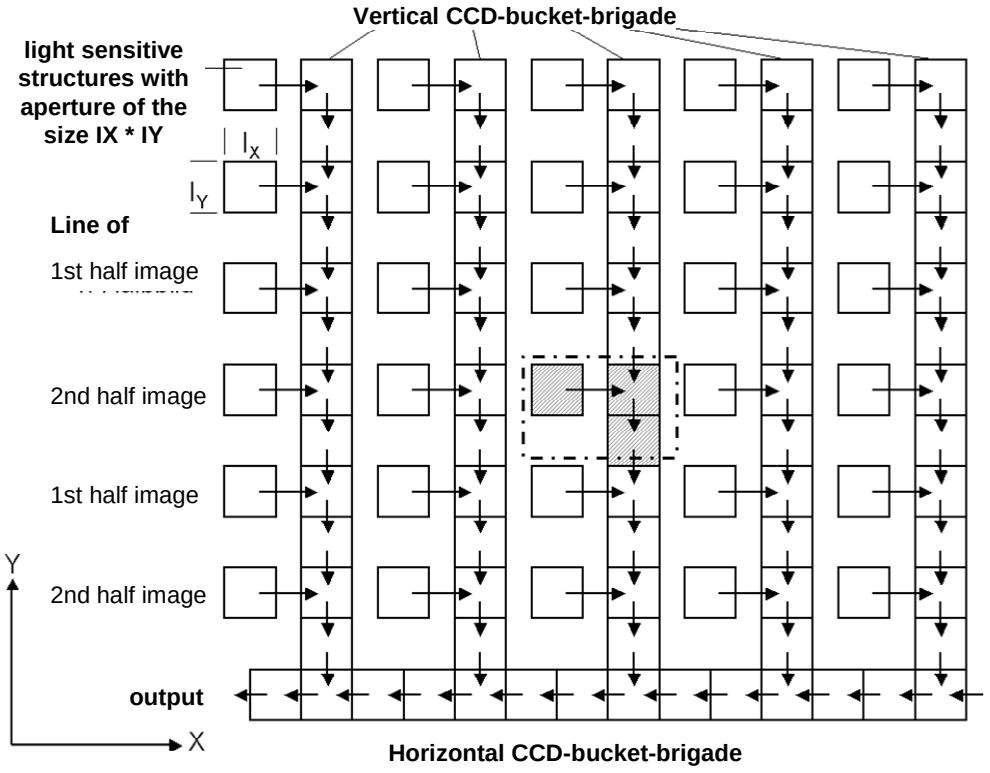

Fig. 6.12: Schematic construction of a CCD camera; frame: individual cell (pixel)

The CCD camera (**C**harge **C**oupled **D**evice) consists of discrete light sensitive elements. The typical number of image dots is 756 x 581 pixels (picture elements). As compared to the electron tube cameras, they are characterised by a somewhat lower resolution limit but a significantly better contrast transfer in the middle of the frequency range (see also L11). Since it features not only a low inertness but also a low tendency for blooming they now have become the standard camera for radioscopic inspection with image intensifiers.

6.3.3 Image intensifier with high resolution cameras

In order to combine the advantage of the fast image intensifier technology with that of a high resolution and the generation of digital signals as realised in the digital detector arrays (L07) the cameras according to the TV standard can be replaced by digital cameras (in most cases) that are capable to resolve more pixels than in the TV standard. As a consequence, these cameras cannot any more just be plugged simply into a TV-monitor but need a computer interface (e.g. USB 2, Firewire or Cameralink).

In order to take advantage of the higher resolution, the analogue signals are converted to digital ones already inside the camera and transferred via a digital interface to an image processing computer. The principle is shown in Figure 6.13.

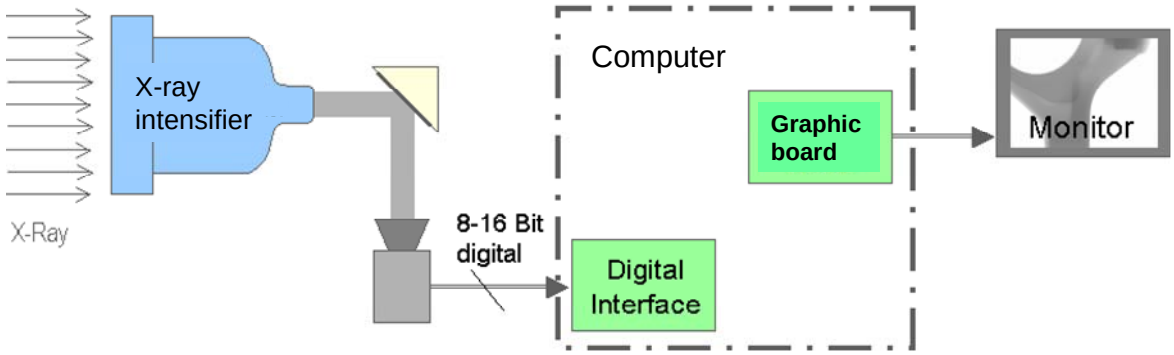

Fig. 6.13: Digital camera linked to an image intensifier

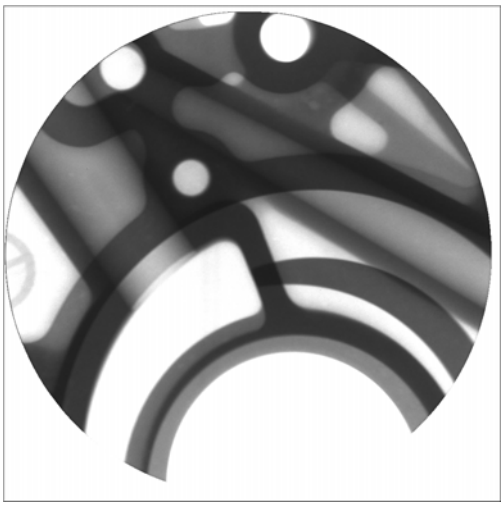

Fig. 6.14:
Image of a aluminium cast part taken with an II and a digital camera

In the following, some technical data are listed on digital cameras:

Active area	7.4 * 7.4 mm^2
Number of active pixels	1000 * 1000
Pixel size	7.4 * 7.4 μm^2
Geometric resolution	4 lp/mm (at 9" II und Zoom2)
Image repetition rate	30 Hz at 1000*1000 Pixel, 40MHz pixel clock
Basic noise	~ 40 electrons
Saturation capacity	~ 40 000 electrons
Signal-to-noise ratio	60dB (1:1000) at 30Hz operation
Image output	Digital, 12 Bit, LVDS (RS644) or Fire-wire

This table demonstrates that these digital cameras offer both a higher spatial resolution and high dynamics as well. Digital cameras in combination with an image intensifier could well be an alternative to digital detector arrays. The high image repetition frequency (real time image) and the moderate price make this advantage. The fact that it requires a lot of space, particularly in depth, has to be taken as a disadvantage.

Fig. 6.14 shows an image of an aluminium cast part taken with an image intensifier and a digital camera.

L 07 X-ray Sensitive Detectors II

Content

7.1 Digital detector arrays

The action principle of digital detector arrays is based on the conversion of the incoming X-rays into electrical charges that are electronically readable. Amorphous silicon (a-Si) is taken as an electrically semi-conducting material for this purpose.

Out of three different conversion principles

- the intrinsic method
- the direct method (conversion via photo conductors)
- the indirect method (conversion into light by means of a scintillator)

only the last two are applied practically for NDT. Each method has specific advantages and disadvantages showing limits for practical applications in imaging systems. In case of the indirect conversion methods, matrices of photo-diodes are employed which are able to convert the radiation (either X-ray or light) into electrical charges. In each photo diode, the charge carrier are integrated over a given time period before they are readout electronically for each single pixel followed by graphic presentation via a suitable data acquisition. Each photo diode is linked to an adjacent TFT switch (TFT = thin film transistor – see also laptop displays) that activates the readout process of the accumulated charges at a given point of time.

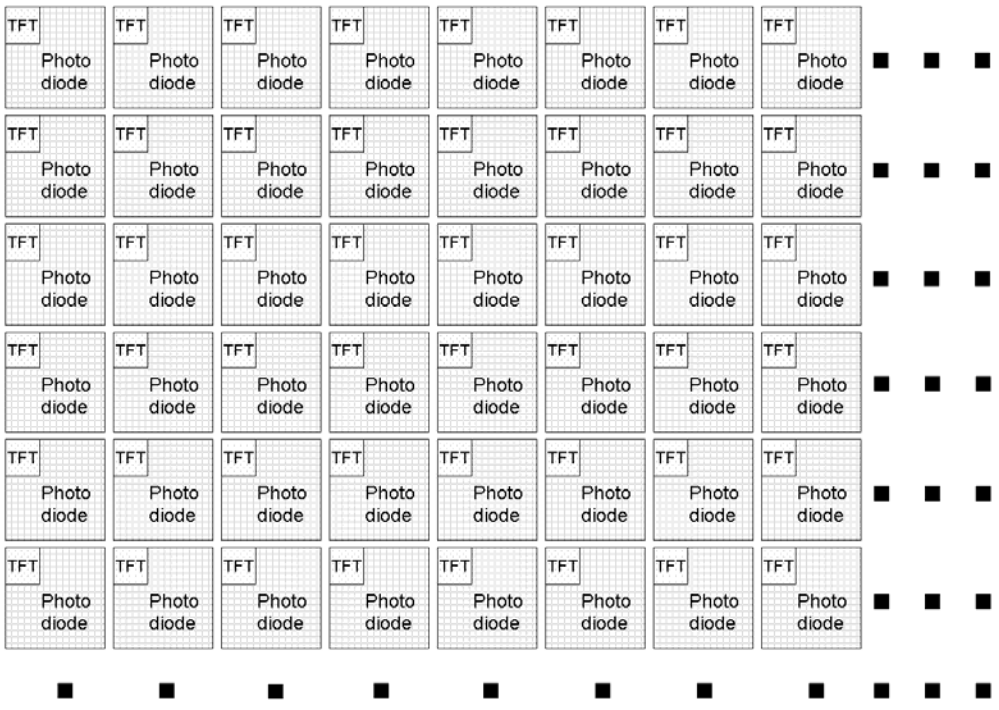

Fig. 7.1: Matrix principle of the arrangement of photo diodes in a digital detector array

The single TFTs are linked together line by line, and column by column, respectively, so the information of each single photo diode can be passed to the *supporting* electronics.

7.2 Intrinsic method

The so-called intrinsic method is based on a direct conversion of the radiation into electric charge carriers inside of a photo diode.

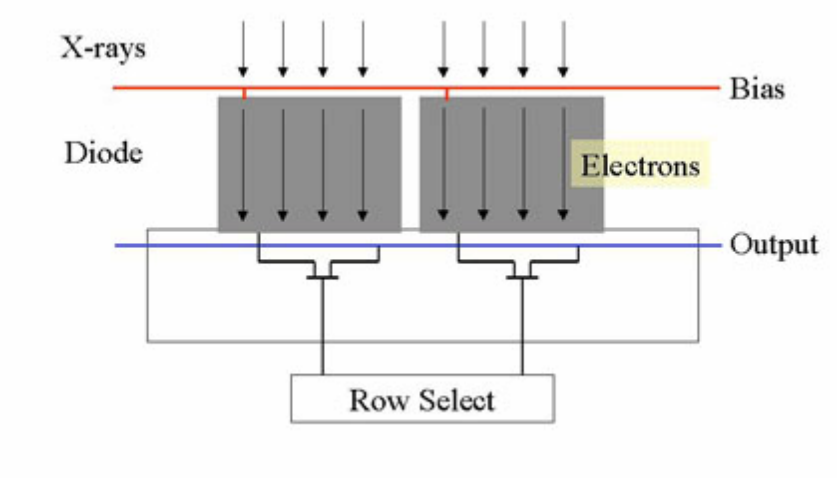

Fig. 7.2: Direct or intrinsic method

The X-rays generate so-called electron-hole pairs within a photo diode. The application of an initial voltage (bias) inhibits a recombination so that the charge carrier can be readout after a given time. Within the silicon, also thin film transistors (TFTs) are attached to the photo diodes to enable the readout of each single photo diode. They are controlled electronically by line and column selectors enabling the transfer of a signal proportional to the radiation intensity to a suitable data acquisition system followed by the display on a monitor.

Unfortunately, the absorption of X-rays is rather poor in silicon. For a typical thickness of a photo diode in the range of some µm, only X-rays with energies below 20 keV can be detected with sufficient efficiency.

7.3 Direct method with photo conductor

In order to gain a higher efficiency as compared to the direct conversion method, a material can be chosen that possesses better absorption characteristics and a higher absorption thickness. This material is attached onto the surface of the electrically conduction layers, and storing the charge carrier is supported by capacitors at these electrodes. The charge carriers need to be stored outside the actually photo-conducting conversion layer since otherwise an overflow to adjacent cell might be possible to occur causing unsharp and smeared images.

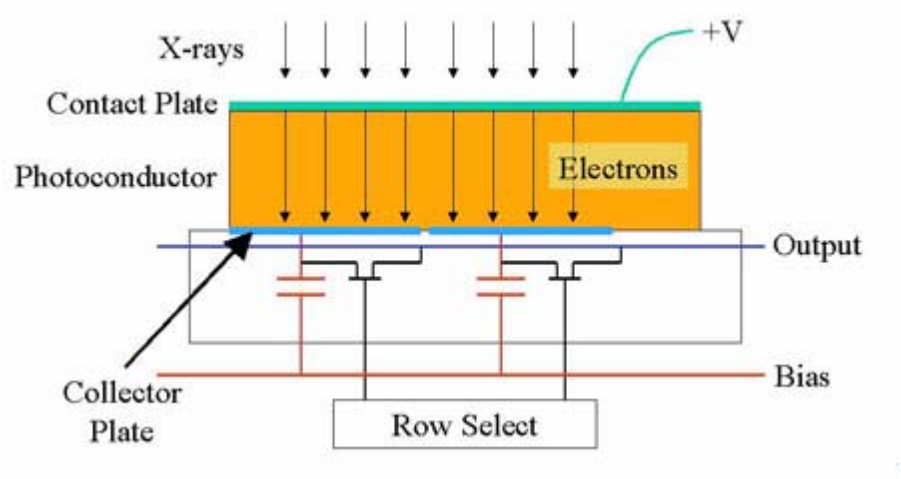

©Varian comp.

Fig. 7.3: Photo-conducting method

An initial tension *(bias)* of some 100 up to 5000 V is applied via a contact plate or layer to avoid a recombination of the charge carriers and to transport the charge carrier in a direct line to the electrodes at the same time. Again, the readout of the charge carrier is accomplished by thin film transistors that are controlled line by line or column by column.

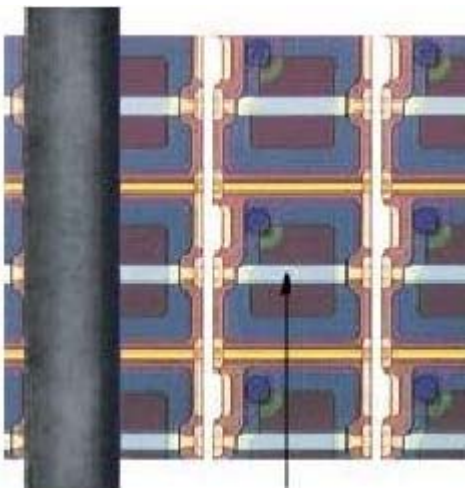

Fig. 7.4: a-Se detector Matrix structure of an a-Se detector

Currently, only one digital detector array is in production working with this a-Se conversion principle. Fig. 7.4 shows such a device, the matrix structure on right panel; a single element is marked with an arrow. A human hair is shown on the left side as a scaling reference. Selenium serves as the photo-conducting conversion layer that features a 10 times improved efficiency as compared to the direct conversion method, but still remains too poorly efficient for energies higher than 100 keV. In the meantime, materials with other conversion properties such as CdTe have entered the market.

The a-Se device features the following technical data:

a-Se layer, 500µm thick; 2560 · 3072 active pixels of 139 µm size; 14 bit digital converter; 300·400 mm^2 active area; 1..30s exposure time, 35s readout and correction time; max. X-ray voltage: 320 kV; *working* temperature range: 10 °C to 35 °C.

7.4 Scintillator method

By this means, a fluorescent layer (scintillator) is covering the amorphous silicon to convert the X-rays into visible light. Scintillator materials are mostly fluorescent substances such as gadolinium oxisulfide (product name: Lanex by Kodak or DRZ by Kasei Optonics).

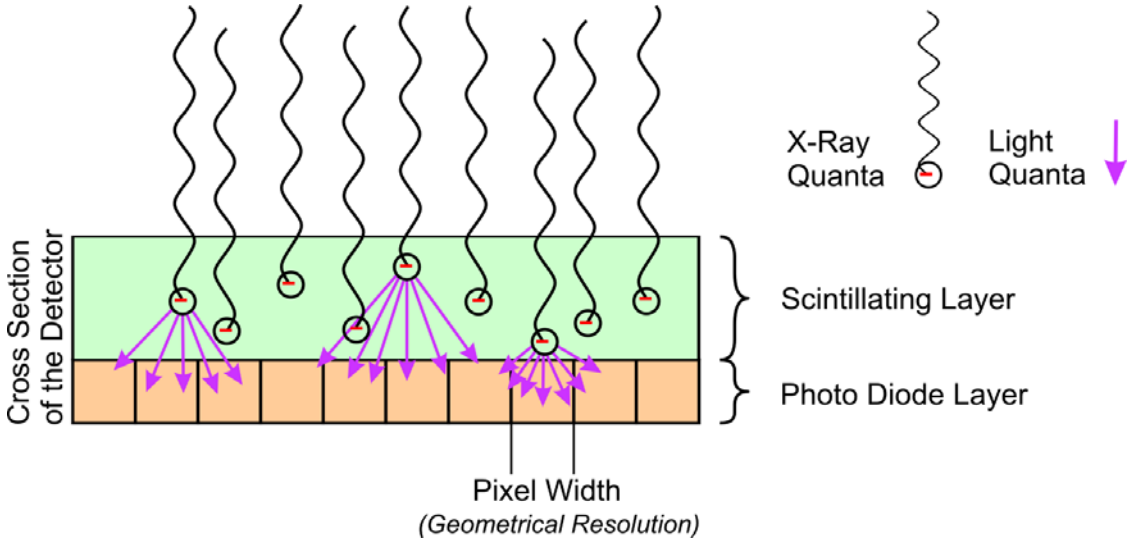

Fig. 7.5: Section through an a-Si detector with scintillator and a photo diode layer

Within the scintillator, an incident X-ray quantum generates multiple light quanta which are converted into electrical charges in the photo diode layer underneath. The thicker the scintillator layer the more X-ray quanta are absorbed and converted. Dissipating of light quanta arbitrarily into any direction causes an unsharpness: The light generated by a single X-ray quantum will be distributed onto several elements by numerous light quanta. Therefore, the thickness of the scintillator has to be chosen to suit the resolution of the detector (width of a single element) to balance optimal efficiency (-> low noise) with the least possible unsharpness (-> perceptibility of details).

A very good compromise between the essential spatial resolution and the light recovery is achieved by the use of a CsI scintillator. The property of CsI to crystallise in needle shaped structures entails that the light is dissipated only within the needle like structures and thus hits focussed just a single element. As a result, higher spatial resolutions can be achieved herewith.

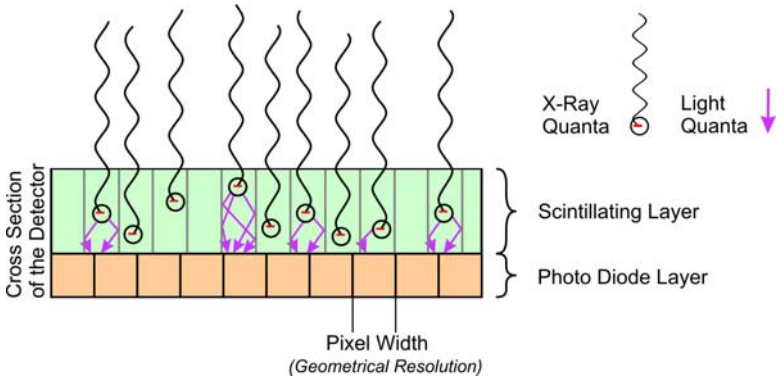

Fig. 7.6: a-Si detector with CsI scintillator showing a needle shaped structure Scintillator structure

The amorphous silicon can be covered with this scintillator substance up to a thickness of 1 mm. This results in a high efficiency in converting X-rays into light. A disadvantage of this structured CsI layer has become evident storing the information of a previous image for a longer time („ghost images“).

The silicon layer incorporates, in addition to the light sensitive photo diodes, also thin film transistors (TFT) to enable the readout of each single photo diode. They all are controlled electronically by means of line and column selectors, respectively, making the transfer of a signal proportional to the radiation intensity to a suitable data acquisition system followed by the display on a monitor.

A digital detector array consists of a million of light sensitive picture elements (pixels) arranged squared in a form of a matrix (Figure 7.1). The readout is achieved by the TFT switching the photo diode to the amplifying electronics followed by measuring the flow of charges that have been generated by the light.

Figure 7.7 shows a single pixel (dashed box) and the downstream electronics.

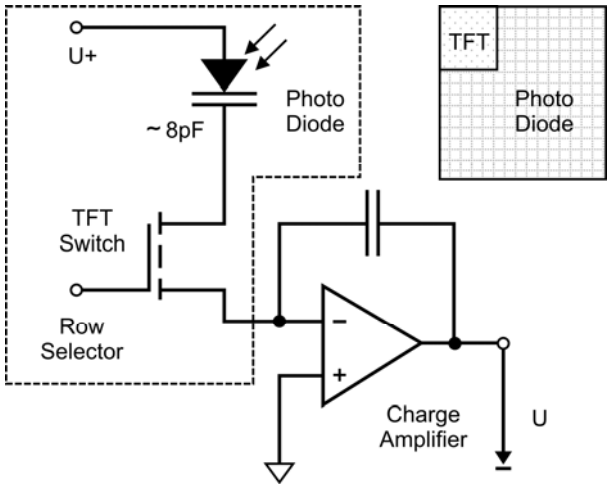

Fig. 7.7: Readout of a photo diode

At the beginning, the capacitor of the photo diode is fully charged. Any incident light discharges the capacitor of the photo diode. At the time of the readout the TFT interconnects. The capacitor is recharged by the readout amplifier; the amount of charges needed for this step is recorded in the capacity of the amplifier. In this context, a voltage U is generated proportionally to the amount of charges which subsequently is digitalised and associated to the pixel. The readout of a pixel lasts 10µs.

The capacitor of the photo diode is discharging itself even without light. Therefore, this loss of charge has to be determined individually for each pixel ("dark image"). This **offset image** will be subtracted subsequently from each image to neutralise this offset.

The individual degrees of efficiency of all photo diodes and the slight variations of the readout electronics from line to line and from column to column results in an amplification individual for each pixel. This has to be determined and will be needed for the image correction **(gain image).**

Digital detector array are offered with various pixel sizes and dimensions (see Table 7.1). The weight of a digital detector array amount to some 8 – 10 kg and thus comes noticeably below that one of an X-ray image amplifier. With respect to the depth of the casing which is less than 100 mm the digital detector arrays are flatter than the image amplifiers.

Currently available a-Si detectors are based on materials developed for medical applications. In 2003, two different basic versions have been realised, one with 127 µm and another one with 200 µm and. 400 µm, respectively. Several providers have assembled their products incorporating one of these two versions.

	Detektor 1	Detektor 2	Detektor 3	Detektor 4	Detektor 5	Detektor 6
Pixel Area / mm	195*244	284*406	284*406	205*205	410*410	410*410
active Pixel Matrix	1408*1888	2240*3200	2240*3200	512*512	1024*1024	2048 * 2048
Pixel Size	127µm	127µm	127µm	400µm	400µm	200µm
geometrical Resolution	4 Lp/mm	4 Lp/mm	4 Lp/mm	1.2 Lp/mm	1.2 Lp/mm	2.4 Lp/mm
A/D Conversion	12 Bit	12 Bit	14 Bit	16 Bit	16 Bit	16 Bit
Energy Range	40 - 150 kV	25 - 160 kV	25 - 160 kV	20 - 160 kV	20 - 450 kV	20 - 450 kV
Scintillator	CsJ	Lanex	CsJ	Lanex Fast	Lanex Fast	CsJ
dynamic range	1000 : 1	1000 : 1	2200 : 1	14000 : 1	14000 : 1	12000 : 1
Sensitivity (quantum efficiency)	high	high	high	medium	medium	high
Image Lag (Geisterbilder)	high	medium	high	low	low	medium
Output time for n integrations	2s + (n*50ms)	3,4s + (n*3400ms)	1,7s + (n*1700ms)	134ms+(n*134ms)	134ms+(n*134ms)	267ms+(n*267ms)
Readout time to PC per frame	50ms	3400ms	1700ms	134ms	134ms	267ms
Mechanical Size of the detector	266,7*317,5 mm	500*366*46 mm	500*366*46 mm	330*320*63 mm	330*320*63 mm	330*320*63 mm
Weight of the detector	8,2 kg with lead cap	9 kg with lead cap	9 kg with lead cap	8,5 kg with lead cap	18kg with lead cap	19 kg with lead cap

Table 7.1: Overview on a-Si detectors (status 2006)

In general, detectors with a larger area per pixel are less noisy since more quanta per time period hit a single pixel.

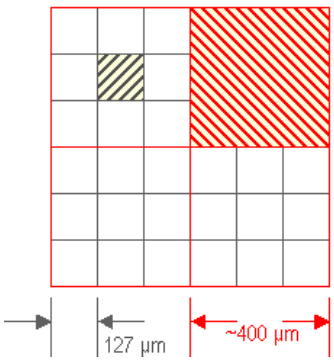

A pixel of the 127 µm dedetcor has an area of 0,0161 mm^2. A pixel fo the 400 µm Detektor has an area of 0,16 mm^2 an thus receives nearly ten times more quanta in the same time. The price for this is a geometric resolution that is worse by the factor of three. To provide the capacity for a larger number of quanta, higher resolving digital converter are provided in this type of detectors (16 bit); in comparison, most 127 µm detectors only have a 12 bit converter. As a consequence, the high resolving detectors are used preferably in weld testing while the 400 µm detector mainly is applied for the inspection of cast components where the contrast range and the short readout times are of bigger importance.

In spite of several disadvantages, the a-Si detectors utilising the scintillator method represent currently the most prevalent technology for digital detector arrays. Their price is

significantly higher than that one of the X-ray amplifier what is restricting their area of application. Enabling even an acceptable price in spite of the sophisticated technology and manufacturing processes has been made possible only by the mass production in electronics and of a-Si structures. This also forms the basis for the screens of laptop PCs (just principally operating the other way round).

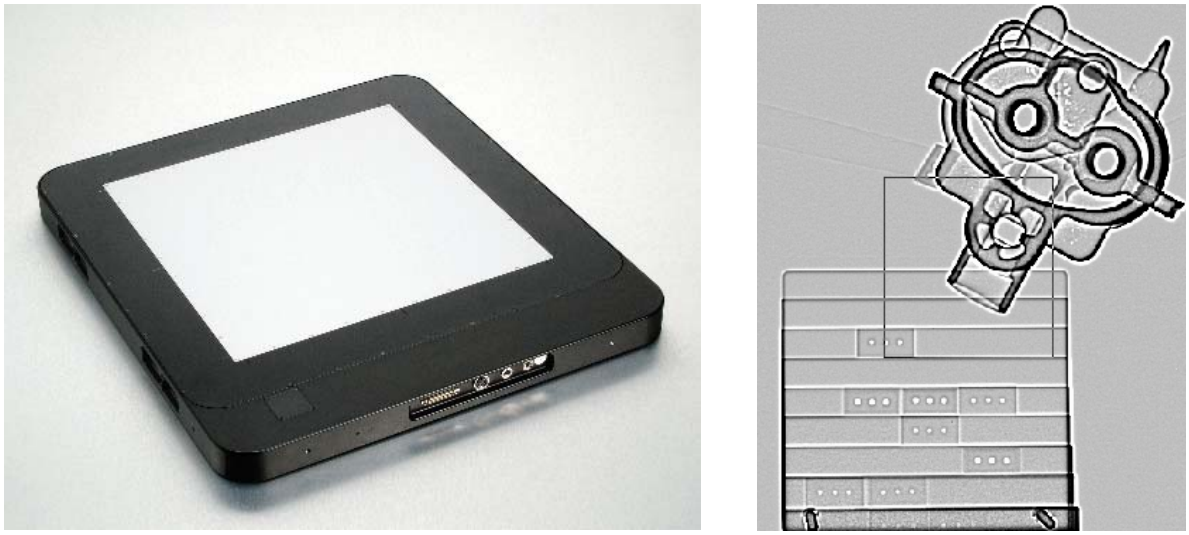

Fig. 7.8: a-Si detector Nr.5 ; 80mm step wedge with diaphragms (high pass filtered)

7.5 CMOS digital detector arrays

CMOS (Complementary Metal Oxide Semiconductor – field effect transistor technology with oxide-insulation) laminar detectors are matrix oriented CMOS photo diodes meshes (Figure 7.1) and have found an application in this form also in digital cameras. The pixel size of a CMOS detector arrays can be larger than that of CCD sensors that allows omitting magnifying optics (see L06). On the other hand, the size of a pixel is smaller than that on of the a-Si detectors with photo diodes and TFT.

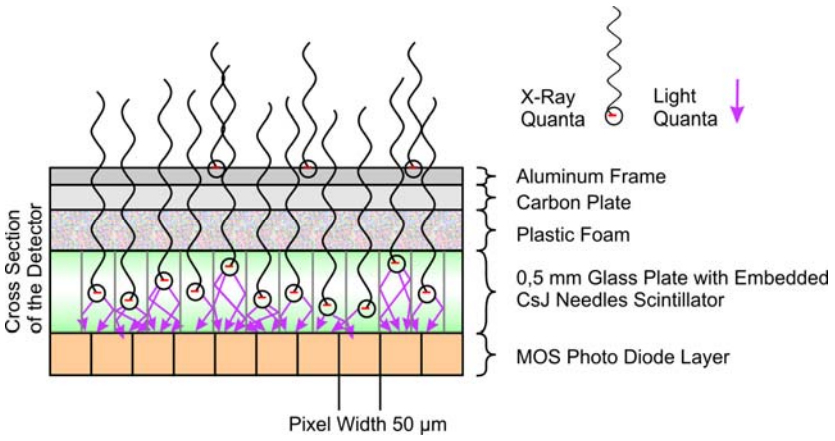

Fig. 7.9: Section through a CMOS detector with a CsI scintillator

The section through the detector (Figure 7.9) shows large similarities with the a-Si detector. A particularly selected scintillator has to be chosen because of the small pixel size; in this case, these are CsI:Tl crystals (s. Figure 7.6, right).

Though this technology has been realised for large series (digital cameras) there are only few systems found in radioscopic applications. The size of the pixel in such systems is 50-100 µm, the readout time for a single image with full resolution amounts to ~ ½ s and the data are processed with a 12-bit converter. The active area ranges from 50*50 mm^2 to 220*180 mm^2. Due to the optimisation of the production of semiconductors filling factors (ratio of the areas of the photo diodes over those of the other electronics per pixel) of 80% are achieved even with 50µm detectors. The CMOS systems currently available produce a considerable electronic noise. The superb resolution makes these detectors being used particularly in specific applications where structures of <100 µm need to be visualised without employing a µ-focus instrument.

Fig. 7.10: CMOS detectors with 50 µm pixel size (max. 8lp/mm resolution)

7.6 A radioscopic system with a digital detector array

The whole system consist of the X-ray sensitive detector itself, a connecting cable, the power supply and the readout electronics with the data acquisition to produce the X-ray image on a monitor. For this purpose, an industry PC is taken normally nowadays (s. a. V8).

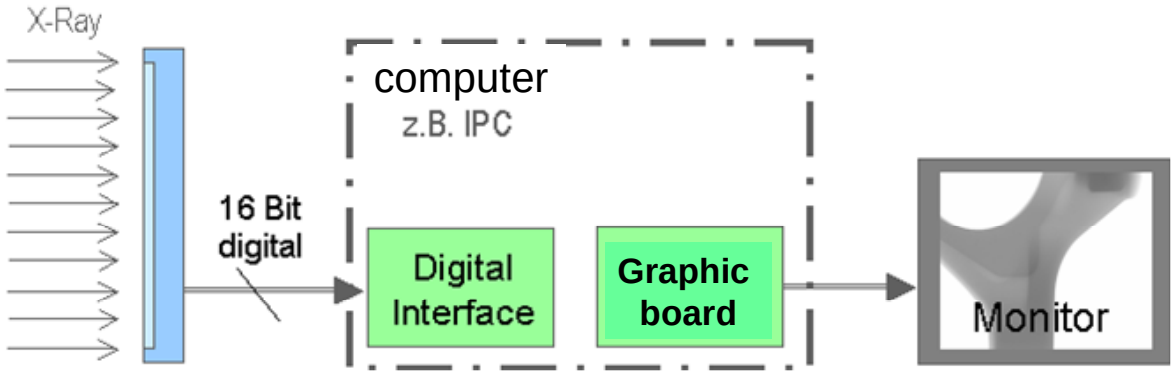

Fig. 7.11: Radioscopic system with digital detector array

The sensitivity of the individual pixels varies arising from the production of the digital detector arrays. In addition, changes in the temperature also have an influence on the detector performance. By this reason, the detector needs to be calibrated periodically (gain and offset adjustment). This is accomplished automatically for each single image by most of the programs.

Moreover, it is unavoidable in the production of photo-diode-semiconductor plates that some pixels are left producing no relevant signal („Bad Pixel“). When calibrating the detector prior to a series of measurements, these pixels are identified and their response is replaced by the mean of the adjacent ones.

7.7 Compensation principles

Contrast-to-noise (CNR) management is the key element for image quality control in digital radiology. Modern DDA calibration techniques allow an extraordinary increase of CNR in comparison to all other digital detectors and film. Contrast reduction due to increase of X-ray energy can be overcompensated by noise reduction. This enables the reduction of acquisition time and increase of the thickness range per radiograph. Even limitations in the spatial resolution, constrained by the individual picture element (pixel) size of the detector, can be compensated with an increased CNR. Bad pixel management of DDAs in combination with CNR enhancement enables the safe application of this technology for film replacement. Considering these points, three compensation principles have been formulated for the implementation of DDAs as a viable film replacement technology:

1st Compensation of reduced contrast (μ_{eff}) by increased signal-to-noise ratio (SNR): If optimization of contrast cannot be achieved, the noise must be reduced (i.e., in-

creased SNR). If contrast can be increased, there is more tolerance for higher noise (moderate or lower SNR can be used).

2nd Compensation of insufficient detector sharpness (high unsharpness) by increased SNR.

3rd Compensation of interpolation unsharpness, due to bad pixel correction, by increased SNR.

7.7.1 General remarks

Contrast-to-noise ratio (CNR) management by increase of radiation dose and specific DDA calibration allows an extraordinary increase of contrast sensitivity [1]. It is obvious that a higher CNR permits the visualisation of smaller defects which inherently have a smaller contrast. **The high contrast sensitivity technique** was developed to improve the testing quality and to prove the compensation principles [1].

7.7.2 Compensation Principle I:

Compensation of reduced contrast (μ_{eff}) by increased signal-to-noise ratio (SNR)

The image quality in digital industrial radiology depends on the product of effective attenuation coefficient μ_{eff}, also called specific contrast, and the signal-to-noise ratio (SNR). This applies for CR, DDAs and X-ray film. Fig. 7.12 illustrates the effect of noise on flaw detection.

The contrast-to-noise ratio (CNR) per wall thickness difference Δw, which is the essential parameter for the visibility of flaws and IQIs of a given size, can be calculated from the detector response (SNR) as a function of exposure dose as follows (small flaws only, see Fig. 7.12):

$$CNR/\Delta w = SNR \cdot \mu_{eff} \qquad (1)$$

Typical IQIs as plate holes (ASTM E 1025) change the hole diameters with its thickness. Therefore, its hole visibility depends on the image unsharpness and the achieved CNR. If the hole diameter is much larger than the unsharpness, the equivalent IQI sensitivity (EPS, defined by IQI thickness in % of the penetrated material thickness for 2T hole visibility) changes proportional to about $1/\sqrt{SNR \cdot \mu_{eff}}$.

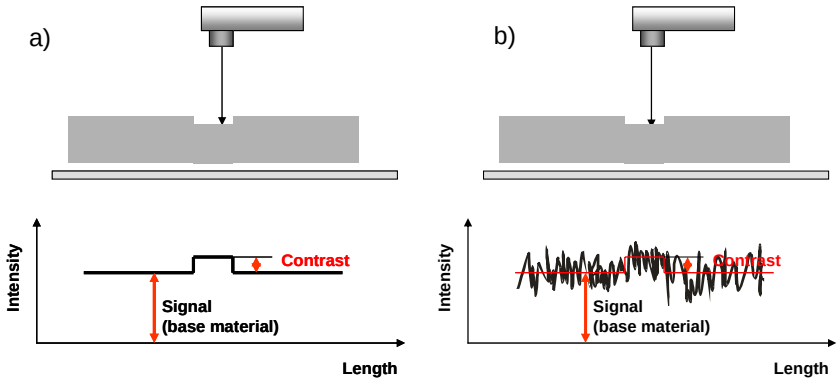

Notch visible!

Contrast/Noise is high
Signal/Noise is high

Notch not visible!

Contrast/Noise is low
Signal/Noise is low

Fig. 7.12: The influence of noise on the visibility of a notch in radiography
a) the notch is visible if the noise contribution can be neglected,
b) the notch is not visible if the noise is just higher than the contrast.

Since the gray values of the pixels in the digital images (assuming signal is linear to dose) depend on noise and signal intensity independent of the contrast and brightness processing for image viewing, the SNR has been proposed and accepted as an equivalence value to the optical density and a certain film system in film radiography (EN 14784-1,-2 and ASTM E 2445, E2446).

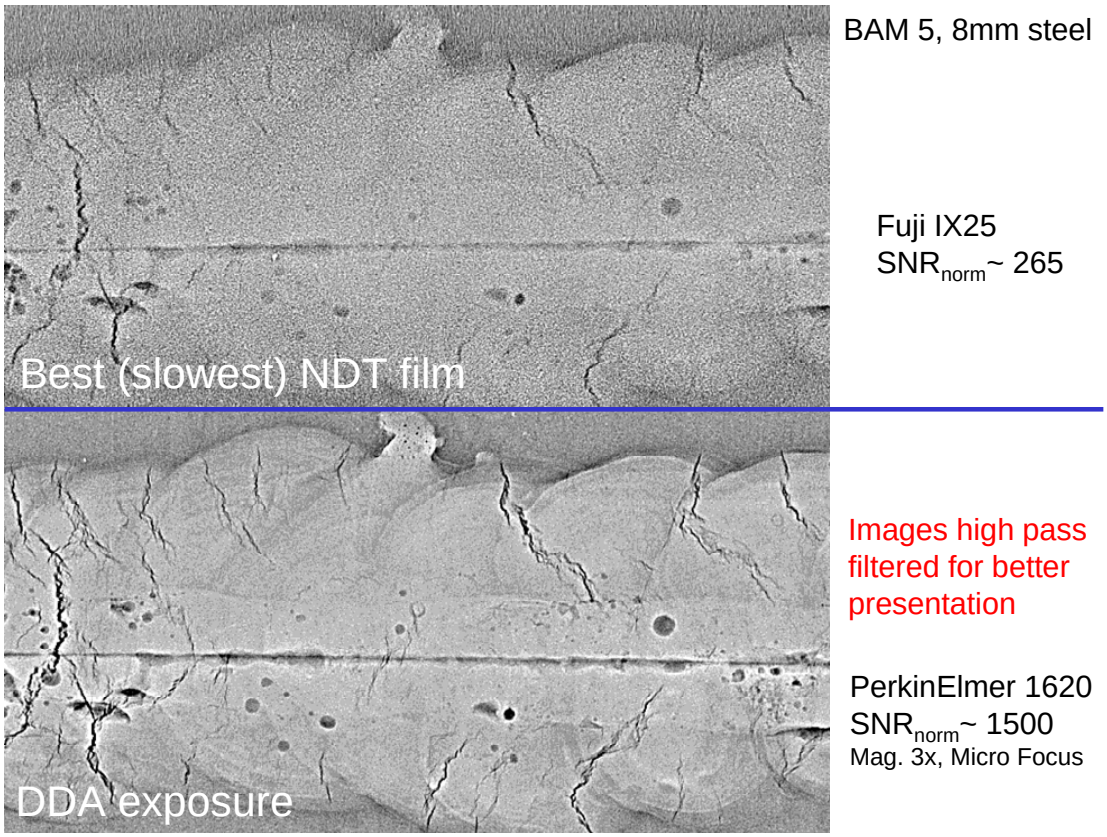

Fig. 7.13: High Contrast Sensitivity Technique: Better detail visibility of flaws by increased SNR of DDA image in comparison to digitized film image of test weld BAM 5.

Four typical noise sources arise in radiography:

- Photon noise depending on exposure dose (e.g. mA·s or GBq·min)
- Structure noise of detector
- Crystalline structure of material (e.g. nickel based steel, mottling)
- Surface roughness of test object

The first two noise sources can be influenced by the exposure conditions and detector selection. The achieved Signal-to-Noise Ratio (SNR) of images depends on the exposure dose (low dose application). The SNR increases with the square root of mA·minutes or GBq·minutes, due to the improved photon quantum statistic. The structure noise of films and imaging plates depends on its manufacturing process and can be influenced basically by the selection of the specific detector type (e.g. fine or coarse grained film). Film development and IP scanner properties contribute also to the final noise figure. The structure noise of detectors and all noise sources depending on the object properties determine the maximum achievable SNR and limit, therefore, the image quality independently on the exposure dose (high dose application). Only with DDAs can the structure noise (due to different properties of the detector elements) be corrected by a calibration procedure, since the characteristic of each element can be measured quite accurately. Fig. 7.13 shows the effect of SNR increase (equivalent to CNR increase) to the visibility of fine flaw indication. The digitized fine grained film provides a SNR of 265 in the base material region. The DDA image was measured with a SNR of about 1500. It shows significantly more fine flaw indications.

In film radiography, it is well understood that the image quality increases if the tube voltage is reduced. In DR, it can also be observed that the image quality increases in a certain range if the tube voltage is increased. The higher photon flow (X-ray intensity behind object) increases the SNR in the detected image faster than the reduction of the contrast by the decreased transmission contrast (also known as specific contrast or effective attenuation coefficient μ_{eff}). This effect depends on the ratio of attenuation decrease to SNR increase (see also eq. 1) since the product of SNR and μ_{eff} controls the contrast sensitivity in the digital radiograph. The effect has been observed if DDAs are used for film replacement. Well calibrated DDAs can be exposed typically at higher tube voltages than films. However, too high a tube voltage may even reduce the attenuation faster than the SNR increases. The maximum achievable SNR is the limiting parameter for the described compensation. It depends on the detector efficiency and the detector calibration of DDAs or the structure noise of imaging plates. It also depends on the noise of the material's structure and the material roughness. Therefore, the compensation by increase of the tube voltage is restricted depending on the detector and material properties and especially on the maximum achievable SNR in the radiograph.

Fig. 7.14a shows a typical example for the compensation of decreased contrast (μ_{eff}) by increased SNR. A step wedge with ASTM E 1025 IQIs (2%) was exposed at different X-ray energies and mA minutes with a constant source to detector distance. The visibility of the 2T hole (denoted with 2 in Fig. 7.14b) was achieved with increasing kV of the tube at shorter exposure time. This cannot be achieved with X-ray films, since they will always be exposed to an optical density between 2 and 4. In this case, the films of a given class always have the same SNR in a small range due to its specific manufacturing process. The increase of the tube voltage from 80 kV to 150 kV allows finally the reduction of exposure time down to 20% for digital radiology in the example of fig. 7.14. All thickness steps of the test object can be inspected with one exposure at 150 kV. The steps with the

smallest thickness are even radiographed with 2-1T quality. Here, the tube voltage increase yields a higher efficiency and an increased thickness range based on the digital “high CNR” technique.

7.7.3 Compensation principle II:

Compensation of insufficient detector sharpness (high unsharpness) by increased SNR.

The European standard EN 14784-2 requires the application of high definition CR systems for X-ray inspection with pixel sizes of less than 50µm for class B inspection (for wall thickness <12 mm and tube voltages <150 kV). Most available systems do not allow a resolution below 50µm pixel size and are excluded for industrial X-ray applications in Europe. Recent trials have shown that DDAs provide a better image quality and IQI visibility than industrial X-ray films [1, 2]. In a high contrast sensitivity mode the DDAs achieve better IQI reading than film exposures. This effect is observed when sub-pixel contrast resolution is achieved. This is the case, if the SNR at the detector is increased considerably. If a wire or crack is smaller than a pixel, it still influences the contrast and can be seen in the image if the contrast is sufficiently higher than the noise. Therefore systems with insufficient spatial resolution can be applied if their high unsharpness is compensated by increased SNR.

Fig. 7.14a: Step wedge of steel with ASTM E 1025 IQIs for determination of image quality.

80kV	1 mA min	2 mA min	5 mA min	10 mA min	20 mA min
0,05 in	1	2	1	1	1
0,07 in	4	2	2	2	1
0,10 in	-	2	2	2	1
0,12 in	4	4	2	2	1
0,15 in	-	-	2	2	2
0,20 in	-	-	-	2	2
0,25 in	-	-	-	-	4

100kV	1 mA min	2 mA min	5 mA min	10 mA min	20 mA min
0,05 in	2	1	1	1	1
0,07 in	2	2	1	1	1
0,10 in	2	2	1	1	1
0,12 in	2	2	1	1	1
0,15 in	4	2	2	1	1
0,20 in	-	4	2	1	1
0,25 in	-	-	1	?	1

150kV	1 mA min	2 mA min	5 mA min	10 mA min	20 mA min
0,05 in	2	1	1	?	?
0,07 in	2	1	1	?	?
0,10 in	2	2	1	?	?
0,12 in	2	2	2	1	?
0,15 in	2	2	2	1	1
0,20 in	4	2	2	1	1
0,25 in	4	2	2	1	2

Fig. 7.14b: Achieved IQI quality (smallest visible hole of 2% IQI. It means: 1: 1T hole, 2: 2T hole, 4: 4T hole) as function of kV, mAmin and wall thickness in inch for test object in accordance to fig. 7.14a.

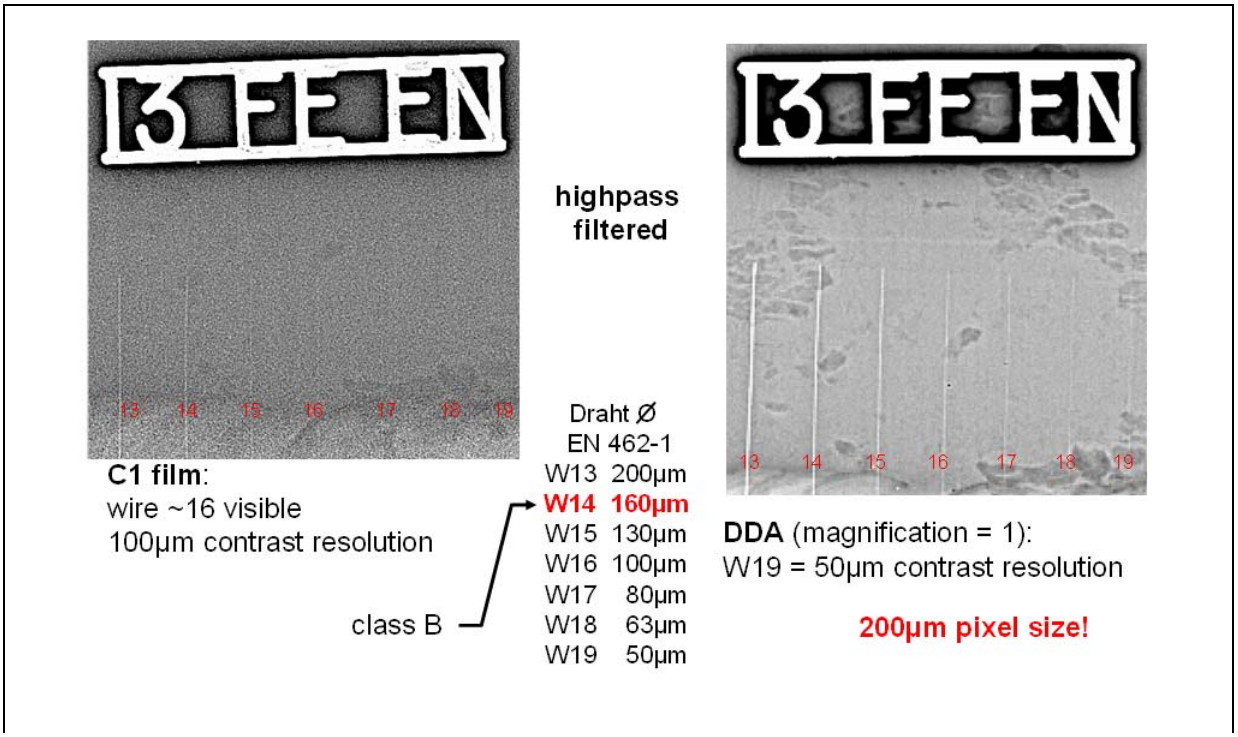

Fig. 7.15: Comparison of visibility of wire type IQIs according to EN 462-1 for film (left) and DDA (right) at 8mm wall thickness (images high pass filtered for better visualization). The improved SNR of the DDA allows to detect the wire W19 (50 µm diameter) at a detector pixel size of 200µm without magnification technique!

It is proposed, to permit the application of unsharp systems, if the visibility of the required wire or step hole IQI is increased by compensation of missing duplex wire resolution through SNR enhancement (see EN 462-5, ASTM E 2002 and requirements of EN 14784-2). Several new standards define minimum duplex wire values for specific applications (e.g. ISO/DIS 10893-7, prEN 1435-2). Typically, one higher (smaller diameter, see EN 462-1) single wire (resulting in higher contrast sensitivity) shall be seen through adjustment of parameters that increase the SNR if an additional duplex wire of spatial resolution is required in the system qualification for a given material thickness and application. It was proposed in CEN TC 138 WG 1 that the compensation should allow maximum 2 wires vs. wire pair compensations. The compensation should be applicable to plate hole IQIs too. This is still under discussion.

This effect has been proven with Perkin Elmer's XRD 1620 detector in combination with YXLON's "Image.3500" software. Even at a magnification of 1 and a basic spatial resolution of 200µm (pixel size), the significantly increased SNR of the DDA allows the detection of crack indications which are hidden by noise in the film image with its much better basic spatial resolution SR_b of 40µm. Fig. 7.15 shows the radiograph of an # 13 wire IQI on a 8 mm steel plate. The radiographs were high pass filtered for better graphical presentation. The digitized film shows wire number 16 and the DDA image shows wire number 19 being visible, which has a diameter of 50 µm. Therefore, the detector shows the wire 19 indication with a sub-pixel resolution.

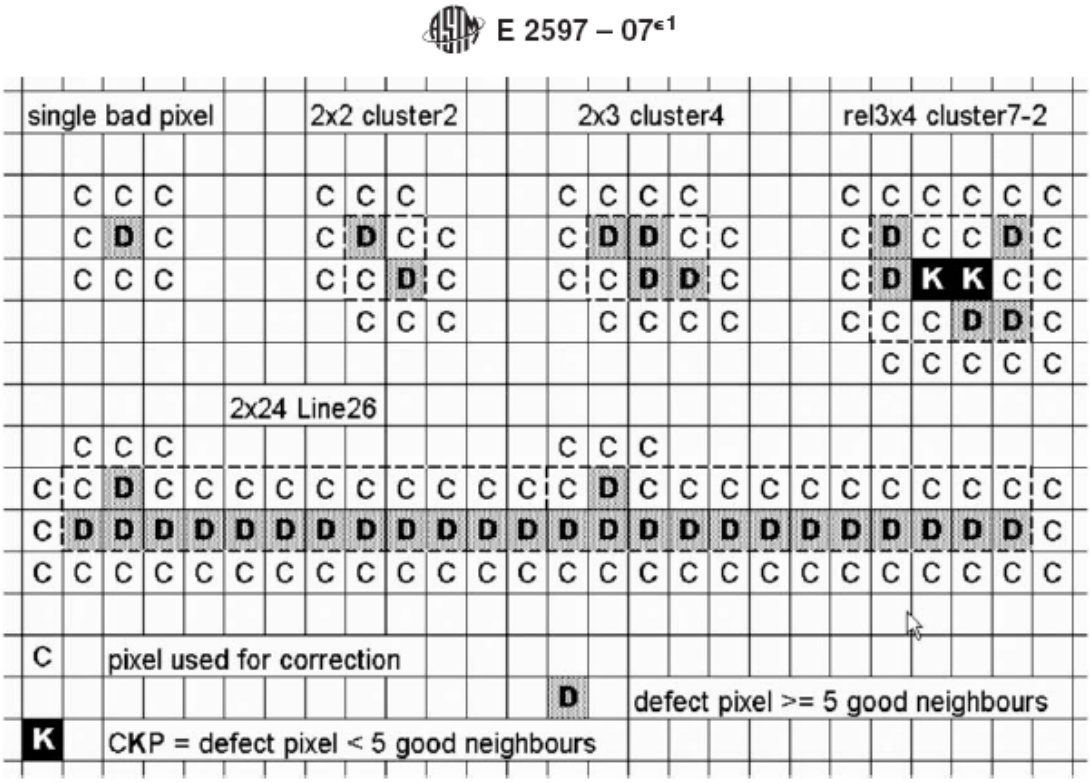

FIG. 7.16: Different Types of Bad Pixel (D) Groups: Cluster, Relevant Cluster, and Bad Line

7.7.4 Compensation Principle III:

Compensation of interpolation unsharpness, due to bad pixel correction, by increased SNR.

The appearance of bad pixels in digital detector arrays has been a controversial topic that has been discussed at length in various standard committees – for instance, ASTM E 2597 defines the different types of underperforming and dead pixels. Generally, the correction of bad pixels is permitted if at least five good pixels can be used for interpolation. Cluster kernel pixels (CKP) are defined as shown in Fig. 7.16, and are not well correctable according to the criterion of E 2597. In praxis all manufacturer offer also corrections for small clusters. The interpolation of bad pixels can reduce the contrast of very small indications as illustrated in Fig. 7.17. The interpolation of the defect pixel reduces the contrast by 15% and the adequate reduction of noise is only achieved indirectly by an increase of the SNR – for instance, an increase of the SNR to 265 will be sufficient to visualise the interpolated indication.

The required CNR for the digital radiographs depends on the ratio of the detectable flaw size to the cluster size of bad pixels. Fig. 7.18 shows a recommended practice for the management of bad pixels and required increase of SNR and corresponding CNR. As mentioned in the section above, increasing CNR and SNR may enable smaller defects to be detected. Figure 7.18 provides guidance on this dependence, as well as the dependence of these metrics on bad pixel management. In Fig. 7.18 three zones are distin-

guished: Best practice zone, zone with risky detection, and zone of negative detection. It shall be noted that there are no exact CNR values agreed on for the limiting lines in Fig. 7.18 yet.

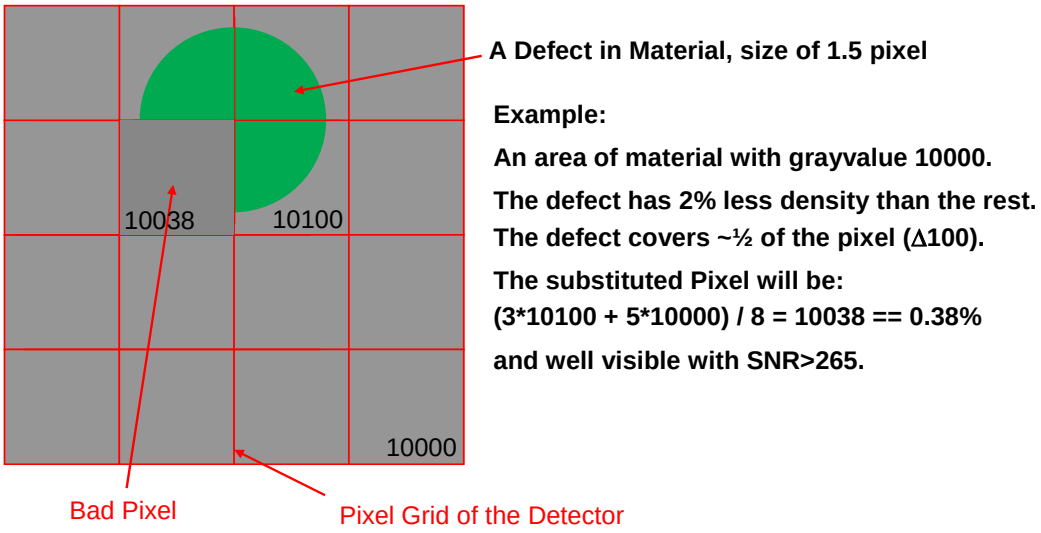

Fig. 7.17: Effect of bad pixel interpolation. The interpolation reduces the contrast of the final indication. The increase of the SNR compensates the CNR to the value of the intact detector image.

The required SNR for the best practice can be recommended as follows: For example, if film and digital detector are applied at the same kV and the specific contrast (μ_{eff}) is comparable, it is sufficient to require a minimum SNR (see eq. 1). Typical SNR values for best practice in film radiography are 150 for fine grained films (at net density =2), and 75 for coarse grained films. Since DDAs have typically higher unsharpness than films, an adequate increase of SNR is recommended. Here, the concept of normalized SNR_N can be applied, and the recommended SNR shall be increased as follows:

$$SNR_{recommended} = SNR_N \cdot \frac{SR_b}{88.6\mu m} \qquad (2)$$

with SR_b – basic spatial resolution (definition see e.g. ASTM E 2597)

If the film application (coarse grained film) provides SNR_N > 75, the adequate DDA radiograph taken by a detector with 200µm effective pixel size (SR_b=200 µm), should exhibit a SNR > 170. This should apply for the last two areas in fig. 7.18 (right side of fig. 7.18 beginning with: isolated bad pixels and irrelevant clusters); best practice line. The SNR selected will depend on the available time allotted to the inspection, and can so be improved using DDAs if time is available to do so. The required minimum SNR depends on the X-ray energy and may vary if compensation principle I and II are applied. The final proof of image quality requires always the visibility of the agreed IQIs as in classical radiography.

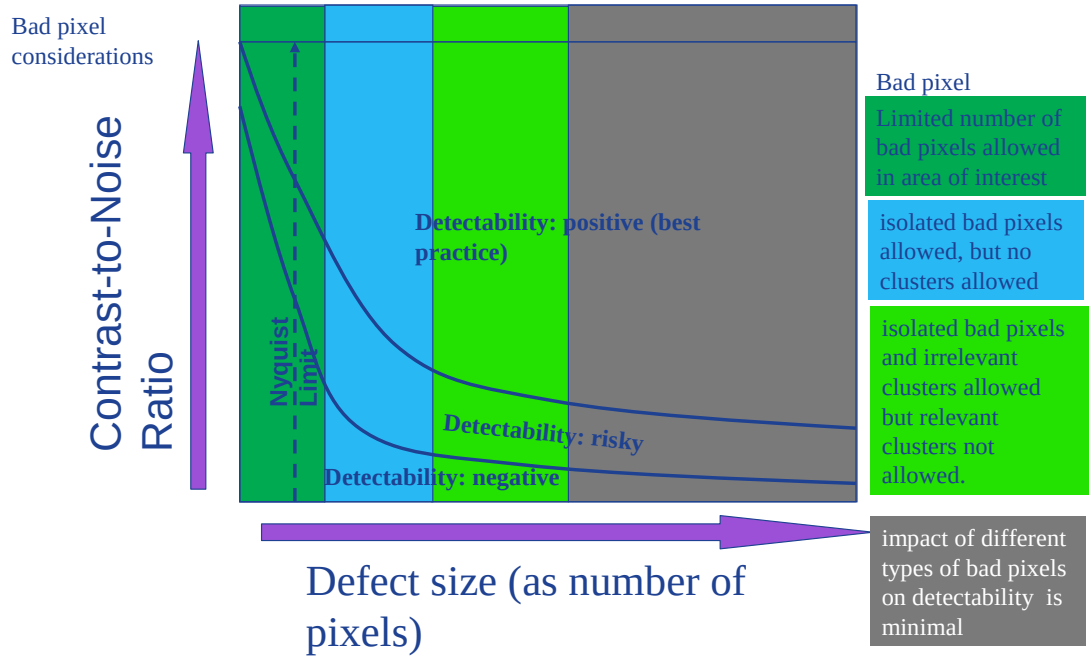

Fig. 7.18: Recommended praxis for selection of minimum SNR for DDA applications with bad pixel management.

7.7.5 References:

[1] Klaus BAVENDIEK, Uwe HEIKE, YXLON International, Hamburg, Germany, William D. MEADE, BOEING Commercial Airplane Group, Seattle, USA, Uwe ZSCHERPEL, Uwe EWERT, BAM, Berlin, Germany, New Digital Radiography Procedure Exceeds Film Sensitivity Considerably in Aerospace Applications, 9th ECNDT, Berlin, 25.-29.9.2006, [2] C. Bueno, A. D. Matula, "Digital Radiography for Gas Turbine Components", Proceedings from ASM Gas Turbine Materials Conference, 12-15 October 1998, Rosemont, IL. P. J. Maziasz; I. G. Wright; W. J. Brindley; J. Stringer; C. O'Brien, editors. ASM International, Materials Park, OH, pp. 119-122.

[2] C. Bueno, A. D. Matula, "Digital Radiography for Gas Turbine Components", Proceedings from ASM Gas Turbine Materials Conference, 12-15 October 1998, Rosemont, IL. P. J. Maziasz; I. G. Wright; W. J. Brindley; J. Stringer; C. O'Brien, editors. ASM International, Materials Park, OH, pp. 119-122.

You should know:

Three compensation principles are recommended for the radiographic practice with digital detectors - e.g. digital detector arrays:

1st Compensation of reduced contrast (μ_{eff}) by increased signal-to-noise ratio (SNR): If optimization of contrast cannot be achieved, the noise must be reduced (i.e., increased SNR). If contrast can be increased, there is more tolerance for higher noise (moderate or lower SNR can be used).

2nd Compensation of insufficient detector sharpness (high unsharpness) by increased SNR.

3rd Compensation of interpolation unsharpness, due to bad pixel correction, by increased SNR.

These compensation principles have been proven for DDA applications. Compensation Principle I enables the reduction of measurement time and an increase in wall thickness range by increasing the X-ray energy in a certain range which reduces the contrast but may be compensated through its improved SNR through greater penetration. The increased SNR yields a wide range of overcompensation of the contrast reduction if the kV is increased compared to film radiography. Compensation Principle II describes the improved visibility of wire and step hole IQIs, as well as flaws with increased SNR. Wires with smaller diameter than the detector pixel size could be visualised. Compensation Principle III is applied to improve the detectibility, through enhanced SNR, of a defect if a portion of it is covered by a correctable bad pixel, and interpolation is used to correct that pixel or cluster of pixels. The increase of the SNR is dependent on the relation of defect cluster size to detectable flaw size. Detailed guidelines are under development.

L 08 Image Processing Systems - Design

Content

8.1 Hardware-setup of an image processing system*

An image processing system essentially consists of the units

- detector interface
- image processing computer unit
- output device

Today, special computer systems with expensive hardware designed for image processing are on necessary any more since the computational power of the actual industry PCs are capable to accomplish most operations of the image processing sufficiently fast.

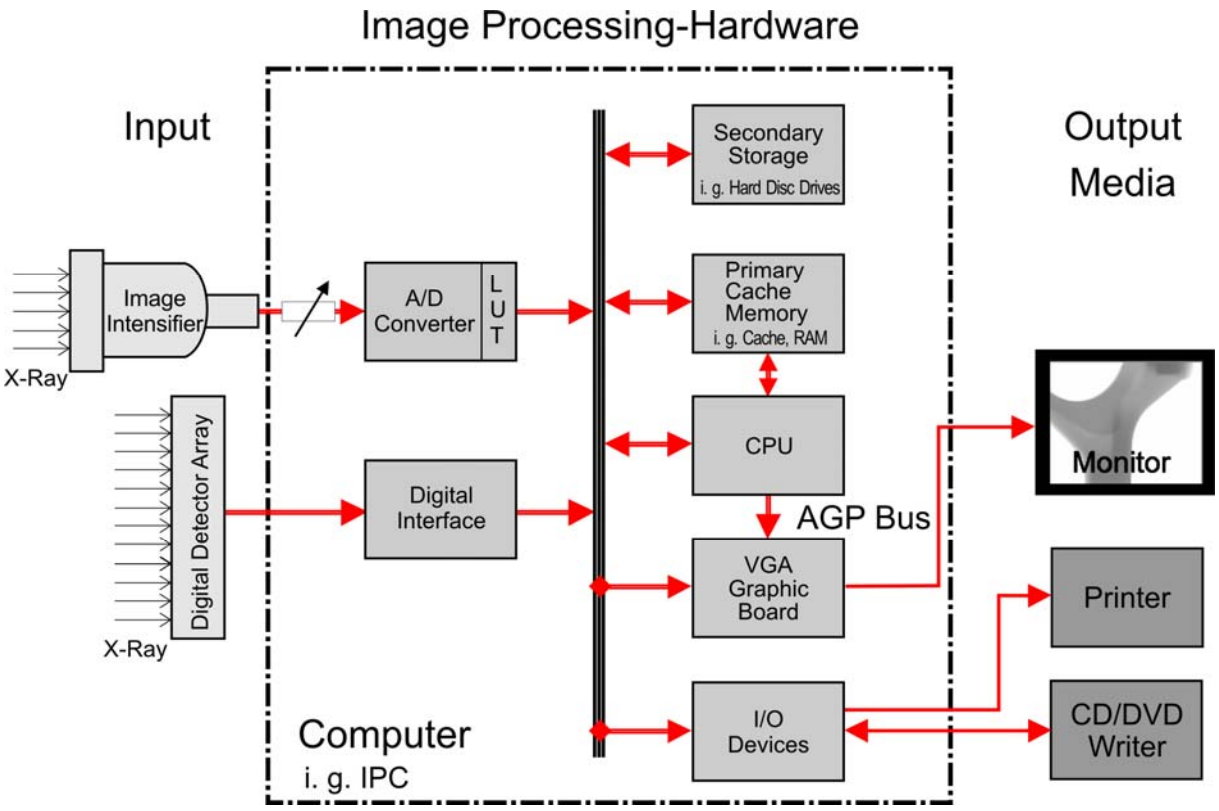

Fig. 8.1: Hardware-design of an actual image processing system

* Status of 2008

8.2 Image signal interfaces

The image signals transferred to an image processing system during an X-ray application are generated either by a camera based image Intensifier (II) or by a digital detector array that are capable to convert the X-rays directly into digital output signals without the aid of a vacuum tube.

The images from image intensifiers are transferred in the format of video images. Normally, this is an analogous signal carrying the image information line by line to the computer (connecting digital cameras is accomplished as described for digital detector arrays). In this case, the image signal interface consists of an analogue-digital converter which converts the signal coming form the camera into discrete and digital picture elements (8 bit per pixel in most cases). The analogous images are discretised in the plane and in a scale of grey values. During this quantisation process a so-called quantisation noise is generated by rounding effects of the scanned values that limits the signal-to-noise ratio. Such a unit consists of a circuit board for the PC; in addition to the A/D conversion, these boards could also achieve an adaptation of the signal intensity (adjustable via software) and are able to fit the digital output signal via a look-up table (LUT) to the desired brightness and contrast. These units subsequently transfer the image to the main memory of the computer. The image size is of 768x574 pixels in most cases according to the CCIR TV-standard; thus an image takes some 440 kbyte of memory.

Commonly, the images from a **digital detector array** have a higher intensity resolution (12 to 16 bit per pixel) and have to be transferred in a digital format to the computer by reasons of interference resistance. Accordingly, the interface for the image signals is a digital one that has the function to transfer the data image by image to the main memory of the computer. The size of the image depends on the type of detector with a spatial resolution ranging from 512 x 512 to 4000 x 4000 pixels. The memory size of the smallest format (512 x 512) amounts to 0.5 Mbyte when having a 16 fit resolution, in case of 4000 x 4000 pixels already 32 Mbyte are necessary for a single image. Just for information: the geometrical resolution of detectors ranges from 400 µm down to 50 µm.

8.3 Bus system

The image processing computers are provided with a system bus that operates with a high transfer rate and cares for the communication between all components of the computer and the exchange of data within the computer. Contemporary industry PCs apply the PCI or PCI Express bus that allows data transfer rates of > 100 Mbytes/s (PCI Express up to 3 Gbytes/s); at an image size of some 0.5 Mbyte it is possible to transfer more than 200 images per second by this way – the TV standard entails 25 images/s.

8.4 Main memory

The image data as well as the program data for the image processing and the operating system are stored in the main or system memory. The size of the memory amounts to some Giga bytes, the access time to each element is less than 10 ns. The size of the main memory is sufficient large to accommodate comprehensive programs and several large images at the same time.

The main memory is a pure semiconductor memory and thus impermanent. I.e. that all data stored in the main memory are lost after switching off the system. As a consequence, it is mandatory to have further storage facilities to save the data permanently.

8.5 Permanent memory

All data of interest for a longer period and therefore should be available also after a system restart are saved in permanent memories. This encompasses the image data for archiving as well as the programs e.g. for image processing. The operating system is also kept in a permanent memory so that the computer has access to meaningful information at a system start-up.

The magnetic disk (hard disk) has bee established as the information storage medium; the usual size ranges around 1000 Gbyte (1,000,000 Mbyte). This gives room for some 1,000,000 images (subtracted the space for programs and the operating system). The data transfer rates reach 100MByte/s in case of large amounts of data; the rate is reduced to <10 Mbyte/s if smaller amounts are transferred.

8.6 CPU

The CPU (Central Processing Unit – main processor) takes over all calculation work in the system. At the same time, it controls all activities in the system including the input and output procedures.

In parallel to the image processing the CPU also can take over other tasks such as the control of the mechanics of an automatic inspection device. In this case, it is recommended to equip the computer with multiple CPU cores which communicate with each other via the system bus so that they can share the tasks. Contemporary operating systems such as MS-WINDOWS or Linux support the multi processor and multi core operation so that the user does not need to worry about the sharing of tasks.

8.7 Image presentations

The user interacts with the computer via the monitor, the key board and the computer mouse. All the responses of the system upon commands entered by the key board or the mouse are displayed to the user on the monitor. This device will be used also to display the processed image in the current image processing systems. This common utilisation allows the presentation to the user's direct view of both, the image itself and also the control panels which are placed preferably closer to the margin of the screen to keep the central area reserved for the pictorial display. Beside the well known (analogous) tube monitors, the (digital) TFT displays are gaining more and more relevance; they exhibit the advantage of an image free of distortions, a higher contrast and, if realised as plain black and white monitors, a higher light density.

Fig. 8.2: Presentation of an X-ray image together with control panels on the same screen

In systems with an image intensifier and a TV camera also the analogue video signal can be displayed directly on a (TV) monitor in addition to the presentation of the digitalised and processed image.

Hint:

The optimal adjustment of contrast and brightness of a monitor should be achieved with the aid of a test image or with the illustration of a step wedge e.g. Figure 8.3 shows an example of a test image following the SMPTE RP133-1991.

(SMPTE = society of motion pictures and television engineers in the USA)

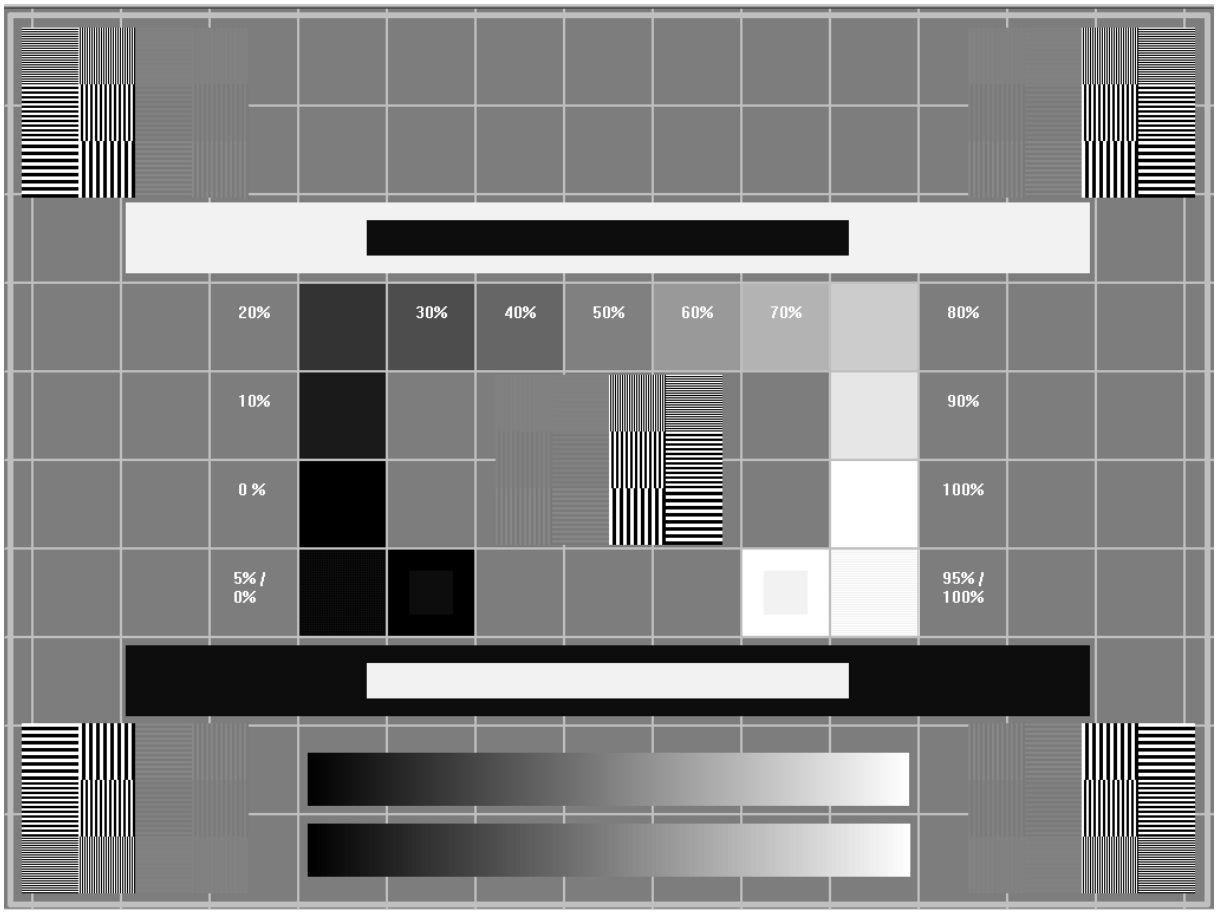

Fig. 8.3: Example of a suitable test image to check the monitor adjustments

8.8 Image archiving

The resulting images can be archived, alternatively to the hard disk, also on other media. The classical way would be on paper, not as a photograph this time but as a printout. A more efficient way, combined with optimal quality, to save the images would be digitally on CDs or DVDs, respectively.

The printout on paper is achieved by a printer. Two different principles are provided as realised in the laser printer and the ink jet printer. The laser printer is very fast and prints on nearly all kinds of paper in comparable quality; on the other hand, it scans the image and converts the grey levels into a density of tiny small black dots. The ink jet printer is capable also to print grey levels and achieves – provided having a good quality paper – the best printing results for the price of being slower (some 10s per image). When archiving on paper it has to be taken into account that a loss of quality has to be accepted during printing and paper printouts will loose quality with time (paper becomes yellow and the printing dye is bleaching out).

The archiving on CDs or DVDs is achieved by means of DC/DVD recorders, also called burners. The media are very close to the music CDs and the video DVDs, respectively. The providers of such media guarantee a life expectance of some 20 to 30 years without any loss of data. Having saved the data digitally on CD/DVD the full information can be retrieved any time in full length (an can be printed out by means of an image processing program). The usual size of a CD is 640 Mbytes that accommodates some 1300 video images. On a DVD, eight times more information can be stored than on a CD. The table of the content of CDs/DVDs keeps rather efficiently records the images provided a meaningful allocation of file names. Additional archiving software enables retrieving fast and reliably a nearly unlimited number of image data.

The low prise of blank CDs/DVDs has made other storage media such as streamer tapes, video tapes, removable magneto-optical disks etc. practically obsolete, they are applied rather rarely.

8.9 Image formats

Numerous formats exist for the storage of digital images. The following have been establishes for standard usage:

TIF oder TIFF **T**agged **I**mage **F**ile **F**ormat; available in numerous versions that are not always compatible with each other. The actual image information is preceded by a header that entails information about the format used. The images can be stored compressed lossless.

BMP Windows **B**it**m**a**p** format; the image data are stored line by line, mostly uncompressed.

JPG oder JPEG **J**oint **P**hotographic **E**xpert **G**roup; Images in the JPEG format are compressed lossy in most cases. Compressing is achieved by cutting off stepwise the information which is barely perceived by the human eye (lossy). Compression rates of up to 50 are in use. This method is being used for X-ray images only if the image size matters and for illustration purposes, not for real image evaluation!

JPEG 2000 **JPEG2000** is based on the wavelet compression in which the images are stored in different resolution levels. JPEG2000 is capable to save either lossless (factor ~2.5) or lossy (up to factor 100). In difference to the “normal lossy JPEG” less artefact appear in JPEG2000 and no more margins can be seen at the borderline of boxes as it may be the case in “normal” JPEG.

DICONDE Emerging standard NDT data format based on DICOM (Digital Imaging and Communication in Medicine), see http://www.nema.org.

In ASTM E 2339 (Standard Practice for **D**igital **I**maging and **Co**mmunication in **N**on**d**estructive **E**valuation (DICONDE) definitions are given for suitable modifications of DICOM for application in NDT. Beside the raw image itself also additional image, inspection and object information is stored in one binary file via extended DICOM tags

In addition to these formats many manufacturers use their own formats which are rarely exchangeable. Particularly for the storage of images derived from digital detector arrays having a grey value range of >8 bits, these special formats are in use by reasons of efficiency.

L 09 Image Acquisition and Pre-processing

Content

9.1 Image acquisition

The image acquisition is the first step of image processing. It is essential to under stan exactly all parameters of the image acquisition for a quantitative image evaluation or assessment. The way from the object to the digital image in the memory of an image processing system can be divided into three separate steps:

- **Visualisation:** the attenuation of the X-rays caused by the *specimen*
- **Imaging:** the three-dimensional *(spatial)* object is projected onto a two-dimensional image plane
- **Digitisation:** the continuous image is converted into a matrix of discrete values of picture elements (pixels). The existing continuous intensity values have to be mapped into a set of grey values (quantisation)

Note: The image acquisition determines the image quality. The subsequent image processing only is capable to visualise or to emphasise what is already present in the image *information*.

9.2 Image specification

Based on the quantum nature of the X-ray radiation a noticeable noise is visible in the X-ray image – depending on the radiation intensity and the readout time of the detector. By this reason, statistical terminology is frequently employed to characterise the image data.

9.2.1 Mean and standard deviation

The mean value is calculated by summing up al individual grey values either within an area of interest or of the total image followed by the division by the number of the averaged grey values.

mean: $$\bar{x} = \frac{1}{N}\sum_{i=1}^{N} x_i$$ denoting: X_i – grey values

N – number of grey values

Whenever X-raying e.g. a homogeneous material the result will be, because of the presence of noise, a distribution of values around a certain mean rather than a constant grey value. More descriptively, the mean value denotes the average grey value of an image or of an area of interest.

The standard deviation s is a parameter for the distance of individual grey values from the mean. The larger the value of s the more the values are scattered around mean value and the broader is the distribution of grey values (s. a. 9.2.2 histogram).

standard deviation: $$s = \sqrt{\frac{1}{N-1}\sum_{i=1}^{N}(x_i - \bar{x})^2}$$

9.2.2 Histogram

The histogram presents graphically the frequency distribution of the grey values within an image or an area of interest. As such it is a valuable tool to analyse an acquired image.

In accomplishing the histogram function the frequencies of the individual grey values are counted within the whole image or an area of interest. These values are subsequently presented in a diagram: The number or frequency, respectively, of the grey values is plotted on the ordinate and the individual grey values on the abscissa. The presentation of the histogram may throughout have various formats (Figure 9.1).

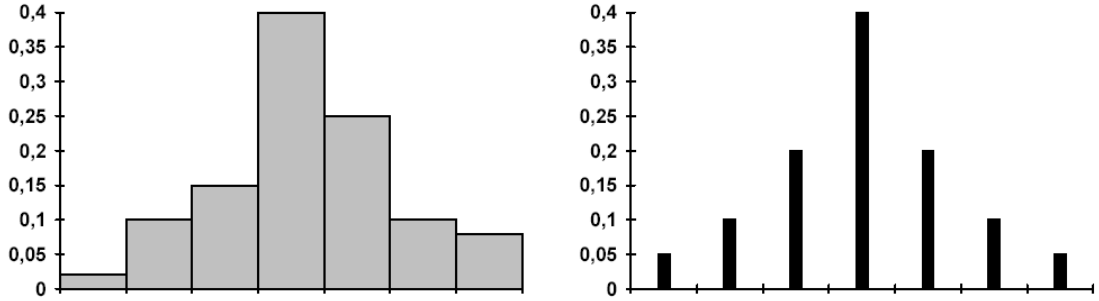

Fig. 9.1: Histogram as a bar and a line diagram
(plot of relative number of grey values over the grey values themselves)

Figure 9.2 presents the histogram of a realistic scenario.

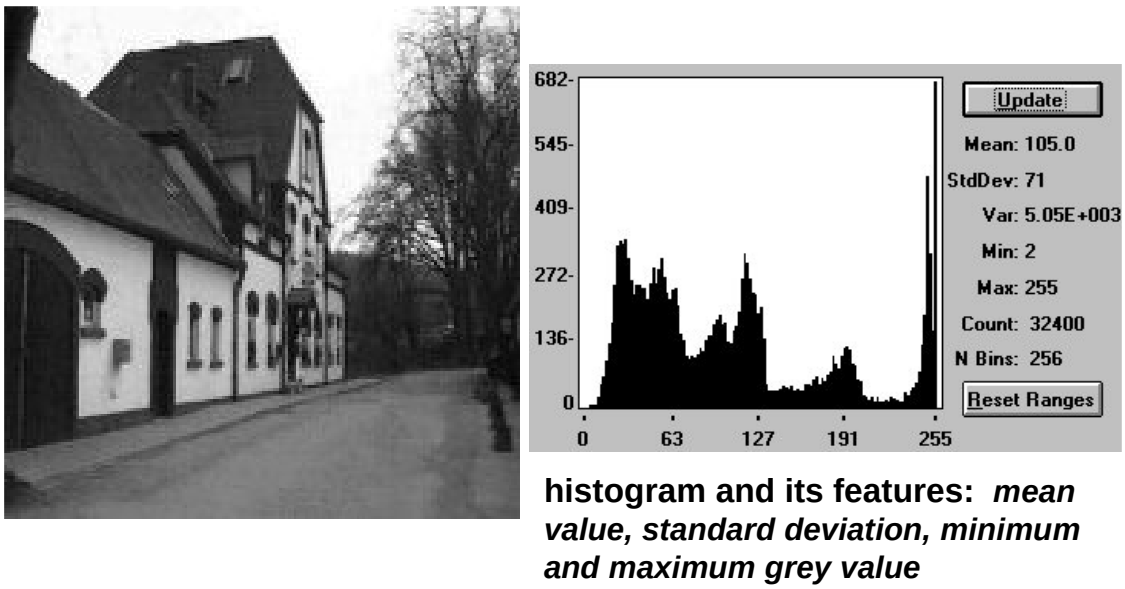

Fig. 9.2: Histogram with the characteristic properties of a realistic scenario

In practical applications, the histogram provides an excellent opportunity to check the saturation degree of an image after its acquisition.

9.2.2.1 Dependency of the histogram from the offset adjustment

Figures 9.3 a und b demonstrate the effect of adjusting the digital offset and brightness on the histogram. The whole profile in the histogram will be shifted either to higher or to lower grey values.

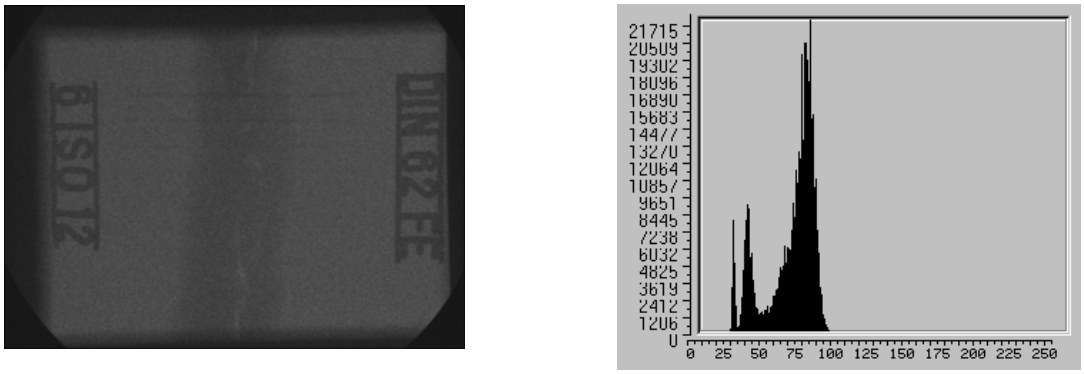

Fig. 9.3 a: Image presentation and corresponding histogram of a dark type of image

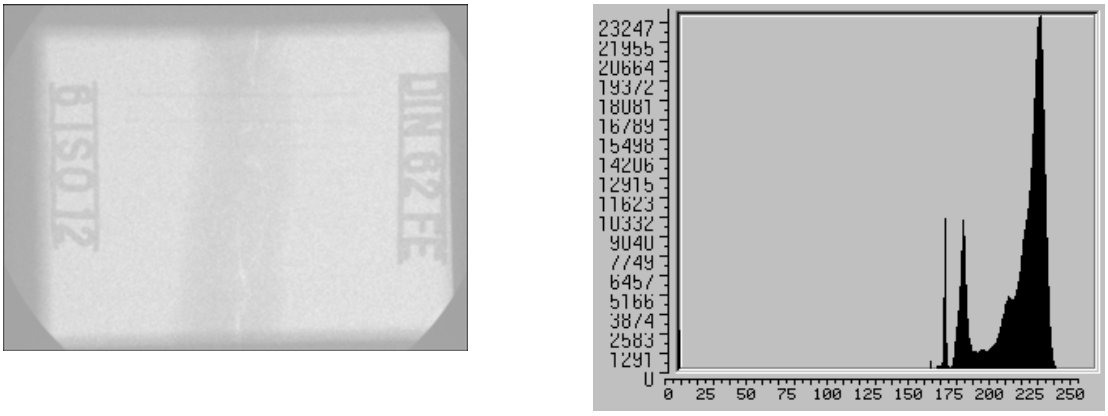

Fig. 9.3 b: Image presentation and corresponding histogram of a bright type of image

9.2.2.2 Dependency of the histogram from the contrast adjustment

The spreading of the grey values present in an image is completed meaningfully e.g. in a way that the smallest occurring grey value is set to zero and the largest one to the maximal digital value. As a consequence, the histogram of an image spread in contrast shows up gaps since certain grey values do not occur any more upon contrast spreading (Figure 9.4 a und b).

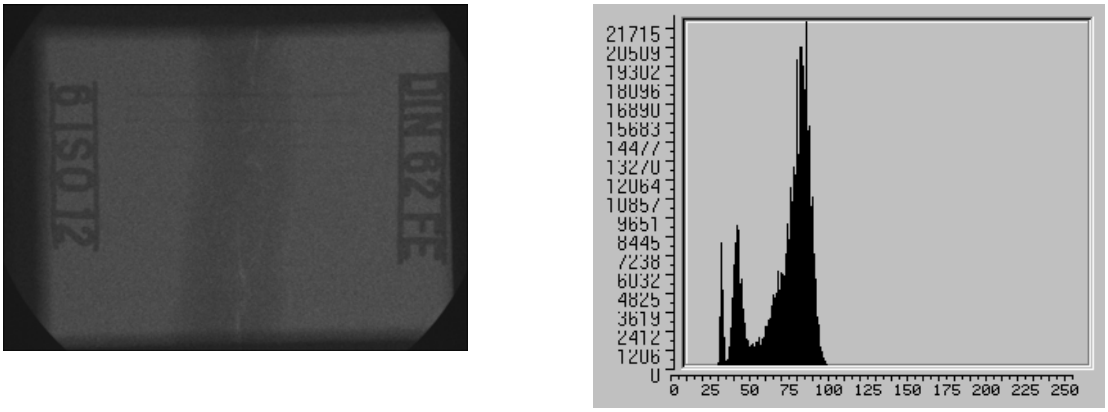

Fig. 9.4 a: Image presentation and a corresponding histogram of an image poor in contrast

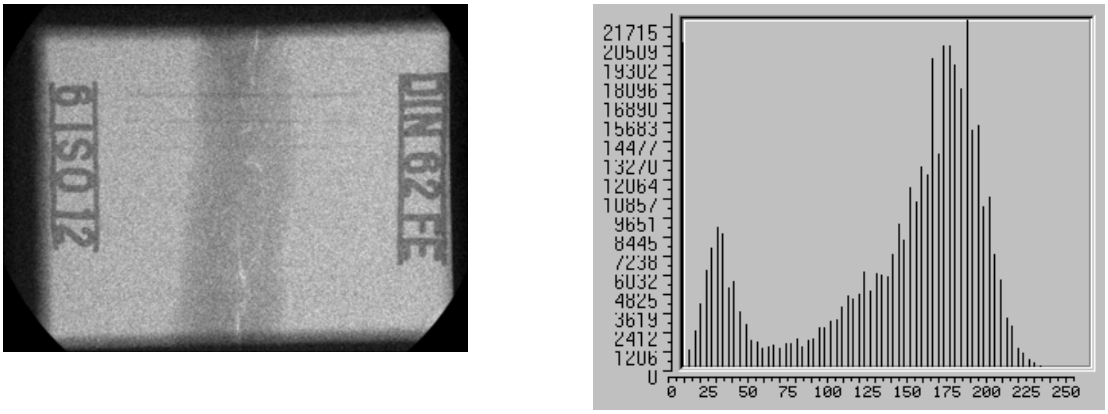

Fig. 9.4 b: Image presentation and a corresponding histogram of an image rich in contrast

Rather often, a scalable presentation of the frequency of the existing grey values appears reasonable to emphasise those of less common grey values in case of large differences in their frequencies.

9.3 Noise reduction

Based on the quantum nature of the X-ray radiation a noticeable noise is visible in the X-ray image – depending on the radiation intensity and the readout time of the detector, therefore, improving the signal-to-noise ration, or a reduction of the noise, respectively, presents an essential step in the image pre-processing. The signal-to-noise ratio SNR is computed as the ratio of the mean grey value and its standard deviation in a region of interest (ROI).

9.3.1 Improving the signal-to-noise ratio by digital image integration

Averaging a number of singe X-ray images **(digital frame integration)** can make a significant reduction of the noise (Figure 9.5).

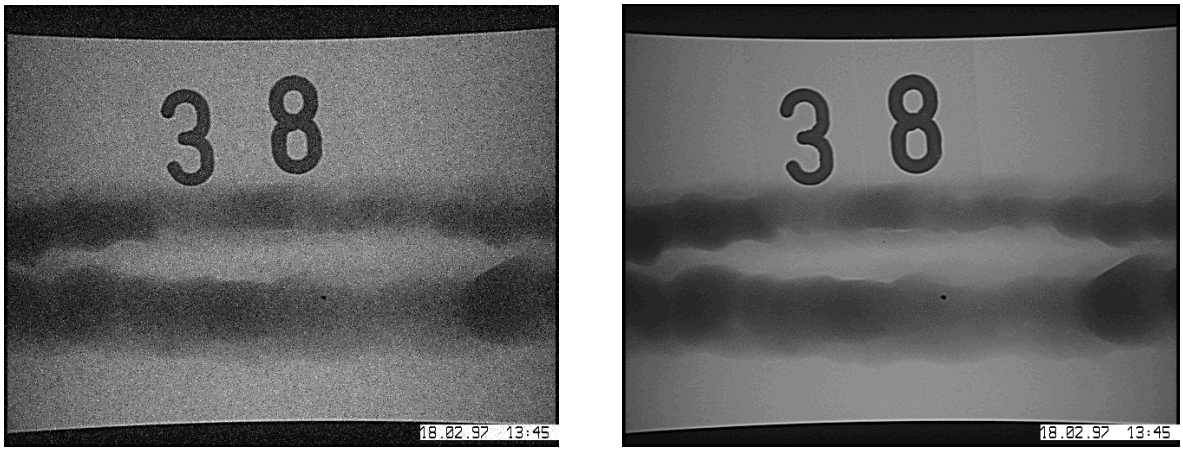

Fig. 9.5: Reduction of noise by digital image integration

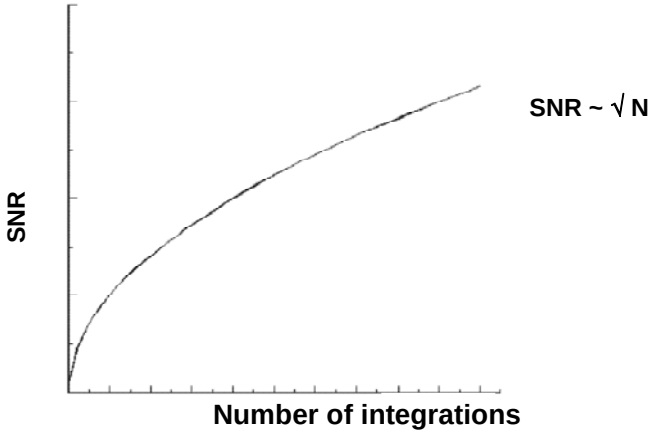

Fig.9.6: Improvement of the signal-to-noise ratio SNR depending on the number of images integrated

A signal-to-noise ratio (SNR) as large as possible is requested in order to detect also details that are small and poor in contrast. This is achieved by calculating the arithmetic mean of the signals collected for a certain period of time or of a certain number N of video images.

Figure 9.6 shows the dependency of an improved signal-to-noise ratio on the number of integrated images or of the intensities. Based on the quantum statistics of the X-ray radiation, there is a relationship to the square root of the number of images integrated. To say it more figuratively, the SNR cannot be improved arbitrarily. Quadrupling the number of images N integrated results in a SNR improvement of the factor 2 whereas nine times longer exposure time only has an improving effect of a factor of 3.

9.3.2 Improving the signal-to-noise ratio depending on exposure time and dosage

Basically, there is no difference in improving the signal-to-noise ratio between the digital image integration and a prolongation of the exposure time of a detector or the increase of the radiation intensity. The improvement of the signal-to-noise ratio as shown in Figure 9.6 also applies here.

In practice, these approaches are frequently limited by the fact that some detectors may become saturated when overexposed or if the electronic noise level rises. This saturation behaviour counteracts any measures to improving the signal-to-noise ratio. As a consequence, a combination of a prolonged exposure time and additional digital frame integration is frequently chosen for digital detector arrays to achieve an optimal signal-to-noise ratio.

9.4 Look-up Table (LUT)

A look-up table is understood as a listing of values that are taken to modify the grey values of the image data in a fast way. The digitised image supposed to be displayed on the monitor is allocated in the image memory of the image processing system. If the original image data are required to be presented differently, this can be achieved with the aid of a look-up table. Contemporary image processing systems offer both, an input and an output LUT. The input LUT is allocated between the camera and the CPU and the output LUT between the CPU and the monitor. Both can be controlled by the software. Commonly said, the output LUT could replace the brightness and contrast controller at the monitor.

9.4.1 Input - LUT

The input LUT allows a weighting of the detector data and thus has a direct effect on the stored image data.

In the following, some examples of different LUTs should be shown and discussed.

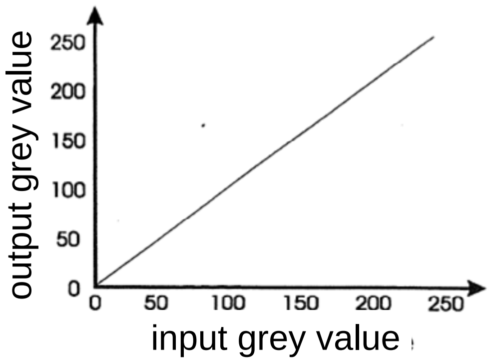

Please describe the function of the LUT:

____

____

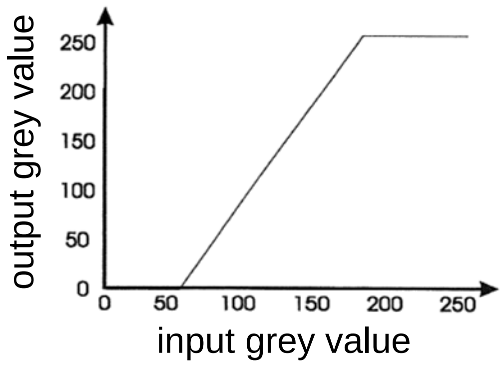

Please describe the function of the LUT:

____

____

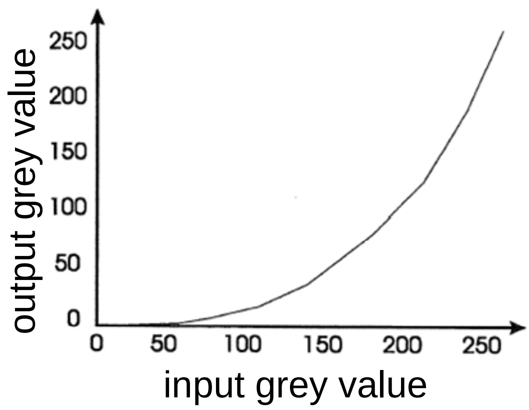

Please describe the function of the LUT:

____

____

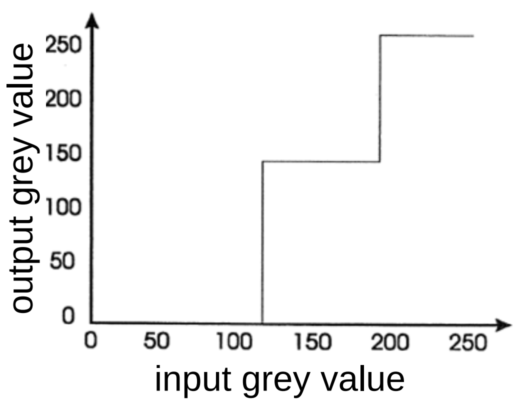

Please describe the function of the LUT:

____

____

9.4.2 Output - LUT

Each point of the image to be displayed passes “through” the LUT to the monitor. The grey value of each image point is taken quasi as an address for the LUT. On the display, the value is presented that has been found at that address.

IMPORTANT:

The point of the image itself remains unchanged, it is only represented differently (Abb. 9.7).

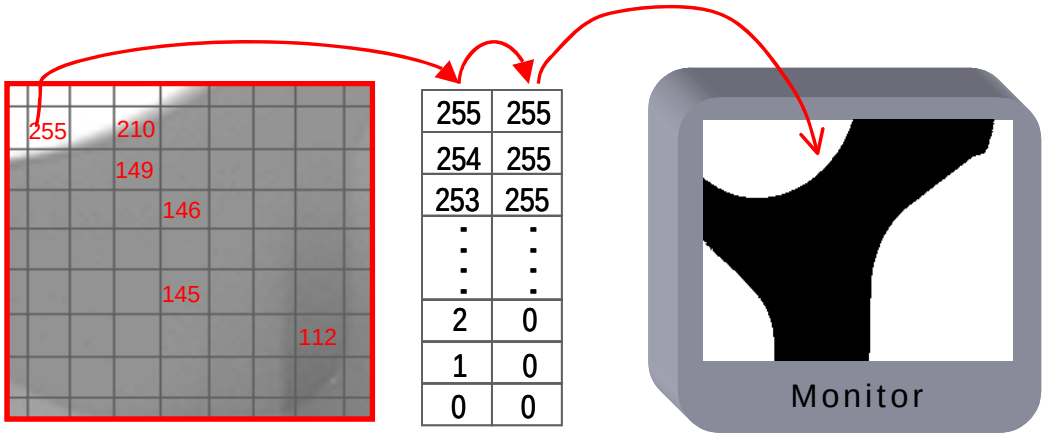

Fig. 9.7: Example of a LUT operation to convert an image to binary

Figure 9.7 shows an example how image data can be converted into binary with the aid of an output LUT. Binary, in this context, means that only two grey values occur in the image (usually white and black). The look-up table is adjusted in a way that all grey values of the original image smaller than e.g. a value of 127 are converted into a grey value of 0 (black) an all pixels with a grey value above 127 appear white (grey value 255).

9.5 Enlargement of digital images

Nearly every commercially available image processing system allows scaling up and down (zooming) of images (Figure 9.8). However, it has to be pointed out clearly that subsequent enlarging of images does not involve any improvement. This has something to do with the fact that zooming digitally a single pixel means just its quadruplicating, or its magnification to an area of 2 x 2 pixels. This leads to an effect that just the pixel structure is emphasised by the digital enlargement. This can be optically compensated by means of suitable interpolating procedures, but this does not result in an improvement of the image quality either.

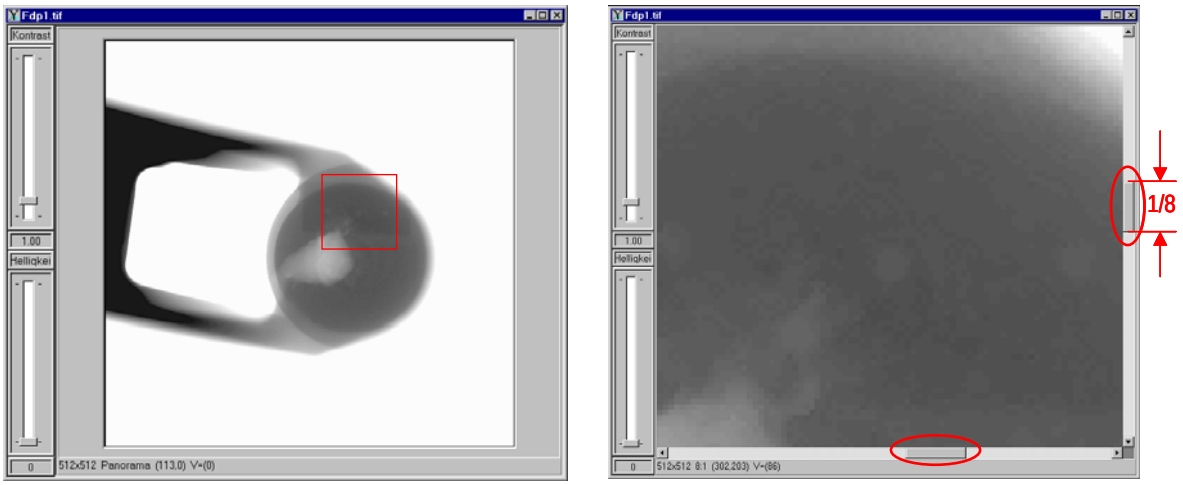

Original image in full size 1:1 area: 100 %

Enlargement (magnification, zoom) factor 8:1 area: 1/64 = 1.5 %

Fig. 9.8: Digital zoom

L 10 Filtering Image Data

Content

10.1 Introduction

Within the digital image processing, the filtering plays a particularly important role. The potential applications range from the suppression of noise, or smoothing of tiny image details, up to the enhancement of structures and small details. Another area of application by means of locally effective filter operations are the detection of basic structures such as edges, object margins, corners or dots. Moreover, it is possible to convert an initial image to a presentation with a diorama (three-dimensional exhibit) like effect. The approaches to detect flaws automatically in weld seams and in cast components are also based on certain filter patterns (s. a. L15).

The core problem of filtering image date is that the image content is purposely altered or manipulated, respectively. By this way, it is possible to make material flaws more clearly visible in an X-ray image, but this can be reverted into an opposite effect when choosing another filter. This means that, when applying digital filtering, the interrelationships and the effects of various filters have to be understood profoundly.

The theoretical fundaments of the image filtering coincide with the theory of signal processing and thus have a strong mathematical orientation. For practical purposes in the daily inspection tasks the knowledge of these subjects is not essentially necessary. By this reason, a descriptive presentation of the digital image filtering is emphasised in this context.

10.2 Point and matrix operations

Principally, the digital image processing is separated into point orientated procedures and those including the proximity, i.e. including adjacent points as matrix.

Point operations are understood as operations within an image not considering any relationships to any other adjacent point but are only related to the point itself (e.g. integration).

The matrix operations are the exact counterparts. In this context, each tackled point always is related to its surroundings. In general, filtering is the typical matrix operation of the digital image processing.

10.3 Practical realisation of a filter operation

First of all, a one-dimensional example (intensities in an image line) should serve to demonstrate the filtering *involving* a so-called filter template and the image information. The following section of an image line should be subjected to filtering:

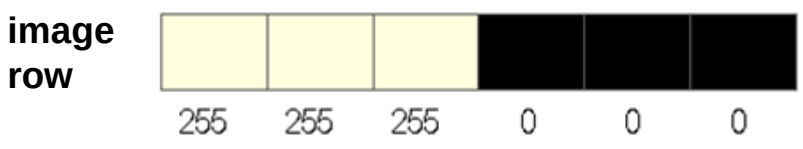

Since the digitalised intensities only assume the grey values 255 (white) and 0 (black), this presents an ideal intensity jump between black and white within this line. The filter template consists of three elements (“coefficients”) and looks like as follows:

filter template

The process of filtering this image line with the filter template is accomplished as follows:

1. The filter template is superimposed onto the original image
2. Each value of the original image is multiplied with the superimposed one of the filter template
3. The sum of the three multiplications will be assigned to the new image point within the filtered image. The resulting point is that one directly positioned underneath the centre of the filter template.

The resulting value is assigned to the marked image point within the resulting image.

4. The filter template is shifted by one image point.

Again, the resulting value is assigned to the marked point within the resulting image.

5. The filter template is shifted by one image point again.

Again, the resulting value is assigned to the marked point within the resulting image.

6. The filter template is shifted by one image point again.

Again, the resulting value is assigned to the marked point within the resulting image.

As a result of the filtering, an image line is yielded with these values:

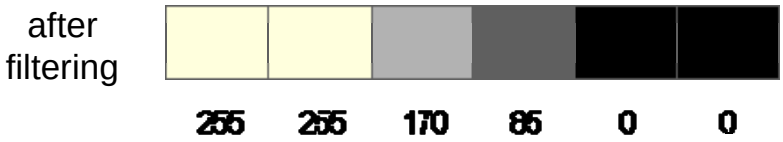

It turns out that the ideal intensity jump of the original image has been “smoothened” (smeared). Obviously, the chosen filter template causes a similar effect as a camera lens that is not properly focussed. This filter is called a “low pass filter”. If a template is taken that has a larger number of elements, the “smearing effect” will be of a larger ex-

tend. In case of a filter template consisting of 5 elements the smearing would be stretched across 4 pixels.

The values of the elements within a filter template are normally chosen in a way that their sum equals to “one” to ensure that the mean grey value remains unchanged.

The filtering of an image is accomplished in analogy to the one-dimensional example. In this case, a two dimensional filter template is necessary for a certain section of the image which is also called filter matrix, filter core or filter kernel. Filters with an odd number of elements always have the centre of the matrix as the resulting point to be calculated. The calculation of the resulting point is accomplished as shown before:

1. The filter template is superimposed onto the original image
2. Each value of the original image is multiplied with the superimposed one of the filter template
3. The sum of the nine multiplications is assigned to the new image point in the filtered image. The resulting point is the one directly underneath the centre of the filter template.

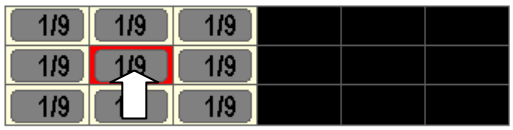

255 255/9 + 255/9 + 255/9
255/9 + 255/9 + 255/9
255/9 + 255/9 + 255/9 = 255

The resulting value is assigned to the marked image point within the resulting image.

4. The filter template is shifted by one image point.

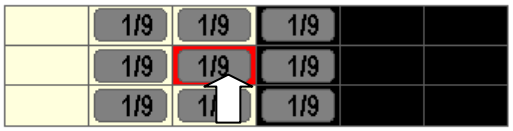

170 255/9 + 255/9 + 0/9
255/9 + 255/9 + 0/9
255/9 + 255/9 + 0/9 = 170

Again, the resulting value is assigned to the marked point within the resulting image.

5. The filter template is shifted by one image point again.

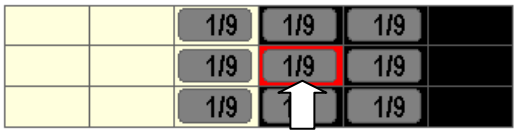

85 255/9 + 0/9 + 0/9
255/9 + 0/9 + 0/9
255/9 + 0/9 + 0/9 = 85

Again, the resulting value is assigned to the marked point within the resulting image.

6. The filter template is shifted by one image point again.

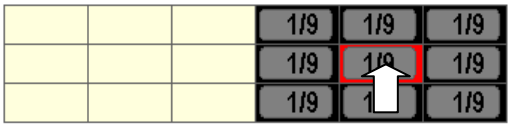

0 0/9 + 0/9 + 0/9
0/9 + 0/9 + 0/9
0/9 + 0/9 + 0/9 = 0

Again, the resulting value is assigned to the marked point within the resulting image.

As a result of the filtering, an image section is achieved with the following values:

255	255	170	85	0	0

Again, it becomes obvious that the ideal intensity jump of the original image is “smoothened” (smeared) by the chosen filter template. This filter is called a “low pass filter”.

Related to a whole image, the following operations will be accomplished with this filter:

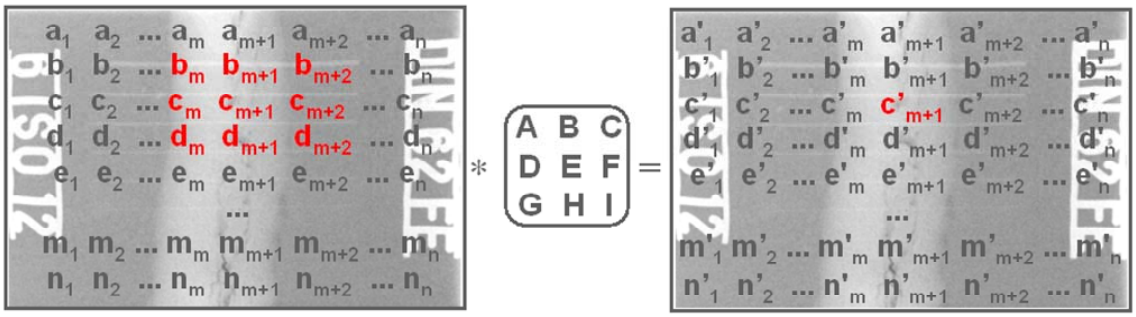

original image **filter template** **resulting image**

wherein the following equation is established for each image point of the result image:

$$c'_{m+1} = b_m{}^*A + b_{m+1}{}^*B + b_{m+2}{}^*C + c_m{}^*D + c_{m+1}{}^*E + c_{m+2}{}^*F + d_m{}^*G + d_{m+1}{}^*H + d_{m+2}{}^*I$$

This formula shows for only one single point the huge number of operations, which need corresponding computational power for large images.

10.4 Various filter templates

10.4.1 Low pass filter

The kind of filter template determines the effect of the filtering on the image. The **low pass filter** introduced before is characterised by the fact that all values of its matrix are positive. If, in addition, all the values are equal, the weighting of all adjacent points is evenly balanced. The effect consists of averaging small alterations of the grey values resulting e.g. in reducing the noise (geometric averaging in opposition to a temporary mean as in an integration process). However, pin sharp images appear “washy” after low pass filtering. The larger the filter template the more pronounced the washing out effect, or the smearing of fine structures, respectively, will occur.

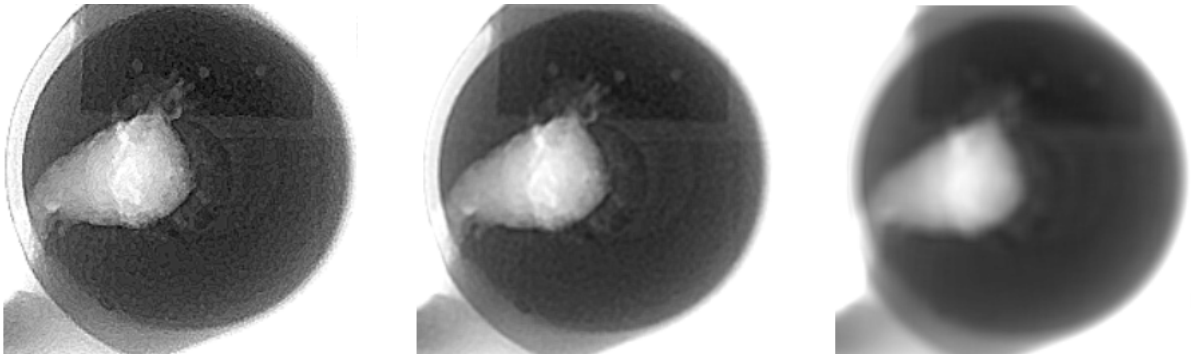

Original image, unfiltered | With small low pass (3x3) | With larger low pass (9x9)

10.4.2 High pass filter

Whenever a negative value occurs in a filter template, this will cause a differentiating effect. If an area of an image only consists of equal values a differentiating filter will deliver a zero value if the all the matrix values sum up to zero. In case of grey value transitions this filter attains a measure for the abruptness of the concerning transition, i.e. the grey value gradient.

The effect is as follows (process in analogy to 10.3):

First, the filter template is left adjusted. Each value of the image line is multiplied with corresponding one of the filter template.

The sum of the three multiplications will be assigned to the new image point in the filtered image. The resulting point is the one directly underneath the centre of the filter template.

In the following steps, the template will be shifted by one image point to the richt each time: This result into the following steps:

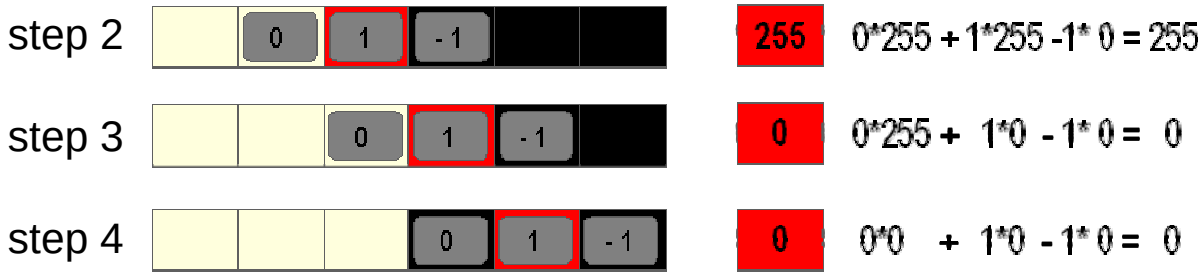

The resulting image looks like as follows:

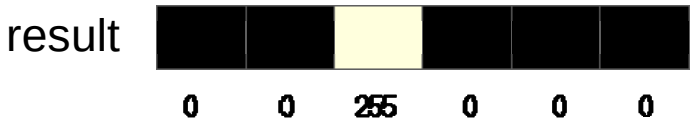

and shows a single high signal different from zero only at the site of the intensity jump.

The two-dimensional high pass has the same effect as shown in the following figure:

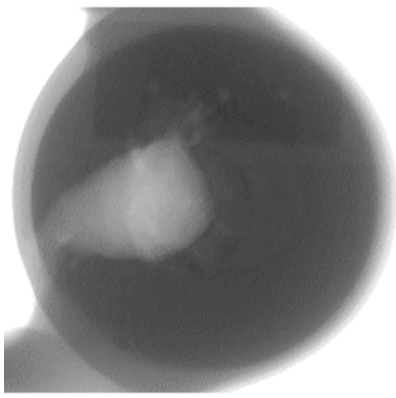

Original image, unfiltered

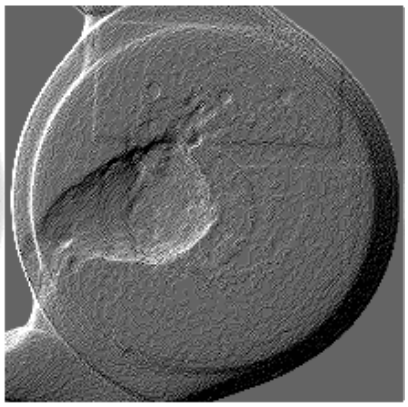

Filtered with high pass

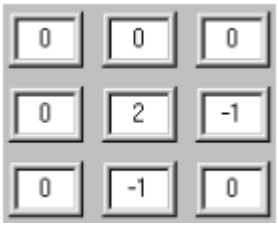

The filter template

It is recognisable that only the grey value transitions have left bright signals.

10.4.3 Band pass filter

The band pass filter combines the differentiating properties to perceive the grey value transitions with the integrating effect to reduce the disturbing interferences. As a consequence, the filter template consists of several positive values in the centre (integrating effect) while negative values closer to the margin produce a rise in brightness at the spots of transits in grey values (differentiating effect).

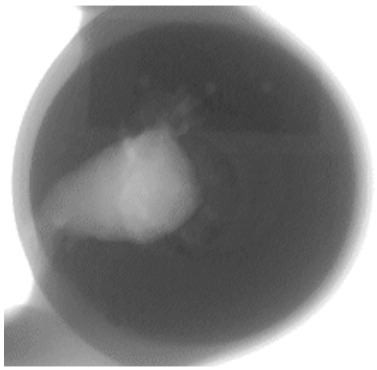

Original image, unfiltered

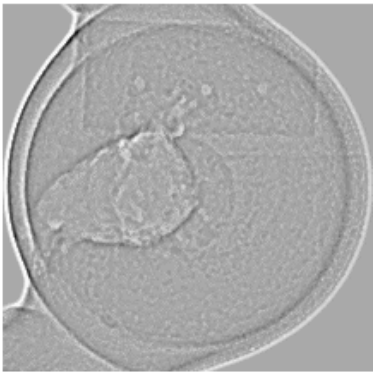

Band pass filtered

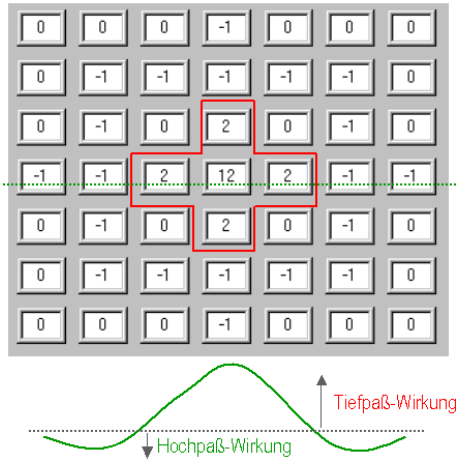

The filter template

The effect of the band pass filter is shown in the image; the centric 5 values care for the low-pass effect, the negative ones outside the centre for the high-pass effect. This filter is called the Difference of Gaussians (DoG-filter) or the “Mexican Hat” because of the profile of the filter matrix.

10.4.4 Effect of a filter in the frequency domain

Large structures in an image have their grey value transitions distributed across numerous pixels. *They may be really large structures*. These are the structures shown to the left and in the centre of Figure 10.1, characterised by the **low** frequencies “2” and “4” and are found on the left side of the frequency diagram. Very small structures are characterised by **high** frequencies as *also* shown in Fig. 10.1, labelled with “32” and showing up in the frequency diagram on the far right. In-between, there are the middle frequencies in the centre of the band with medium sized structures tagged “8” and “16”.

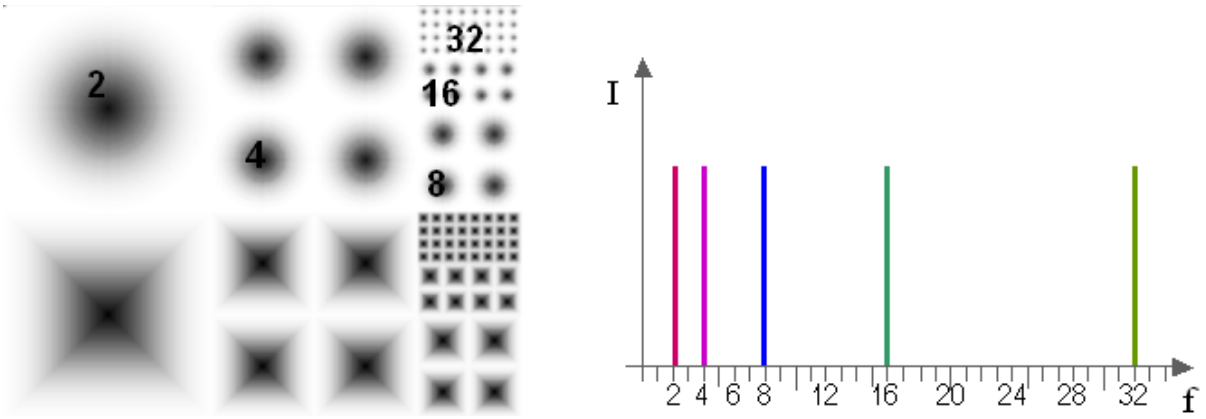

Fig. 10.1: Spectrum of frequencies in an image

The low pass leaves the low frequency passing and suppresses (filters) the high frequencies.

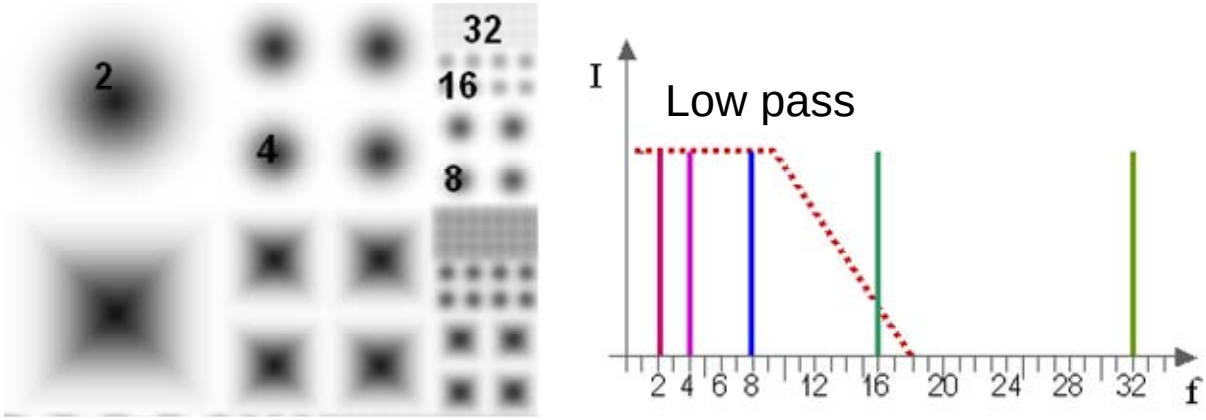

Fig. 10.2: Frequency spectrum after low pass filtering in the image

The frequencies of 16 and higher are markedly attenuated; the 32 frequencies are barely perceivable.

The band pass leaves the frequencies in the median range (centric band) passing and suppresses (filters) the lower and the higher ones.

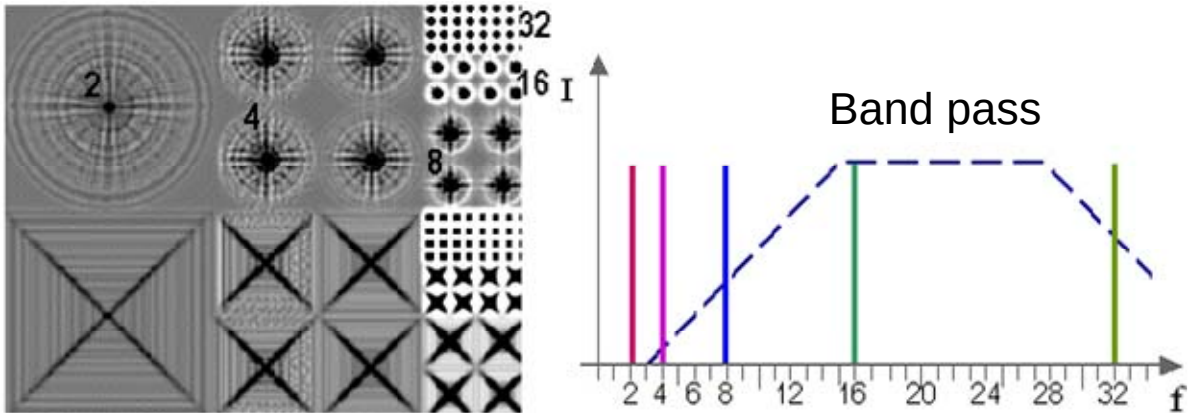

Abb. 10.3: Frequenzspektrum nach Bandpassfilterung in dem Bild

The high pass leaves the high frequency passing only and suppresses (filters) the (low) *all the other* ones.

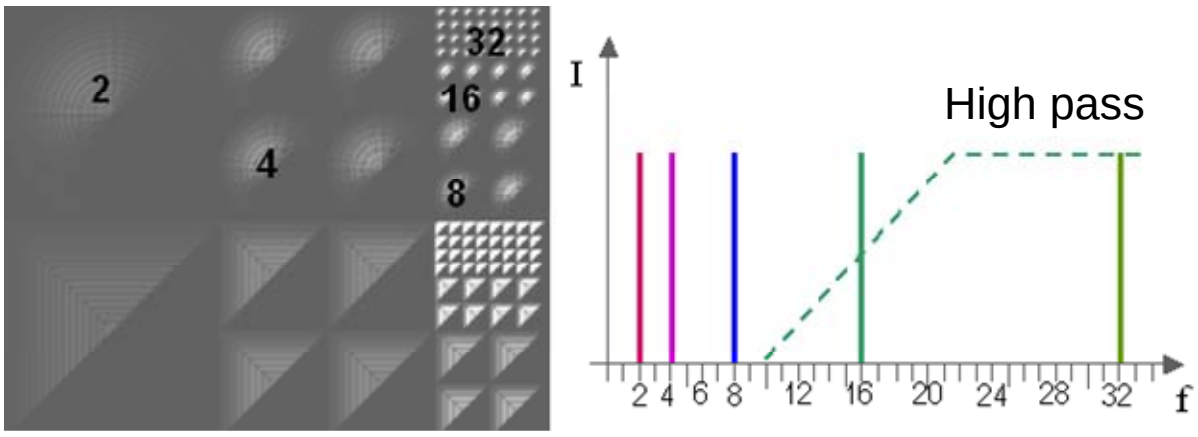

Abb. 10.4: Frequenzspektrum nach Hochpassfilterung in dem Bild

Only the high frequencies 16 and 32 remain while the large structures associated with the low frequencies are suppressed (“damped away”).

10.5 The median filter

The median filter is a very computationally intensive ranking filter that smoothens contours on one hand and preserves edges on the other hand at the same time.

The grey values within the superimposed “filter template” are sorted according to their values first.

The Figure to the right shows a section of an image in the size of 9 pixels.

The three values “2” are listed first (position 1 to 3), then the value “3”, the three values “4”, the value “5” and finally the outlier value “15”.

The value that is allocated exactly in the centre of this array of pixel values - in this example the value “4” at the fifth position - will become the new grey value of the pixel in the resulting image.

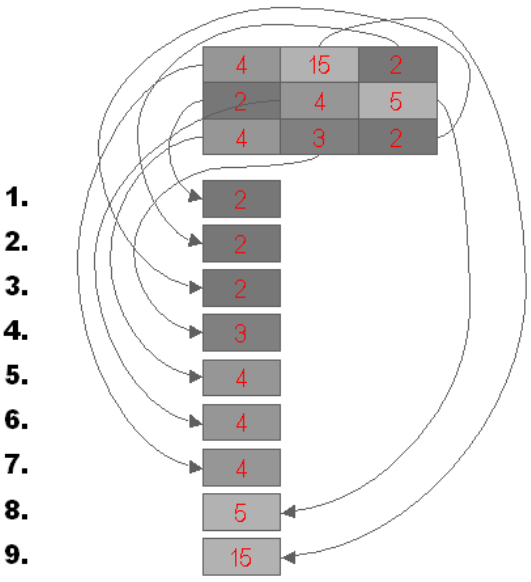

The effect of the median filter is shown in the following figure, in comparison to the low pass filter.

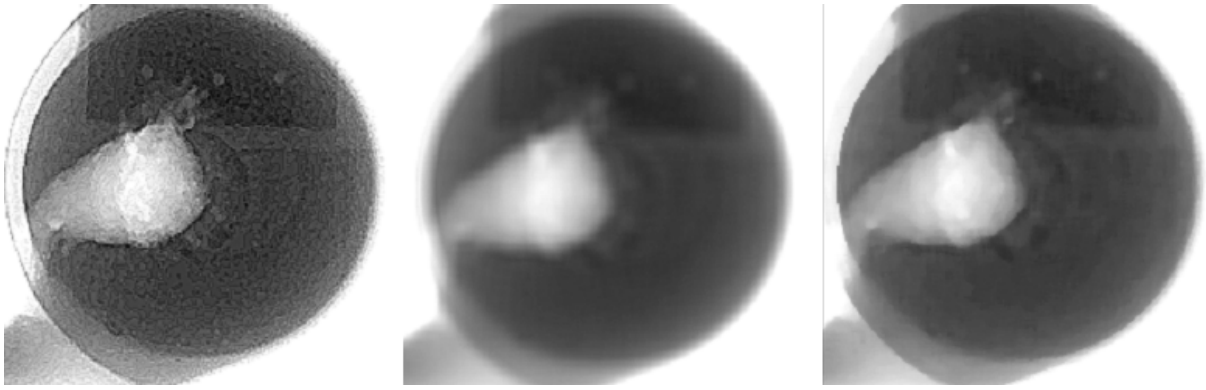

Fig. 10.5: Original Low pass filtered Median filtered

It is well recognisable that the three holes in the attached penetrameter are highly smeared when low pass filtered, in difference to the median filter which preserves them nearly completely. In addition, the image leaves a less smeared impression.

L 11 Application of Digital Filters I

Content

11.1 Filters for the suppression of noise

In the chapter L10, the geometric integration (integration on a plane) has been introduced as a counterpart to the temporal integration (chapter V9). In general, the temporal integration should be preferred – as far as possible – since the perceptibility of details may be impaired by the geometric integration. In case of an already acquired image, only the geometric integrations is left as a possibility to suppress the noise.

The noise appears in an image as tiny and irregular structures that are changing with time. Thus, the noise does not contribute to the desired image information at all.

11.1.1 Low pass filters

The standard filter for the suppression of noise is the low pass one since it blocks the tiny structures. Commonly the low pass is characterised by possessing only positive values in the filter mask. The size of the filter mask determines the strength of the effect since all those values of the image are averaged that are within the filter template.

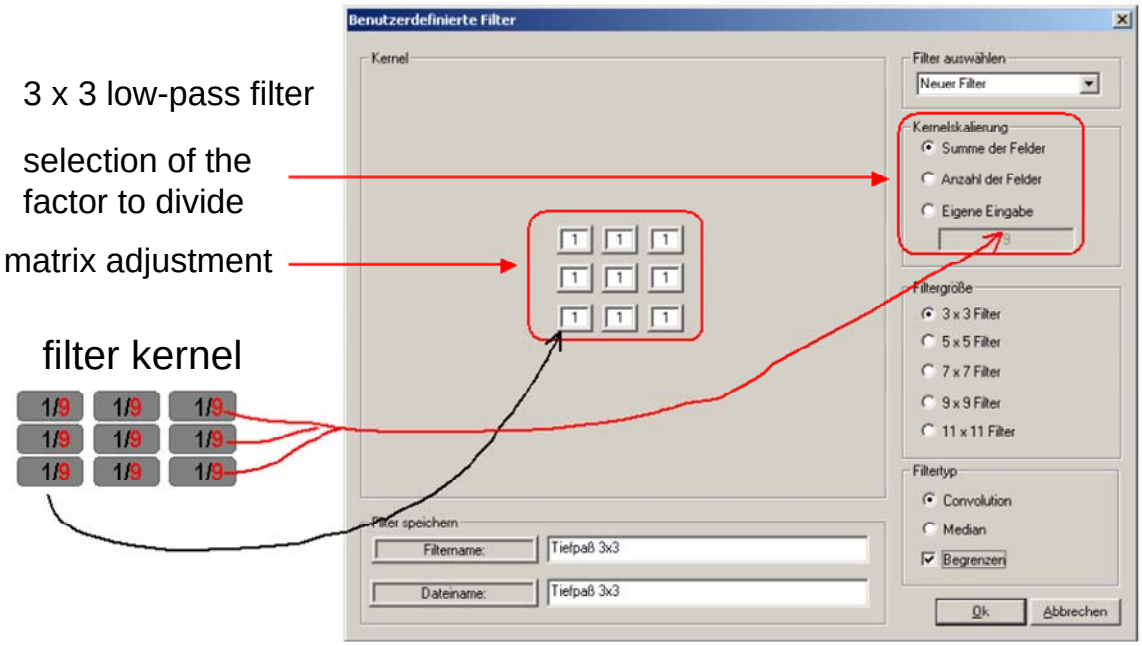

Fig. 11.1: Parameter selection for a 3x3 low pass filter

Since all the values within the filter kernel, or the template, respectively, have the same denominator to be divided by (9 in this case) it can be omitted in the template matrix as a common scale for the kernel; at the end of the multiplication, all values will be divided by this common denominator. Many image processing systems offer an automatic summation of all template values for this purpose (as in example 9). This leaves the overall brightness of the image unchanged.

The numerators of the kernel values can be entered into the corresponding boxes of the matrix. Since all values are positive in this case it will become a low pass filter. The presence of 9 matrix elements will make a 3 x 3 low pass filter.

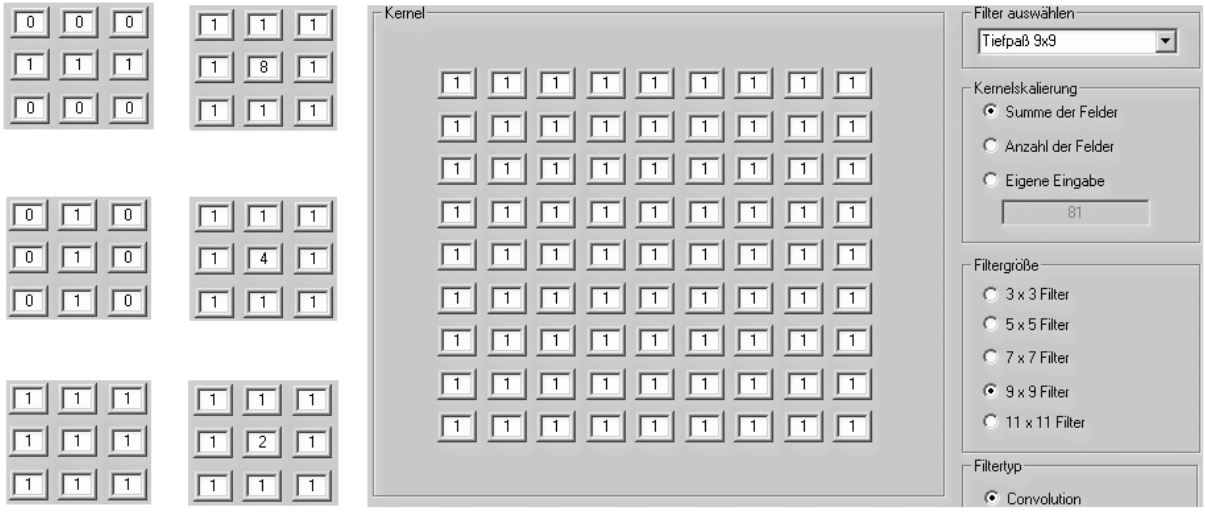

Fig. 11.2: Various low pass filters for noise suppression

Figure 11.2 shows various filter kernels for the noise suppression; a small one is shown in the left column with a 1x3, another one with a 3x1 and on the lower left with a 3x3 filter. The 1x3 filter averages only the elements of a line, as shown in chapter L10.3.

The central column shows three filters which are increasingly intensive from top to bottom. The smaller the number in the centre the stronger becomes the effect onto the adjacent pixels, i.e. the more intense the filter operates.

The filter kernel on the right shows 9x9 low pass filter; the size of the kernel amounts to 81 elements because of the product of 9x9. The effect of this filter is shown in Figure 10.5.

11.1.2 Median filters

The median filter is also suitable for noise suppression. It preserves more efficiently edges and structures in the image. The median filter is particularly suited for the suppression single corrupted pixels as the may occur in digital detector arrays. The mode of operation and the effect of the median filter are described in chapter L10.5 and shown in Figure 10.5.

11.2 Filters to emphasise structures

Certain filters have been already introduced in chapter L10.4 that emphasise structures (transitions of grey values). These are filter containing also negative values in their kernel. These negative values make enhancing, or emphasising, respectively, the grey value transitions by interaction with the positive ones.

11.2.1 Sharpening filters

With this image, the aim is to improve the visibility of the flaws in a weld seam in parallel with that of the wire IQI and the hole-penetrameter.

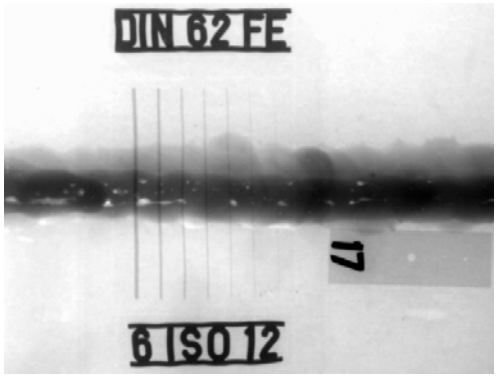

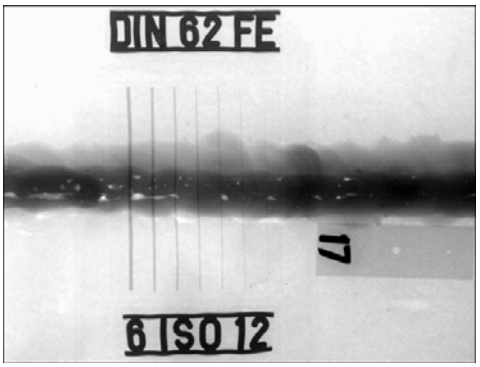

Fig. 11.3: Image of a weld seam ... treated with a sharpening filter

The structures are slightly enhanced by the soft sharpening filter with the matrix shown to the right; the value in the centre of the matrix refers to the intensity of the original image. The values in the direct vicinity are subtracted and thus generate a gradient which is added to the original image. The ratio is 6 : -4.

0	-1	0
-1	6	-1
0	-1	0

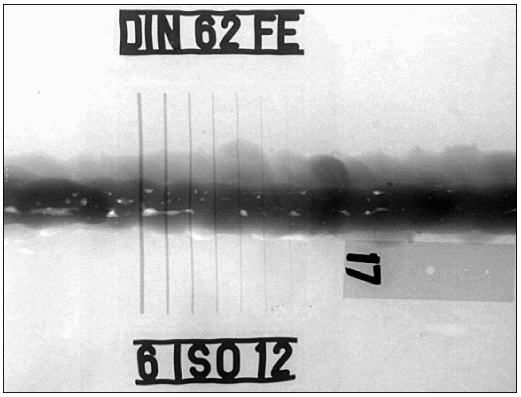

0	-1	0
-1	5	-1
0	-1	0

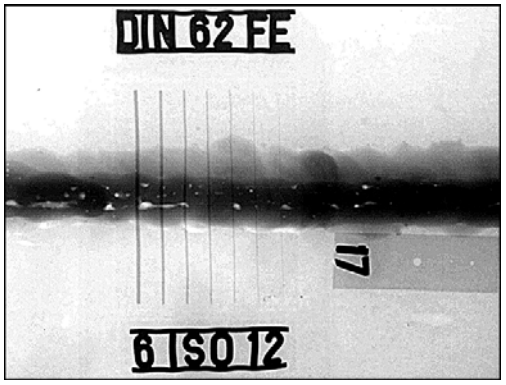

0	0	-1	0	0
0	-1	0	-1	0
-1	0	10	0	-1
0	-1	0	-1	0
0	0	-1	0	0

Fig. 11.4: Strong 3x3 sharpening filter 5x5 sharpening filter with the filter matrix

In the left panel of the Figure 11.4 the ratio of original value over the gradient is lowered down to 5 : -4 increasing the sharpening effect. When choosing a larger matrix, e.g. 5x5, more pixels can be included into the determination of the gradient. By this way, the effect even can be enhanced.

11.2.2 Pseudo-plast filters (pseudo-3D exhibiting)

Further emphasising of structures can be achieved by the simulation of light and shadow. This results in gaining a three-dimensional impression ("pseudo-3D") of the specimen. Different orientations are realisable by the adequate choice of the filter matrix:

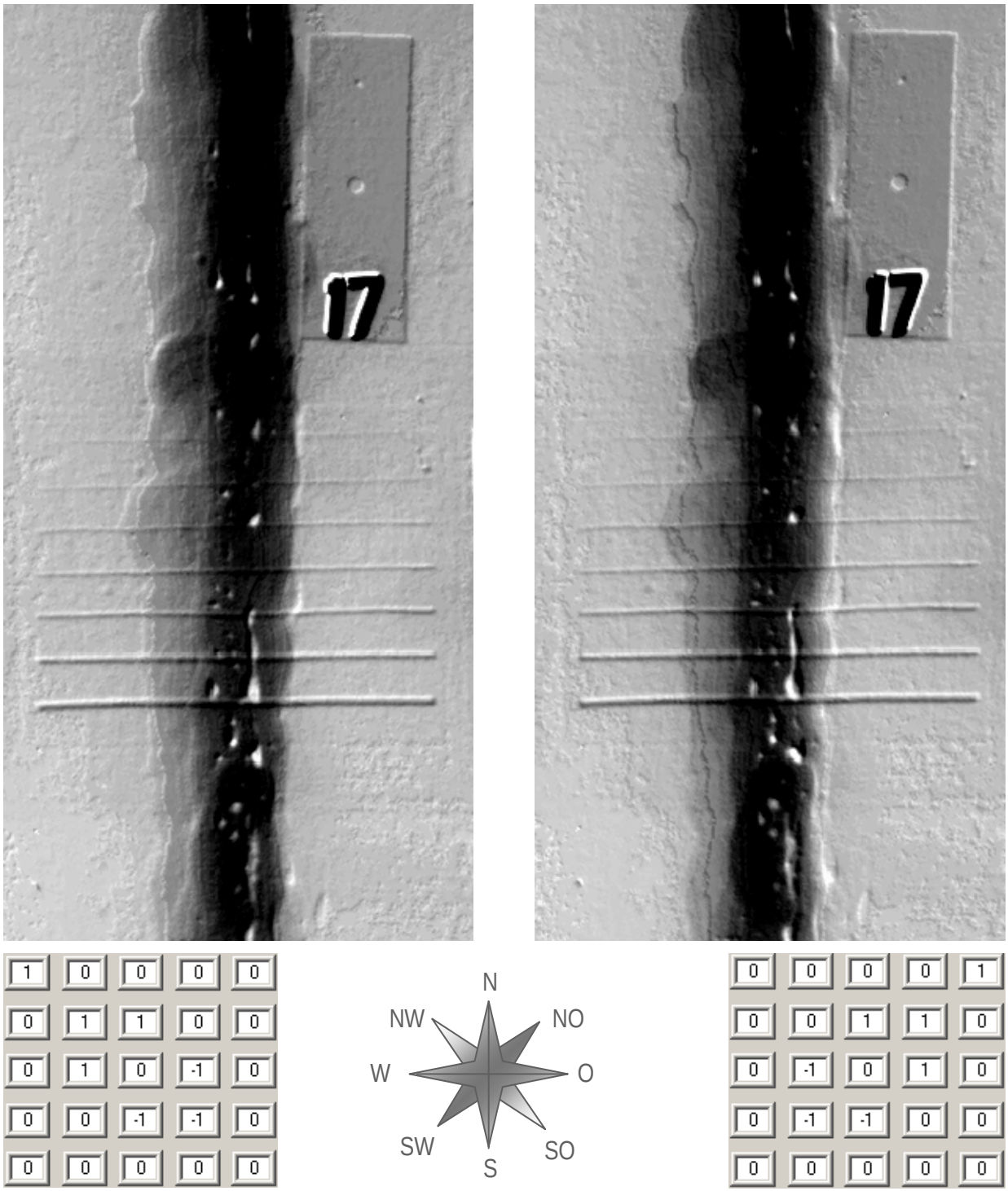

Fig. 11.5: "Pseudo-3D" filter, direction NW

"Pseudo-3D" filter direction north east (NO)

11.3 Filters to extract edges and structures

Structures and edges can be extracted from images by certain filters so that e.g. the contour lines appear. Particularly the edges could be an interested feature of an object. An edge image is defined by the grey values of each point representing the gradient and the height of an edge that may eventually cross an object shown. The enhancement or the **extraction of edges** can form a valuable tool to facilitate an improved image evaluation. When examining an image the attention of the visual sense is primarily focussed on edges and corners present in an image. Only after that, a scanning of the planar regions is accomplished.

In certain cases just the edges of an imaged object may be of interest only for the interpretation of an image as it might be the case in comprehending the shapes of cast or other components and their inspection. It would be an asset in such cases to yield a binary line chart just showing the edges by means of suitable algorithms for noise suppression and edge enhancements.

In reality, only sketchy line drawings can be extracted in most cases, i.e. edges may appear as broken lines in the resulting image. The edges in the image of an electric iron are extracted by an ordinary and an optimised algorithm. The red arrows mark the incomplete extraction of edges. It is anything than trivial to choose the appropriate filter for such a task.

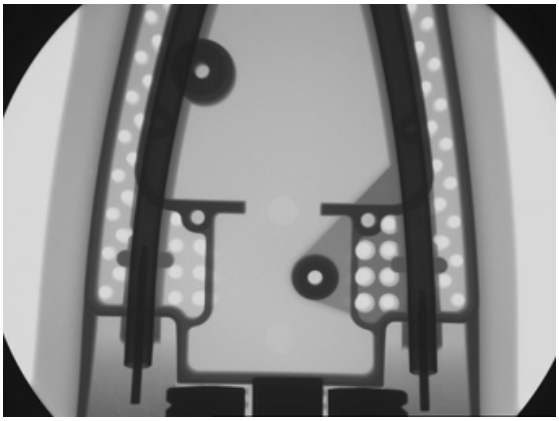

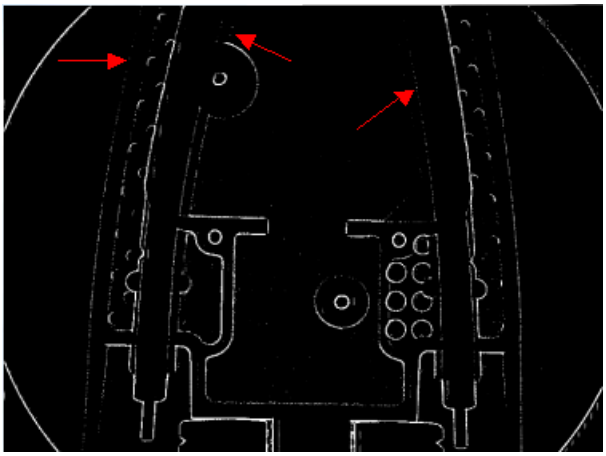

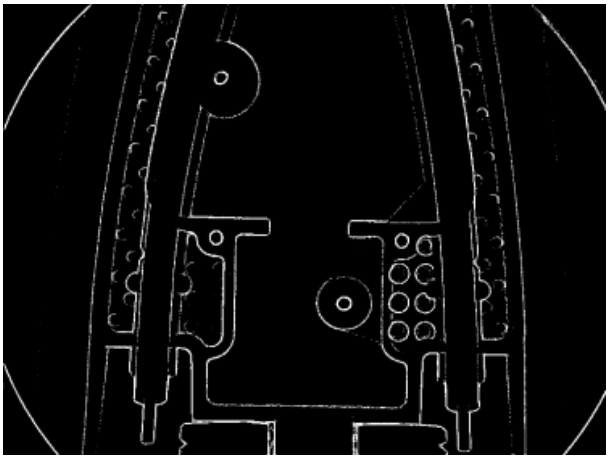

Fig.11.6: Incomplete edge extraction Improved edge extraction

Classical edge operations based on the filter technology are the **Sobel** and the **Laplace operators as well as band pass filters**. They differ in the size and the content of their various filter matrices (convolution kernels) for the treatment of the images. They represent two-dimensional filter templates of 3x3 elements or larger.

11.3.1 The Sobel operator

The Sobel operator is a filter combination. Commonly, it operates with two successive convolution kernels which are twisted by an angle 90° to each other. By this way, both the horizontal and the vertical edges are enhanced as well. The Sobel operator yields appreciable results mainly because of calculating the differences to the next but one column or line, respectively. This makes suppressing small interfering signals in the close vicinity and the noise in the resulting image. The final image consists of the sum or the maximum of the two successive operations.

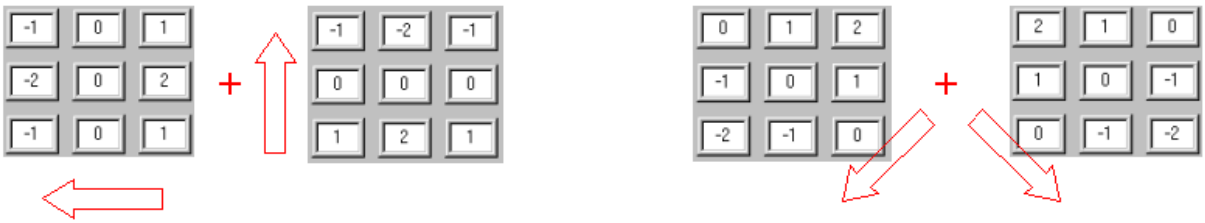

Fig. 11.7: Convolution kernels of the Sobel operator twisted by 90° to each other

In addition to the vertical and horizontal pair of Sobel convolution kernels others are available turned by 45° which achieve better results in case of diagonally crossing edges.

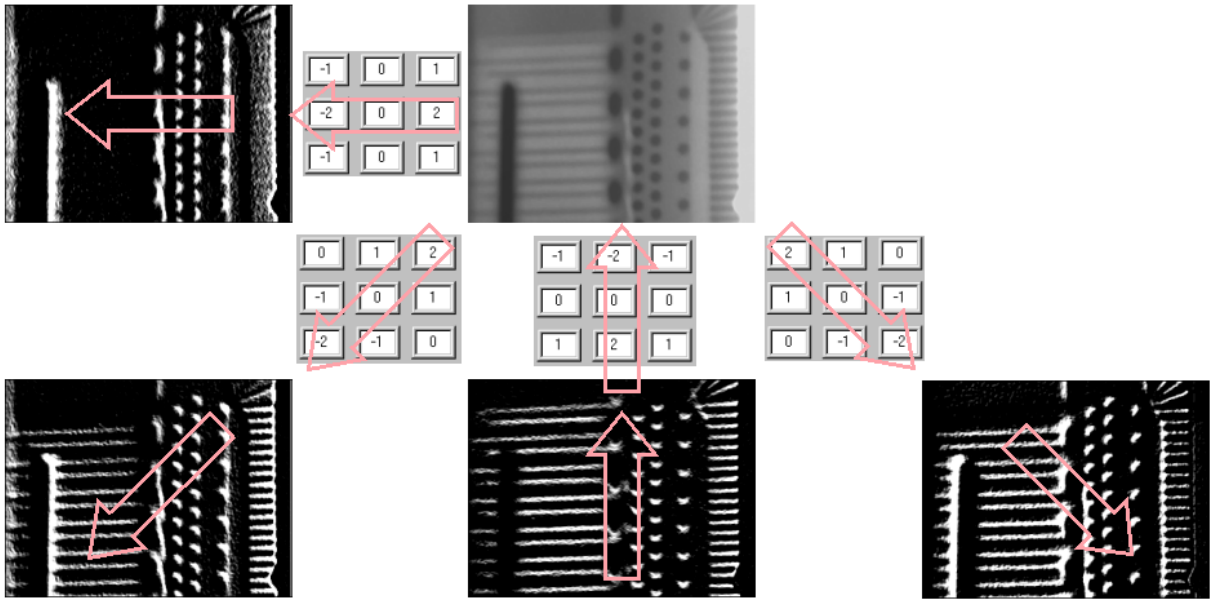

Fig. 11.8: Effect of the 4 convolution kernels of the Sobel operator example: turbine blade

The direction in which the filtering is accomplished plays an important role in case of operations to enhance edges. If applied improperly these filters are also capable to erase edge indications from an image. In the first image, all horizontal structures are ex-

tracted, in the corresponding one centrally at the bottom, which is twisted by an angle of 90°, all the vertical structures. The two outer panels below show the corresponding Sobel operators twisted to each other by an angle of 45° to each other together with their result images.

The next image shows the result of the combination of the two Sobel images. The structures of the turbine blades are clearly visible.

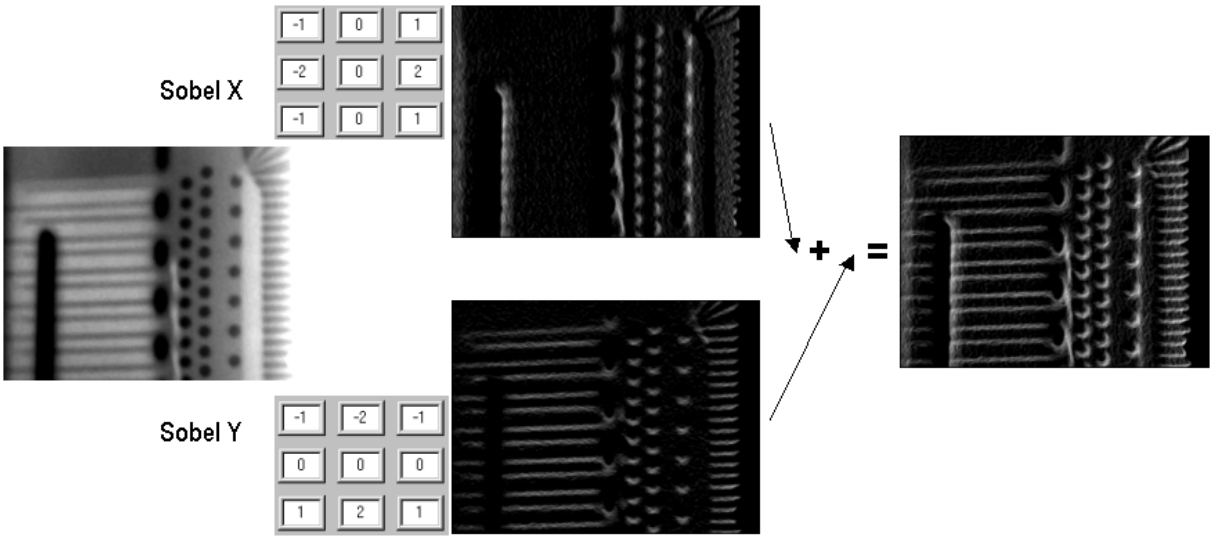

Fig. 11.9: Combination of Sobel-X and Sobel-Y with a turbine blade

11.3.2 The Laplace operator

The Laplace operator works only with a single filter matrix and equally in all directions.

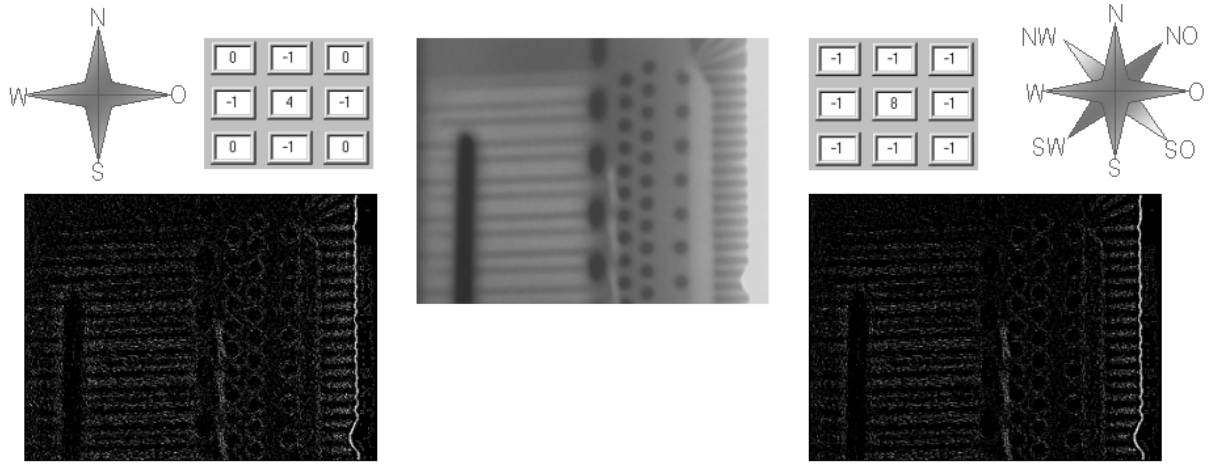

Fig. 11.10: Laplace operator with 2 different filter matrices

The result shows values different from zeros only at those sites where a gradient is present in the image. The difference between the two matrices shown in Figure 11.10 con-

sists of the fact that the left kernel only filters in 2 directions (horizontally and vertically) while the right on operates into all directions.

The main disadvantage of the Laplace filter consists of its high sensitivity to noise. A remedy would be enlarging the filter matrix so that more image pixels are included in the calculation – and thus in the averaging of values. The price for that is a slightly longer computation time what should be not a problem any more with the industry-PCs available nowadays.

A 3x3 filter needs some 20 operations per image pixel, the amount for a 5x5 filter would be about 50 operations.

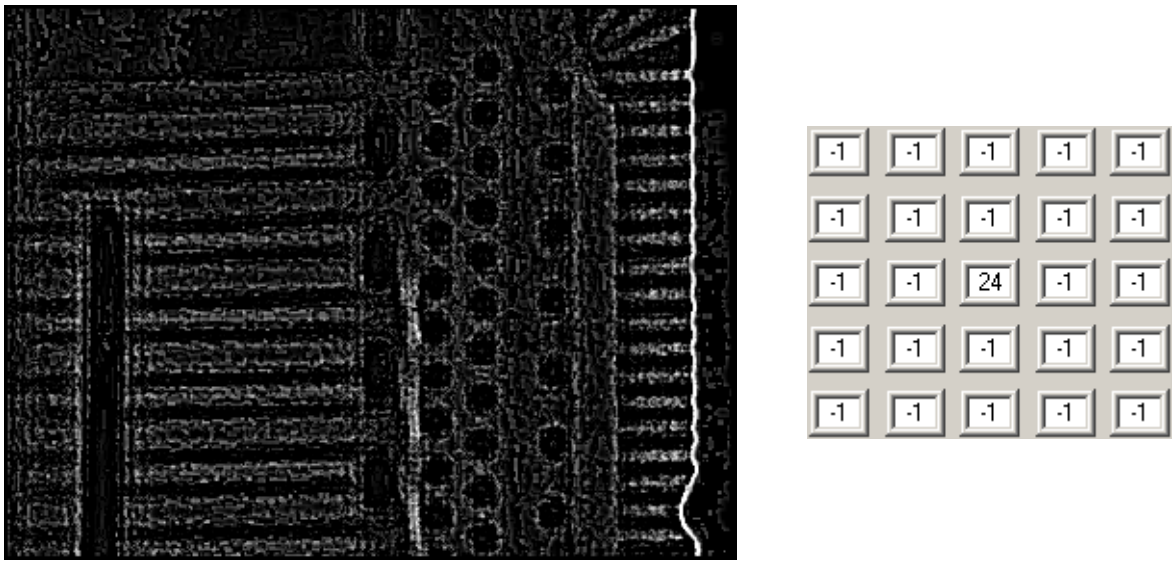

Fig. 11.12: Laplace operator with a 5x5 matrix

11.3.3 The band pass operator

Like the Laplace operator, the band pass filter works only with a single filter matrix. A typical application would be the following filter called the “Difference of Gaussians” (DoG).

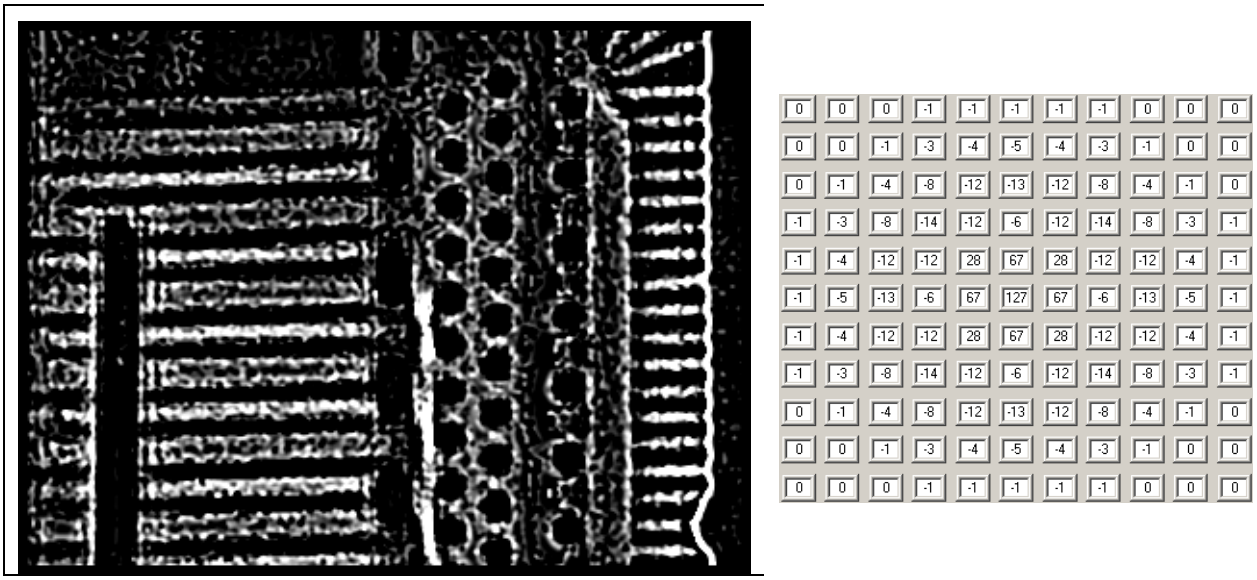

Fig. 11.13: Band pass Filter with the corresponding filter matrix (11x11)

Provided properly chosen values in the matrix the result is only different from zero at sites where gradients exist in the image. By choosing its size the noise can be reduced and the size of the structures selected that should be visualised by the filter.

As a rule of thumb, the resulting line width is roughly determined by the area of positive values within the filter kernel.

The most serious disadvantage of the DoG filter consists of the computation power needed; about 250 operations are necessary for each image pixel for an 11x11 filter.

L 12 Measuring Functions within the Image

Content

12.1 Measuring lengths, areas and intensities

The detection of discontinuities in an image is one subject, another one is the evaluation and classification. Important parameters for the evaluation are presented by the measures of the discontinuity within the image, be it in the image plane (X and Y) or in the depth (Z direction).

Each measurement has to be preceded by calibrating the system in order to provide the computer with the information to convert distances between pixels or grey values into real dimensions such as millimetre.

12.1.1 Calibration of measurements

Prior to any measurement, a calibration is accomplished with a reference specimen whose dimensions are known. An attached penetrameter e.g. may serve as a reference specimen. Then the calibration result is saved for each image, and the lengths within the image can be determined directly.

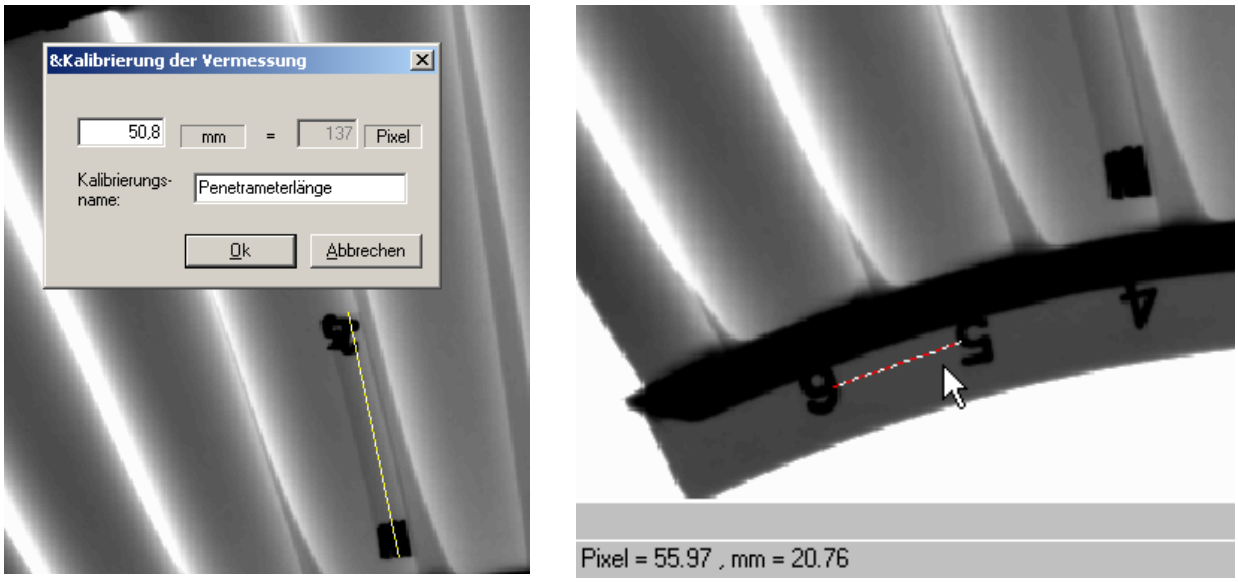

Fig. 12.1: Calibration succeeded by a measurement of a length displaying in mm

12.2 Measuring of lengths

Contemporary digital systems are capable for measurements directly in the image. The usual measuring directly on TV-monitor screens with a ruler has become history.

After the calibration the measurement within the image is accomplished by placing two or more marks with the PC mouse. The computer subsequently converts the distance from pixels to mm.

12.3 Measuring of areas

The measurement of areas is accomplished similarly to that one of lengths. Most image processing systems offer predefined measurement templates such as rectangles or circles. With the aid of those measurements can be achieved as shown in the next Figure.

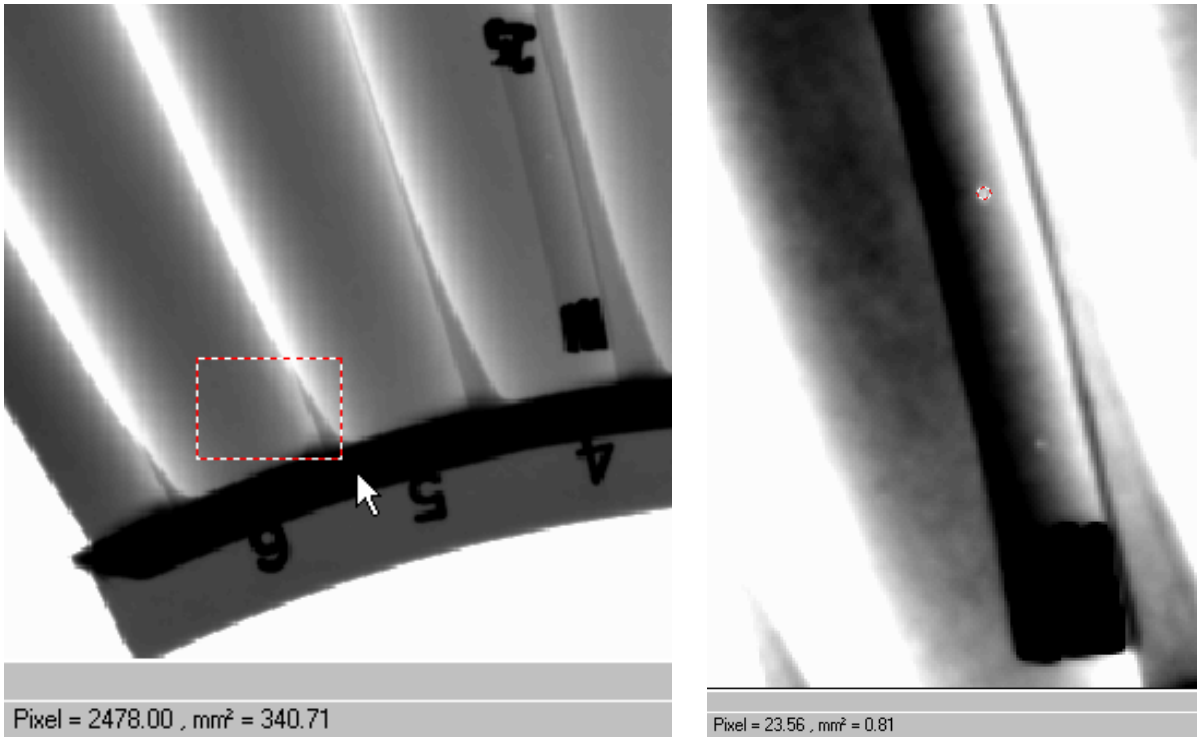

Fig. 12.2: Measuring a rectangular area Measurement with an elliptic function

Frequently, tiny and even the smallest details need to be sized. For this purpose, it is recommended to magnify the image digitally and then to use it for measurements. The right Figure *(panel)* shows the measurement of a hole in the penetrameter of 1 mm diameter.

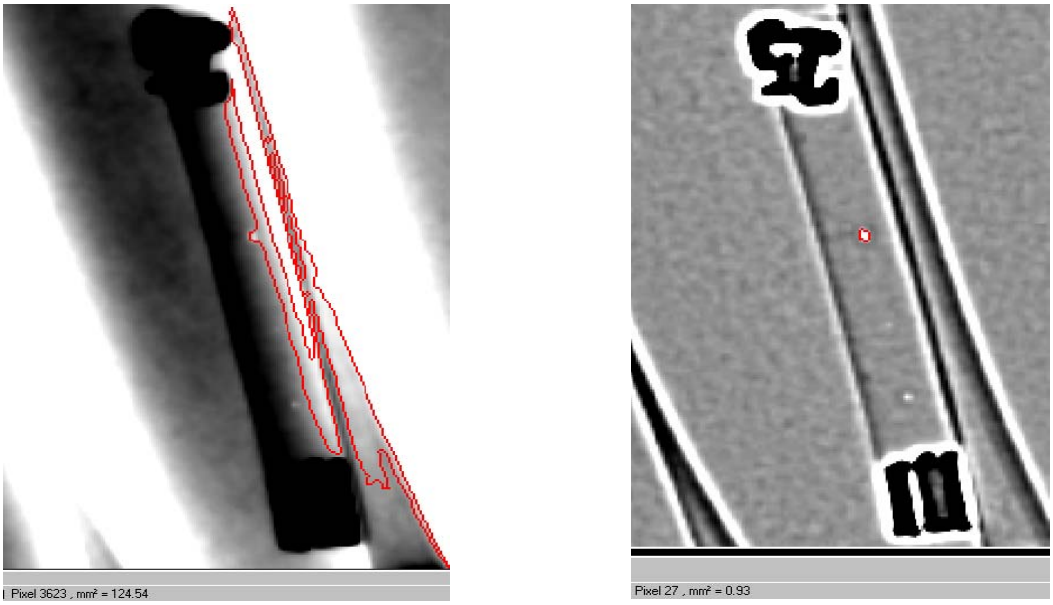

Fig. 12.3: Automatic filtering after elimination of the gradient by filtering

When measuring it is not always clearly visible in the image where exactly the rim of a flaw is located, or of a hole, structure or anything else in may cases. Particularly if the object to be measured is superimposed by a gradient of grey values as shown in Figure 12.3, a high or band pass filtering is recommended to remove the absolute grey values from the image leaving only the grey value gradients (s. chapter L11.3). In such images, an automatic measurement can be applied with a so-called “magic wand function” that automatically recognises and fills the geometry of a structure.

12.4 Measuring of intensities

While the measurement of lengths and areas is accomplished in the X/Y space measuring intensities is achieved by evaluating differences between grey values.

12.4.1 Calibration of intensity measurements

Analogously to the measurements of lengths and areas the system has to be calibrated with a standard specimen before any measuring to have a relationship between the grey value differences and the thicknesses of various materials.

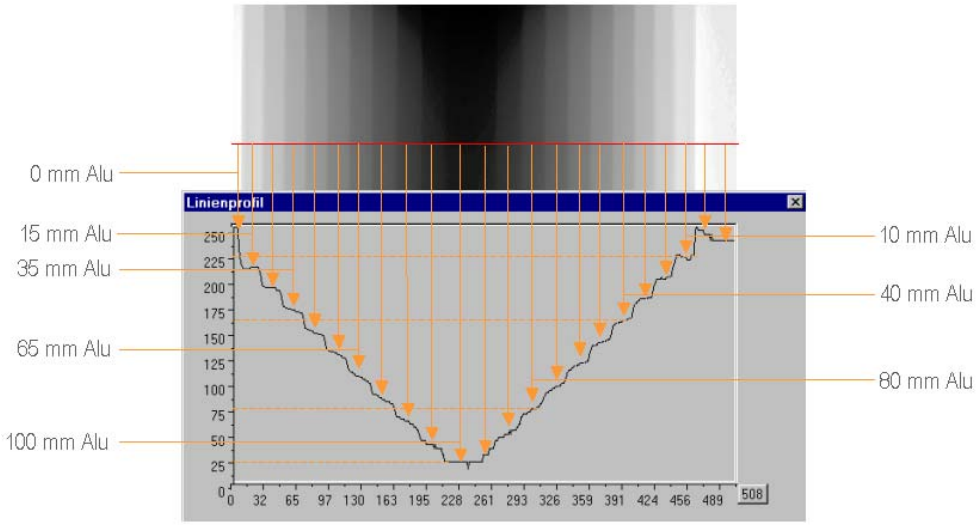

Fig. 12.4: Calibration of intensities (grey values related to material thickness)

The result of the calibration procedure is a table listing the different material thicknesses and the corresponding grey values, e.g. a layer of 100 mm aluminium shows a grey value of 26 which increases to 165 with 40 mm. With that the computer calculates the corresponding material thickness within the image for each single measured grey value. Values between the calibrated levels are interpolated by the computer.

12.4.2 Accomplishing of intensity measurements

The measurement of intensities is normally achieved by means of histograms, line profiles (V9) or simply by a point measurement of the grey value at the position of the mouse pointer. Figure 12.5 shows an example for such a point measurement. The values in brackets in front it indicate the coordinates of the mouse pointer in the image. By this way the location of measurement is exactly indicated.

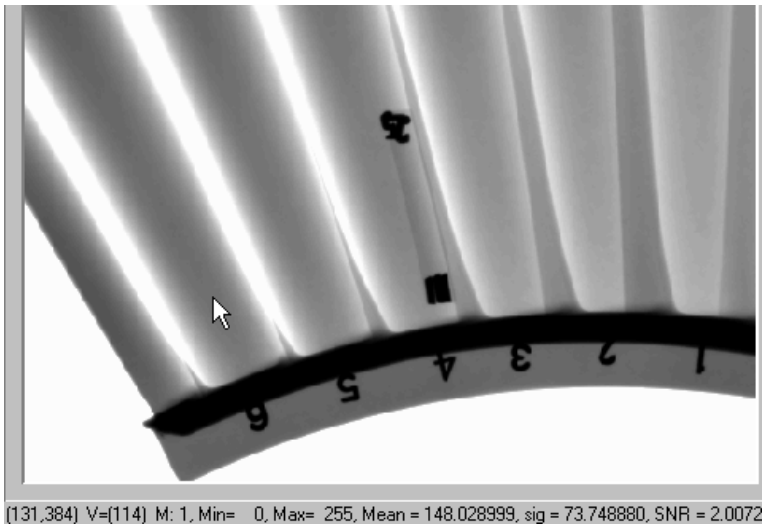

Fig. 12.5: Display of the grey value at the mouse pointer position

12.5 Determination of depth by stereo technique

The X-ray image is a shadow projection. By this reason, the material defects or details of an object are imaged on a plane while the information about the true depth of an item is lost. No information can be achieved about the position of a flaw perpendicular to the *imaging plane* from just a single image.

The position in the depth can be estimated by acquiring a second image with an altered exposure geometry in some circumstances. A perfect resolution of the depth of flaws can only be achieved with the computed tomography (CT) whereby it should be considered that the efforts are balanced with the expected result.

Figure 12.6 presents the principle of stereo radioscopy. Two Irregularities or flaws O1 und O_2 within an object are viewed at from two different aspects A_1 und A_2 by radioscopic means.

The extent of the shift of an object in the corresponding images (distance C1 or C2, resp.) depends on the depth, i.e. on the distance between the object and the imaging plane (X1 or X2, resp.). The larger the object to imaging plane distance the bigger is the shift of the image of the object.

Taken from the geometry of the image acquisition the following relationship applies for the calculation of the imaging shift between the two exposures of the corresponding flaw:

$$C = \frac{X}{e\text{-}X} * f$$

If several flaws are superimposed, i.e. are in line with the direction of the radiation beam, the individual objects only can be separated by one or multiple stereo exposures from different aspects.

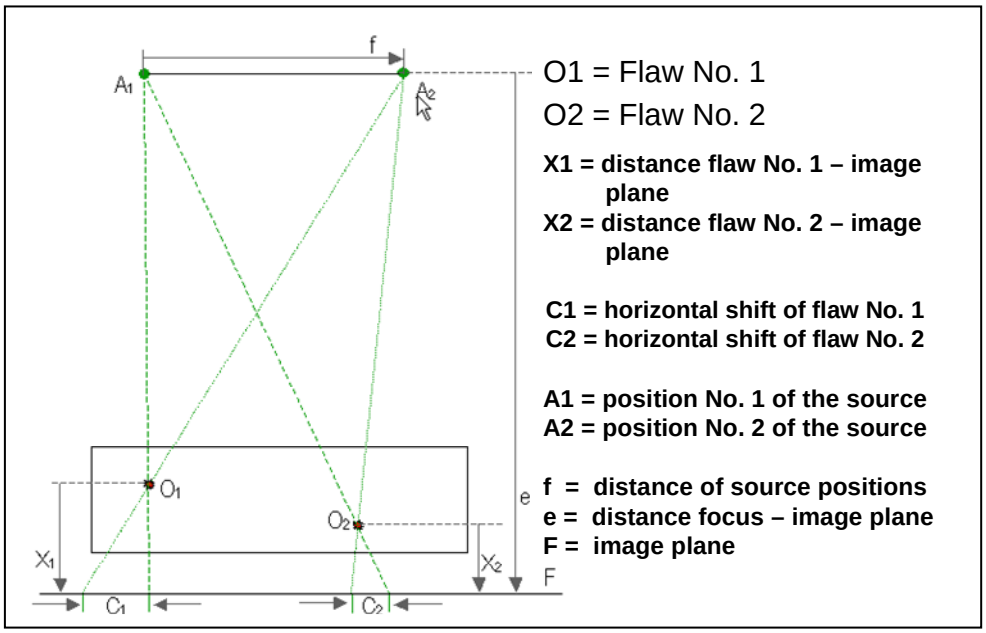

12.6: Exposure geometry to determine the depth

Further information about the determination of the depth or the estimation of a three-dimensional structure of a specimen, respectively, will be presented in L16.

L 13 Evaluation of Digital Image Data

Content

13.1 Requirements for the quality of digital images

The evaluation of irregularities requires their detection first which is inevitably combined with basic technical efforts. No wording can be sufficient to achieve the whole task qualitatively and quantitatively. It is thus easier to define limits that ensure achieving an optimised image quality adequate to the inspection task. This has been accomplished in terms of testing classes that are requested depending on the size of flaws to be detected. While the test class A is commonly sufficient for the inspection of cast components, the test class B is required for weld seam inspections entailing higher demands. Typical rules and standards stating the relationship between the quality class (requirements for a weld seam) and the testing class are represented by the DIN EN 12062 or ISO 17635. Since these requirements are only defined for the film radiography and not for the radioscopy, a selection of the testing class as well as the evaluation of irregularities only can be achieved according to those.

Excerpt from EN 12062 or ISO 17635:

Class according to ISO 5817	Radiography test class	Class EN 13068-3
B	B	SB
C	B (number of sub-parts acc. to A)	SB
D	A	SA

It has to be ensured that a radioscopy system complying with SC1 according to EN 13068-1 and EN 13068-2 has to be used to achieving the testing class SB.

The control of the image quality (see also V4) is achieved by image quality indicators according to EN 462-1 and EN 462-5 (or ISO 19232-1 and ISO 19232-5) that have to be applied for the radioscopic inspection.

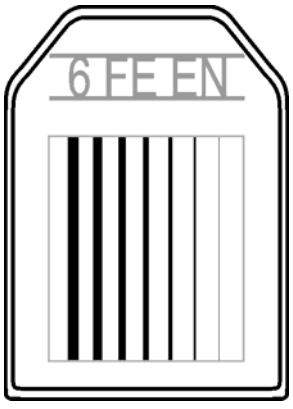

Fig. 13.1: EN 462-1 wire IQI

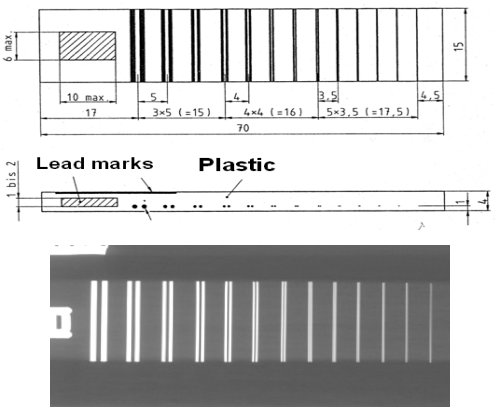

Fig. 13.2: EN 462-5 duplex wire IQI

Position of the image quality indicators:

If the focal spot is larger than the internal unsharpness of the detector system, the image quality indicators are positioned at the side towards to the radiation source.

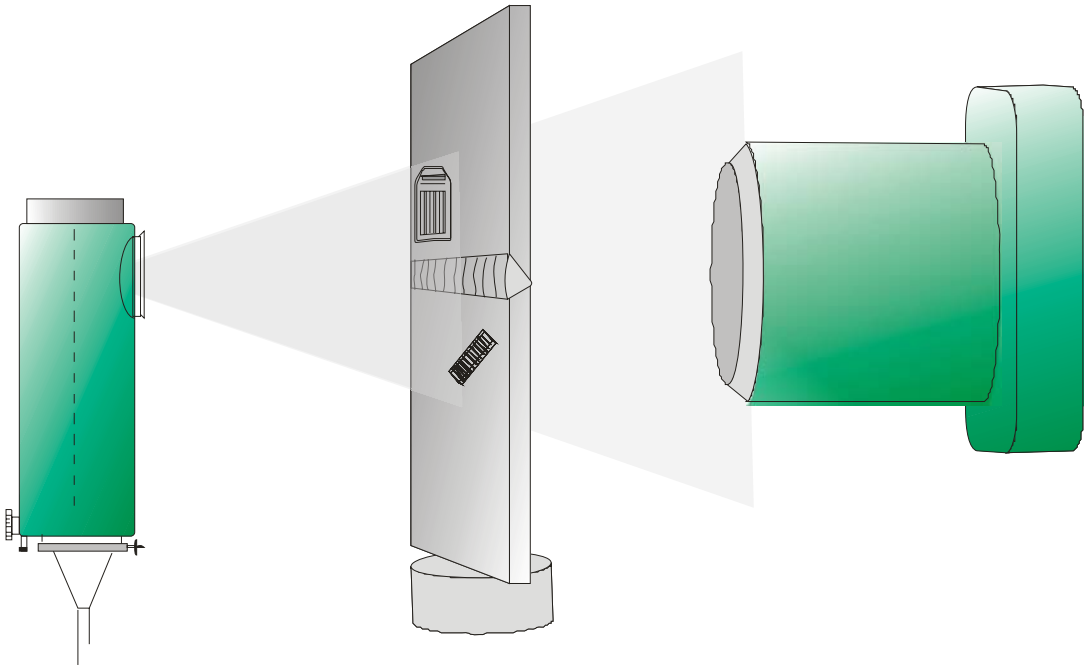

Fig. 13.3: Position of the IQI if $d_{Tube} > Ui_{Detector}$ applies

If the focal spot size d of the radiation source is smaller than the internal unsharpness of the detector the IQI is attached to the specimen on the side close to the detector.

Depending on the penetrated wall thickness the perceptibility of the required wire number (image quality value) has verifiably to be reached as well as the required pair of duplex wires (duplex element) according to table 5 in the EN 13068-3. The image quality indicator has to be chosen which contains the respective wire necessary to proof the image quality value W_{xx}. The wires are grouped together like that: W 1–7; W 6–12, W 10–16 und W 13–19.

SA			SB		
System class SC2			System class SC1		
thickness [mm]	IQI wire No.	IQI duplex wire	thickness [mm]	IQI wire No.	IQI duplex wire
1,2-2,0	W17	11D	-1,5	W19	13D
2,0-3,5	W16	10D	1,5-2,5	W18	12D
3,5-5,0	W15	9D	2,5-4,0	W17	11D
5,0-7,0	W14	8D	4,0-6,0	W16	10D
7,0-10	W13	7D	6,0-8,0	W15	9D
10-15	W12	7D	8,0-12	W14	9D
15-25	W11	7D	12-20	W13	9D
25-32	W10	7D	20-30	W12	9D
32-40	W9	7D	30-35	W11	9D
40-55	W8	7D	35-45	W10	9D
55-85	W7	6D	45-65	W9	9D

Table 13.1: Table 5 of the EN 13068-3

The performance of the system has been achieved whenever the required or a higher image quality value is reached. If this is not the case then the parameters have further to be optimised. The tables 2 und 3 of the EN 13068-3 could serve as a guideline for the maximal tube voltage. Only the image integration, contrast and brightness adjustments are allowed for the image quality control. The image is viewed on a monitor in a *some-what* darkened room.

Steel		Aluminium and light alloys	
wall thickness [mm]	maximal tube voltage [kV]	wall thickness [mm]	maximal tube voltage [kV]
1,2 to 2,0	90	≥ 5	45
2,0 to 3,5	100	≥ 10	50
3,5 to 5,0	110	≥ 15	55
5,0 to 7,0	120	≥ 25	65
7,0 to 10	135	≥ 35	75
10 to 15	160	≥ 45	85
15 to 25	210	≥ 55	95
25 to 32	265	≥ 70	110
32 to 40	315	≥ 85	125
40 to 55	390	≥ 100	140
55 to 85	450	≥ 120	160

Table 13.2: Table 2 and 3 of the EN 13068-3

13.2 Documentation

Whenever a test report is requested for a radioscopic inspection, it should contain at least the following information:

1. Name of the testing laboratory
2. An unambiguous report number
3. Specimen inspected
4. Material
5. Stage of production
6. Nominal thickness
7. Radioscopic technology, testing class and system class
8. Tag system if labelled
9. Radiation source, type and size of the focal spot and device employed
10. Tube voltage and current or activity of the radiation source
11. Beam direction (if not perpendicular to the object)
12. Filters and collimators applied

13. Integration time, focus-detector-distance and geometric magnification
14. Kind and position of the image quality indicator (IQI) applied
15. References about the IQI and the required/achieved image quality value
16. Specification of the accomplished image processing, if applicable
17. File format and file name of the stored data
18. Compliance with the agreed standards
19. Deviations from the agreed standards
20. The responsible persons' names, certifications and signatures
21. Date of the inspection and of the report

The data mentioned in item 17 of the inspection report should consist of the unprocessed images on an external storage medium. This medium has to be capable to archive the data for a long time without any loss of *information*.

13.3 Evaluation according to Rules and Standards

In numerous cases the flaws that have been detected in a specimen visually by an operator should also be evaluated and subjected to a classification. This should be in accordance to common refereed criteria that have been applied for evaluating.

In case of aluminium cast components the American standard ASTM E155 represents de facto the standard.

13.3.1 The ASTM E155 film catalogue and digital reference images E 2422

The ASTM is an American organisation for standardisation who defines the guidelines and rules for methods and procedures including e.g. NDT (group E07).

The E 155 is a guideline established in the 1960s that

- defines 8 classes of flaws in cast aluminium and further 6 classes of flaws for cast magnesium
- separates the classes of flaws into 8 levels each wherein the toughest one is level 1.
- (The allocation of the corresponding flaws to each level is accomplished by numerous expert opinions basing on film radiographs.)
- refers to 1/4" as well as to 3/4" thickness *gages*, wherein the 1/4" are taken up to 1/2", beyond this the 3/4" applies ("= inch = 25,4mm)

ASTM sells a set of 13 * 8 * 2"*2" large X-ray films; these radiographs serve as a physical reference (on a light box). The original plates themselves are stored in a safe with the company Parker in Hartford, Connecticut.

Fig. 13.4: Size of a ASTM E155 plate (reference hardware)

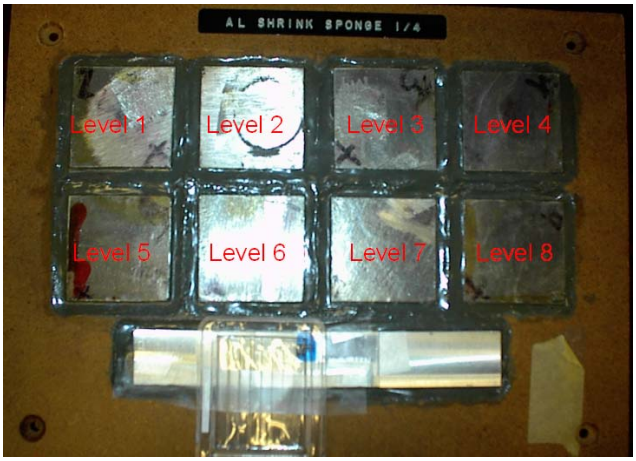

Fig. 13.5: Arrangement of a plate with assignment to the levels

Since 2006 the ASTM provides to E 2422 digital reference images with digitised E 155 films. Using special software for reference image comparison, the acquired digital image can be compared directly with an ASTM reference image on a monitor screen.

ASTM E155 reference plates

	1/4 "	3/4"
Aluminium Gas Holes	X	X
Aluminium Shrinkage Cavity	X	n.a.
Aluminium Foreign Material, less density	X	X
Aluminium Foreign Material, more density	X	X
Aluminium Shrinkage Sponge	X	X
Aluminium Gas Porosity Round	X	X
Aluminium Gas Porosity Elongated	X	X

Fig. 13.6: Flaw classification according to E155

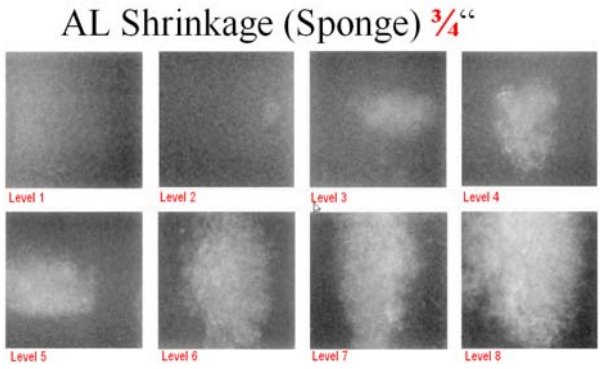

Image of a film (inverted)

Recent computer programs are designed in a way that reference images can be displayed simultaneously; all deviations in size and grey value scaling will be also superimposed onto the reference image so to ease the allocation for the viewer.

2 DVD's containing digitised films of E 155 in 10 µm pixel resolution can be installed on the computer in the pixel resolution of the used detector. The pixel resolution of the detector has to be provided during the installation process. So both images can be compared side by side on a monitor screen.

13.3.2 Evaluation of weld seam irregularities according to ISO 5817

Preface

In the course of a non-destructive inspection the operator is expected not only to detect irregularities but also to evaluate them, i.e. to assess the specimen with respect to the acceptability for its intended use. There is no commonly applicable recipe for the definition of the necessary assessment category related to the component. It thus depends on numerous factors which quality may be required for a weld seam within a certain component, e.g. on constructional conditions, subsequent procedures, surface treatments, kinds of mechanical load, conditions of operation, consequences of a prior defect and economic considerations.

The decision about the quality a weld seam should be developed meaningfully together with the designer, manufacturer and the user, i.e. in an interdisciplinary co-operation. Since the quality parameters are cost relevant and have to remain calculable the quality requirements should be agreed on before ordering, if possible included in the quote. It has to be assumed principally that nearly every weld seam shows irregularities while nevertheless constituting a sort of "quality". If the level 2 operator is provided with a guideline by the designer, the production or the approvers that states e.g. a maximum occurrence and size of an irregularity which should not be exceeded he will be in a position to classify an irregularity with respect to this guideline.

According to ISO 5817 three evaluation classes are available in accordance to the mechanical stress they may be subjected to:

Evaluation class	D	For low mechanical stress
Evaluation class	C	For medium mechanical stress
Evaluation class	B	For high mechanical stress

For these evaluation classes there are different limits of irregularities (limiting values for the size of the irregularities) that become less severe from class B to class D. All three quality levels are defined with regard to their characteristics in the standard. The interpretation of the standard becomes difficult if several irregularities are superimposed at a single spot so that the maximal limit cannot be applied any more for a single indication and a general evaluation becomes necessary.

The external appearance of a weld seam should **be inspected visually**, if an access is feasible, and assessed with the aid of measurement by gauging tools. The assessment of internal irregularities is accomplished alternatively by an X-ray inspection (film radiography or radioscopy, respectively), by evaluation of the fracture surface or by an ultrasonic inspection.

It has to be taken into account that the limit values given in the ISO 5817 are real sizes of flaws that might be only conditionally detected by non-destructive testing. In marginal cases the method of measuring the irregularity is of great importance, or further NDT methods have to be applied.

Identification of irregularities in weld seams

The first step is the identification of an irregularity. The terms of the DIN EN ISO 6520 should be used here. A formatted record sheet may serve as a help.

Evaluation record:

Weld seam tag:_____

Irregularities according to DIN EN ISO 6520:

section of seam	101 (Ea)	102 (Eb)	103	104 (Ec)	2011 (Aa)	2012	2013	2014	2016 (Ab)	202 (K)	301 (Ba)	3011	304 (H)	3041	401 (C)	4011	4013	402 (D)	5011 (F)	5013	507	511	515	517	further assign-ment no.

101 longitudinal crack	2011 gas pore	301 slag inclusion	401 lack of fusion	5011 continuous undercut	511 incompletely filled groove
102 transversal crack	2012 porosity	3011 slag line	4011 lack of side wall fusion	5013 shrinkage groove	515 root concavity
103 star shaped crack	2013 clustered porosity	304 metal inclusion	4013 root fusion	502 excess weld material	517 poor restart
104 crater crack	2014 linear porosity	3041 tungsten inclusion	402 lack of penetration	504 excess penetration	
105 crack cluster	2016 worm holes			5041 root drop	601 stray arc
106 branched crack	202 shrinkage cavity			507 linear misalign-ment	602 sputter

assessed according to	evaluation class	comply / does not comply

remarks:

Classification of weld seam irregularities

Classification is understood as the assignment of irregularities to a certain quality level (group of acceptance). This is accomplished in accordance to the kind, the size, the frequency and the position of the irregularity occurred.

The specifications of an evaluation class essentially needed for classifications have to be given by the construction. In this course various irregularities can be assigned to different evaluation classes. Practically this specification is made for a whole weld seam in most cases.

It is possible by true to measure measurements (see 12.3) to determine the extent of an irregularity. Adding the parts of the surface of the individual irregularities yields the cover rate. The following Table lists the admissibility of cracks, cavities and solid inclusions in accordance to ISO 5817. The evaluation class applies when the irregularities stay within (≤) the limit values.

indication	**ISO 5817 evaluation class**		
	B	**C**	**D**
Cracks	not permitted	not permitted	not permitted
Terminal crater cracks	not permitted	not permitted	not permitted
Pores (2011, 2012) (…%) = single layered	Ø ≤ 0,2 · t (max. 3 mm) cover: ≤ 2 % (1,0%)	Ø ≤ 0,3 · t (max. 4 mm) cover: ≤ 3 % (1,5%)	Ø ≤ 0,4 · t (max. 5 mm) cover: ≤ 5 % (2,5%)
	related to the area = seam width · 100 mm seam length		
Clustered porosity (2013)	$Ø_{Pore}$ ≤ 0,2 · t (max. 2 mm) cover: envelope ≤ 4 %	$Ø_{Pore}$ ≤ 0,3 · t (max. 3 mm) cover: envelope ≤ 8 %	$Ø_{Pore}$ ≤ 0,4 · t (max. 4 mm) cover: envelope ≤ 16%
	related to the area = seam width · 100 mm seam length		
Elongated cavities, solid inclusions (2015, 300)	single width: h ≤ 0,2 · t (max. 2 mm) single length: l ≤ t (max. 25 mm)	single width: h ≤ 0,3 · t (max. 3 mm) single length: l ≤ t (max. 50 mm)	single width: h ≤ 0,4 · t (max. 4 mm) single length: l ≤ t (max. 75 mm)
	related to 100 mm seam length		
Worm holes (2016)	Like gas channels (caution: length may be not measurable)		
Linear porosity (2014) pore distance: ≥ smaller Ø	Ø ≤ 0,2 · t (max. 2 mm) cover: ≤ 4 % (2%)	Ø ≤ 0,3 · t (max. 3 mm) cover: ≤ 8 % (4%)	Ø ≤ 0,4 · t (max. 4 mm) cover: ≤ 16 % (8%)
	related to the area = seam width · 100 mm seam length		

L 14 Compilation of a Written Procedure

Content

14.1 Preface

According to DGZfP's qualification guidelines (corresponding to EN 473 and ISO 9712) and related recommendations such as the American SNT TC 1A, an operator qualified on level 1 should be in a position to complete a radioscopic inspection or other tasks of the digital radioscopy professionally and to compile a record of the results following oral or written instructions.

The operators of the level 2 should also be able to work independently in accordance to the standards and other rules. They should also be in a position to compile inspection instruction and to evaluate testing records.

A person who holds a level 3 certificate should have the competence to supervise and to instruct inspection personnel and to take the responsibility for the personnel and the testing facilities. In addition, he has to be capable to evaluate and to assess the inspection results according to the applicable rules, standards and specifications.

14.2 Purpose of a written procedure

There is a rather manifold palette of various DR - tests: Commonly, these are serial inspections of components in large numbers. Moreover, the expected statements about the inspected parts could be of different nature: in some cases, a plain yes/no-decision is sufficient to judge if a component satisfies the reliability criteria. In other cases, the customer expects also some sort of quantification. In **each** case, the appropriate steps of the inspections have carefully to be selected as well as a consistent planning of the performance of the inspection and explicit instructions for the inspection personnel!

In many cases all the briefings will be given in form of a written procedure. This should ensure that

- the statement requested by the customer to assess the specimen will be produced,
- a subsequent challenge of the inspection result by reason of imprecise working instructions will be avoided,
- repeated inspection or those applied to several identical components will be accomplished always under the same conditions,
- economic aspects will be considered while working.

14.3 Procedure of compiling an written procedure

Creating an overview first!

Before commencing a compilation of an written procedure it is important to achieve an exact impression about the specimen and its environment for one's own sake. In case of unfamiliar specimens they should be viewed at on site together with the actual operator / customer. The aim of the inspection and the basic conditions should be discussed and scrutinised in detail.

In case of components integrated into plants and within a strange environment (i.e. outside the acquainted testing laboratory) many questions may be raised that need a clarification: Is the area of inspection accessible? Who is the person of contact on site and is able to help? Are there any specific safety precautions necessary?

If the specimen has already been in use then it has to be questioned what kind of media it has been in contact with, if these entail poisonous substances, may be combustible or may bear any health risk. It has also to be discussed in which way and by whom the specimen has to be cleaned prior to the inspection. Independently from cost considerations it is always of benefit to take advantage of the customer's competence and responsibility in this case.

Please consider: Circumstances taken for granted by a conscious and experienced operator or head of a group of inspectors may be taken less seriously by a somewhat inexperienced one! Therefore, all facts to be considered and all results expected to be achieved as well as the format of the requested documentation have to be stated clearly and unambiguously in an inspection instruction. It is always a problem if an operator has nothing more to say in a critical discussion about the quality of the inspection performance and/or the correctness of the inspection results than: "How should I have known that you wanted to have it differently?"

14.4 Design and content of an inspection instruction

In the following, some aspects are tackled that have to be taken into account when compiling a written inspection instruction.

First of all, the inspection instruction must contain the precise description of the inspection task to be completed. This is followed by the exact indication of the testing procedure, the requirements necessary to perform the inspection and the experimental setup together with the necessary equipment as well as a description of how to accomplish the inspection. This is completed by the statements on the documentation with all the relevant facts and the expected inspection results.

In case of a general instruction that eventually should be made accessible to customers or outsiders it could make sense to **explain** some **terms** in the beginning so everyone involves “speaks the same language”.

The aim of the inspection: what should be achieved?

The inspection instruction should begin with a precise description of the task to be accomplished by stating the aim of the inspection. This entails, in addition to the exact identification of the specimen, the time and the site of inspection also the aim in words.

Who is allowed to inspect?

If the inspection personnel or the inspection supervision needs a certain qualification or expertise these have to be stated in the inspection instruction. The inspection personnel should be well acquainted with the testing technology applied in every case.

Even if the work will be accomplished not always by the inspection personnel, these essential prerequisites for the performance have nevertheless to be defined and stated in the instructions. In this context, it is important to appoint precisely the work to be done. Not only the cost allocation but also the responsibility should be determined.

Where to leave the results?

At least in the conclusion, the written procedure should entail how to report the achieved results. In this context, it has to be stated which results are supposed to be documented and how the document should be formatted. If these details are missing it may happen that important intermediate results or data are lost and may eventually only be retrieved by a repetition of the whole inspection. In many cases, an appended **testing record sheet** or a **measurement data collection sheet** may provide the operator with some clarity.

14.5 Meaningful structure of an inspection instruction

An analysis of numerous inspection instructions of various enterprises has shown that all relevant items are included in an inspection instruction when following this structure:

	Cover sheet	Showing the identification number, testing method, coverage and release notes, author's name
0	**Content**	
1	**Coverage and purpose of the inspection**	Short description of the subject; applicable rules and documents
2	**Inspection personnel**	e.g. information about the minimally required qualification
3	**Prerequisites to accomplish the inspection**	Preparatory work such as dismantling and defining the inspection scope, cleaning
4	**Safety precautions**	Protective measures for the personnel and for the equipment
5	**Equipment**	Type, measuring range, precision etc.
6	**Inspection setup**	With a sketch, if required!
7	**Preparation of the inspection**	Work to be accomplished by the inspection personnel
8	**Workflow of the inspection**	Going into details!
9	**Repetition of the inspection**	Procedure after a touching up has been accomplished
10	**Recording of the results / inspection record**	Good work has to be sold accordingly!

14.6 Written Procedure (short schedule format, testing record)

Task:

You are receiving the order to inspect the following cast component:

Catch plate : 2000 pieces

Dimensions : see plot

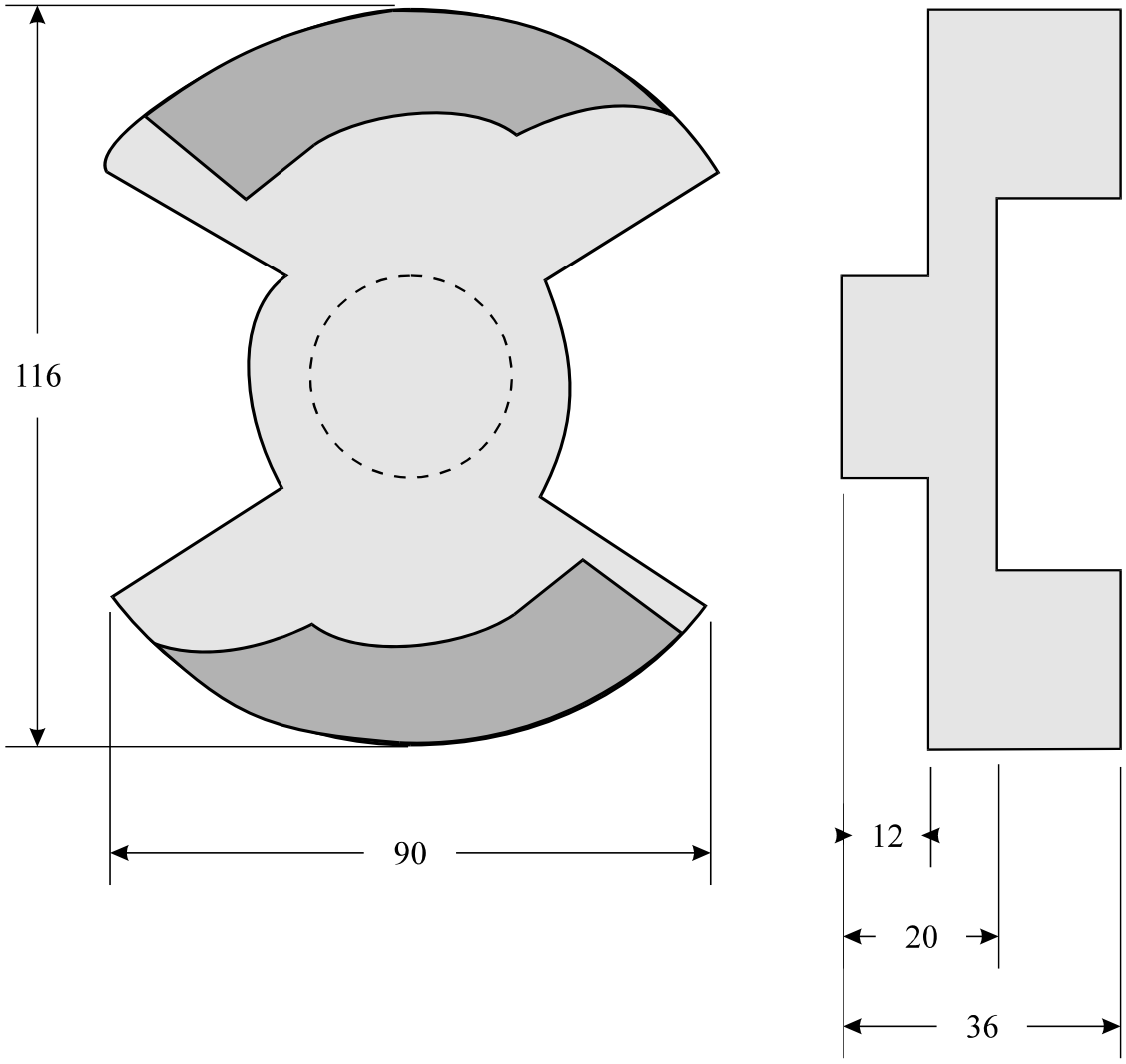

Specification of the specimen:

Testing obbject: Catch plate Identification: serial number	Testing procedures: EN 13068 -3 Testing class: IQI set: SA EN 584-1 W6 Al
Material: Al Max. penetrated thickness: 24 mm	Dimensions: Coverage: ∅ 116mm, x 36 mm 100%

Relevant inspection data:

Test positions:	1	perpendicular	projection
Inspection sequence:	1		
Type of radiation source:	YXLON 160 kV	Y.TU 160 DO 02	
Focal spot size d [mm]:	0.2 mm		
Pre-filter:	no		
Diaphragm:	adjusted to	Size of part	
Masking:	Lead in segments		
Tube voltage [kV]:	65 kV		
Tube current [mA]:	5 mA		
SDD:	500 mm		
SOD:	300 mm		
Geometrical magnification:	1.7		
Detector, SR_b:	Image Intensifier	0.2 mm	
Input screen size:	200 mm (8”)		
IQI required / achieved:	W 9 / W10	D7 / D7	
Integration time:	2 s		
Image Processing:	yes		
Filter sequence 1:	High Pass	Customer 1	
Filter sequence 2:			
Filter sequence 3:			

Location:	Date:	Operator:
BAM Berlin	12. Dec. 2008	Expert B

Remarks:

L 15 Automatic Image Evaluation

Content

15.1 Semi automatic and automatic image evaluation

The term **semi automatic** means that the image evaluator controls partly operating image processing algorithms and has to select from various alternatives of automatic partial procedures. The partially operating image improvement algorithms are assembled interactively by the inspection supervisor with sample images in the first instance. It depends predominantly on the inspection purpose which sections could be automated – from acquiring the X-ray image up to the object detection and classification that involves the image evaluation.

The term **automatic** means that the whole inspection process is accomplished automatically. This starts with the acquisition of the X-ray image followed by the automatic image processing and concludes with the automatic evaluation of the image. A prerequisite for the feasibility of such completely automatic processes is a high similarity between all the specimens of the series.

15.2 Methods and mode of operation of the automatic image evaluation

The following methods for the image processing have already been introduced and are applied in the (semi) automatic image evaluation:

-	Contrast optimisation	LUT spreading / 16 to 8 Bit conversion	(L09)
-	Noise suppression	integration (with time) / low pass filtering	(L05&L11)
-	Filtering	high pass filtering / low pass filtering	(L11)
-	arithmetic operations	difference of original and filtered image	(L05&L15)
-	threshold setting	binary coding / segmentation	(L15)
-	object measurements	area or diameter measurements	(L12)

In many cases, subtracting an “unsharp” image from the original one is taken as an **arithmetic function** for the purpose of an automatic image evaluation. Here, the filter is designed in a way that it makes potential flaws disappearing as far as possible; when calculating subsequently the difference only the parts “filtered away” reappear. This method is applied whenever grey value gradients are present in the image.

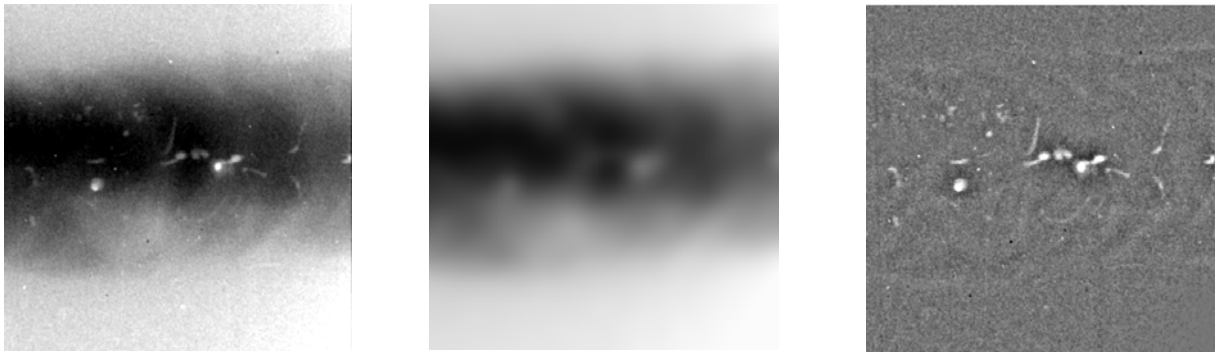

Original image - Filtered image = Difference image

The **setting** of a **threshold** is applied to separate discontinuities in a specimen from the regular structures and thus to segment them. The segmentation is understood as the separation of the feature searched for and the back ground. In cases of discontinuities within weld seams or cast components these features are displayed with a high (bright) grey value in the radioscopic image. Now the threshold has to be found that separates the bright grey values from the dark ones in the digital image. This results in a binary image where the bright areas indicate the potential discontinuities while the remaining ones remain black.

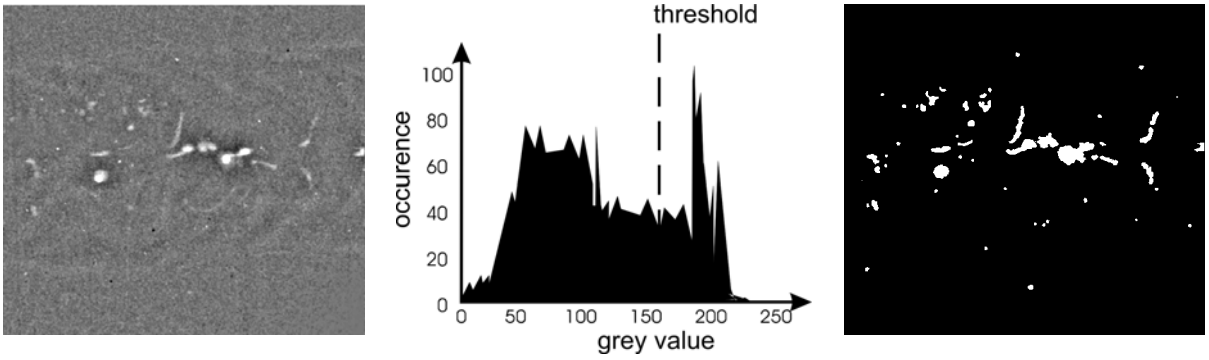

Difference image Histogram and threshold Binary image with potential flaws

15.3 Flow of a semi automatic image evaluation

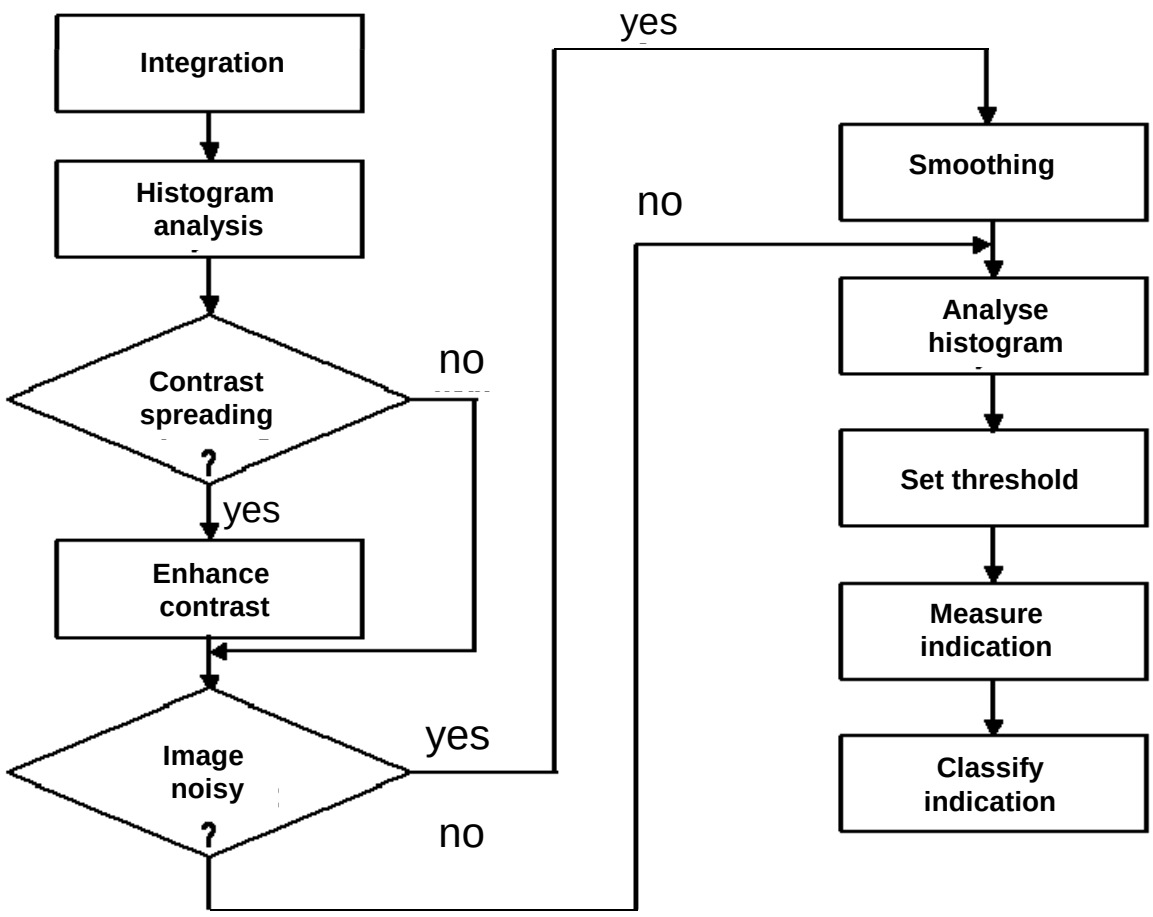

Fig. 15.1: Flow of an image evaluation

Presumed that the X-ray parameters are chosen optimally for the specimen to be interrogated the number of images has to be determined that have to be integrated in order to achieve an image of sufficiently low noise. An analysis of the histogram then indicates if the contrast really is sufficient; a LUT may be involved to spread the contrast. In spite of the integration of noisy images additional smoothing might be applied using an appropriate filter. In case of a semi automatic image evaluation this is the moment to choose an appropriate threshold. Conclusively, the object is measured and classified, if desired. The essential problem consists of finding always the appropriate threshold for the segmentation. For this purpose, the image evaluator should have some experience.

The following Figure demonstrates the resulting images of each single step of the image processing as given by the flow shown in Figure 15.1. Different threshold values have been tested here for the segmentation to choose the most appropriate one.

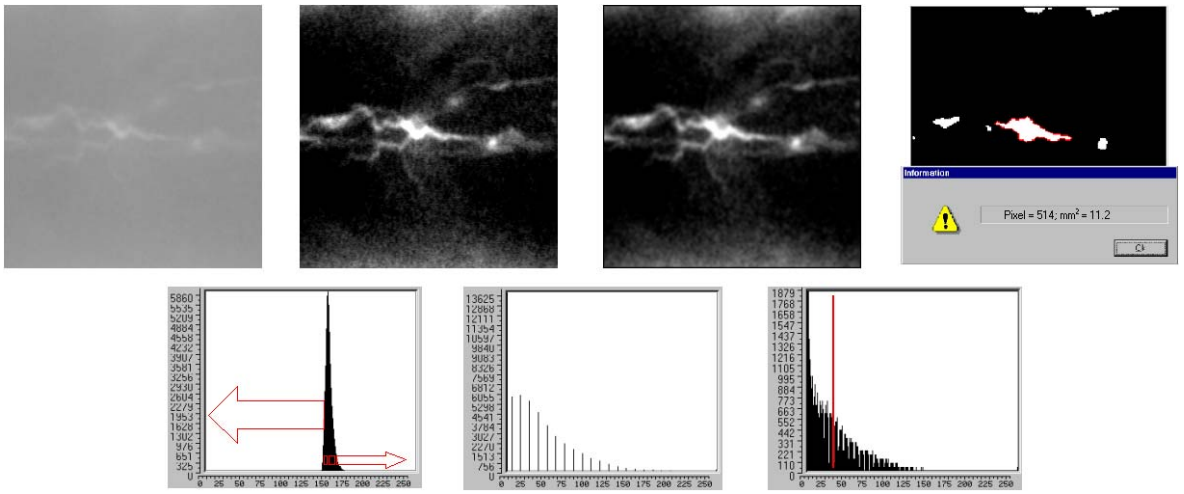

Fig. 15.2: Approach of semi automatic image processing in accordance to Fig. 15.1

The semi automatic image processing leaving the decision making to the operator still is the optimal mode of inspection for many kinds of objects since the specimens may not allow an automatic inspection – as for example weld seams (L15.4.1), or the number of identical specimens is not large enough to justify the efforts of an automatic inspection (L15.5).

15.4 Automatic evaluation of weld seams

There are several reasons why the fully automatic image evaluation for weld seam images has not yet been realised in an industrial extent. The main reason consists in the fact that contrast variances, the distribution of grey values, unsharpness etc. are so drastic that a once accepted setting of image processing parameters may apply to other images only in a very limited range; all other images may remain falsely evaluated.

The diversity of the possible shapes if crack indications should be considered that could be imaged in really various ways and may only appear fragmentally. In spite of these difficulties some working groups have developed algorithms to detect flaws and to classify them. These are in a position to evaluate images of weld seams with the aid of new mathematical approaches such as fuzzy logic and neuronal network technologies showing a reliability that comes close to that one of a visual evaluation. However, these technologies are only found in the laboratory up to now.

15.4.1 Limits of the automatic weld seam evaluation

The limits of the automatic image evaluation should be demonstrated with an example showing the image of a weld seam. In Figure 15.3, a section of an image is shown which is subjected to the standard steps of the image processing. Problems occur in selecting an appropriate threshold value for segmentation when attempting to detect a long crack that is clearly visible for the human viewer. Various threshold values did not achieve a satisfying result.

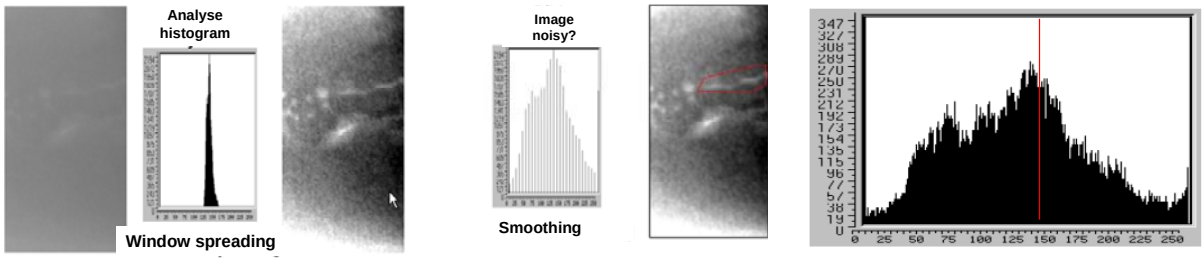

Fig. 15.3: Approaching the segmentation

The enframed crack is clearly visible for the human viewer but not retrievable within the histogram on the right. It is thus impossible for the computer to make an appropriate decision for a threshold value. Various threshold settings lead to the following results:

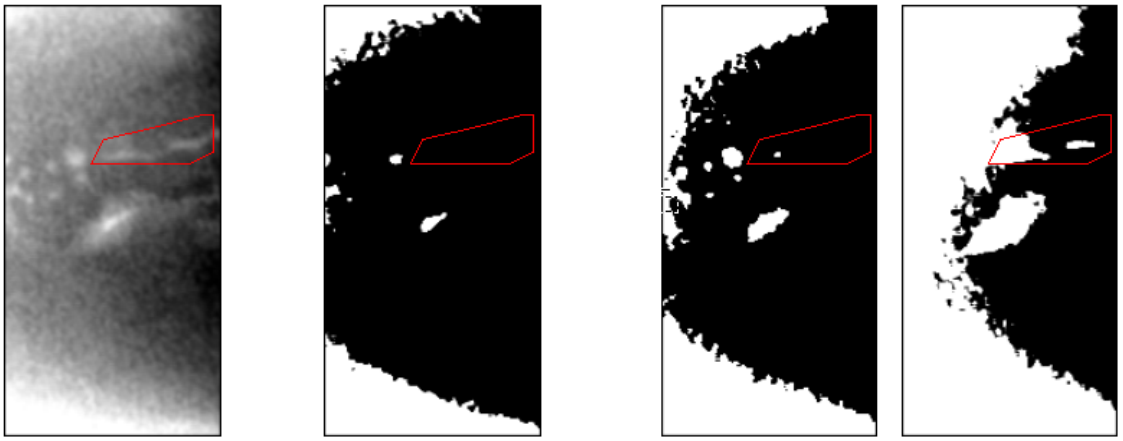

The crack cannot be recognised completely in any of these binary images. Therefore, the mode of image processing is changed to the difference image method:

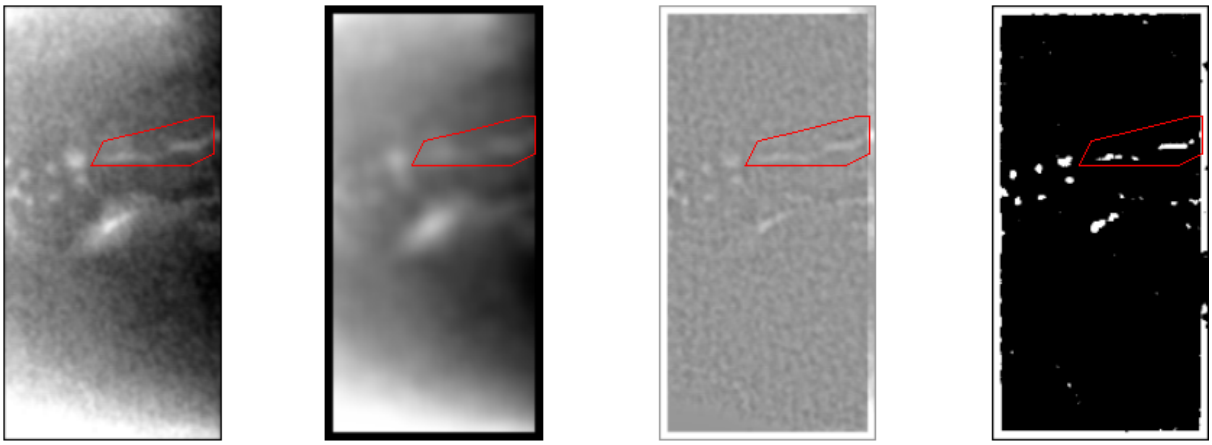

Now a straight forward search for a threshold value allows a glimpse of the crack: The thresholds shown below lead to the following results:

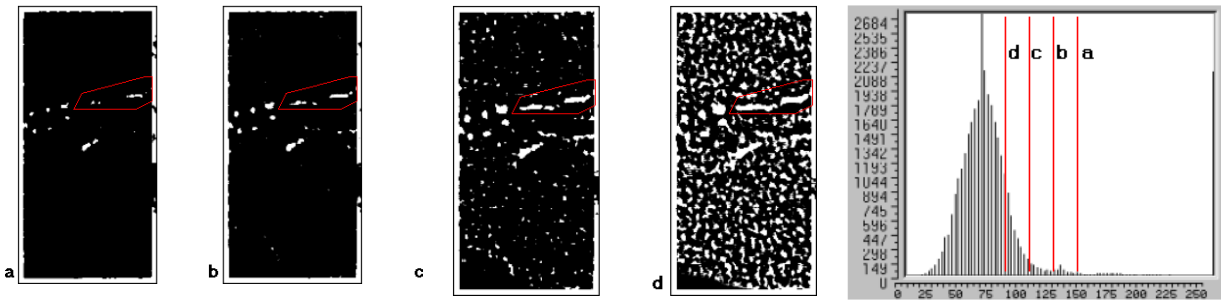

Fig. 15.4: Segmentation thresholds

The enframed crack cannot be detected in its whole extent with any of the thresholds shown; starting with the threshold “c” unreasonably many pseudo features are added so that an automatic procedure cannot make a meaningful decision any more between real flaws and pseudo features.

Some automatic systems have been tried successfully for selected applications such as in laser weld seams of automotive steel rims; however, these weld seams are characterised as particularly smooth and flat ones.

15.5 Automatic image evaluation of cast components

The automatic image evaluation plays an essential role with safety-relevant components in the automotive industry when inspecting cast components, particularly those made of aluminium, since flaws never can be excluded by physical reasons during the manufacturing process. Independently from the viewer’s current alertness, identical decision should be made for comparable flaws as far as possible, and this should be achieved increasingly in shorter time intervals, the pace of the production line.

The manufacturers of automobiles mostly issue definite instructions for the inspection. These entail limiting either the flaw area or its diameter; in addition, the flaw density is confined frequently in order to cover also porosities or clusters of cavities. A classification of flaws according to their origin, e.g. gas bubbles, voids or surface *links* is not realised yet at the status of 2003; the main obstacle for that might be the high similarity between all those flaws in an X-ray image – rather often, the type of flaw may be determined doubtlessly only by means of the position of the flaw within the specimen.

15.5.1 Requirements for the fully automatic evaluation of cast components

Practically, rather differently severe requirements are made for a fully automatic evaluation system for detecting flaws in X-ray images:

- A fully automatic system has to ensure that flaws that lead to a rejection according to the quality demands are really recognised by the system and classified as to be rejected.
- The pseudo-rejection rate, i.e. the number of parts that have been wrongly classified for exclusion by the inspection system, has to be kept negligibly low already by economic considerations. This includes demanding also a high reliability of the system.
- The unimpaired operability of such a system has to be ensured periodically by an autonomously accomplished self-test.
- The fully automatic inspection should not take longer than a visual inspection.

These requirements that are competing each other, i.e. high economic efficiency on one hand and high reliability on the other hand have to be considered for both, choosing the approach for a resolution and designing the automatic operating device.

15.5.2 Flow of the fully automatic cast component inspection

Fully automatic X-ray inspection devices are designed for maximal throughput. Nowadays the mechanical transport and moving devices are limiting a further reduction of the inspection time. The automatic image evaluation is normally faster than the mechanics – albeit by means of parallel computation.

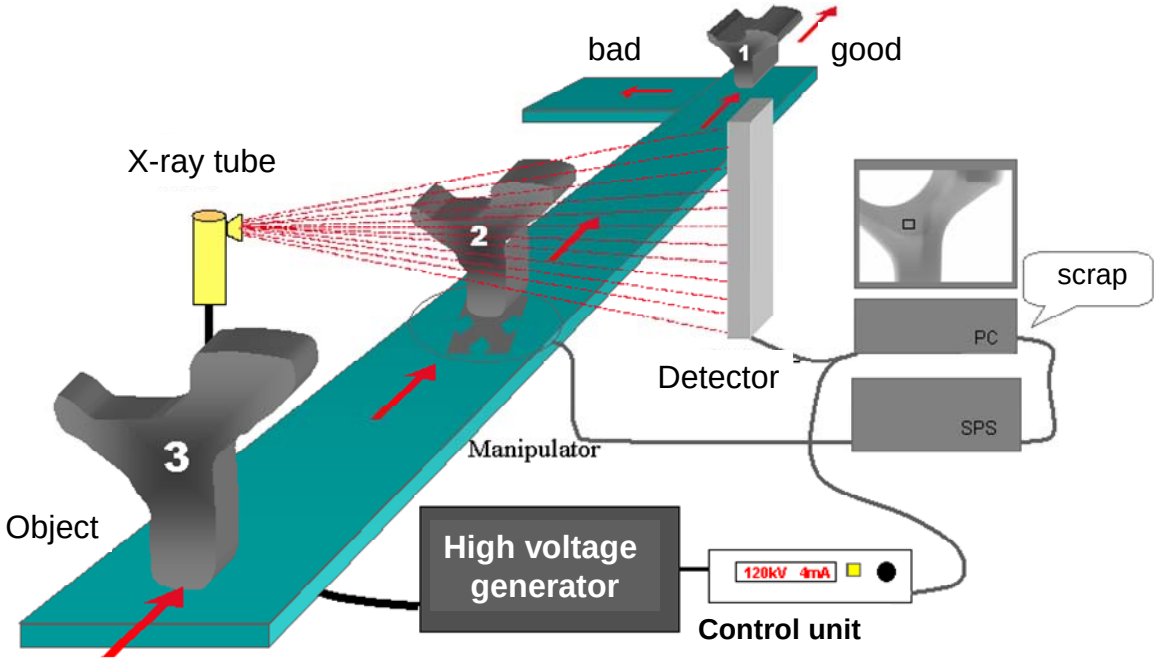

Fig. 15.5: Flow of the automatic inspection of cast parts

The principle flow of the inspection is shown in Figure 15.5: While the specimen No. 3 is waiting, the inspection of the object No. is in progress. The object No. 1 is already checked and is waiting for the final decision of the computer. This is accomplished time delayed with respect to the X-ray procedure since the last position still has to be evaluated and to be adjusted across all positions if required. A flaw is labelled in the first X-ray image, and the part is directed away from the production line towards the rejections. The computer also controls this mechanical point, i.e. no human eye controls any more the decision of the computer in most cases. It thus become obvious that a poorly adjusted image processing program either is dangerous (leaving the passage of too many faulty components) or dumping to many acceptable parts to the rejections (pseudo-rejection is very expensive!).

The X-raying itself is position-based (start-stop operation). For every specimen, an individual mechanical inspection program is established that contains numerous different positions for inspections in most cases. The specimen either is moved by a manipulator into the beam line or lies on a palettes that are pushed into the beam line. An image processing program has to be compiled which is capable to detect the potential flaw safely in the corresponding position according to the inspection specifications. The actual flaw detection has to be proven to the customer by means of sample components with real flaws or with prepared specimens (*faked flaws*) – e.g. by drilled holes or, better, by attached image quality indicators with hollow balls. These sample parts are also suited for the periodical testing of the device later on in operation.

15.5.3 The use of the reference image technology

In the first drafts of the image processing in such a position-bastes system an approach was chosen to generate an averaged reference image that has been subtracted from each single acquired one during the process.

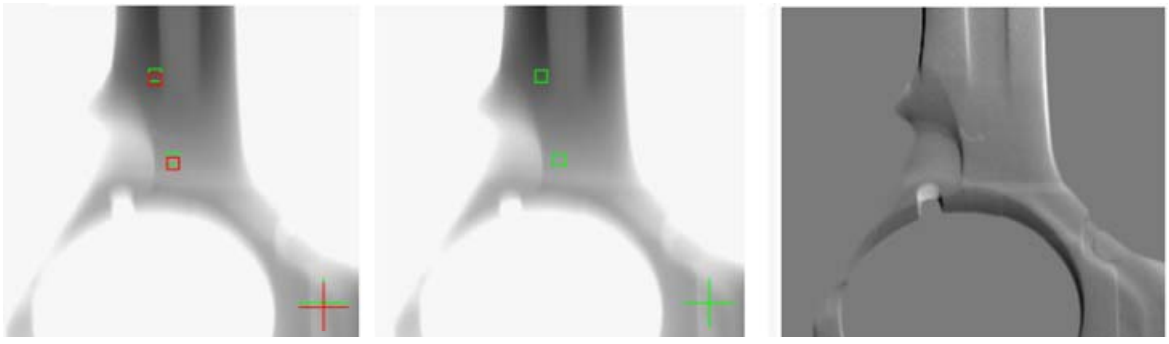

Fig. 15.6: Difference image with a reference shifted only by 3 pixels

Figure 15.6 shows a deviation of 3 pixels towards the bottom in the actual image (ca. 0,8mm), no lateral shift is been found. Despite of this extremely low deviation in the mechanical position the spread difference image shows a relatively high signal beside the large cavity. If it is attempted right now to extract the large cavity with a threshold the problem occurs which is shown in Figure 15.7 that many other structures appear in the

binary image beside the cavity – moreover, it has to be stated that the cavity is detected rather lately (the 4th threshold value) in its whole shape in contrast to the regular structures of the specimen.

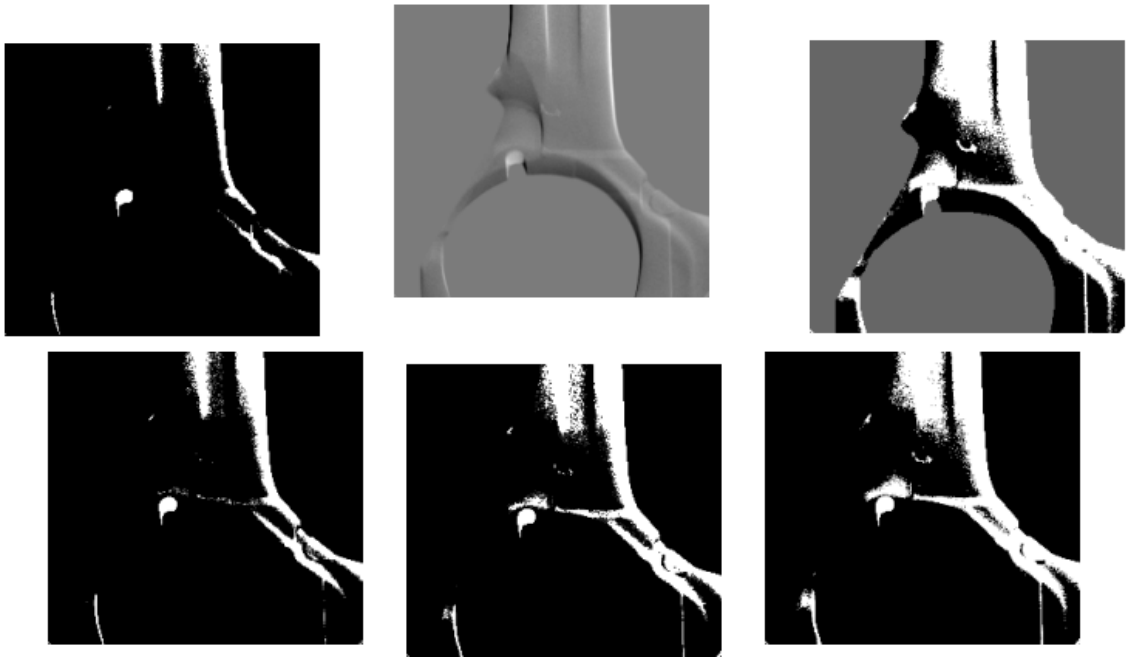

Fig. 15.7: Application of 5 different threshold values for the segmentation

This reference image technology leads to a very high pseudo-rejection rate since

- the manipulator claws or the palette trays cause tolerances in positioning
- the specimens deviate from their required design form (also in thickness)
- the X-ray scatter and the scanning (quantification) may vary

Therefore, this approach is abandoned in this form. Modern systems apply suitable filters to the actually acquired image and take a reference image only for purposes to determine deviations in the position and to correct the regions for specifications *of interest*.

15.5.4 Procedure of the Automatic Defect Recognition (ADR)

The contemporary **A**utomatic **D**efect **R**ecognition (ADR) operates with the following steps:

1. contrast optimisation of the acquired image
2. matching of the area of inspection with the actual image
3. filtering with special, properly adjusted filters
4. differentiation: original image minus filtered image
5. converting to binary of the differential image with a threshold (segmentation)

6. classification of the defects according to the specification
   while removing regular structures (“pseudos”) – if possible

This flow of activities is shown in Figure 15.8 with a series of images. Image A shows the already contrast optimised image with the marked regions of inspections which now are corrected in accordance to the shift of the specimen in the actual image. Image B displays the image A filtered with a large low pass filter. In the next image, the contrast spread difference image can be seen [A-B]. This image is converted to binary with a threshold extracting the indicated segments.

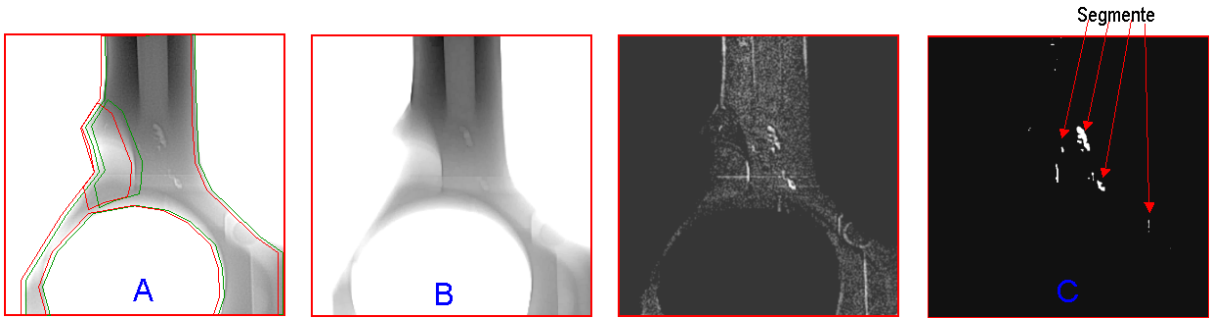

Fig. 15.8: Sequence of the image processing for the automatic cast component inspection

The following Figure shows the result of the segmentation superimposed to the image in comparison to a pseudoplast (“pseudo 3D”) filtered image. It becomes evident that the shape of the flaws has been met in large, but also false detections are present.

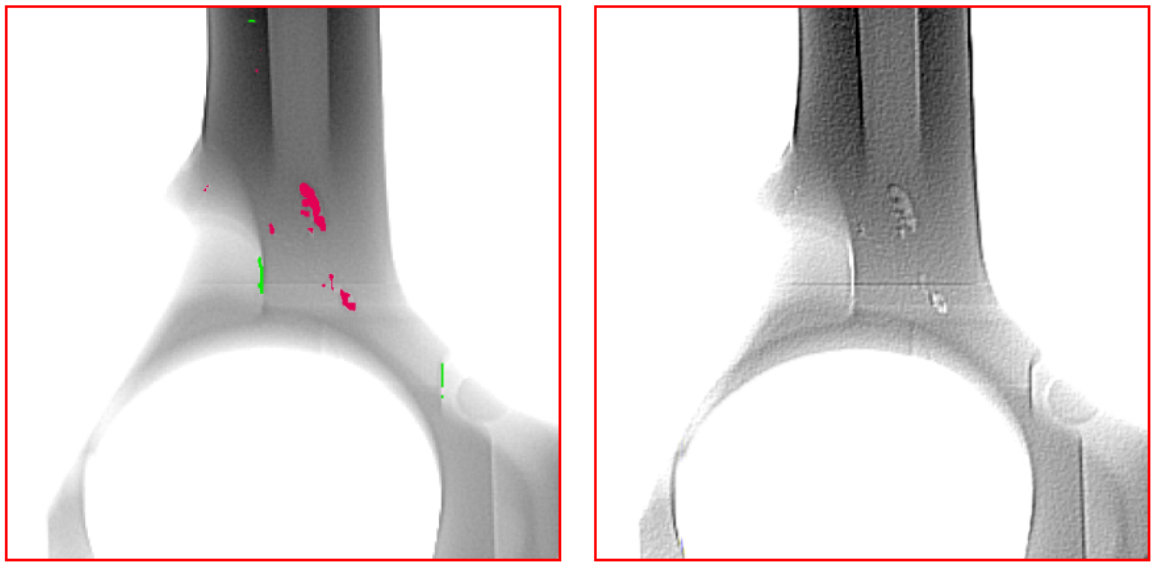

Fig. 15.9: Result of the segmentation as compared to a pseudoplast filtered image

In the last step, the segments have to be classified. The “learnt” regular structures are removed first, and then the closely adjacent flaws are grouped together. The corresponding size of the flaws is calculated – the area of the flaw in this example. Conclusively the determined flaws are matched with the specifications; in this example, both apply the size of the individual flaws as well as the flaw density (size of the faulty area). The inspection has doubtlessly come to a decision: rejected.

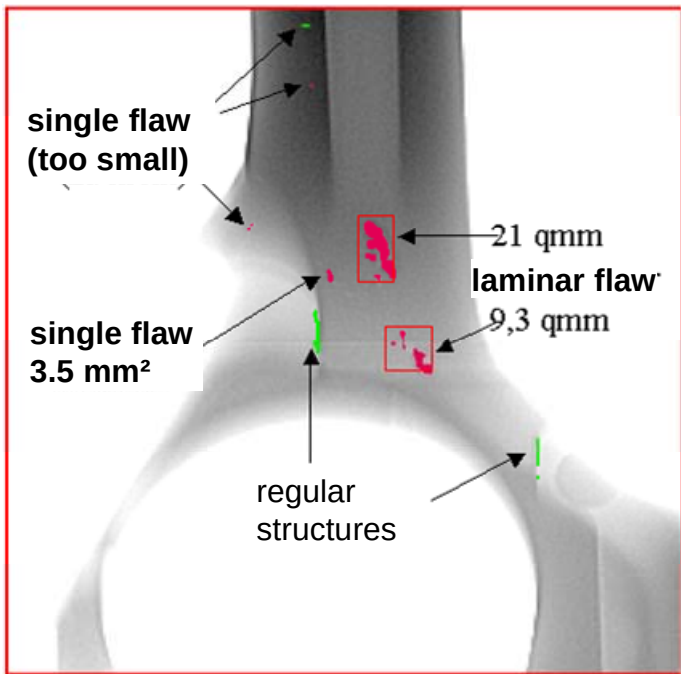

Fig. 15.10: Result of the classification

15.5.5 Problems encountered with the automatic defect recognition (ADR)

The adjustment of the image processing for an ADR takes relatively much time and requires fundamental knowledge as well as experience in image processing itself. The reasons for the time needed as follows:

As a general rule, a single filter is not sufficient for one image; in most cases, it has to be divided in several regions that have to be processed each with other filters or with different filter parameters, respectively.

The established types of filters are the difference image technology, the ranking filters (e.g. median) as well as the linear filters (e.g. the low pass). A special role plays the band pass filter (e.g. the DoG) where the segmentation is accomplished without differentiation. The corresponding optimal filter has to be chosen and checked in comparison with alternatives.

When choosing the filter kernel it has to be taken into account that normally only objects can be detected that fully fit into the filter kernel, i.e. are not larger than the filter kernel. Otherwise, only the rim of an object might be segmented in most cases so that the size of the flaw area is underestimated in the subsequent measurement.

If a regular pattern is present in the image, e.g. parallel aligned longwalls, then the filter kernel can be selected in a way that only objects are recognised perpendicular to those structures (see L11: Sobel filter). For such cases, modern ADR-systems offer menus with a compass rose to align the filter kernel so that the pattern direction coincides with that one of the compass and the structures along the compass direction are ignored. In this context it has to be considered that those flaws in parallel with the pattern cannot be recognised for sure with this filter.

15.6 Differences between visual and automatic inspection

- The inspection is accomplished not in motion (visually) but in exactly defined positions (highest demands are made to their precision since tolerances herein directly result in an increased rate of rejections, or “pseudo rejections”, resp.).
- The human vision is capable to cope with the presence of noise in the image since it is “filtered away”. In the automatic inspection, noise may lead to false (“pseudo”) rejections or even to the risk that existing flaws are covered by the noise.
- Man is capable to distinguish between 40 grey values only, thus he prefers an image that is adequately adjusted, rather poor in contrast. The computer needs a contrast as high as possible.
- The inspection specifications currently in use or the quality assurance rules are designed for the visual testing; up today (status 2008) no algorithmic realisations of inspection specifications are available.
- The accessibility for inspections has poorly been considered in the construction of a component; rather frequently a type label, a control stamp or even a flexible drilling may cause serious problems for the automatic inspection.
- A human operator easily is able to inspect various specimens, the automatic system has to identify the different parts first and then to initiate the respective programs.
- ADR systems make high demands on the control software because there is nor more human supervision.

15.6.1 Application areas of the visual and automatic inspection

By means of the parameters throughput and expenses it can be estimated from when on an automatic inspection is more cost effective than a visual inspection. There are also cases where the customer stipulates an automatic inspection making the cost aspect of minor importance.

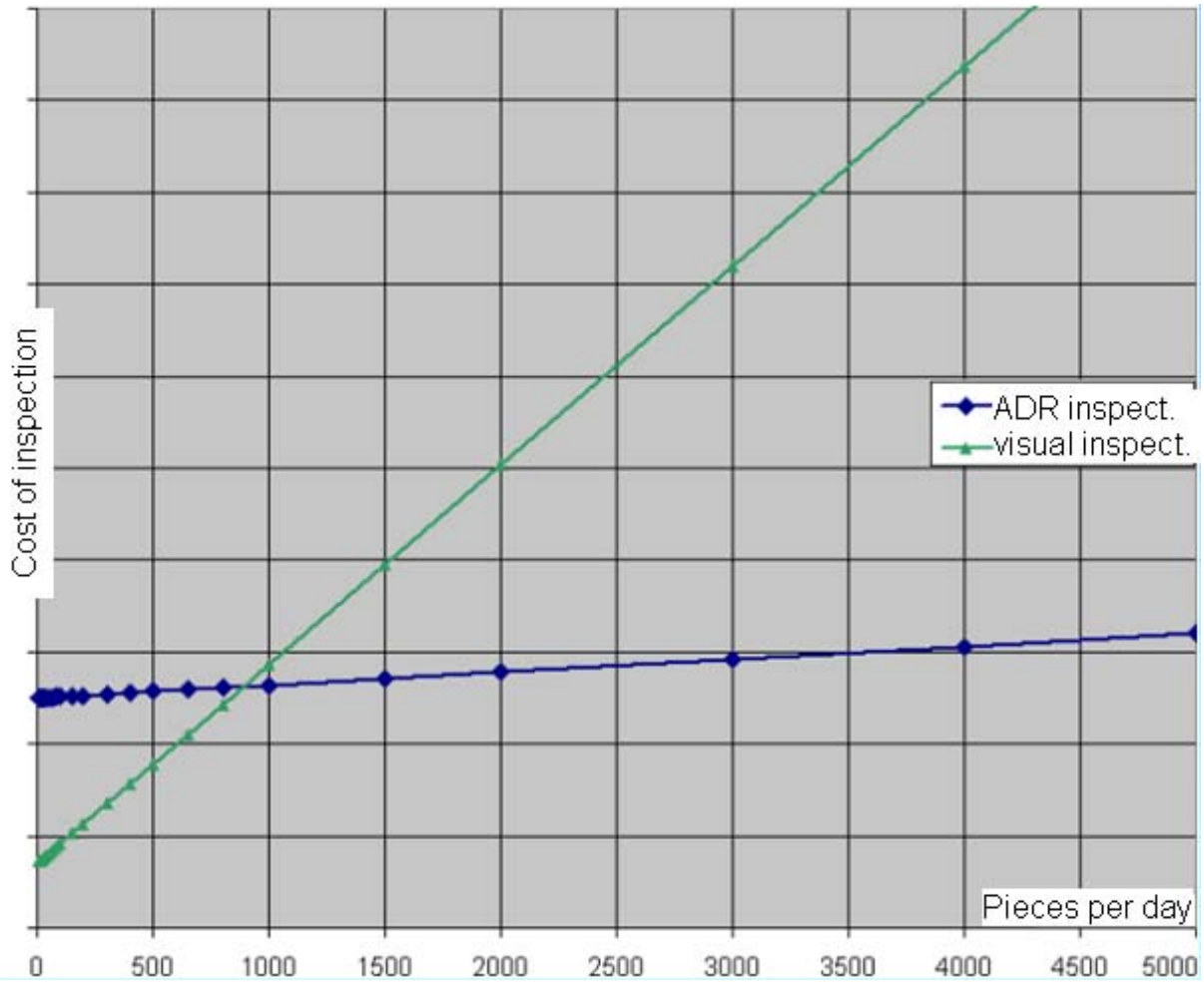

Assumptions for the plot (empirical values or typical system utilisation):

Specimen an ADR requires 12s for with 5 inspection positions including import and export. A visual inspection takes 40 s. The ADR is used 360 days a year in a 3-shift operation (24h) while the visual inspection is accomplished in a one-shift operation with one or more operators 200 days a year. An availability of 95% is assumed. The expected useful life amounts to 2 years. For this example, an ADR device is paying off from some 1000 parts a day by cost considerations.

These exemplary data can be transferred also to other specimens or even to other objects to be inspected.

15.7 Process optimisation by X-ray inspection

Modern quality strategies require a consequent avoiding of rejections. This make a targeted control of the casting process necessary before rejections occur. With the aid of early warning thresholds given by experts in casting from their knowledge of the process the production can be optimised in a way that any running astray of the process are realised in time so that corrections can be made. In this context, the ADR image processing works like an “ordinary sensor” giving signals for the in-process control.

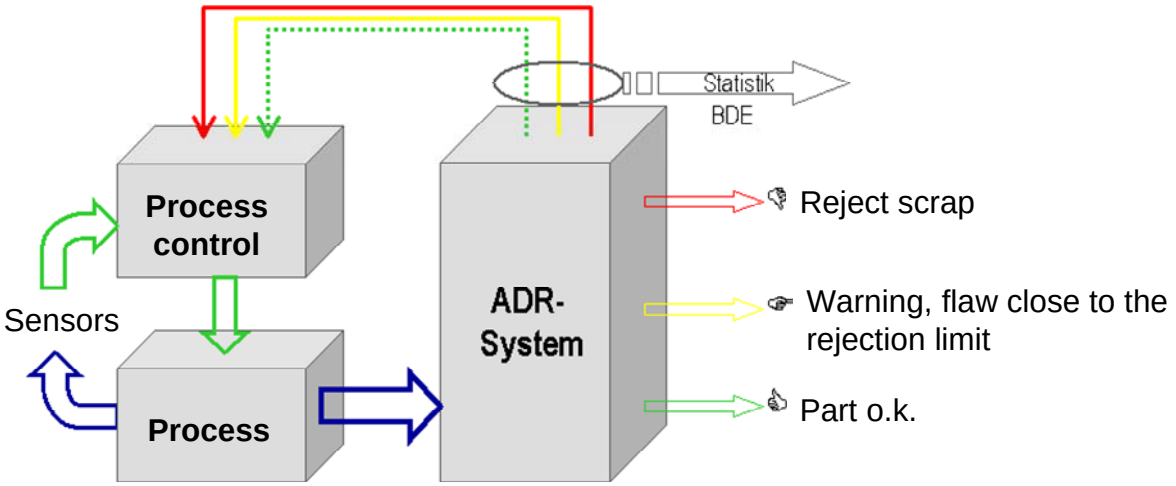

Fig. 15.11: Feed-back of the results from an ADR system for in-process optimisation

A permanent control of the occurrence frequency distribution of flaws across all the coquilles allows conclusions o their individual operability or the wear and tear – as far as they are separable.

The transfer of the results to the data management of the enterprise demonstrates another practical use of the ADR equipment.

L 16 Computed Tomography

Content

16.1 Introduction

The specimen located between the X-ray source and the detector when inspected by means of X-rays is projected onto the detector like an X-ray image converter. As a consequence of the projection technology details are superimposed along the radiation beam; details arranged one after the other partly cannot be separated anymore from each other in the X-ray image, the depth information and that about the extent in the direction of the radiation are lost, please see L13.

Fig. 16.1 shows two X-rays of a human foot with two metal brackets taken perpendicularly to each other. Only the evaluation of both exposures together makes evident that the two brackets do not touch each others and are positioned in different depth.

Fig. 16.1: X-ray exposure in 0 degree und 90 degree angular directions

When tracing back the path of the radiation beam through a detail in two exposures taken in two different angular directions (ideally: with 90 degree), it is possible to determine the depth or the extent in the direction of the beam. However, this method fails in case of complex geometries in a component, or if numerous structures of similar type such as pores are present so that an unequivocal correlation remains impossible.

By means of the computed tomography (CT) it is possible to generate cross sections that show the internal structures without any overlay. This technology has been developed for the medical diagnostics in the seventies. In order to accomplish the calculations for the cross sections, it is essential to have X-ray images from all directions. For this purpose, the object is rotated around an axis by 360 degree in total. In case of large ob-

jects the specimen remains fixed while the source and the detector are rotated around the object on a circular path (orbit).

16.2 Data acquisition

Medical scanners are designed for the examination of humans that means to keep the radiation exposure as low as reasonable. Thus the maximum energy and the geometric resolution vary only slightly from system to system.

The large diversification of technical CT-systems is reflected in the various types of the instruments. The CT installations range from those with a linear accelerator to inspect the empennages of airliners down to devices with a micro-focus X-ray tube to investigate seeds.

It is differentiated between the two-dimensional and the three-dimensional computed radiography (2D-CT and 3D-CT). In case of the two-dimensional CT, cross sections are produces in difference to volume data with the three-dimensional CT.

16.2.1 Two-dimensional Computed Tomography

The first medical scanners consisted of an X-ray tube and a single detector. The source and the detector are mounted on a traverse in opposite to each other with the patient in-between. Both, the source and the detector are shifted in parallel during the process of data acquisition measuring the intensity distribution along the traversal direction. After completion the traversal arrangement is rotated around the patient reaching the position for the next projection. For the next generation of the first medical scanners several detectors have been integrated into the traverse. This kind of CT-scanner is commonly called a translation-rotation scanner. These scanners are frequently encountered in the industrial 2D-CT devices.

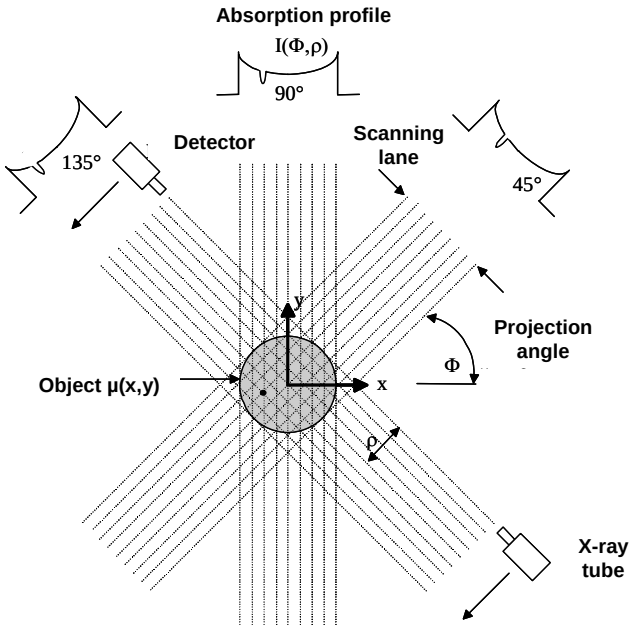

Fig. 16.2: Scanning in a parallel beam geometry

As a consequence of the translation and rotation movements the scanning time is considerably high with the CT-scanners of the first and second generation.

Contemporary CT systems have line detectors incorporated with up to 2048 detector elements. The cone beam of the X-ray tube is limited to a narrow fan beam by means of collimators to reduce the scattered radiation. The “section height” can be adjusted with the aid of a collimator attached to the line detector in most cases. Any linear movement of the detector and the source has become obsolete due to the projection with up to 2048 single measurements; only the rotation of the specimen is left. Since the reconstruction algorithm requires having the whole cross section of the specimen always within the fan beam, those objects larger than the length of the line detector are frequently scanned with a translation-rotation movement.

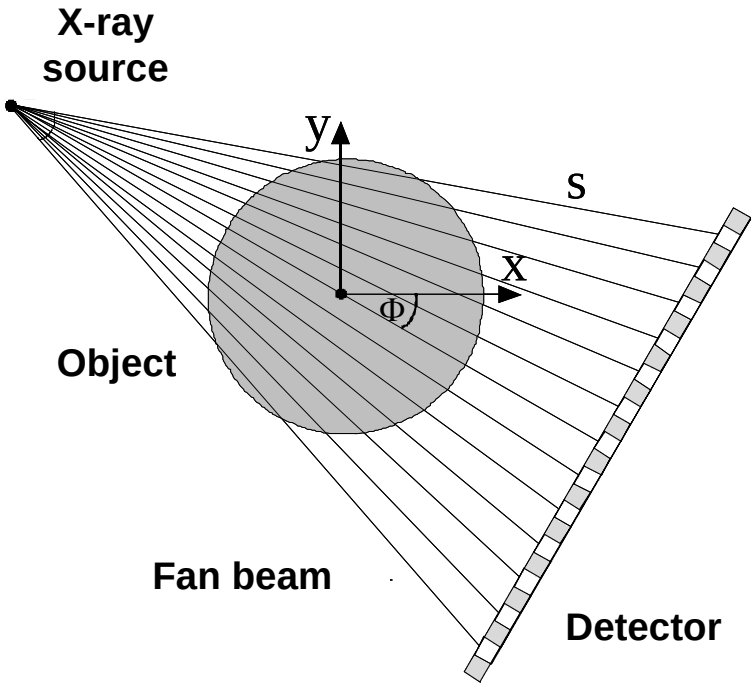

Fig. 16.3: Scanning in fan beam geometry

16.2.2 Three-dimensional CT

Inspecting the whole volume by means of the 2D-CT takes really much time since many sections have to be produced in different height levels. For the purpose of investigating the volume of an object, the three-dimensional CT (3D-CT) has been developed in which two-dimensional projection data are acquired by means of a digital detector array. The principal scanning geometry is shown in Figure 16.4. The specimen positioned on a turntable within the beam cone of an X-ray tube is projected magnified onto the digital detector array. The projection data are converted into digital while the specimen itself is rotated by 360 degree *at the end*.

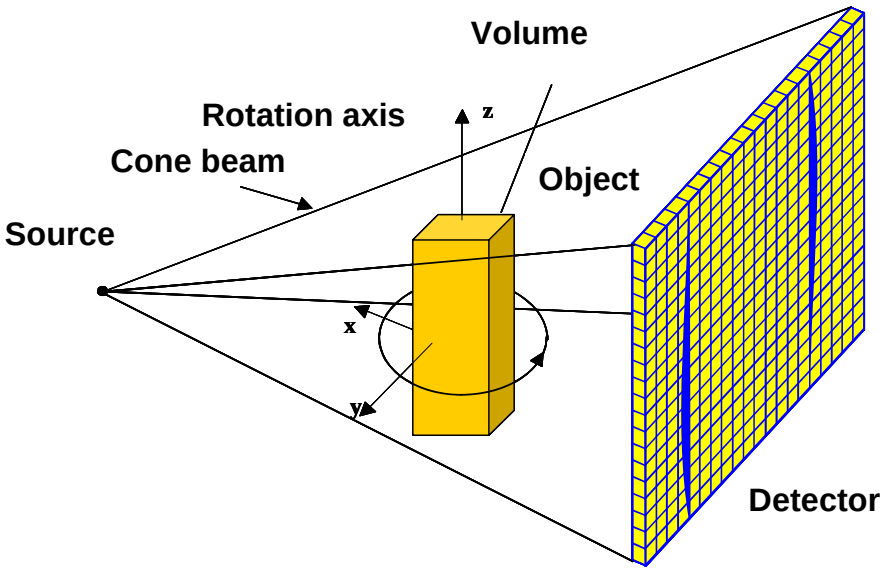

Fig. 16.4: Scanning in cone beam geometry

16.2.3 Requirements for the setup of a CT-system

High requirements are postulated by the CT for the manipulation mechanics in all the technologies presented here. The mathematics behind the computed tomography has to take precisely the geometric conditions into account with the installation of the X-ray tube, the specimen and the detector to ensure that the expected result really represents a true image of the specimen. All axes should, depending on the (sub-) task, be oriented exactly perpendicular or parallel to each other. In principle, the CT is capable also to compensate skew axes, however, this increases the computational effort unnecessarily. The rotation axis has to be capable to exert equidistant steps in the range of the resolution in any case where the measurements are running in a stop-and-go mode. Whenever a CT works with a continuous rotation (as it may be the case in 2D-CTs) it has to be accomplished without any fluctuation in velocity.

At the source, it has to be ensured that the stability of the X-ray beam is stable for the time of the whole measurement. If a reference detector is available for determining the intensity of the X-ray beam, the tube beam is allowed to vary during the measurement. Otherwise the current in the X-ray tube has to be kept very constant. Any undefined fluctuation of the energy is undesired indeed since it impairs the quality of the results.

At the site of the detector, also stable conditions are required since fluctuations in the image (contrast or geometry) diminish the quality of the reconstruction. Image intensifiers have been used in the beginning of the CT. However, they are conditionally suited for this purpose since they have a curved input screen that distorts the image. In addition, the image is also distorted by alterations of the ambient magnetic field. Particularly the last-mentioned circumstance can be compensated only with tremendous efforts. The

image amplifiers have been displaced by the emergence of digital detector arrays in high-end applications. Today, they are only found in low-cost systems or changed over ones.

Also with respect to the computational effort the CT is extremely extensive. Computer clusters are used in the area of 3D-CT employing detectors with a pixel number of 1024 x 1024 and larger since the performance and the memory size of a single computer remains insufficient. As an example, duplicating the size of a layer leads to an eight fold increase of the computational effort in the reconstruction! A further factor influencing the computational effort is the number of projections during a measurement. The large the number of projections the higher is the computational effort paralleled by an improved resolution.

16.2.4 Accomplishing a measurement

In each CT-technology when preparing a measurement it has to be considered that any over exposure (saturation) of the detector has to be avoided during the total measurement. This should be achieved by means of pre-filtering. The energy applied has to be sufficient to penetrate the specimen from any aspect that occurs in the whole course of the measurement. This should be assured by approaching the position of the longest beam pathways through the specimen *in a pre-measurement*.

The requested resolution that should be achieved after the reconstruction is determining the number of angular steps and the size of the reconstruction matrix which is related the detector implemented. As a rule of thumb, the whole rotation should contain as many angular positions as pixels exist in the horizontal directions of the detector. It should be stated principally that increasing the number of angular steps results in an improved spatial resolution in the volume while increasing in parallel the computational effort.

Of course the resolution also depends on the chosen magnification. In this context, the same constraints apply in relation to the unsharpness as they are known from the radioscopy.

Normally the angular positions are distributed across a whole circle (360°). Principally, 180° plus the angle covered by the detector may be also sufficient. This can be of advantage in case of specimens with a disadvantageous geometry.

16.3 Noise

Following the noise in each single projection all the reconstructed cross-sections also appear noisy. The lower the noise level in the projections the less noise appears in the reconstructed cross-sections. By prolongation of the measuring time, e.g. with longer integration times per projection or by increasing the tube current, respectively, the noise can be reduced accordingly (see also chapter 3). The noise will become more intense in the reconstruction with increasing resolution (smaller size of pixels or voxels).

The noise in the reconstruction can also be decreased by choosing more angular steps while acquiring the images, i.e. by increasing the number of projections. However, this prolongs the duration of the measuring at the same time, on the other hand, the reconstructions commonly show a better perceptibility of details.

16.4 Artefacts

16.4.1 Definition of the term

Aberrations may occur in a reconstructed image by reasons of physical effects. These are called reconstruction artefacts. They are manifested in most cases by false attenuation coefficients that are assumed at sites within the volume where other coefficients really exist. Fig. 16.5 shows a reconstruction afflicted with artefacts. Radial grey shadows are clearly visible around the true contour of the component itself where air is present in the real part. In addition, the contour of the component appears diffusely and cannot be determined unequivocally.

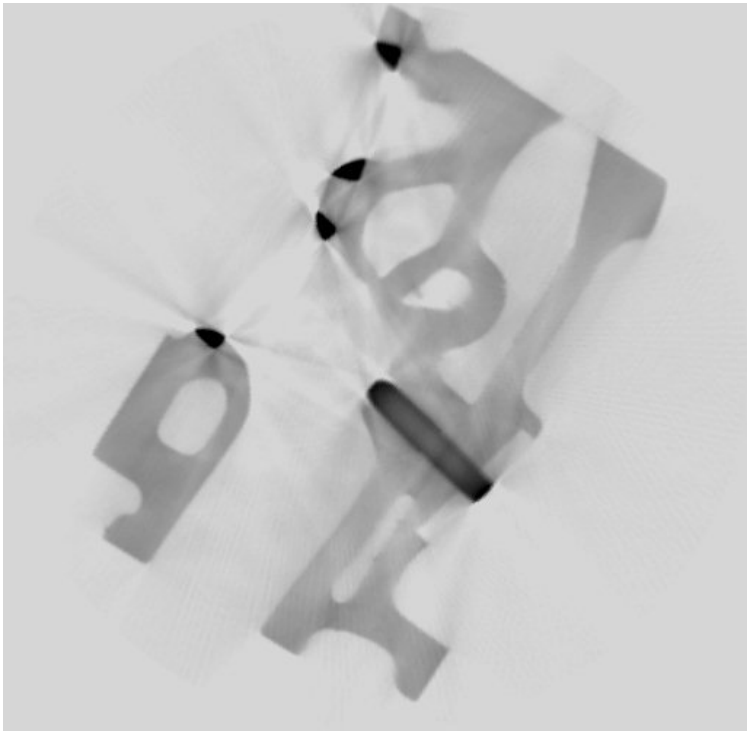

Fig. 16.5: Reconstruction afflicted with artefacts

16.4.2 Reasons for artefacts

There are numerous reasons for generating artefacts in the reconstruction. Those will be tackled first that emerge from external influences and can be avoided interactively by the operator.

- Wrong geometry:
    - The object diameter is larger than the reconstructed cross section, i.e. the specimen protrudes laterally over the fan beam. The artefacts caused hereby may prevent a meaningful evaluation.
    - The position of the rotation axis is incorrect, the specimen is shifted during the measurement, or the adjustment of the axis is faulty: Additional structures are created, the edges become unsharp.
- Wrong adjustments of the source and the detector:
    - Blooming of the detector: edges appearing washed, missing object details in areas of low wall thicknesses.
    - Incorrect detector calibration: circular artefacts.

These problems can be resolved by the operator e.g. by a readjustment of the axes, by improving the detector corrections and by a new adjustment of the source of the application of filters.

In addition, there are physical effects giving rise to artefacts. These cannot be compensated by simple interaction. At the time being, methods exist to minimise the effects:

- Scatter radiation: This is a secondary radiation generated by scattering within the object or also in the manipulator causing image information in the detector that carries no information at all about the specimen. The scatter radiation lowers the contrast in the image and leads to washed looking edges.
- Beam hardening: The energy spectrum of the X-ray is not *attenuated* linearly during penetration. By this reason the relationship between the measured grey value and the material thickness becomes not interpretable. This leads to an exaggerated elevation of edge structures and a false reconstruction of absorption coefficients in certain areas of the volume (see Fig. 16.5).
- Insufficient penetration: Grey shadows and false reconstruction of the absorption coefficient, incomplete object structures.

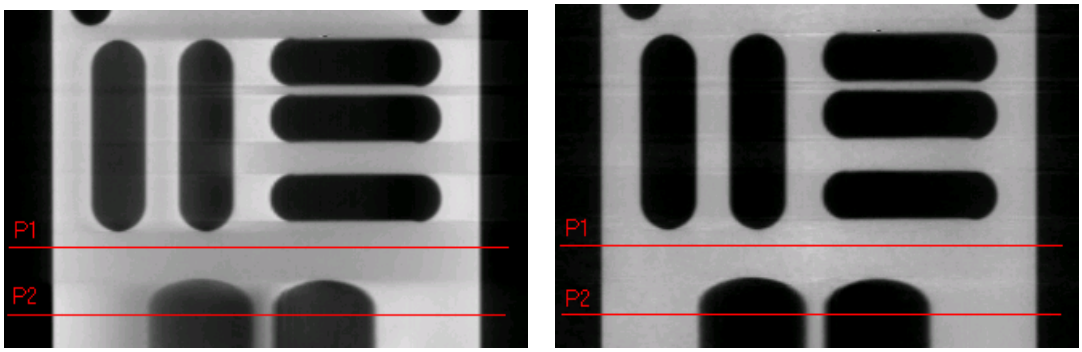

Fig. 16.6: Reconstruction without (left) and with (right) correction of the beam hardening

For the effects of both, the scatter radiation and the beam hardening mathematical procedures exist that are able simulate them and also partly to correct them. The Fig. 16.6 shows the difference between the reconstructions accomplished without and with the correction of beam hardening.

The scatter radiation can be mechanically shielded particularly in case of the 2D-CT. For this purpose, collimators are in use that restrict the utilisable beam as small as even required (fan shape). The collimation is achieved on both sides, at the source as well as at the collimator. The Fig. 16.7 shows how this can be effective to the quality of the reconstruction. This image has to be compared with that one shown in Fig. 16.5 which has been achieved without collimation.

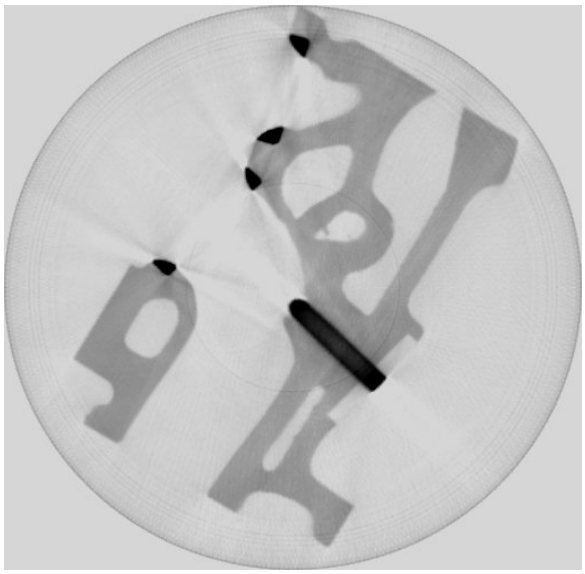

Fig. 16.7: Reconstruction with fan collimation

16.5 Visualisation and evaluation

The reconstruction yields a three-dimensional representation of the investigated object. Now the data are available in a way that allows different kinds of visual presentations.

The simplest method consists of sections through the volume. Like grinding patterns they allow a presentation of a desired plane of the specimen. Within the selected plane assessments can be made on the density distributions and on various dimensions such as wall thicknesses. Contemporary visualisation systems allow cutting arbitrarily sections through the reconstructed volume and thus provide the opportunity to inspect from various aspects without the need of destroying the specimen (see Fig. 16.8 und Fig. 16.9).

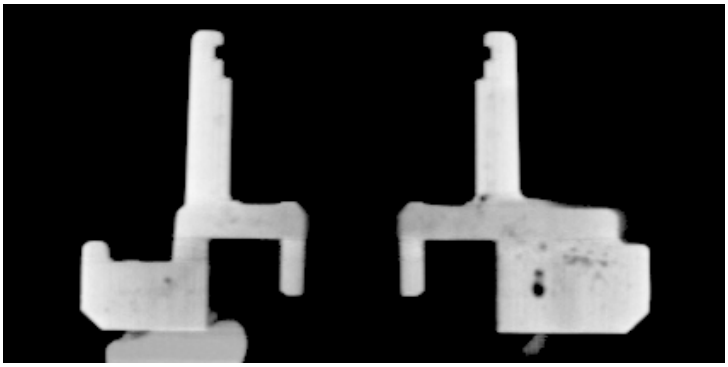

Fig. 16.8: Section through the YZ-plane of the tomography of a component

Fig. 16.9: Section through the XY-plane of the tomography of a component

More effort is needed for a 3D visualisation in space. Software systems with this capability display the data as a virtual body as shown in Fig. 16.10. They allow various views arbitrarily from different spatial aspects, are capable to display certain materials transparently or have the tools to produce animations such as to simulate a flight through the specimen.

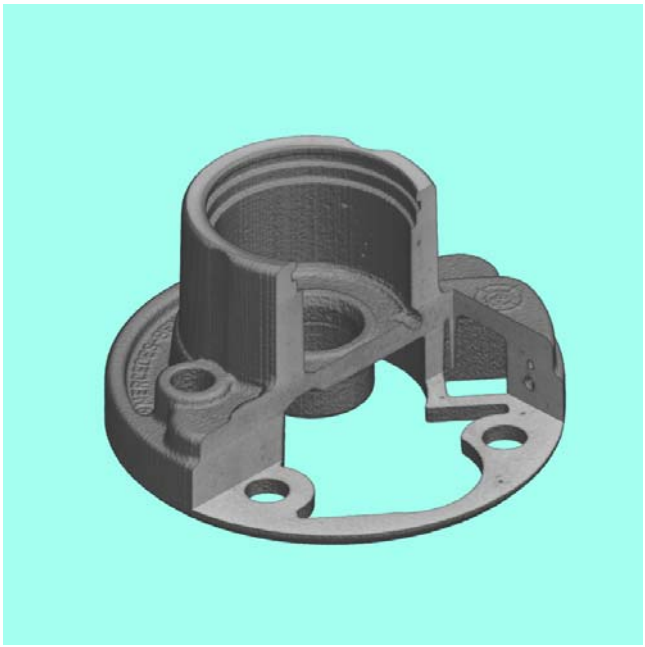

Fig. 16.10: 3D visualisation of a tomography with a virtual cut

16.6 Fields of application

The computed radiography is suitable e.g. for the following applications:

- Analysis of imperfections
  - Characterisation of cavities, pores, inclusions of impurities, crack configurations.
  - Integrity analysis.
  - Assessment of material transitions and combinations.
- Measurements
  - Wall-thickness measurement.
  - Nominal/actual value comparison.
- Reverse engineering
  - Reverting dimensions of real components to CAD-data.

Moreover, numerous detail problems are resolvable by CT whenever the internal structures of the test objects are involved. If a specimen consists of different material such as synthetics and aluminium their absorption differences can be visualised in the CT. However, it remains impossible to determine the exact material composition with the aid of CT.

Specification of the specimen:

Testing object: Identification:	Testing procedures: Testing class: IQI set:
Material: Max. penetrated thickness:	Dimensions: Coverage:

Relevant testing data:

Testing positions:			
Inspection sequence:			
Type of radiation source:			
Focal spot size d [mm]:			
Pre-filter:			
Diaphragm:			
Masking:			
Tube voltage [kV]:			
Tube current [mA]:			
SDD:			
SOD:			
Geometrical magnification:			
Detector, SR_b:			
Input screen size:			
IQI # required / achieved:			
Exposure time per frame:			
Integration number:			
Image processing:			
Filter sequence 1:			
Filter sequence 2:			
Filter sequence 3:			

Location:	Date:	Operator:

Remarks:

Image Acquisition with Computed Radiography

The available test object should be inspected.

1.1 System set-up

1.1.1 Adjust the monitor properly.

1.1.2 Place the test object including single and duplex wire IQIs on a CR cassette. Choose the correct settings for voltage and current at the X-ray tube

(please use EN 13068 – 3 testing class SB)

X-ray voltage = ... kV, current = ... mA

1.2 Geometrical magnification:

1.2.1 Measure the distances and calculate the geometrical magnification factor.

Calculation: .....M =

1.3 Selection of exposure time

1.3.1 Choose a suitable exposure time for minimum SNR of 100 in base material.

Selected exposure time: .....

---1

1.3.2 Acquire an image with the chosen exposure time.

1.3.3 Store the resulting image on the computer hard drive.

---1

1.4 Protocol

1.4.1 Please complete the testing record on the following page in such a way that it can be used for subsequent inspections.

Specification of the specimen:

Test object: Identification:	Testing procedures: Testing class: IQI set:
Material: Max. penetrated thickness:	Dimensions: Radiographic coverage:

Relevant testing data:

Test positions:		
Inspection sequence:		
Type of radiation source:		
Focal spot size d [mm]:		
Pre-filter at tube port:		
Diaphragm:		
Masking:		
Tube voltage [kV]:		
Tube current [mA]:		
SDD:		
SOD:		
Geometrical magnification:	V =	
Detector, SR_b:		
Input window size:	Zoom:	
Verification of image quality:	Wire type IQI acc. to EN 462-1: $W\#_{required}$: $W\#_{achieved}$:	Duplex wire IQI acc. to EN 462-5: $D\#_{required}$: $D\#_{achieved}$:
Exposure time:		
Image processing:		
Filter sequence 1:		
Filter sequence 2:		

Location: Date: Operator:

Optimisation, Analysis and Flaw Detection

Load the image from the USB stick into ISee! with the file name:

Images\Corrosion\ FilmC4_Mg_casting_300dpi.tif

Test object: connector pipe, Al/Mg casting of Al, wall thickness 4mm, outer diameter 70 mm

2.1 Contrast Enhancement

The casting parts should be inspected for volume defects in the center pipe region.

2.1.1 Which functions are you using to evaluate possibilities for contrast enhancemment?

Please list the function: .....

2.1.2 Decide if there exist possibilities to enhance the contrast of the single wire IQI.

If yes, please apply the contrast enhancement.

Displayed grey value range before and after contrast enhancement for IQI reading:

Before: gv_{min} = ... gv_{max} = ...

After: gv_{min} = ... gv_{max} = ...

Which imperfections are visible?

Please list:.....

.....

2.1.3 Please check if the IQI visibility is achieved according to EN 13068 testing class SB.

Required W# = ...

Achieved W# = ...

2.1.4 Please store the optimised image.

Hint: use <Alt Gr> <Prnt Scrn> for Windows copy into Clipboard and <Ctl> <V> for insertion of clipboard content into Word or Paint for image storage!

2.2 Segmentation of the flaw region shown in the image:

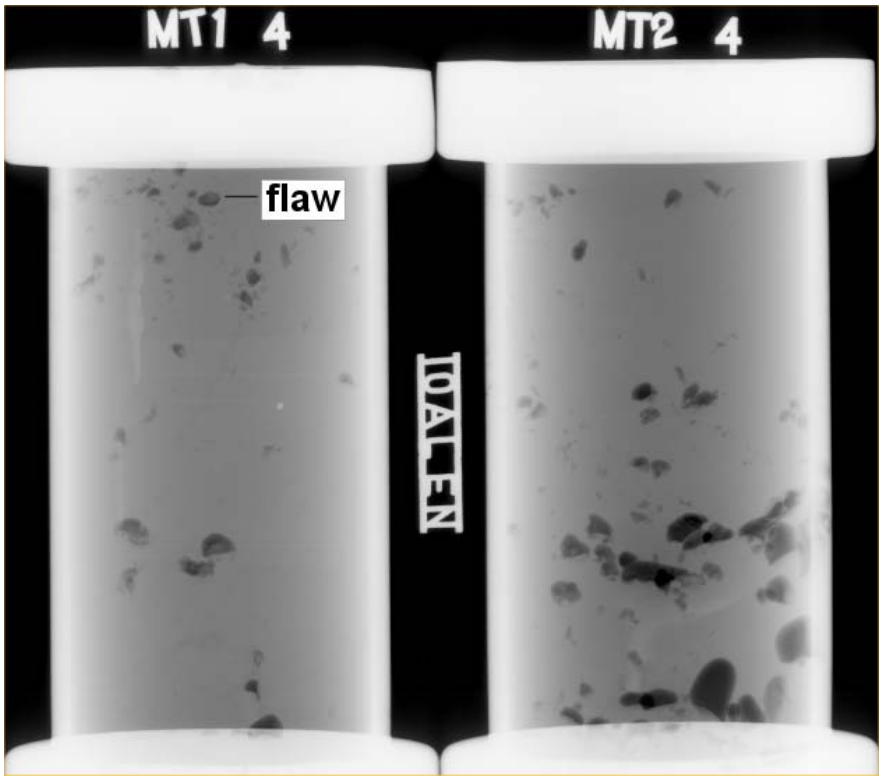

2.2.1 Please choose a suitable sequence of filtering and/or operations to segment the depicted flaw indication.

Please list each of the steps:

1) .....

2) .....

3) .....

Grey value after Segmentation:

$gv_{threshld}$ = ...

2.2.2 Apply these operations.

2.3.3 Please store the segmented image under a useful name.

Wall thickness measurement of a stepped pipe by projection radiography

Load the image from the USB stick into ISee! with the file name:

Corrosion\ StepPipe148mm_Ir-192_CR_DPS_linear.tif

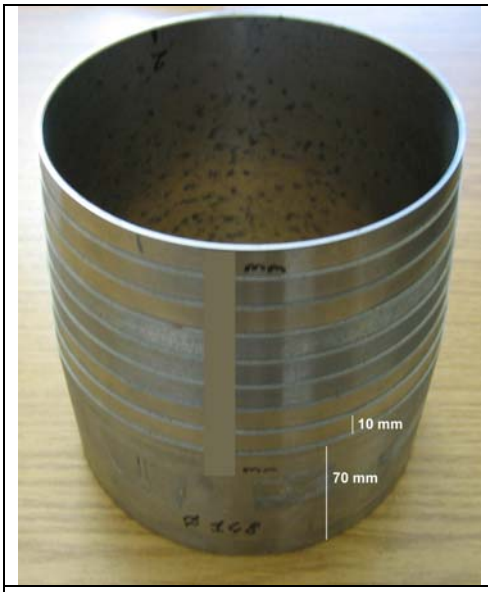

Image 1: View of the stepped pipe

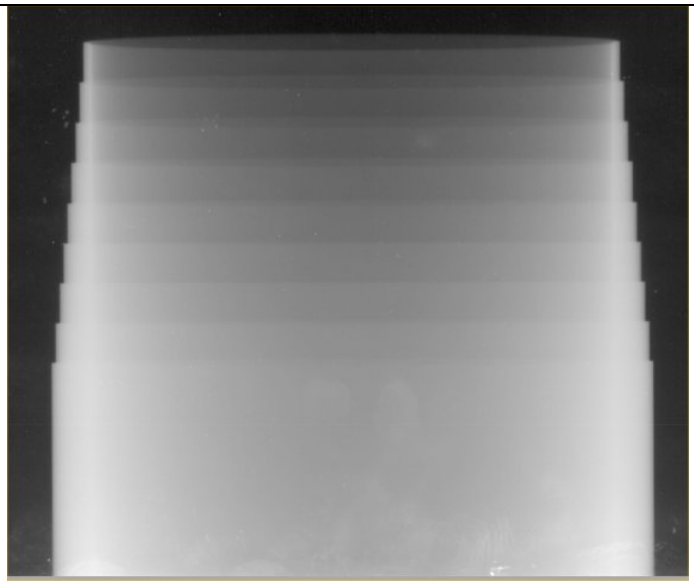

Image 2: CR radiograph of the stepped pipe (Ir- 192)

3.1 Calibration (see Image 1)

Describe the procedure of calibration. Use as reference the outer pipe diameter of 148 mm.

.....

.....

.....

3.2 Measurement (see Image 2, step 1 on top)

step 1 / mm		step 6 / mm	
step 2 / mm		step 7 / mm	
step 3 / mm		step 8 / mm	
step 4 / mm		full pipe / mm	
step 5 / mm			

3.3 Storage of the image with measured wall thickness annotations

Hint: use <Alt GR> <Prt scr> for Windows copy into Clipboard and <Ctl> <V> for insertion of clipboard content into Word or Paint for image storage!

EUROPEAN STANDARD

NORME EUROPÉENNE

EUROPÄISCHE NORM

EN 13068-3

August 2001

ICS 19.100

English version

Non-destructive testing - Radioscopic testing - Part 3: General principles of radioscopic testing of metallic materials by X- and gamma rays

Essais non destructifs - Contrôle par radioscopie - Partie 3: Principes généraux de l'essai radioscopique à l'aide de rayons X et gamma des matériaux métalliques

Zerstörungsfreie Prüfung - Radioskopische Prüfung - Teil 3: Allgemeine Grundlagen für die radioskopische Prüfung von metallischen Werkstoffen mit Röntgen- und Gammastrahlen

This European Standard was approved by CEN on 25 July 2001.

CEN members are bound to comply with the CEN/CENELEC Internal Regulations which stipulate the conditions for giving this European Standard the status of a national standard without any alteration. Up-to-date lists and bibliographical references concerning such national standards may be obtained on application to the Management Centre or to any CEN member.

This European Standard exists in three official versions (English, French, German). A version in any other language made by translation under the responsibility of a CEN member into its own language and notified to the Management Centre has the same status as the official versions.

CEN members are the national standards bodies of Austria, Belgium, Czech Republic, Denmark, Finland, France, Germany, Greece, Iceland, Ireland, Italy, Luxembourg, Netherlands, Norway, Portugal, Spain, Sweden, Switzerland and United Kingdom.

EUROPEAN COMMITTEE FOR STANDARDIZATION
COMITÉ EUROPÉEN DE NORMALISATION
EUROPÄISCHES KOMITEE FÜR NORMUNG

Management Centre: rue de Stassart, 36 B-1050 Brussels

Ref. No. EN 13068-3:2001 E

Contents

Foreword

This European Standard has been prepared by Technical Committee CEN/TC 138 "Non-destructive testing", the secretariat of which is held by AFNOR.

This European Standard shall be given the status of a national standard, either by publication of an identical text or by endorsement, at the latest by February 2002, and conflicting national standards shall be withdrawn at the latest by February 2002.

EN 13068 comprises a series of European Standards of radioscopic systems which is made of the following:

EN 13068-1, *Non-destructive testing - Radioscopic testing - Part 1: Quantitative measurement of image properties.*

EN 13068-2, *Non-destructive testing - Radioscopic testing - Part 2: Qualitative control and long term stability of imaging devices*.

EN 13068-3, *Non-destructive testing - Radioscopic testing - Part 3: General principles of radioscopic testing of metallic materials by X- and gamma-rays*.

According to the CEN/CENELEC Internal Regulations, the national standards organizations of the following countries are bound to implement this European Standard: Austria, Belgium, Czech Republic, Denmark, Finland, France, Germany, Greece, Iceland, Ireland, Italy, Luxembourg, Netherlands, Norway, Portugal, Spain, Sweden, Switzerland and the United Kingdom.

Introduction

This part specifies fundamental techniques of radioscopy with the object of enabling repeatable results to be obtained economically. The techniques are based on generally accepted practice and the fundamental theory of the subject.

The goal of this standard is to define a radioscopic technique as close as possible to the radiographic standard EN 444 and EN 462. Due to the specific differences the following deviations are essential:

1) The limited inherent unsharpness of the intensifier based systems in comparison to the film technique requires careful handling with IQI´s. Therefore, the usage of the double wire IQI corresponding to EN 462-5 is additionally introduced for each measurement. The maximum permissible unsharpness is defined in dependence on the wall thickness. The values are calculated from the permissible geometric unsharpness corresponding to the equation f_{min} of EN 444. Due to technical and economical reasons up to the double unsharpness corresponding to EN 444 was accepted for the lower wall thickness range in Table 4 and 5. Contrast enhancement by a lower maximum tube voltage and the requirement for the same minimum wire IQI values corresponding to EN 462-3 yield a compensation for the limitations in the spatial resolution. No values for step hole IQI´s are defined because wire IQI´s are more typical for small structures to detect.

2) The principle of compensating the limited spatial resolution by contrast enhancement requires the necessity for image integration for most applications. Thus, the image quality defined in Table 5 for testing of metallic materials is based on radioscopic test images acquired with image integration. Real time testing yields advantages for the perceptibility of oriented structures by the dynamic testing principle and should be applied always as a first step for system and positioning optimization. The wide application of radioscopy for light alloy testing justifies the definition of special limited requirements for this application area in Table 4. Here, class SA testing can be performed by real time radioscopy and class SB testing only needs additional image integration. The user may decide if he does apply Table 4 or 5 depending on his testing problem.

1 Scope

This European Standard specifies general rules for industrial X- and gamma-radioscopy for flaw detection purposes, using radioscopic techniques, applicable to the testing of metallic materials.

It does not lay down acceptance criteria of the discontinuities.

2 Normative references

This European Standard incorporates by dated or undated reference, provisions from other publications. These normative references are cited at the appropriate places in the text and the publications are listed hereafter. For dated references, subsequent amendments to or revisions of any these publications apply to this European Standard only when incorporated in it by amendment or revision. For undated references the latest edition of the publication referred to applies (including amendments).

EN 462-1, *Non-destructive testing - Image quality of radiographs - Part 1: Image quality indicators (wire type) - Determination of image quality value*

EN 462-3, *Non-destructive testing - Image quality of radiographs - Part 3: Image quality of radiogrammes - Part 3: Image quality classes for ferrous metals*

EN 462-5, *Non-destructive testing - Image Quality of radiographs - Part 2: Image quality indicators (duplex wire type) - Determination of image quality value*

EN 473, *Non-destructive testing - Qualification and certification of NDT personnel - General principles*

EN 1435, *Non-destructive examination of welds - Radiographic examination of welded joints*

EN 12544-1, *Non-destructive testing - Measurement and evaluation of the X-ray tube voltage - Part 1: Voltage divider method*

EN 12544-2, *Non-destructive testing - Measurement and evaluation of the X-ray tube voltage - Part 2: Constancy check by the thick filter method*

EN 12544-3, *Non-destructive testing - Measurement and evaluation of the X-ray tube voltage - Part 3: Spectrometric method*

EN 12681, *Founding - Radiographic inspection*

EN 13068-1, *Non-destructive testing - Radioscopic Testing - Part 1: Quantitative measurement of image properties*

EN 13068-2, *Non-destructive testing - Radioscopic Testing - Part 2: Qualitative control and long term stability of imaging devices*

3 Terms and definitions

For the purposes of this European Standard, the following terms and definitions apply:

3.1
nominal thickness, *t*
nominal thickness of the material in the region under testing [EN 444]

Manufacturing tolerances do not have to be taken into account.

3.2
penetrated thickness, *w*
thickness of material in the direction of the radiation beam calculated on basis of the nominal thickness [EN 444]

3.3
source size, d
size of the source of radiation (in accordance with EN 12679), focal spot size of the used X-ray tube (in accordance with EN 12543-1 to EN 12543-5)

3.4
focus-to-detector distance, FDD
distance between the source of radiation and the detector measured in the direction of the beam

3.5
focus-to-object distance, FOD
distance between the source of radiation and the source side of the test object measured along the central axis of the radiation beam

3.6
terms describing spatial resolution (see annex A)
geometric unsharpness, U_g
inherent (screen) unsharpness, U_i
total unsharpness, U_t

3.7
system parameter (see annex A)
geometric magnification, M

3.8
blooming
light overshoot or streaking in areas with high intensity contrast

4 Radioscopic testing

4.1 Classification of radioscopic techniques

The radioscopic techniques are divided into two classes:

Testing class SA: Basic techniques

Testing class SB: Improved techniques.

Testing class SB techniques will be used when testing class SA may be insufficiently sensitive.

Better techniques compared with testing class SB are possible and may be agreed between the contracting parties by specification of all appropriate testing parameters and improved minimum requirements of the radioscopic system.

The choice of radioscopic technique shall be agreed between the parties concerned.

4.2 Minimum requirements to radioscopic detector systems

The equipment used for radioscopic work can differ in the quality of the results depending on the type of test system.

Three system classes of radioscopic test systems are defined. The standard defines the minimum system class which shall be used for a particular purpose.

Criteria for the classifications are the inherent detector unsharpness, the distortion and the homogeneity in accordance with Part 1 of this standard (Table 1) measured without geometric magnification. The values shall be measured with a 6 mm steel plate as test object at 100 kV. Furthermore a check of inherent unsharpness for long term stability is necessary. The measurement shall be done in accordance with EN 13068-1 and EN 13068-2.

Table 1 – Minimum requirements for radioscopic detector systems

Parameter	System classes		
	SC 1	SC 2	SC 3
inherent detector unsharpness U_i better than	0,4 mm	0,5 mm	0,6 mm
distortion $V_{d,i}$ better than	5 %	10 %	20 %
homogeneity $H_{d,i}$ better than	10 %	20 %	30 %

These features shall be measured at a signal to noise ratio better than 50. Distortion and homogeneity shall be measured at 75% of the radius of the used image field.

Systems which do not meet the system classes SC 1 to SC 3 are not subject of this standard.

5 General

5.1 Protection against ionizing radiations

Warning - Exposure of any part of the human body to X-rays or gamma-rays can be highly injurious to health. Wherever X-ray equiment or radioactive sources are in use, appropriate legal requirements are applied.

Local or national or international safety precautions when using ionizing radiation shall be strictly applied.

5.2 Surface preparation and stage of manufacture

In general, surface preparation is not necessary, but where surface imperfections or coatings might cause difficulty in detecting discontinuities, the surface shall be ground smooth or the coating shall be removed.

5.3 Identification of radioscopic images

If documentation is necessary, a clear identification shall be affixed to each section of the object being inspected. The images of these symbols shall appear in the radioscopic image outside the region of interest where possible and shall ensure unequivocal identification of the section. In case where a documentation is necessary a clear identification of each image shall be guaranteed.

Alternatively the identification of radioscopic images can be performed by inserting a symbol or reference number into the image, the image header or a parameter file by electronic means. The reference shall be stored as part of the radioscopic image.

5.4 Marking

If documentation is necessary permanent markings on the object to be tested shall be made in order to accurately locate the position of each radioscopic image.

Where the nature of the material and/or its service conditions do not permit permanent marking, the location may be recorded by means of accurate sketches.

5.5 Overlap of images

When testing an area with two or more separate images/video frames, these shall overlap suffiently to ensure that the complete region of interest is radioscopically tested. This can for example be verified by a high density marker on the surface of the object which will appear in the image.

5.6 Personnel qualification

It is assumed that radioscopic testing is performed by qualified and capable personnel. In order to prove this qualification, it is recommended to certify the personnel in accordance with EN 473 or equivalent.

6 Recommended techniques for radioscopic images

6.1 Test arrangements

Where applicable, testing arrangements shall be determined by the specific application standards.

6.2 Radioscopic imaging devices

The imaging properties of the system shall be given in terms as described in EN 13068-1 and EN 13068-2.

6.3 Alignment of beam

The beam of radiation shall be directed to the centre of the area being tested and should be normal to the object surface at that point, except when it can be demonstrated that certain tests are best revealed by a different alignment of the beam. In this case, an appropriate alignment of the beam may be permitted.

Between the contracting parties other ways of radioscopic testing may be agreed upon. Other testing geometries may be carried out with reference to testing related standards.

6.4 Use of filters and collimators

In order to reduce the effect of scattered radiation and blooming, direct radiation shall be collimated as much as possible to the section under testing. Scattered radiation shall be reduced by collimators, filters and masks.

6.5 Choice of tube voltage

To maintain a good flaw sensitivity, the X-ray tube voltage (in accordance with EN 12544-1 to EN 12544-3) should be as low as possible. The maximum values of tube voltage versus penetrated thickness are given in Table 2 for aluminium and light alloys and in Table 3 for steel.

Table 2 – Maximum X-ray voltage for aluminium and light alloys

Penetrated thickness mm	Maximum X-ray voltage kV
5	45
10	50
15	55
25	65
35	75
45	85
55	95
70	110
85	125
100	140
120	160

Table 3 – Maximum X-ray voltage for steel

Penetrated thickness mm	Maximum X-ray voltage kV
1,2 to 2,0	90
2,0 to 3,5	100
3,5 to 5,0	110
5,0 to 7,0	120
7,0 to 10	135
10 to 15	160
15 to 25	210
25 to 32	265
32 to 40	315
40 to 55	390
55 to 85	450

For some applications with microfocus equipment it can be necessary to use a slightly higher voltage. Then the geometric magnification shall be increased to reach the necessary IQI sensitivity (see Tables 4 and 5). But it should be noted that an excessively high tube voltage will lead to a loss of defect detection sensitivity.

By agreement between the contracting parties gamma ray sources may be used according to EN 1435 and EN 12681.

6.6 Sampling of image data

The image is provided as an electronic signal which undergoes statistical variations caused by the photon flux. In the visual representation on a tv-screen this appears as an optical noise in the image. Noise reduction can be achieved by increasing the number of photons at the entrance screen used for the image or by integration of the image signal.

The integration or averaging shall be done at least until the required image quality is reached, better until no further improvement can be detected.

The image quality shall be controlled by use of image quality indicators (IQIs). It is recommended to use the IQI defined in EN 462-1 and EN 462-5.

Minimum requirements for the visibility of the wire type IQI in accordance with EN 462-1 and the duplex wire in accordance with EN 462-5 as a function of penetrated thickness are given in the Tables 4 and 5 for different applications.

The IQI´s shall be fixed on the source side of the object (for focal spot sizes larger than the inherent detector unsharpness) or on the detector side of the object (for focal spot sizes smaller than the inherent detector unsharpness) under an angle of approximately 45°. In addition the wire penetrameter and the duplex wire shall be visible under the same system conditions like the testing will be done.

Table 4 – System performance for aluminium and light alloy

Testing Class	SA		SB	
System Class	SC3		SC2	
penetrameter	wire no.	duplex no.	wire no.	duplex no.
penetrated thickness mm				
5	W 12	8 D	W 16	10 D
10	W 11	7 D	W 14	9 D
15	W 10	7 D	W 13	9 D
25	W 9	7 D	W 12	9 D
35	W 8	7 D	W 10	9 D
45	W 7	7 D	W 9	9 D
55	W 6	7 D	W 9	9 D
70	W 5	7 D	W 8	9 D
85	W 5	7 D	W 8	9 D
100	W 5	7 D	W 8	9 D
120	W 4	7 D	W 7	9 D

NOTE For light alloy testing the **testing class SA** is based on the requirements of real-time serial testing which are covered especiallyby standard minifocus X-ray tubes (0,1 ...1 mm focal spot size according to the serie EN 12543).

The **testing class SB** is based on the requirements beyound serial testing for higher geometric resolution and contrastsensitivity (in accordance with EN 462-3).

Table 5 – System performance for metallic materials testing class SA and SB except aluminium and light alloys

Testing Class	SA		SB		Testing Class
System Class	SC 2		SC 1		System Class
IQI	wire no.	duplex no.	wire no.	duplex no.	IQI
penetrated thickness mm					penetrated thickness mm
1,2 to 2,0	W 17	11 D	W 19	13 D	to 1,5 *)
2,0 to 3,5	W 16	10 D	W 18	12 D	1,5 to 2,5 *)
3,5 to 5,0	W 15	9 D	W 17	11 D	2,5 to 4,0 *)
5,0 to 7,0	W14	8 D	W 16	10 D	4,0 to 6,0 *)
7,0 to 10	W 13	7 D	W 15	9 D	6,0 to 8,0
10 to 15	W 12	7 D	W 14	9 D	8,0 to 12
15 to 25	W 11	7 D	W 13	9 D	12 to 20
25 to 32	W 10	7 D	W 12	9 D	20 to 30
32 to 40	W 9	7 D	W 11	9 D	30 to 35
40 to 55	W 8	7 D	W 10	9 D	35 to 45
55 to 85	W 7	6 D	W 9	9 D	45 to 65
*) In case of difficulties to reach the necessary geometric magnification in testing class SB the required duplex wire number may be reduced by one in the wall thickness range up to 6,0 mm under agreement between the contracting parties.					

The testing classes SA and SB of Table 5 are based on EN 462-3.

NOTE The human eye has already an integration time of approximately 0.2 sec. The quality of a single video frame is worse than the image on a tv-screen.

6.7 Image storage and treatment

After measurement, the images shall be stored as raw data on an external storage. The device shall be suitable for long term storage to fulfil the requirements of testing documentation.

Radioscopic images can be further processed by digital image processing for enhancement of the defect visibility or automated evaluation. For the image quality test only image integration, contrast and brightness adjustment are permitted.

It has to be agreed between the contracting parties whether the raw data, only the processed images or both shall be stored for documentation.

6.8 Image viewing conditions

The evaluation of radioscopic images shall be carried out in a darkened room on a monitor.

7 Test report

If a test report is necessary for each radioscopic image, or set of images, a test report shall be made giving information on the testing technique used, and on any other special circumstances which would allow a better understanding of the results.

Details concerning form and contents should be specified in special application standards or be agreed on by the contracting parties. If testing is carried out exclusively to this standard then the test report shall contain at least the following topics:

a) name of the testing company;

b) unique report number;

c) object;

d) material;

e) stage of manufacture;

f) nominal thickness ;

g) radioscopic technique, testing class and system class;

h) system of marking, if applied;

i) radiation source, type and size of focal spot and equipment used;

j) tube voltage and current or source activity;

k) alignment of the beam (if not normal to the object);

l) filters and collimators used;

m) integration time, focus-to-detector distance and magnification used ;

n) type and position of image quality indicators;

o) type and reading of image quality indicators;

p) specification of image processing, if applied;

q) data format and file names of stored data;

r) conformance to this standard;

s) any deviation from agreed standards;

t) name, certification and signature of the responsible person(s);

u) date of testing and report.

Annex A
(informative)

Test arrangements; relation between geometric unsharpness and geometric magnification

The X-ray projection enlargement is shown graphically in Figure A.1.

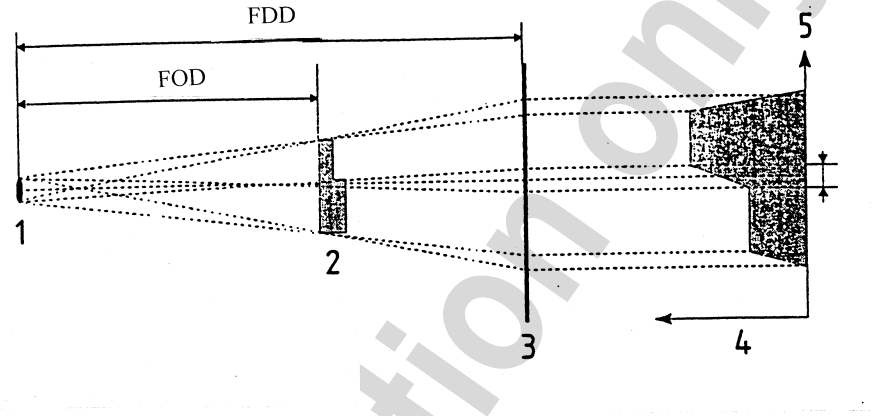

Key

1 focus
2 specimen
3 detector
4 intensity
5 location

Figure A.1 – X-ray projection enlargement

The geometric unsharpness U_g has to be calculated by the focus-detector distance FDD, the focus object distance FOD and the focal spot size d.

$U_g = d \times (FDD - FOD) / FOD$ (A.1)

or

$U_g = d \times (FDD/FOD - 1)$ (A.2)

With the geometric magnification M = FDD/FOD:

$U_g = d \times (M - 1)$ (A.3)

The smallest discontinuity observable is controlled by two types of unsharpness, the geometric and inherent unsharpness U_i of the detector. Both together define the resolution of the radioscopic system, U_t. This is equal to the square root of the sum of the squares of the geometrical and inherent unsharpness:

$$U_t = \sqrt{(U_g^2 + U_i^2)} \quad \text{(A.4)}$$

The theoretical minimal unsharpness of the system U_t is obtained if the optimal geometric magnification M_{opt} is choosen (for $d \geq 0{,}1$ mm):

$M_{opt} = 1 + (U_i / d)^2$ (A.5)

Any deviation of the theoretical Mopt leads to an increase of the unsharpness of the system.

Bibliography

EN 444, *Non-destructive testing - General principles for radiographic examination of metallic materials by X- and gamma-rays*

EN 12543-1, *Non destructive testing - Characteristics of focal spots in industrial X-ray tube assemblies for use in non destructive testing - Part 1: Scanning method*

EN 12543-2, *Non destructive testing - Characteristics of focal spots in industrial X-ray tube assemblies for use in non destructive testing - Part 2: Pinhole camera radiographic method*

EN 12543-3, *Non destructive testing - Characteristics of focal spots in industrial X-ray tube assemblies for use in non destructive testing - Part 3: Slit camera radiographic method*

EN 12543-4, *Non destructive testing - Characteristics of focal spots in industrial X-ray tube assemblies for use in non destructive testing - Part 4: Edge method*

EN 12543-5, *Non destructive testing - Characteristics of focal spots in industrial X-ray tube assemblies for use in non destructive testing - Part 5: Measurement of the effective focal spot size of mini and micro focus X-ray tubes*

EN 12679, *Non-destructive testing - Determination of the size of industrial radiographic sources - Radiographic method*